Development of a Concentric Internally Heat Integrated Distillation Column (HIDiC)

Development of a Concentric Internally Heat Integrated Distillation Column (HIDiC)

Proefschrift

ter verkrijging van de graad van doctor
aan de Technische Universiteit Delft,
op gezag van de Rector Magnificus prof. dr. ir. J.T. Fokkema,
voorzitter van het College voor Promoties,
in het openbaar te verdedigen op dinsdag 23 oktober 2007 om 12.30 uur

door

Aris DE RIJKE

scheikundig ingenieur
geboren te Delft.

Dit proefschrift is goedgekeurd door de promotor:
Prof. dr. ir. P.J. Jansens
Toegevoegd promotor:
Dr. Sc. Ž. Olujić

Samenstelling promotiecommissie:

Rector Magnificus	voorzitter
Prof. dr. ir. P.J. Jansens	Technische Universiteit Delft, promotor
Dr. Sc. Ž. Olujić	Technische Universiteit Delft, toegevoegd promotor
Prof. Dr. -Ing. G. Wozny	Technische Universität Berlin
Prof. dr. ir. H.E.A. van den Akker	Technische Universiteit Delft
Prof. dr. ir. P.J.A.M. Kerkhof	Technische Universiteit Eindhoven
Dr. J.A. Hugill	Energy research Centre of the Netherlands (ECN)
ir. C.J.G. van Strien	Akzo Nobel

Printed by Gildeprint drukkerijen, Enschede, Netherlands.

Summary

Increasing energy demand, consequently high oil prices and growing concern about carbon dioxide emissions are important drivers for the development of more energy efficient and environmentally friendly processes and unit operations in the chemical and process industries.
Distillation is by far the most applied separation technology. A major drawback is the degradation of energy associated with the distillation process, due to the temperature difference between the reboiler and condenser of a distillation column. This degradation of energy causes the thermodynamic efficiency of distillation to be low, typically around 10%. During the last decades several technologies have been developed and implemented to improve the thermal economy of distillation. The main focus has been on heat integration of a train of distillation columns. Vapour recompression is a way to improve the energy efficiency of a single distillation column and is industrially applied for the separation of close-boiling mixtures.
An internally Heat Integrated Distillation Column (HIDiC) combines advantages of vapour recompression and diabatic operation to reduce the energy requirements of a single distillation column. The theoretical advantage of HIDiC over a vapour recompression column is that in a HIDiC the compressor operates only over the stripping section of the column. Therefore a HIDiC should operate at a lower compression ratio and consequently lower compressor duty than a vapour recompression column. In a HIDiC the stripping section is physically separated from the rectifying section. Heat is transferred inside the distillation column from the rectifying to the stripping section, because the operating pressure of the rectifying section is increased by means of the compressor. Although the HIDiC concept was introduced around 1970, it is still not implemented in industrial practice due to difficulties related with equipment design and lack of experimental data at sufficiently large scale to prove the HIDiC principle.
A novel type of concentric HIDiC was developed at the TU Delft in which a low pressure annular stripping section is configured around a high pressure rectifying section. Heat panels can be placed on the active tray area of the stripping section in order to obtain a sufficiently large surface area for heat transfer. An experimental study was performed to prove this concept of intra-column heat transfer and to study the effect of internal heat transfer on the mass transfer efficiency, which results were used to validate the model predictions.

Heat Transfer inside a Concentric HIDiC with heat panels

Large scale experiments have been performed with a 0.8 m diameter concentric HIDiC column, operated with the model system cyclohexane/n-heptane. The overall heat transfer coefficient was determined for heat transfer panels placed in the downcomer and on the active tray area of a sieve tray respectively. The heat panels appeared to be sufficiently wetted by the splashing froth present above the tray deck. The overall heat transfer coefficient strongly depends on the temperature driving force between the rectification and stripping section, because of the laminar flow conditions at the condensation side of the heat panels. Overall heat transfer coefficients were between 700 and 1500 W/m^2K for operating conditions of practical interest to HIDiC.

The Alhusseini model appeared to be the most suitable for predicting heat transfer coefficients for an evaporating liquid film in the transition regime between laminar and turbulent flow. The Nusselt model was in good agreement with the experimental condensation side heat transfer coefficient, except for the low Reynolds numbers, indicating partial wetting of the heat transfer surface.

The vapour inlet manifold to the heat transfer panels must be carefully designed in order to avoid stagnant zones inside the panels.

Separation Efficiency of an Annular Sieve Tray

Experiments were carried out to establish the effect of the annular tray layout on the separation efficiency and to determine the influence of the presence of heat transfer panels on tray hydraulics and the overall tray efficiency.

Comparison of the data obtained in this study with measurements by the Fractionating Research Institute shows that separation efficiency of an annular sieve tray resembles that of a conventional cross-flow sieve tray.

The Garcia and Fair model was used to predict the overall tray efficiency. The tray pressure drop was modeled with the Bennett model. Both measurements and calculations showed that the heat panels did not influence tray pressure drop.

Heat transfer panels do have a positive influence on tray hydraulics and enhance the separation efficiency of the tray with roughly 10%, which is an important advantage of the proposed column design with heat transfer panels placed on the active tray area. The main reason for the increase in tray efficiency appears to be a reduction of back mixing by the panels. This additional effect could be simulated by regarding the two-phase froth as a number of ideally mixed pools in series.

The heat panel surface provides extra interfacial area which has a small enhancing effect on the separation efficiency.

Design of HIDiC for Different Industrial Distillation Applications

A HIDiC version of a state of the art propylene-propane splitter is introduced. The base case is one of the worlds largest, heat pump assisted, stand alone columns. The actual plant data formed the basis for a techno-economic evaluation, which indicated that HIDiC could become economically attractive for new designs.

The thermal efficiency of an internally Heat Integrated Distillation Column (HIDiC) is very sensitive to the column configuration, i.e. the way in which the rectifying and stripping sections stages are thermally integrated. Secondly, the distribution of the internal heat duty along the column appears to be very important. Since a HIDiC is essentially a fractionating heat-exchanger, the temperature profile dictates the trays which are feasible for internal heat transfer. A better exploitation of driving forces for heat transfer reduces the overall need for heat transfer area and moreover results in a more feasible design. The choice for an ideal HIDiC without external reboiler or a partial HIDiC depends strongly on the model system. HIDiC appears to be favourable for the separation of close boiling mixtures in moderate to high pressure applications, where an optimum HIDiC design reduces the energy need by 50% compared to conventional heat pump technology.

Table of Contents

Chapter 1:

Introduction to Heat Integrated Distillation

Scope of Thesis

1.1 Introduction

Distillation is a widely implemented separation technique for the separation of bulk liquid mixtures. A major disadvantage however is the large energy degradation associated with distillation processes. In a distillation column, heat is used as separating agent. High temperature heat is introduced in the reboiler, which is withdrawn at low temperature from the condenser. This external introduction and removal of heat causes the overall thermodynamic efficiency of distillation to be well below 10%. (Humphrey, 1991)

Multiple effect methods
In the past decades several methods for improving the thermal economy of distillation were proposed and implemented in industry. Most research and simulation efforts went into the heat integration of a sequence of distillation columns. The basic idea of multiple effect methods is to use the heat content of the distillate vapour generated in one column to supply some of the heat required in the reboiler of the next column. In order to provide the necessary temperature difference, the columns must be operated under different pressures (Linnhoff ,1993; Glenchur, 1987; Lang, 1996).

Thermal Coupling
An alternative way of improving the energy efficiency of two or more distillation columns is thermal coupling. Thermally coupled arrangements are realised by setting up two-way vapour/liquid flow between different columns of a distillation sequence. Thermal coupling often eliminates the condenser/reboiler of one column and introduces a vapour/liquid connection. Thermally coupled distillation was first patented by Brugma (1937, 1942) and re-introduced by Petlyuk et al. (1965). For some specific ternary separations thermal coupling in a Petlyuk column (Wolff et al 1995, Halvorsen et al 1999, Shah, 2002) or a Divided Wall Column (Wright 1949**,** Kaibel, 1988, Schultz 2002), which is essentially a Petlyuk column in one shell, has lead to substantial energy savings.

Direct Vapour Recompression
In contrast to the multiple effect methods, direct vapour recompression has been primarily a method for enhancing the thermal economy of a single column (Freshwater, 1951, 1961; Null, 1976; Smith, 1995; Sulzer Chemtech 1998). Heat pump assisted distillation (*figure 1)* is very effective because it attacks the problem of introduction and removal of heat from the column at the source: the pressure and temperature of the overhead vapour is upgraded by means of a compressor to such a level that it can be used as heat source for

the reboiler. Although vapour recompression is a very useful technique for saving energy, it is capital intensive and appeared to be economical only for close boiling mixtures, where due to a small temperature difference between top and bottom, small compression ratios and consequently small compressor duties are required. Indeed, the potential for energy saving is largest in the separation of a low relative volatility mixture, because high reflux ratios and a consequently large reboiler duties are required to separate these mixtures.

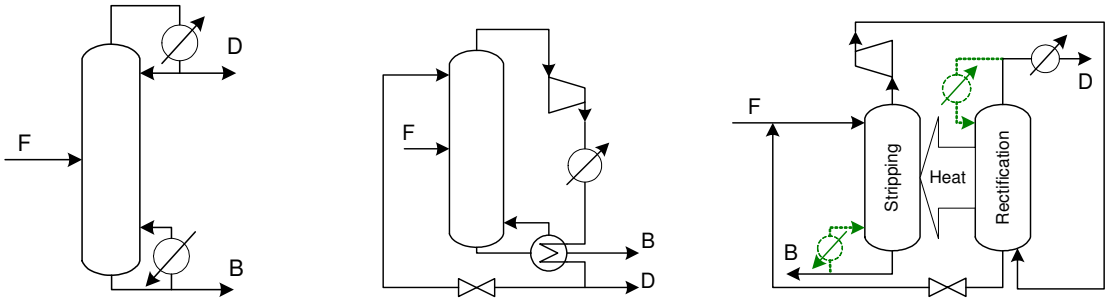

Figure 1: Conventional distillation column, vapour recompression column and the HIDiC concept

Diabatic Distillation

Another concept for energy saving in a single distillation column, which is not implemented in practice so far, is the so-called diabatic distillation column. (Le Goff, 1996; Rivero, 2001). Compared to the classical adiabatic distillation column, a diabatic column replaces the reboiler and the condenser, normally connected to the bottom and at the top of the column, by a condenser and reboiler integrated in the rectification and stripping sections, respectively (*figure 2*). Because of the gradual supply/removal of the heat along the stripping and rectification sections, diabatic distillation offers the benefits of a more efficient use of the heat of condensation and the heat of evaporation. Heat transfer takes place at a lower temperature difference, which implies smaller exergy losses associated with heat transfer. The effect of internal heat transfer on the distillation process can be evaluated with the help of the McCabe-Thiele diagram (*figure 2*). In a conventional distillation column, the two straight operating lines have slopes, the ratio of which is equal to the ratio of the molar flow rates of liquid and vapour flowing counter-currently in the rectification and stripping sections of an adiabatic column. In the diabatic column, the two straight lines are replaced by a continuous operating curve, which is parallel to the equilibrium curve. A measure for the irreversibility of the process is given by the distance between the operating and the

equilibrium curve. If, in the limit, these curves overlap then the exergy losses would be zero and the distillation process would be perfectly reversible. As, however, bringing these two curves together, while reducing the exergy losses to a minimum, would result in an inoperable column, a finite difference must be maintained. Obviously, the theoretical potential for energy/exergy savings cannot be exploited, and, similar to conventional distillation, a trade off between operating reflux and the number of stages is required.

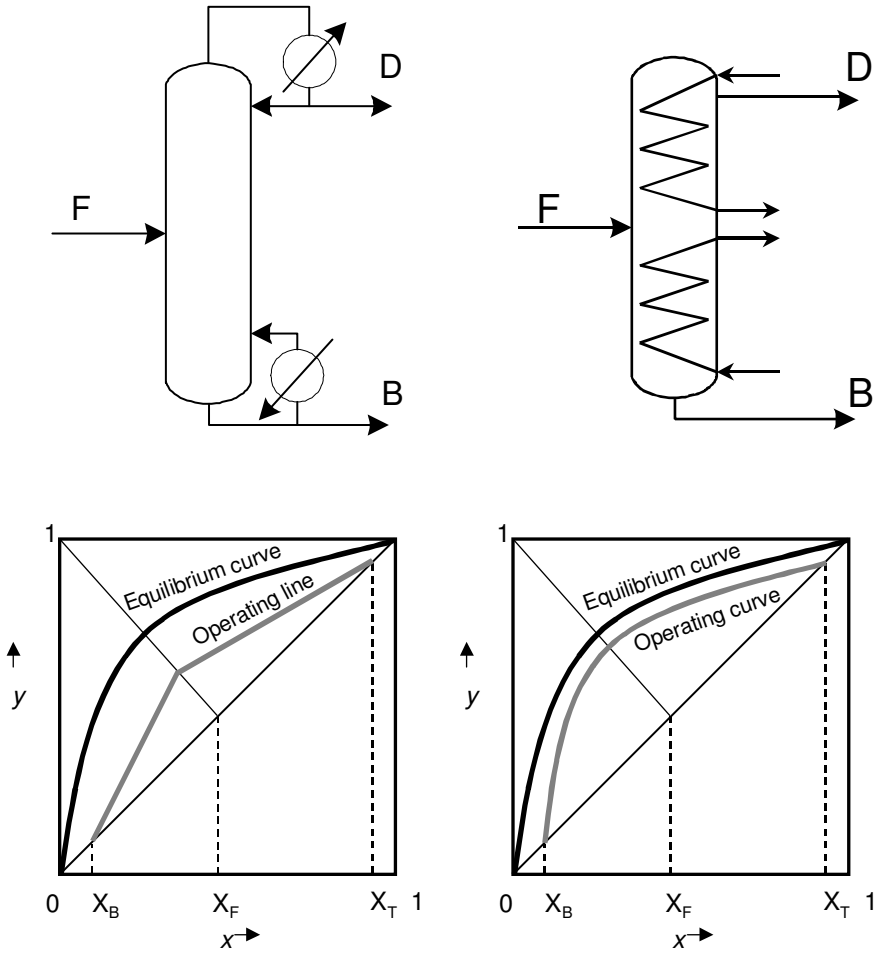

Figure 2: Schematic representations and McCabe-Thiele diagrams of a conventional and a diabatic distillation column.

Another disadvantage of this concept is that it requires the use of a special heating liquid in the reboiler. Finally, the utilities leaving the condenser and reboiler are at such a temperature that they can hardly be utilised in the process.

Internally Heat Integrated Distillation Column

Another possibility for internal heat integration is the so-called Heat Integrated Distillation Column (HIDiC), which combines the advantages of vapour recompression and a diabatic distillation column. In a HIDiC, heat is transferred from the hotter rectification section to the colder stripping section (*figure 1*), leading to a gradual evaporation along the length of the stripping section and a gradual condensation along the length of the rectifying section. In order to realise a temperature driving force between the rectifying and the stripping sections, the rectifying section is operated at higher pressure than the stripping section. Direct vapour recompression is applied to increase the pressure of the vapour leaving the top of the stripping section. Vapour recompression requires the heat pump to operate over the complete temperature difference that exists in the system. In fact, the main advantage of HIDiC compared to a conventional heat pump system is that HIDiC can operate at a significantly lower compression ratio. Theoretically it can operate without reboiler and condenser. Moreover the height of a HIDiC column could be significantly lower, in the best case just half the normal column height.

The first one to apply an extensive thermodynamic analysis to distillation processes and to suggest heat transfer from the rectifying section to the stripping section of a single distillation column, in order to narrow the temperature range to be overcome by the heat pump, was Freshwater. (1951, 1961). Flower and Jackson (1964) worked out the idea systematically and showed the advantages of this technique by simulation studies based on the second law of thermodynamics. From 1977, Mah and co-workers thoroughly evaluated the HIDiC concept under the name “Secondary Reflux and Vaporization” (SRV) (Mah, 1977; Fitzmorris 1980). During the ’70 s and ’80 s, several equipment related patents were filed (Haselden, 1977; Seader, 1980; Govind, 1986, 1987). Since 1985, Nakaiwa et al are working on HIDiC. They performed both simulation studies and pilot plant experiments in which they proved that HIDiC can save a substantial amount of energy compared to its conventional counterpart. Takamatsu et al. (1996) indicated the possibility for operation without either a reboiler or a condenser, in a so-called ideal HIDiC. A new type, shell & tube heat integrated distillation column was proposed and patented (Aso et al 1998). An extensive literature review of their work in this field can be found elsewhere (Nakaiwa et al, 2003).

The Kyoto protocol and recent trends towards more sustainable developments gave a strong impulse resulting in initiation of new research groups dealing with heat integrated distillation. Emphasis is ranging from process design (Kjelstrup, 1995; Aguirre, 1997), thermodynamic analysis (Niang, 1995; Rivera-Ortega, 1999) and process operations (Liu; 2000) to mass and heat transfer mechanism (Kaeser, 2003)

In 2000, the Separation Technology group of Delft University of Technology started to investigate HIDiC. A feasibility study was carried out to evaluate the energy saving potential of HIDiC. Like a VRC, HIDiC appeared to be especially attractive for close boiling mixtures. (Jansens et al, 2001; Olujic et al, 2003). Focus is now on problems related to practical implementation of HIDiC, i.e.: equipment design and heat and mass transfer efficiency.
Most recently a patent was filed (De Graauw et al, 2003) on a concentric HIDiC in which the lower pressure stripping section is configured around a higher pressure rectifying section. Heat transfer panels can be placed in either the stripping or rectifying section to obtain a large and variable heat transfer area. The design is applicable for both tray columns and packed columns and can be utilised in HIDiC configurations other than a concentric column (Gadalla, 2003).

In this introductory chapter, the equipment design related work on HIDiC is reviewed. A thermodynamic analysis is presented, revealing the process parameters which mainly determine the energy consumption of HIDiC. Advantages and drawbacks of the different HIDiC design options which are proposed in literature are discussed.

1.2 Thermodynamic Analysis

In a conventional distillation column heat is supplied in the reboiler and withdrawn in the condenser. Because of the temperature difference between the heating media used in the reboiler and condenser respectively, the separation of components is always accompanied by a degradation of energy, even when heat losses are neglected.
To realise a closer approach to a reversible distillation column, one could use intercoolers and interheaters, instead of a separate reboiler at the bottom and a separate condenser at the top of the column. The idea is basically to distribute the addition and removal of heat from the distillation process more uniformly along the length of the column. The thermodynamic advantages of a more equal partition of energy introduction and removal from a distillation column have been reported by several authors. (Haselden, 1958; Flower, 1964; Le Goff, 1996; Rivero, 1991, 2001; Aguirre, 1997; De Koeijer, 2002; Schaller, 2002). Equipartition of entropy production was introduced as a general concept by Tondeur and Kvaalen (1987). They suggested that the “optimal design” (in the sense of the second law) is the one where the entropy production is uniformly distributed among process variables. In his review article on future challenges for basic research in chemical engineering, Villermaux (1993) addresses the equipartition of entropy production as a new design principle. This design principle is applied in both a diabatic or quasi-reversible distillation column and a HIDiC.

In a HIDiC the design principle of equipartition of entropy production is combined with a heat pump operating over a narrowed temperature range, compared to a conventional heat pump system. This combination of advantages leads to a very powerful, possibly ultimate design of a distillation column with respect to energy saving.
The thermodynamic efficiency of an ideally heat integrated distillation column has been discussed by Nakaiwa (2003) and Liu (2000).

1.2.1 Thermodynamic Efficiency of HIDiC

For a separation process the minimum amount of work required to make a complete separation is given by:

$$W_{\min} = F(\Delta H - T\Delta S) \qquad [1]$$

Where, F is the feed flowrate (kmole/s). ΔH (kJ/mole) and *ΔS* (kJ/mole·K) are the changes in enthalpy and entropy respectively. For an ideal mixture of *n* components the minimum work for separation can be expressed as:

$$W_{\min} = FRT \sum_{i=1}^{n} x_i \ln x_i \qquad [2]$$

Where *R* (kJ/mole·K) is the gas constant, *T*(K) is the mixture temperature and x_i (-) is the mole fraction of component *i* in the feed.
W_{min} is the thermodynamic minimum independent of any particular process. Actual processes operate with finite driving forces that are irreversible and therefore use more energy than the thermodynamic minimum.
For a conventional distillation column, the minimum energy required ($Q_{min,conventional}$) to separate an ideal binary mixture completely, when feed is at its bubble point, can be reduced to (Keller & Humphrey, 1997):

$$Q_{\min,conventional} = F\Delta H_{vap,B}\left[\frac{1}{\alpha_{12}-1} + x_{F1}\right] \qquad [3]$$

where $\Delta H_{vap,\,B}$ (kJ/kg) is the heat of vaporisation of the bottom product, α_{12} (-) is the relative volatility of the components and x_{F1} (-) is the mole fraction of component 1 in the feed.
The maximum thermodynamic efficiency (E_{max}) is defined as the minimum work for separation (W_{min}) divided by the minimum energy required for a separation process (Q_{min}), thus for conventional distillation of an ideal system:

$$E_{\max,conventional} = \frac{W_{\min}}{Q_{\min,conventional}} = \frac{RT\sum_{i=1}^{2} x_i \ln x_i}{\Delta H_{vap,B}\left[\frac{1}{\alpha_{12}-1} + x_{F1}\right]} \qquad [4]$$

According to Eq. [4], the maximum thermodynamic efficiency for a conventional distillation column, appears to be very low, typically below 10%. (Keller & Humphrey 1997, Olujic et al 2003). The relative volatility (α_{12}) is the most important parameter. A relative volatility close to unity leads to a very high reflux requirement and consequently to a high energy requirement in a conventional distillation column. The systems with low relative volatility are therefore the best candidates for energy saving in distillation. As a rule these close boiling systems are mainly binary or nearly binary mixtures.

In the case that a binary mixture is separated in an ideal HIDiC, operating without reboiler and condenser and feed thermal condition is at bubble point, the separation can be completely driven by shaft work of the compressor. The compressor duty is equal to:

$$Q_{HIDiC} = W_{compressor} = VRT_{in}\,\frac{K}{K-1}\left[\left(\frac{P_{out}}{P_{in}}\right)^{\frac{K-1}{K}} - 1\right] \qquad [5]$$

where V (kmole/s) is the molar vapour flow rate leaving the top of the column, K (-) is the ratio of the specific heat at constant pressure to that at constant volume, P_{in} (kPa) is the absolute inlet pressure, in this case the pressure of the stripping section and P_{out} (kPa) is the absolute outlet pressure, which is equal to the pressure of the rectifying section.

So the thermodynamic efficiency of the HIDiC for the separation an ideal system may be expressed as:

$$E_{HIDiC} = \frac{F \cdot RT \sum_{i=1}^{2} x_i \ln x_i}{V \cdot RT_{in} \frac{K}{K-1} \left[\left(\frac{P_{out}}{P_{in}} \right)^{\frac{K-1}{K}} - 1 \right]} \qquad [6]$$

The compressor duty determines the energy efficiency of HIDiC. From Eq. [5] follows, that the compressor duty depends on two variables: the pressure ratio (P_{out}/ P_{in}), and the vapour flow rate entering the compressor (V). This vapour flow rate is also influenced by partial vaporization of the high pressure liquid, which is fed back from the rectifying section. To maximize the thermodynamic efficiency of HIDiC, the compression ratio and vapour load should be minimised.

1.3 Potential energy savings

1.3.1 Partial HIDiC

The ideal HIDiC, in which the separation is completely driven by shaft work of the compressor, and hence is able to operate without a reboiler or condenser, was introduced by Takamatsu et al (1996). The simulation studies by Mah et al (1977, 1980) and Seader et al (1980) were based on a partial HIDiC, where only part of the heat is transferred internally from rectifying to stripping section. Both an external reboiler and condenser are still required. Mah et al (1977) suggests vapour recompression between the top vapour and the bottom reboiler to enhance the thermal economy of the partial HIDiC, which they called Secondary Reflux and Vaporization (SRV) column (Figure 3).

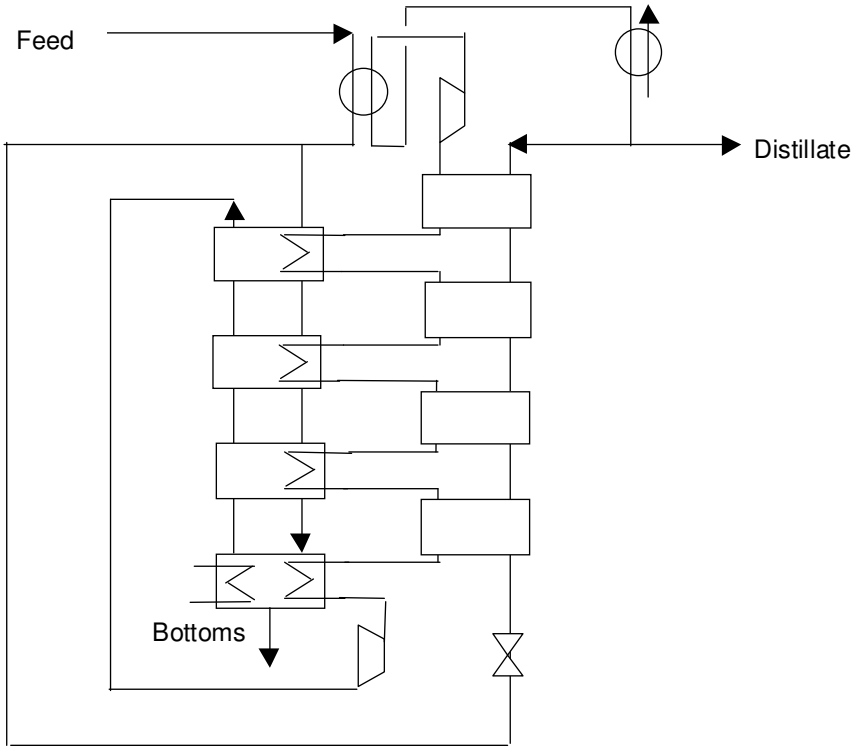

Figure 3: Distillation with Secondary Reflux and Vaporization

Primary reflux is obtained in the conventional way by feeding part of the condensed top product back in the column, the secondary reflux is achieved by internal condensation in the rectifying section due to the heat transfer between rectifying and stripping section. As a consequence two compressors are needed in the concept of Mah et al. The first compressor is the SRV compressor which compresses the vapour leaving the stripping section into the bottom of the rectifying section and the second compressor is the VRC compressor which compresses the vapour leaving the top of the column into the bottom reboiler. The binary mixtures investigated by Mah et al (1977) were ethylene-ethane, propylene-propane and trans-2-butene and cis-2-butene. The system ethylene-ethane appeared to be the most promising application (table 1).

Seader reports energy savings of 56% for the system ethylene-ethane in a partial HIDiC operated without an extra vapour recompression compressor.

Table 1: Reported Energy savings of a partial HIDiC for different model systems

Model system	α_{12}	Pressure ratio P_{out} / P_{in}	Energy requirements partial HIDiC vs conventional		Reference
			Steam consumption	Cooling water requirements	
Ethylene/ethane	1.8	3.0	- 54 %	- 77%	Mah et al. (1977)
			- 56 %	- 75 %	Seader et al. (1980)
Propylene/propane	1.15	2.2	+ 71 %	- 61 %	Mah et al. (1977)
Trans-2-butene/cis-2-butene	1.08	2.4	- 15 %	- 35 %	Mah. et al (1977)

In the simulation studies of the system propylene-propane and of the butene mixture, the column pressures were set so that the conventional distillation condensers required refrigeration and SRV distillation condensers could be operated with cooling water. In industrial practice, however, these separations are not carried out with sub ambient condenser temperatures; which makes these simulation results less relevant from a practical point of view. The temperature difference between stripping and rectifying section was preset to 27,8 ºC, for reasons not made explicit. This temperature difference leads to a too high compression ratio for the propylene/propane case and explains the rise in steam consumption. For the butene mixture this preset temperature difference lead to a compression ratio of 2,4 between the stripper and rectifier. Because of the lower relative volatility of the butene mixture the partial HIDiC is still favourable at this compression ratio.

For the ethylene-ethane mixture both the condenser of the conventional column and that of the SRV-column required refrigeration. The condenser temperatures were respectively 191K and 219K (temperature difference 28 K). For the PP-splitter the temperature difference between the conventional column condenser and the SRV column condenser was 29K and for the butene mixture 26K. The absolute increase of the condenser temperature is approximately the same for the three cases. However, because the operating temperature of the ethane-ethylene column is far below ambient temperature, this temperature increase of the condenser leads to much less energy consumption for the SRV case, when duties are translated to equivalent

steam requirements and equivalent cooling water requirements. In other words: from energy saving point of view it is more interesting to increase the operating temperature of the condenser form –80ºC to –50ºC than to increase it from 5ºC to 35ºC. The main conclusion from Mah et al. was therefore that low operating temperatures are favourable for SRV.
Care must be taken to apply this conclusion to the ideal HIDiC, because an ideal HIDiC doesn't have an external condenser and the effect of operating temperature should be less pronounced.

1.3.2 Ideal HIDiC

Both simulation studies (Nakaiwa et al, 1997, 2001, 2003; Liu et al, 2000) and experimental validation in a HIDiC pilot plant (Naito et al, 2000) were carried out for the ideal HIDiC using the model system benzene/toluene. Energy savings of 60% were reported for this model system (*table 2*). A substantial energy saving is indicated for HIDiC, but the number of stages is increased with a factor 2 to 3, compared to the conventional column.
The main conclusions from the feasibility by Jansens et al, 2001, Olujic et al 2003 were that HIDiC is especially attractive for close boiling mixtures and moreover that HIDiC indeed is able to operate at a lower compression ratio than heat pump as was expected from theory. Benzene-toluene was taken as reference system, however in this case with the same number of stages as the conventional column.

Table 2: Reported Energy savings of a ideal HIDiC for different model systems

Model system	α_{12}	Pressure ratio P_{out} / P_{in}	Energy requirements ideal HIDiC vs conventional	reference
Benzene/toluene	2.4	2.0	- 60%	Nakaiwa et al. (1997, 2000)
		3.0	- 52%	Liu et al. (2000)
		2.1	- 60 %	Jansens et al. (2001)
Ethyl benzene/styrene	1.4	2.3	- 80 %	Jansens et al. (2001)
Propylene/propane	1.15	1.4	- 90 %	Jansens et al. (2001)

From this simulation study, it can be concluded that a HIDiC PP-splitter can save upto 90% of energy, although Mah et al concluded that SRV was not favourable for the separation of propylene-propane. The most important parameter appears to be the compression ratio, which was 1,4 in this simulation study of Jansens et al. and was 2,2 in the work of Mah et al.
It can be concluded (Mah 1977, Jansens et al 2001, Olujic et al 2003, table 1, table 2) that HIDiC is especially feasible for separations with low relative volatility and tight product specifications. In the case of a sub ambient condenser temperature, a heat pump can eliminate the use of refrigerants.

1.4 Design Options for Heat-Integrated Columns

Although HIDiC appears to be very attractive in energy efficiency, it poses great difficulties in realizing an effective configuration. Smart equipment design is the key to industrial implementation of HIDiC. Some design guidelines and proposed configurations are introduced below.

Close boiling separations require large reflux ratios in order to generate enough liquid-vapour contact for a required product purity. In high pressure applications, the column diameter is relatively small, due to the increased density of the vapour. The combination of a large reflux ratio and a small column diameter leads to a large liquid flow rate, relative to the cross sectional area of the distillation column. It is known from industrial practice that

structured packing cannot handle these large liquid loads. For high pressure applications, where structured packing cannot be used, sieve or valve trays are applied (Fischer, 2004). Hence, a HIDiC design should allow *trays as distillation internal.*

From energy saving reason a low temperature difference between rectifying and stripping section is preferred for HIDiC (Olujic et al, 2003; Sun et al, 2003). This leads to a rather large heat transfer area requirements per stage. The HIDiC design should therefore allow for *large heat transfer area* inside the column.

Because of the changing vapour flows in the column a very important pre-requisite for a heat-integrated column design is that it allows *changing area for vapour flow*. This could be done by changing the diameter of stripping section and rectifying section stepwise along the height of the column and/or by a variation of the tray layout.

1.4.1 Inter-coupled Columns

The first one who considered a practical design for an internally heat-integrated distillation column was Haselden (1977). His concept is based on two separate parallel columns interconnected on every distillation tray by piping. The tubular heat transfer bodies are submerged in the liquid/vapour mixture on the tray. This concept is applicable for tray columns and allows flexible, but relative small heat exchange area per stage. A drawback of this design is the large amount of piping between the adjacent columns, which leads to extra investment costs and extra heat losses to the environment.
Beggs (2002) introduces a separate stripping and rectifying section which is not connected at every tray, but uses a single heat transfer loop, which means much less tubing than in the concept of Haselden. An external pump is required for transport of the heat transfer fluid, which is heated along the length of the rectifying section and subsequently cooled along the length of the stripping section. Special heat transfer trays with serpentine ducts inside the tray are used, which implies that total heat transfer area is restricted to the tray surface. Overall heat transfer coefficients between 2,2 and 4,0 kW/m2K are reported for the system water-methanol (Kaeser 2003).

1.4.2 Column with a Partitioning Wall

Seader (1980) filed a patent on a column with two semi-cylindrical sections in which the heat transfer is realised by heat pipes mounted through the wall and the trays of the stripping section. The high internal heat transfer coefficients and negligible pressure drop along the heat pipes permit effective heat transfer over small temperature differences (Beggs, 2002). A special heat pipe

fluid is required, which means introduction of at least one extra component in the process. His concept is applicable for tray columns and allows flexible heat transfer area per stage.
Heat tranfer measurements were done by Seader (1984) in a bench-scale distillation column equipped with heat pipes. The heat pipes were finned copper tubes with water as the working fluid. Pure water was distilled in both the low pressure and the high pressure distillation column. Heat transfer coefficients of 4,7 KW/m^2K ± 22% were reported, based on the bare tube area at temperature driving forces between 12,4 and 22,7ºC. However, one should take into account that heat transfer coefficients for hydrocarbon mixtures will be considerably lower than the values reported for pure water. Moreover a very interesting aspect of intra-column heat transfer is the effect of heat transfer on the mass transfer efficiency of the distillation tray, which was not taken into account in this study.

1.4.3 Concentric Column

Govind and Glenchur (1986, 1987) proposed a concentric HIDiC in which the annular stripping section is configured around the rectifying section. This concentric configuration has in principle ideal properties with respect to heat transfer because the heat in the rectifying section cannot leak to the environment i.e. the heat has no way to go than to the stripping section. This concept was proposed for tray columns, with the heat transfer area restricted to the area of the column wall. Consequently, the heat transfer area is relatively small i.e. insufficient and the design does not allow any flexibility for changing the heat transfer area per stage.

1.4.4 Shell & Tube Column

The problem of limited heat transfer area as encountered in the design of Govind et al is alleviated by adopting a multiple tube in a shell concept as proposed by Aso et al. (1998). In this way, actually a fractionating heat exchanger is constructed rather than a heat-exchanging distillation column. This design exhibits very good heat transfer properties. Like in the concentric column, the heat can only be transferred to the stripping section, which is configured around the tubes. In addition, this design allows a large and flexible heat transfer area. Drawback of the shell-and-tube HIDiC is that it is not suitable for trays in both rectifying (small diameter tubes) and stripping sections (very complex tray design). Proposed HIDiC configurations are illustrated schematically in Figure 5

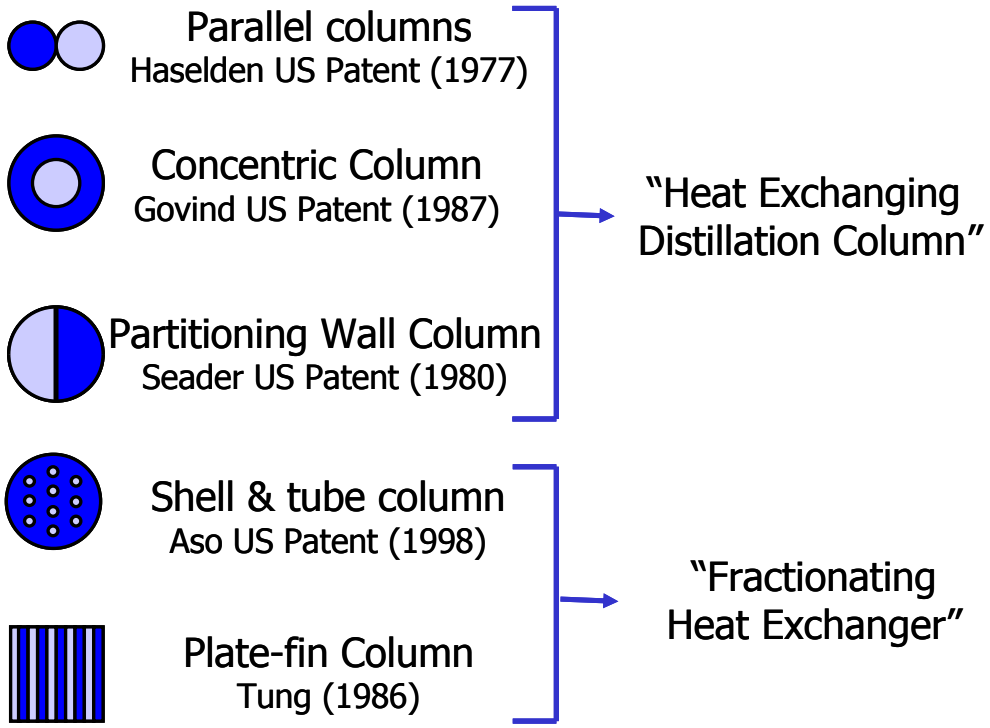

Figure 5: Proposed configurations for a heat-integrated distillation column

1.4.5 Plate heat exchanger Column

Tung (1986) suggested constructing a heat-integrated distillation column from a plate-fin heat exchanger. In a plate-fin device, alternate and adjacent vertical channels serve as strippers and rectifiers. In this design the heat transfer area is large and flexible. By changing the channel and fin dimension, heat transfer area can be changed along the length of the column. Difficulties will arise in the (re)distribution of liquid and vapour over the set of parallel columns.

A model was developed (Tung 1986) to predict the heat transfer rates and influence of internal heat transfer on the separation efficiency of a plate-fin device. The model appeared to be in good agreement with experimental data.

Aitken (1998) filed a patent on a plate-heat exchanger for combined heat and mass transfer in which the space between the vertical plates is equipped with corrugated sheets similar to that of a structured packing.

An alternative idea, which deviates more from current plate fin heat exchanger designs, is to use non-parallel plates with a constant fin spacing. (Hugill 2003, Hugill et al 2005).

1.4.6 Concentric Column with heat panels

De Graauw et al, 2003 filed a patent on a concentric column equipped with heat panels (*figure 6*). Distillation internals can be trays, random or structured packing. Heat transfer bodies can be placed in either the stripping or rectifying section. In the bottom part of the HIDiC where relatively much space is available in the rectifying section, heat transfer bodies are preferentially placed in the rectifying section.

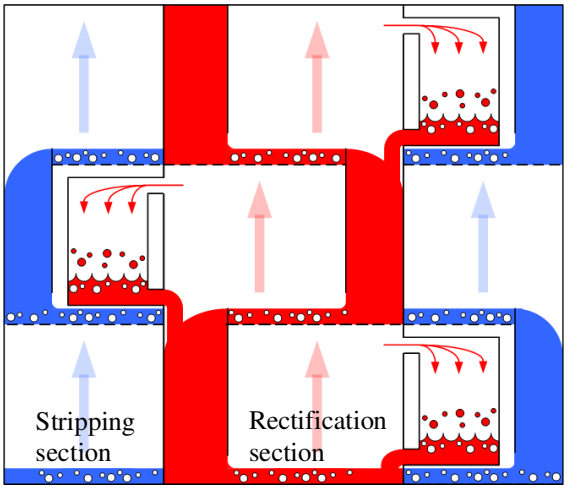

Figure 6: Cross section of concentric HIDiC with heat panels in stripping section

On the other hand in the upper part of the HIDiC heat panels are preferentially placed in the stripping section. In contrast to the heat pipes in the design by Seader (1980), the panels in this concept are in open connection with the other section of the distillation column. Hence panels placed in the stripping section (*figure 6)* are in open connection with the rectifying section so that vapour from the rectifying section can enter the panels, condense inside and liquid can flow back to the rectifying section. On the outer surface of the panels present in the stripping section simultaneous evaporation of liquid will take place. This implies that the panels should be well wetted. In the case, that heat transfer bodies are positioned in the rectifying section *(figure 7*), liquid from the stripping section enters the heat transfer element via the open connection and evaporates partially inside. Vapour will flow back in the stripping section. On the outer surface vapour present in the rectifying section will condense simultaneously.

In this concept heat transfer internals can be placed in either the downcomer or in the active area between two distillation trays, which results in a *large and flexible heat transfer area*. A strong advantage of this concept is that it allows the designer to exclude certain trays with low, or negative temperature driving forces, from the heat transfer process i.e. no heat panels are installed on

these trays. The heat transfer panels should be wetted by froth and entrainment from a tray.

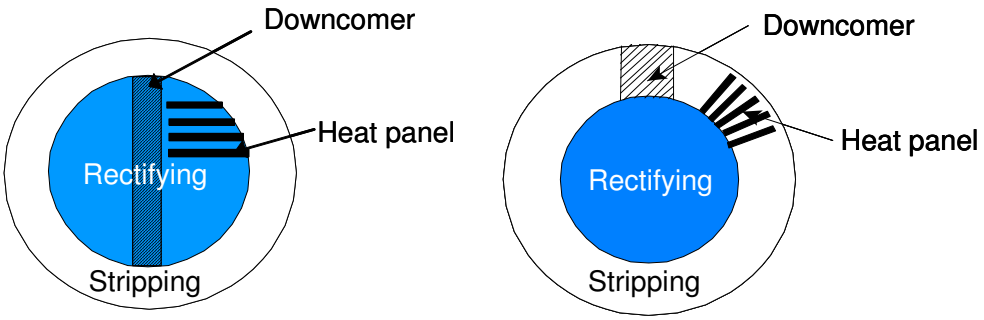

Figure 7: Placement of heat transfer panels in rectifying or stripping section

1.5 Scope of Research

HIDiC is probably the ultimate concept with respect to energy saving potential in distillation, because it combines the advantages of vapour recompression and quasi-reversible operation of a diabatic distillation column. This study was carried out in a research consortium granted by the Dutch Ministry of Economic Affairs (grant EETK10125), in cooperation with the Energy research Centre of the Netherlands (ECN), ABB-Lummus, BP, DSM, SHELL, and Sulzer Chemtech. The scope of the EET-project was to develop a technically feasible HIDiC and to determine for which industrial applications HIDiC could be a viable technology both from energy saving and economic point of view.

The aim of this PhD study project at the TU Delft was to design and to develop an industrially viable internal Heat Integrated Distillation Column, which is constructed as a concentric column using trays as separation internals which are equipped with heat panels.

1.5.1 Technical & Scientific Challenges

As the key parameter in HIDiC design is the overall heat transfer coefficient inside the distillation column, a pilot plant was built to prove the principle of this method of internal heat transfer, to determine the overall heat transfer coefficient at relevant scale and to study the influence of process conditions on the heat transfer performance of HIDiC.
The main task of the distillation column, namely separation of a feed mixture, should not be violated, the second objective of this work was to study the influence of the heat transfer panels on the tray hydraulics and the separation

efficiency of the distillation column and to determine the mass transfer performance of an annular sieve tray, compared to a conventional cross flow sieve tray.
The third objective of this work was to determine the influence of process parameters, column configuration and the degree in which the stripping section and rectifying section are thermally integrated on the energy savings and economical feasibility of HIDiC compared to conventional vapour recompression technology for various industrially important separations.

1.5.2 Approach

Since very little is known from literature about the heat transfer coefficient inside an operating distillation column, the overall heat transfer coefficient should be modeled but also determined experimentally.
Only the overall heat transfer coefficient can be measured but it is obviously necessary to distinguish between the condensation side heat transfer coefficient and the heat transfer coefficient of the evaporation side. The experimental approach was as follows:

1) Measure the overall heat transfer coefficient of a set of heat panels equipped with a liquid distributor, using saturated steam as heating medium. Since the heat transfer coefficient of condensing steam is known from literature, the heat transfer coefficient of the evaporation side can be calculated.
2) Measure the overall heat transfer coefficient of the same set of heat transfer panels, equipped with the same liquid distributor, using hydrocarbon vapour as heating medium. Because the outside heat transfer coefficient is the same as in the previous experiments, the condensation side heat transfer coefficient of the hydrocarbon mixture can be calculated.
3) Measure the overall heat transfer coefficient of the same set of panels placed on the active area of an operating sieve tray using the hydrocarbon model mixture as heating medium. The condensation side coefficient will not change compared to the previous experiments. Consequently the outside heat transfer coefficient of the froth present on the distillation tray can be calculated.

Simulation studies indicated that HIDiC is most favourable economically at low driving forces for heat transfer, leading to a large internal heat transfer area and consequently to a tray which is densely packed with heat transfer panels. These panels will most likely influence the tray hydraulics and therefore the separation efficiency. The experimental approach with respect to the mass transfer performance of HIDiC is given below:

1) Measure the tray efficiency of an annular tray using a well known model system for distillation in order to compare the performance with a conventional cross flow sieve tray.
2) Measure the tray efficiency of the annular tray, which is densely packed with “cold” heat transfer panels. The panels are not heated to determine the effect of the presence of the panels on tray hydraulics and separation efficiency.
3) Measure the tray efficiency of the annular tray, with the same but now “hot” heat transfer panels. The heat transfer panels are heated with hydrocarbon vapour to determine the enhancing effect of the preferential evaporation of the light component on the tray efficiency.

1.5.3 Outline of Thesis

Chapter 2 describes the development and operation of the experimental facilities.

In Chapter 3, the heat transfer mechanisms playing a role are theoretically evaluated. Attention is given to pressure drop in the vapour entrance of the heat transfer panels. Experimental heat transfer coefficients are evaluated and compared to model predictions for both heat panels placed in the downcomer and heat panels placed on the active tray area.

Chapter 4 describes the mass transfer model which was used to predict the tray efficiency. Experimentally obtained tray efficiencies of the annular tray used in this study are discussed and compared to literature results of a conventional cross flow sieve tray. The influence of heat panels on tray efficiency is modelled and validated with experimental results.

In chapter 5, the opportunities of the proposed HIDiC technology for the separation of propylene-propane are presented. Actual plant data of a large stand alone vapour recompression column are used for the techno-economic evaluation. The asymmetric feed stage location in an industrial PP-splitter, leads to several possibilities for heat integration of the rectifying and stripping section. The way in which the stripping section and rectifying section are thermally integrated appears to have a strong influence on energy efficiency.

In Chapter 6 the technical and economical feasibility of HIDiC for other industrial model systems is evaluated. The design of the HIDiC PP-splitter is further optimised by considering a constant heat transfer area per stage instead of a constant heat transfer duty per stage. Optimized HIDiC designs are presented for the separation of methanol-water and ethylbenzene-styrene. The energy efficiency and total annual costs are compared with those of state of the art commercial columns.

Chapter 7 introduces opportunities for further development of HIDiC technology.

Appendix 1 presents the possible decrease of carbon dioxide emissions as a result of the implementation of HIDiC for the separation of close boiling mixtures.

1.6 Nomenclature

E_{max}	maximum thermodynamic efficiency (-)
F	Feed flow rate (mol/s)
H	Enthalpy (J/mol)
P_{in}	inlet pressure of compressor, in this case equal to pressure of stripping section (kPa)
P_{out}	discharge pressure of compressor, in this case equal to pressure of rectifying section (kPa)
Q_{min}	minimum energy required (J/s)
R	gas constant (J/mol·K)
S	Entropy (J/mol·K)
T	temperature (K)
V	vapour flow rate through compressor (mol/s)
$W_{compressor}$	compressor duty (J/s)
W_{min}	minimum amount of work to make a complete separation (J/s)
x_i	mole fraction of component i (-)
α_{12}	relative volatility of components 1 and 2 (-)
$\Delta H_{vap,B}$	enthalpy of vaporization of the bottom product (J/mol)
K	the ratio of the specific heat at constant pressure to that at constant volume (-)

1.7 References

Aguirre, P., Espinosa, J., Tarifa, E. and Scenna, N., *Ind. Eng Chem Res*, **36**: 4882-4893 (1997)

Aitken, W.H., Apparatus for combined heat and mass transfer, U.S. Patent 5,722,258 (1998)

Aso, K., Takamatsu, T. and Nakaiwa, M., Heat Integrated Distillation Column, U.S. Patent 5,873,047 (1998)

Beggs, S. Meng project report, University of Edinburgh UK, (2002)

Brugma, A.J., Dutch Patent No. 41.850 (1937)

Brugma, A.J., US Patent 2,295,256 (1942)

De Graauw, J., Steenbakker, M.J., de Rijke, A., Olujic, Z. and Jansens, P.J., Distillation column with heat integration, EP Patent Application (2002)

De Graauw, J., Steenbakker, M.J., de Rijke, A., Olujic, Z. and Jansens, P.J., Distillation column with heat integration, Dutch Patent P56921NL00 (2003)

De Koeijer, G.M., Kjelstrup, S., Van der Kooij, H., Gross, B., Knoche, K.F., and Andersen, T.R., Positioning heat exchangers in binary tray distillation using isoforce operation, *Energy Conversion and Managment*, **43**, 1571-1581 (2002)

De Swaan Arons, J. and van der Kooi H., The thermodynamic analysis of distillation-some parallels with living systems, *Proceedings of ECOS*, Tokyo Institute of Technology, Tokyo: **3**: 0-11 (1999)

Fischer, M and Tonon, Loris, VGPlus Trays: Improving the Proven, *Sulzer Technical Review*, (1), 12-14 (2004)

Fitzmorris, R.E. and Mah, R.S.H., Improving Distilation Column Design using Thermodynamic Availability Analysis, *AIChE J,* **26**, 265-273 (1980)

Flower, J.R., Jackson, R., *Trans Inst Chem Eng,* **42**, 249-258, (1964)

Freshwater, D.C., The Heat Pump in Multicomponent Distillation *Brit. Chem. Eng..,* **6**, . 388-391 (1961)

Freshwater, D.C., Thermal Economy in Distillation, *Trans. Inst. Chem. Eng.,* **29**, 149-160 (1951)
Govind, R., Distillation Column and Process, U.S. Patent 4,615,770 (1986)

Gadalla, M., De Rijke, A., Olujic, Z. and Jansens, P.J., A Thermo-Hydraulic Approach to Conceptual Design of an Internally Heat Integrated Distilallation Column (HIDiC), *article in press*

Glenchur, T. and Govind, R., Study on a continuous Heat Integrated Distillation Column, *Separation Science and Technology*, **22**(12), 2323-2338 (1987)

Govind, R., Dual Distillation Columns, U.S. Patent 4,681,661 (1987)

Haselden, G.G., An approach to minimum power consumption in low temperature gas separation, *Trans. Instn. Chem Engrs*, **36**, 122-132 (1958)

Haselden, G.G., Distillation Processes and Apparatus, U.S. Patent 4,025,398 (1977)

Halvorsen, I.J. and Skogestad, S., Optimal Operation of Peltyuk Distillation: Steady State Behaviour, *J. Process Control*, **9**, 407-424 (1999)

Hugill, J.A., System for stripping and rectifying a fluid mixture. International patent application, WO 03/011418 A1, (2003)

Hugill, J.A., and Van Dorst, E.M., Design of a Heat Integrated Distillation Column based on a Plate Fin Heat Exchanger, Sustainable (Bio)Chemical Process Technology, incorporating the 6th international conference on Process Intensification, Delft, The Netherlands, eds P.J. Jansens, A.I. Stankiewicz and A, Green, 33-46 September 27-29, (2005)

Humphrey, J.L., Seibert, A.F. and Koort, R.A.*,* Separation technologies advances and priorities, Final Report for US Department of Energy, Office of Industrial Technologiest, Washington DC*,* (1991)

Jansens, P.J ., Fahkri, F., de Graauw. J. and Olujic, Z., Energy saving potential of a heat integrated distillation column, *Proceedings of the Topical Distillation Symposium*, AIChE 2001 Spring Meeting Houston, 22-26 April, 19-25 (2001)

Kaeser, M. and Pritchard, C.L., Heat Transfer at the Surface of Sieve Trays, *Proceedings of the UK Heat Transfer 2003 Session*, (2003)

Keller G.E. and Humphrey, J.L., Separation Process Technology, McGrawHill, New York (1997)

Kjelstrup, R.S., Sauar, E., Lien, K.M., and Hafskjold, B., *Ind Eng Chem Res*, **34**: 3001-3007 (1995)

Lang, L., Dynamic Behaviour and Operational Aspects of Heat-Integrated Distillation Processes, *Chem. Eng. Technol.,* **19**, 498-506 (1996)

Le Goff, P., Cachot, T. and Rivero, R., Exergy Analysis of Distillation Processes, *Chem. Eng. Technol.*, **19**, 478-485 (1996)

Linnhoff, B, Pinch Analysis, A State of the Art Review, *Trans. I Chem E*, **71,** 503-515 (1993)

Liu, X.G. and Qian, J.X., *Chem Eng Technol*, **23**: 235-241 (2000)

Mah, R.S., Nicholas, J.J. and Wodnik, R.B., Distillation with Secondary Reflux and Vaporization, a comparative evaluation, *AIChE J*, **23** 651-658 (1977)

Naito, K., Nakaiwa, M., Huang, K., Endo, A., Aso, K., Nakanishi, T., Nakamura, T., Noda, H. and Takamatsu, T., Operation of a bench-scale ideal heat-

integrated distillation column (HIDiC): an experimental study, *Computers and Chemical Engineering*, **24**, 495-499 (2000)

Nakaiwa, M., Huang, K., Naito, K., Endo, A., Akiya, T., Nakane, T. and Takamatsu, T., Parameter analysis and optimization of ideal heat-integrated distillation columns, *Computers and Chemical Engineering*, **25**, 737-744 (2001)

Nakaiwa, M., Huang, K., Owa, M., Akiya, T., Nakane, T., Sato, M. and Takamatsu, T., Energy savings in Heat-Integrated distillation columns, *Energy* **22**(6), 621-625 (1997)

Nakaiwa, M., Internally Heat Integrated Distillation Columns: a review, *Trans IChemE,* **81** Part A, (2003)

Niang, M.B., Cachot, T. and Le Goff, P., *Proceedings of Second Law Thermodynamics Workshop*, 333-338 (1995)

Null, H.R., *Chem. Eng. Progress*, **78**, pp. 58-64 (1976)

Olujic, Z., Fakhri, F., de Rijke, A., de Graauw, J. and Jansens, P.J., Internal heat integration – the key to an energy conserving distillation column, *J Chem Technol Biotechnol*, **78**, 241-248 (2003)

Petlyuk, F.B., Platanov, V.M. and Slavinskii, D.M., Thermodynamically Optimal Method for Separating Multicomponent Mixtures, *Intl. Chem. Eng.,* **5** (3), 555-561 (1965)

Rivera-Ortega P., Picon-Nunez, M., Torres-Reyes, E. and Gallegos-Munoz, A., *Appl Therm Eng*, **19**: 819-829

Rivero, R., Cachot, T., Ramadane, A., Le Goff, P., Analysis of Thermal and Energy Systems, *Proceedings of the International Conference, Athens, Greece, June 3-6, 1991*: 129-140 (1991)

Rivero, R., Exergy simulation and optimization of adiabatic and diabatic binary distillation, *Energy*, **26**, 561-593 (2001)

Schaller, M., Hoffmann, K.H., Rivero, R., Andresen B., Salamon, P., The influence of Heat Transfer Irreversibilities on the Optimal Performance of Diabatic Distillation Columns, *J. Non-Equilib. Thermodyn.*, **27**(3), 257-269

Schultz, M.A., Stewart, D.G., Harris, J.M., Rosenblum, S.P., Shakur, M.S. and O'Brien, D.E., Reduce Costs with Dividing Wall Columns, *Chem. Eng. Progress*, **98** (5), 64-71 (2002)

Seader, J.D., Continuous Distillation Apparatus and Method, U.S. Patent 4,234,391 (1980)

Seader, J.D. and Baer, S.C., Continuous Distillation Apparatus and Method, final report, University of Utah, Salt Lake City (1984)

Shah, P.B., Squeeze more out of Complex Columns, *Chem. Eng. Progress*, **98** (7), 46-55

Smith, R., *Chemical Process Design* (McGraw-Hill New York), pp. 341-354 (1995)

Sulzer Chemtech, Distillation and Heat Pump Technology, Brochure 22.47.06.40-V.91-100

Sun,. L, de Rijke, A., Olujic Z. and Jansens, P.J. paper presented at the *Process Innovation and Intensification Conference*, 13-15 oktober 2003, Maastricht, The Netherlands

Takamatsu, T., Nakaiwa, M., and Nakanishi, T., *Journal of Chemical Engineering Japan*, **29**: 344 (1996)

Tondeur, D., and Kvaalen, E., Equipartition of Entropy-production. An optimalitility criterion for transfer and separation processes, *Ind. Engng Chem Res,* **26**, 50-56 (1987)

Tung, H.H., Davis, J.F. and Mah, R.S.H., Fractionating Condensation and Evaporation in Plate-Fin Devices, *AIChE Journal*, **32**(7) 1116-1124 (1986)

Villermaux, J., Future Challenges for Basic Research in Chemical Engineering, *Chemical Engineering Science*, **48**(14): 2525-2535 (1993)

Wolff, E.A. and Skogestad, S., Operation of Integrated Three Product (Petlyuk) Columns, *Ind. Eng. Chem. Res.,* **34**, 2094-2103 (1995)

Wright R.O., U.S. Patent 2,471,134, (1949)

Chapter 2:

Experimental Facilities

2.1 Introduction

As the aim of this research programme was to develop an industrially viable heat integrated distillation column, two experimental set-ups were designed and built in order to develop and validate predictive models for heat and mass transfer efficiency, respectively and to demonstrate the technical feasibility of a patented, concentric tray column with heat panels placed in the stripping section.

The first setup was a bench-scale plant specifically developed to determine the outside heat transfer coefficient of an evaporating falling liquid film distributed along the heat transfer panels used in this study.

The second experimental setup, a pilot scale concentric distillation column was designed and constructed to determine the overall heat transfer coefficient of heat transfer panels placed on the active tray area or in the downcomer of an operating sieve tray, to study the influence of the annular tray geometry on the tray efficiency and to determine the effect of the heat transfer panels on tray hydraulics and on tray efficiency.

The patent of De Graauw et al (1) allows for different types of internal heat exchangers both of tubular or plate design. In our study so-called heat panels were used. (Figure 1 a and c).

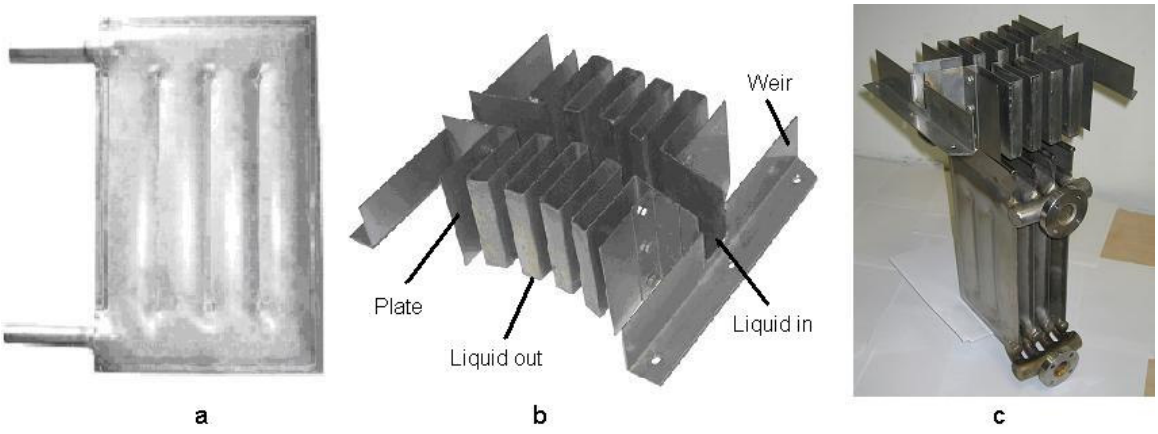

Figure 1: a) Heat panel, b) liquid distributor with splash baffle, c) small set of heat panels used in downcomer experiments

These panels consist of two stainless steel plates, which are laser-weld together and reformed under elevated temperature and high pressure in order to form channels for vapour/liquid flow. The strong advantage of this type of heat exchangers is the flexibility in panel dimensions and channel layout. Moreover these heat exchangers have proven their robustness in process industry e.g. as plate heat exchangers or as column top condensers and are cheap to manufacture, compared to tubular heat exchangers. Finally it was

assumed that due to the smooth shape these panels will have less influence on the tray hydraulics, when placed parallel to the flowing froth present on a sieve tray, than heat exchangers of a tubular design.

2.2 Heat panel test setup

Figure 2 shows the flow sheet of the heat panel test setup. As the main components of the setup were constructed of glass, the setup is operated atmospherically for safety reasons. Single or multiple heat transfer panels can be placed in vessel (VE-1) A trough type liquid distributor with 3 mm holes in the bottom (pitch 25 mm) is placed on top of the heat transfer panel to create a uniform falling liquid film. (Figure 1). The panel dimensions are 200 mm length and 350 mm height. The dimensions of the channels are 60 mm x 13 mm. Stainless steel 316L sheets with a thickness of 1,5 mm are used as construction material.

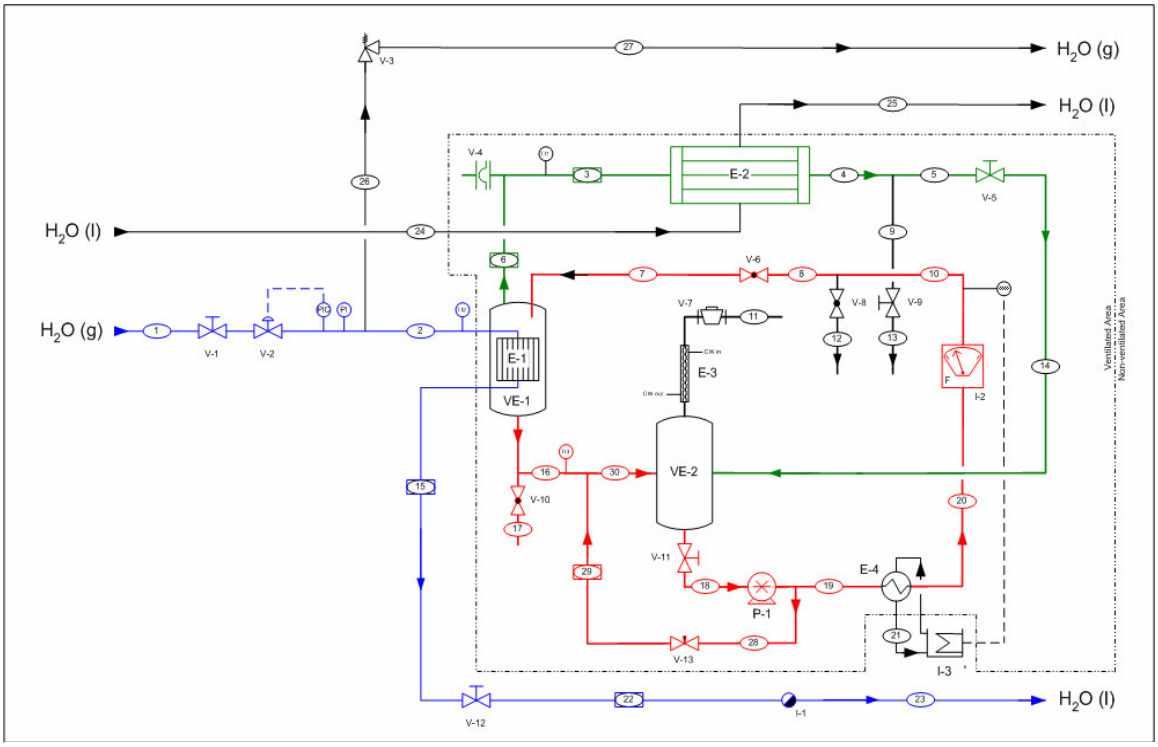

Figure 2: Flow sheet of Heat panel test setup

The model system is either pure (n)-heptane or a mixture of cyclohexane/(n)heptane as this is a well known mixture in distillation literature and also the boiling temperature of (n)-heptane is around 98ºC, allowing to use saturated steam as the heat source. Inside the heat panel (E-1) steam will condensate thereby evaporating the liquid film on the outside of the panel. The steam temperature can be controlled by changing the vapour pressure of the steam. The pressure can be changed with an accuracy of 0.01 bar changing from 1 tot 4 bar absolute pressure. The temperature range

associated with the pressure range is 100-134 ℃. The steam is fed to the panel at the upper side of the panel and the condensate leaves the panel at the bottom. A condensate trap prevents vapour to pass through the condensate exit. As flows are small, the amount of condensate is measured with a laboratory balance. The hydrocarbon liquid is pumped from a buffer vessel (VE-2) using a rotary pump (P-1) with a maximum capacity of 500 l/hr. The speed of the pump is controlled using a frequency controller. The temperature of the liquid inside the buffer vessel will be below the saturation temperature of the liquid.

The hydrocarbon liquid is pumped from a buffer vessel (VE-2) using a rotary pump (P-1) with a maximum capacity of 500 l/hr. The speed of the pump is controlled using a frequency controller. The temperature of the liquid inside the buffer vessel will be below the saturation temperature of the liquid. A coiled double pipe countercurrent heat exchanger is used to heat the liquid to saturation temperature. The temperature of the process liquid is controlled by a thermostatic bath filled with mineral heating oil.

The saturated liquid is fed to the liquid distributor placed just above the panel. This liquid film evaporates partly on the panel surface. The remaining liquid falls from the panel and is collected in the bottom of the vessel (VE-1) from where it is transported back to the buffer vessel.

Figure 3: Heat Panel Test Setup

The vapour formed on the panel will be condensed in glass spiral condensers (E-2). The condensers are cooled using tap water. The condensed hydrocarbon vapour falls down into the buffer vessel from which the liquid is pumped back into the cycle.
To make it possible to determine the separating performance of the heat panels, two sample points are contained in the setup. The first one, to determine the feed composition, is located in the feed line just before the heat panel. Furthermore, a sample of the liquid falling from the heat panel can be taken.

2.3 HIDiC pilot plant

An annular sieve tray column was built in parallel to the existing total reflux distillation pilot plant present at TU Delft (figure 4, figure 5).The column data are summarized in table 1.

Table 1: Distillation pilot plant data

Diameter outer column	800 mm
Diameter inner column	300 mm
Number of trays	3
Tray spacing	500 mm
Hole size	10 mm
Hole pitch	30 mm
Tray area	0.38 m^2
Downcomer area	0.08 m^2

The setup comprises the following main parts: the distillation column itself, a steam operated falling film reboiler with an area of 19.5 m^2, a condenser with an area of 40 m^2 and a buffer vessel of 900 liters. A number of pumps is used to circulate the liquid flows through the process. Construction material of the setup is stainless steel. Al major equipment and piping is insulated to prevent heat loss to the environment. Temperature and pressure are monitored at several locations in the process. A computerized control system allows for easy operation and data acquisition. The column is operated with a mixture of cyclohexane/(n)-heptane.

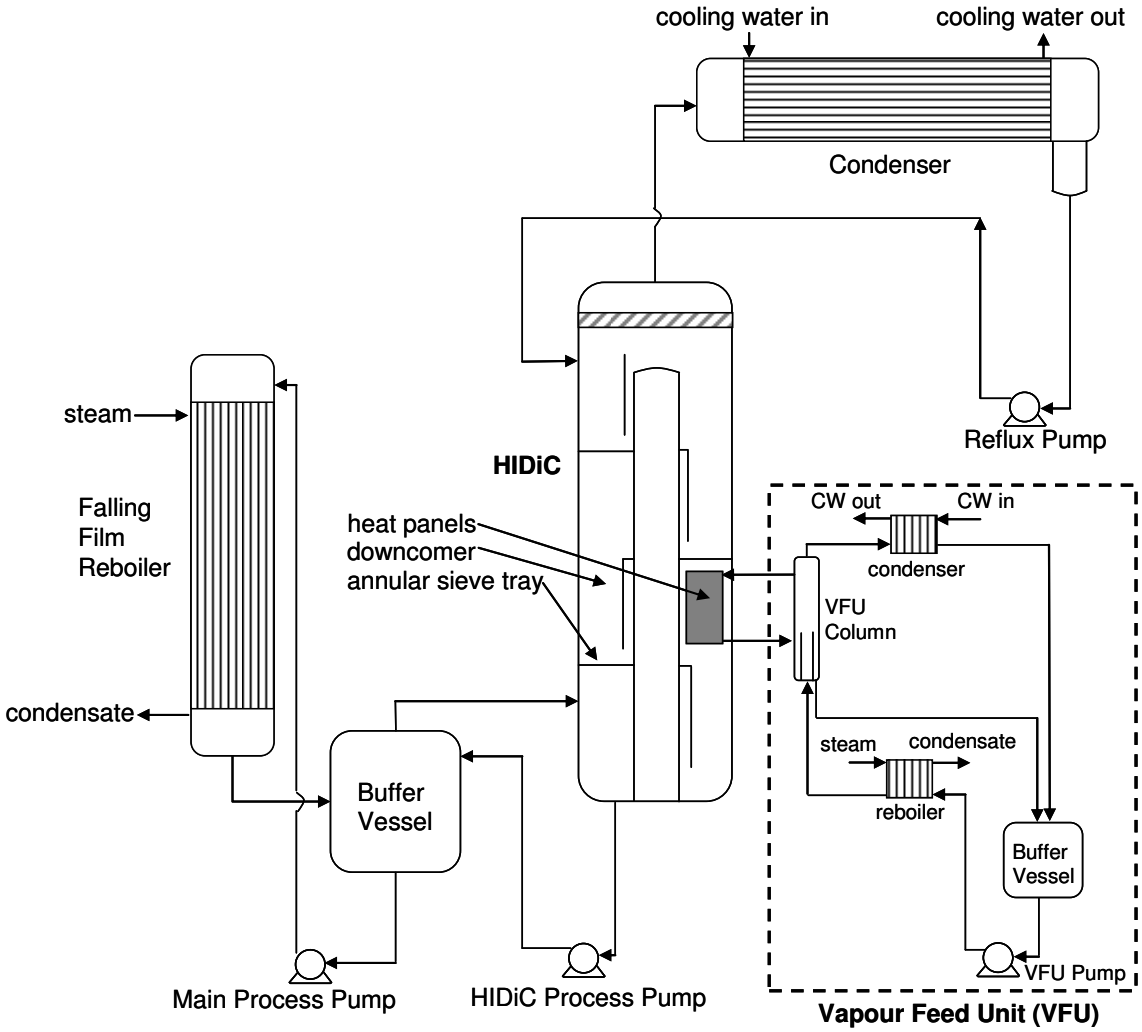

Figure 4: Process Flow Diagram HIDiC Pilot Plant

Figure 5: Annular Sieve Tray Distillation Column

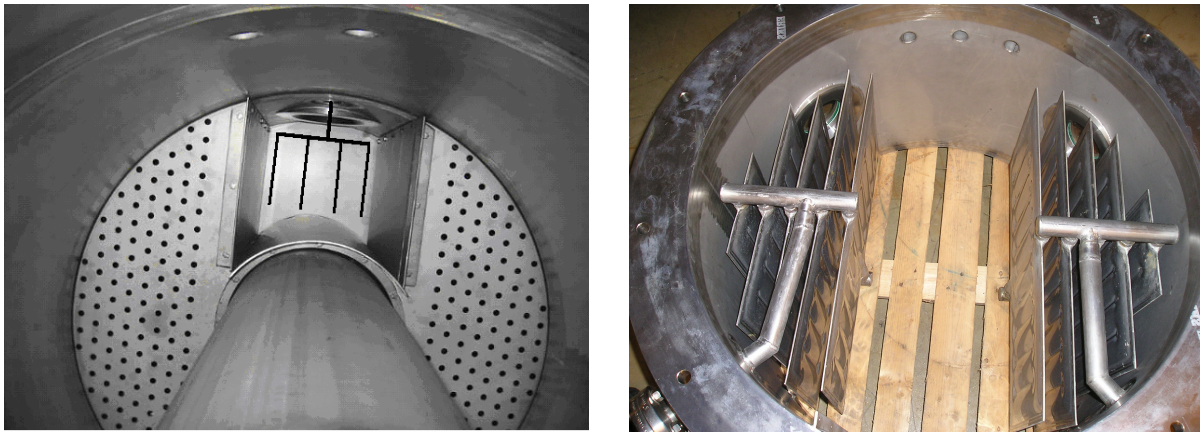

a **b**

Figure 6: a) placement of heat transfer panels in downcomer b) layout of large set of heat panels on tray active area

Tray temperatures and pressure drop of the center tray were measured. Heat panels can be placed in either the downcomer (Figure 1, 6) or on the active tray area (Figure 6). Samples can be taken just after the condenser and from the bottom of the column in order to determine the separation efficiency. Flows are measured with coreolis mass flow meters.
In order to feed the heat panels with hydrocarbon vapour, a separate so-called vapour feed unit was designed and built. A process flow diagram of this setup is shown in Figure 8. Liquid is pumped from the 120 l liquid vessel to the reboiler by the main process pump. The reboiler is a plate type heat exchanger, in which the feed is evaporated using steam. The hydrocarbon vapour is slightly overheated to prevent condensation before the vapour has entered the heat panels. Vapour leaving the reboiler flows to the vapour vessel, which simulates the rectifying section of a HIDiC.

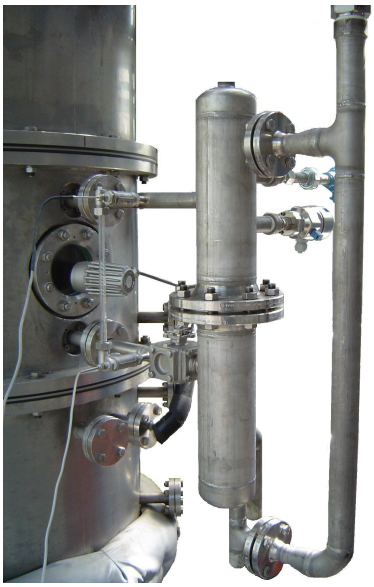

Figure 7: Vapour Feed Unit

The vapour vessel is a column with a height of 0.6 m and diameter of 0.112 m. Vapour enters the vessel through a distributor to create a uniform flow. The vapour vessel is connected to a set of heat panels placed in the HIDiC. Part of the vapour flowing upwards through the vapour vessel will enter the panels, condense inside and flow back to the liquid vessel. The condenser is a plate type heat exchanger, cooled with cooling water from the same system that is used for the distillation column condenser. From the condenser the liquid flows back to the storage vessel. The amount of condensate is measured with a coreolis mass flow meter. A small liquid level is maintained in the vapour vessel with the aid of a control valve in order to ensure free outflow of condensate and moreover to prevent vapour from entering the mass flow

meter. The pressure of the setup can be controlled by the cooling water flow to the condenser.

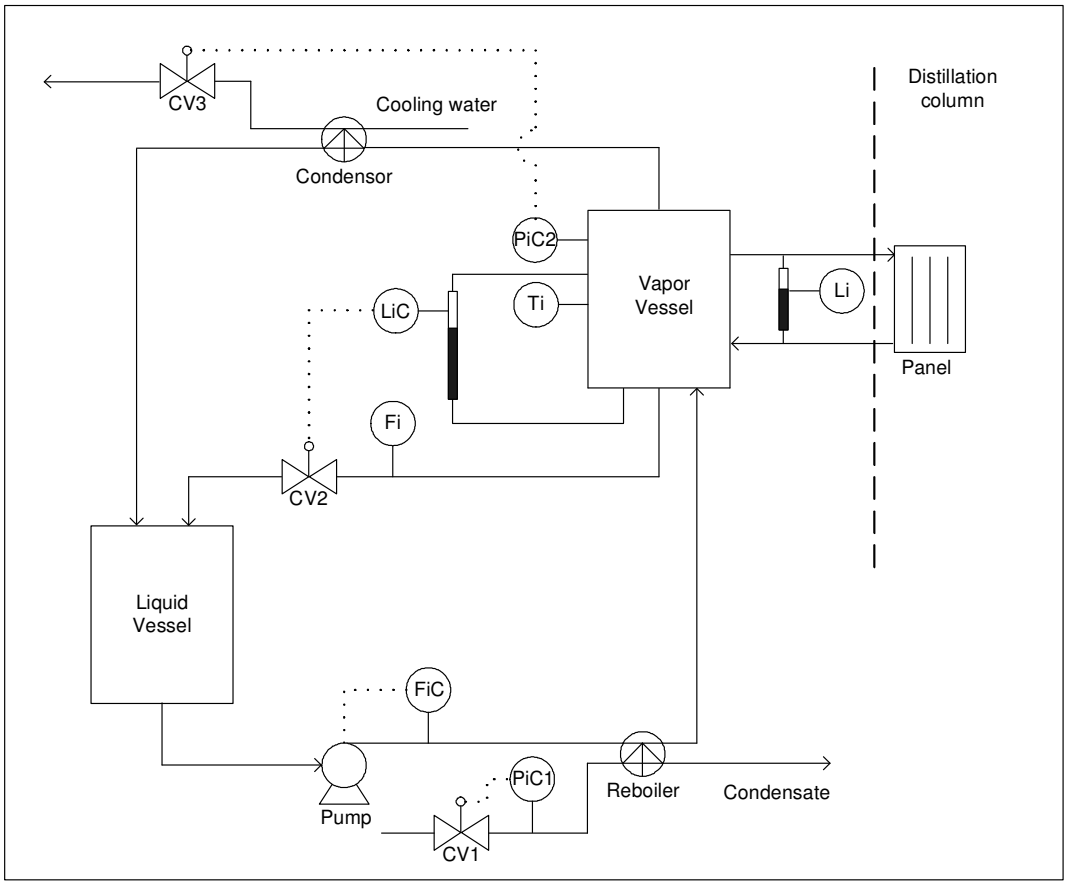

Figure 8: Process Flow Diagram of Vapour Feed Unit

2.4 Analysis

The composition of the samples was determined with a Gas Chromatograph, equipped with a Chrompack 9002 column, with FID detector. The column used was 25 mm in length with a film of Cp-sil-5Cb. The mass fraction analysis was within an accuracy of 0,4 %.

2.5 References

(1) De Graauw, J., Steenbakker, M.J., de Rijke, A., Olujic, Z. and Jansens, P.J., Distillation column with heat integration, World Patent WO03061802 (2003)

(2) VDI-Wärmeatlas, 7. Auflage, 1994, Ja 1-8

(3) Olujic, Z., Fakhri, F., de Rijke, A., de Graauw, J. and Jansens, P.J., Internal heat integration – the key to an energy conserving distillation column, *J Chem Technol Biotechnol*, **78**, 241-248 (2003)

Chapter 3:

Heat Transfer Characteristics of a Concentric Heat Integrated Distillation Column

Abstract

An internally heat integrated distillation column, HIDiC, offers maximum energy saving potential for difficult, energy intensive separations, such as a propylene-propane. A novel type of HIDiC was developed, namely a concentric distillation column in which a low pressure annular stripping section is configured around a high pressure rectifying section. Heat transfer panels are placed either in the downcomers or on the active area of the distillation trays to provide a flexible and sufficiently large amount of heat transfer area. Experimental results are presented and compared to model predictions. The overall heat transfer coefficient was found to depend strongly on temperature difference between rectification and stripping section due to laminar flow conditions at the condensation side. Laminar film condensation inside the panels appeared to be the rate determining step in the heat transfer process, leading to the same values for the overall heat transfer coefficient for both the downcomer and tray layout. Overall heat transfer coefficients ranged from 700 to 1500 W/m^2K for the temperature range which is of practical interest to HIDiC.

3.1 Introduction

An internally Heat Integrated Distillation Column (HIDiC) combines advantages of a vapour recompression column and diabatic distillation and is therefore probably the ultimate concept for energy saving in a single distillation column (Chapter 1). Although the HIDiC concept (*Figure 1*) is known since the 1970s (1-3), it appeared to be a great challenge to find an effective column design for HIDiC (4-7, Chapter 1).

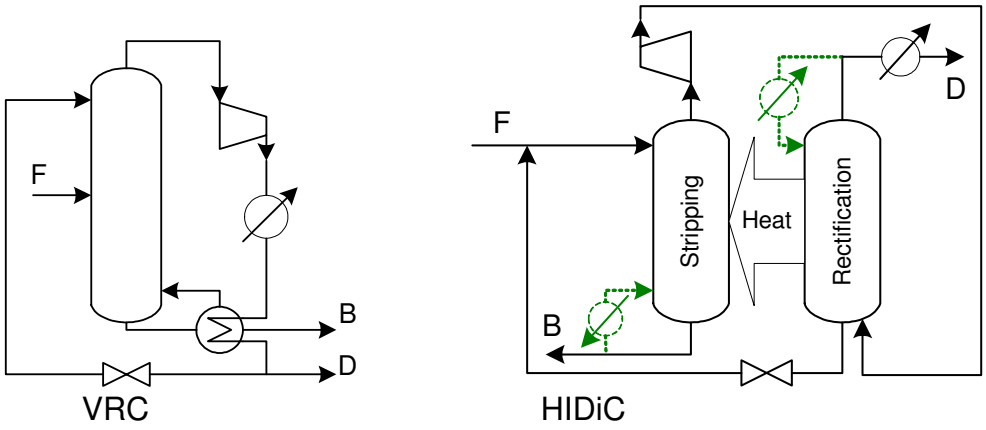

Figure 1: Schematic representation of the vapour recompression column and the HIDiC

The column concept for HIDiC introduced by de Graauw et al (8) is based on a tray distillation column. Simulation studies proved that HIDiC is especially favourable for the separation of close boiling mixtures, however a lot of internal heat transfer area is required (9). It is known from industrial practice that close boiling mixtures are separated in tray columns as structured or random packing cannot handle efficiently the large liquid loads in these applications. Therefore a tray appeared to be the preferred column internal for a HIDiC. In the proposed HIDiC design, which is basically a concentric distillation column, an annular stripping section is configured around the rectifying section. Heat transfer area is provided by heat transfer panels which are placed in the stripping section. Panels can be placed in either the downcomer or on the active tray area (*figure 2*).

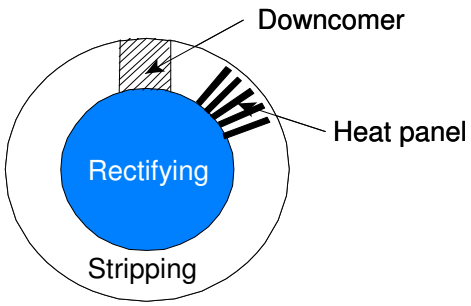

Figure 2: Placement of heat transfer panels in stripping section

Vapour from the rectifying section should enter the panels condense inside and the condensate will flow back into the rectifying section. On the outer surface of the panels simultaneous evaporation of liquid will take place in the stripping section. It should be noted here that the driving force for vapour to enter the panels must be delivered by the condensation process itself, as there is virtually no pressure difference between the inlet and outlet of the panels. Although pressure drop calculations show that the condensation process should start spontaneously, it is clear that this should be validated experimentally to prove the principle of this way of heat transfer between stripping and rectifying section. Moreover very little is known of heat transfer characteristics of chosen panels in the froth regime of an operating distillation tray.

Heat transfer measurements were done by Seader (10) in a bench-scale distillation column equipped with heat pipes. The heat pipes were finned copper tubes with water as the working fluid. Pure water was distilled in both the low pressure and the high pressure distillation column. Heat transfer coefficients of 4700 W/m^2K ± 22% were reported, based on the bare tube area at temperature differences between 12,4 and 22,7ºC. It should be noted here that simulation studies show that HIDiC is only feasible for low driving forces for heat transfer, i.e: between 2 to 10 ºC (2, 9). Also, one should take into account that heat transfer coefficients for hydrocarbon mixtures will be considerably lower than the values reported for pure water. Moreover a very interesting aspect of intra-column heat transfer is the effect of heat transfer bodies on the mass transfer efficiency of the distillation tray, which was not taken into account in the study of Seader (see Chapter 4).

Experimental values for both heat transfer coefficient and Murphree tray efficiency for a laboratory scale, tray deck heated sieve tray column were reported by Kaiser et al (11) for the model system methanol-water.

The overall heat transfer coefficient should be determined experimentally for a given HIDiC configuration. The objective of this paper is to describe the experimental effort and obtained results on overall heat transfer coefficient associated with the operation of an annular sieve tray equipped with heat panels. The obtained experimental data is used to validate a predictive model, which can be used to make a reliable estimate for the purpose of design of an industrial scale HIDiC.

3.2. Experimental

The type of heat transfer internal to be installed inside a distillation column is very important and will strongly influence the feasibility of HIDiC. In the present study so-called heat panels were used as shown in Figure 3. These commercially manufactured panels consist of two stainless steel plates, which are laser-weld together and reformed under elevated temperature and high pressure in order to form channels for vapour/liquid flow. The strong advantage of this type of heat exchangers is the flexibility in panel dimensions and channel layout. Moreover these heat exchangers have proven their robustness in process industry e.g. as plate heat exchangers or as column top condensers and are relatively cheap to manufacture.

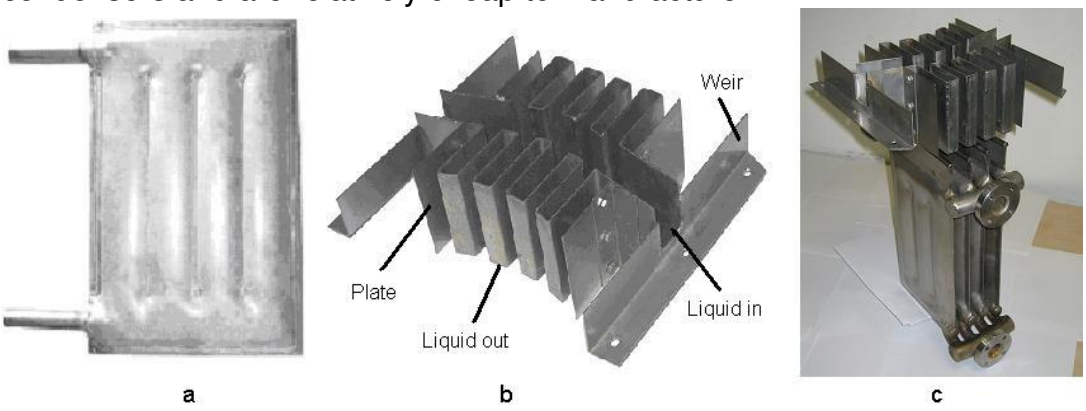

Figure 3: a) Heat panel, b) liquid distributor with splash baffle, c) small set of heat panels used in downcomer experiments

3.2.1 Heat panel test setup

A dedicated bench-scale unit was built to determine the heat transfer characteristics of the heat panels (*Figure 4*). One or more heat transfer panels could be placed in a glass insulated vessel in order to have the possibility for a visual observation of the evaporating liquid film. The setup was operated atmospherically. Pure heptane or a binary mixture of cyclohexane/heptane was circulated over the outside wall of the panel using a frequency controlled gear pump. The liquid feed was heated to boiling temperature with an electrical heating bath. A trough type liquid distributor with holes in the bottom

(*Figure 3*) was applied in order to obtain a controlled falling film at the outside of the heat transfer panels. Steam was used as heating medium, because the heat transfer coefficient of condensing steam is accurately available and consequently the outside heat transfer coefficient could be calculated from the measured overall heat transfer coefficient. The mass of condensed steam was measured with a laboratory balance. Experiments were carried out at overall temperature differences between 4 and 12K. Samples of the condensed top and bottom product could be taken in order to determine the separation performance of the heat transfer panels, caused by the preferential evaporation of the light component. The composition of the liquid samples was determined using a gas gromatograph.

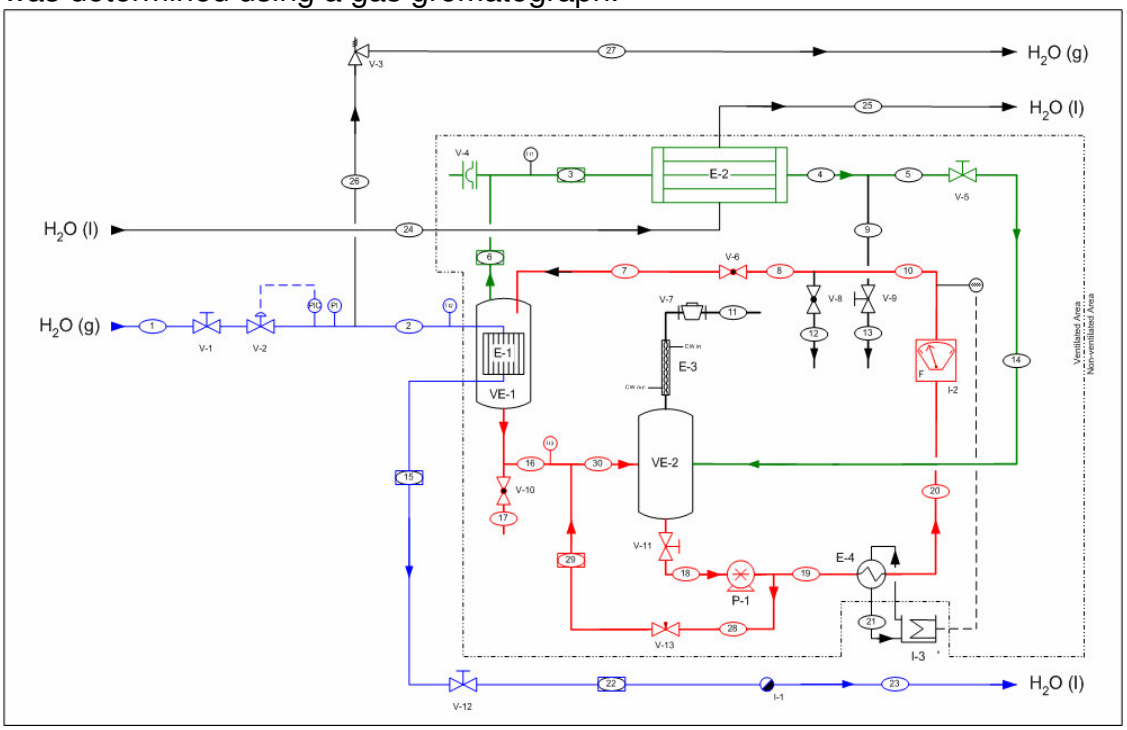

Figure 4: Flow sheet of heat panel test setup

3.2.2 HIDiC pilot plant

A pilot plant was built, which is basically an annular sieve tray column in which heat transfer panels can be placed in either the downcomer or on the active area of an operating tray (*Figure 5*). The column data are summarized in *table 1:*

Table 1: Distillation pilot plant data

Diameter outer column	800 mm
Diameter inner column	300 mm
Number of trays	3
Tray spacing	500 mm
Hole size	10 mm
Hole pitch	30 mm
Downcomer area	0.08 m^2

The model system for this study was cyclohexane/(n)-heptane. The column was operated under total reflux and samples can be taken from the top and bottom products in order to determine the separation efficiency. View glasses were mounted in order to visually observe the hydraulic behaviour of the interacting phases on the annular sieve tray.

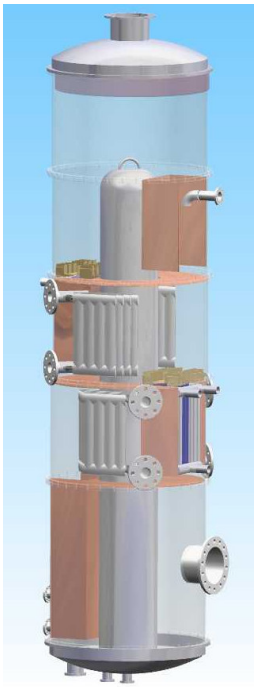

Figure 5: 3D image of HIDiC pilot column, equipped with annular sieve trays. Heat panels can be placed on tray deck or in the downcomer

A separate setup was built to feed the heat transfer panels with hydrocarbon vapour (Figure 6). The vapour vessel is an empty cylinder through which vapour flows upwards at slightly increased pressure. In this way the process conditions of the rectifying section could be simulated. Pure cyclohexane and mixtures of cyclohexane/(n)-heptane were used as model systems. The vapour was slightly superheated to avoid condensation inside the setup, before the vapour entered the heat transfer panels. Part of the vapour flowing

upwards in the vapour vessel, will enter the heat panels and condense subsequently. The condensate quantity was measured with a coreolis mass flow meter.
In the case that the heat panels were placed inside the downcomer, part of the liquid leaving the tray was fed over the panels with the same liquid distributor as used in the heat panel test setup (Figure 3). This was done to obtain the same flow behaviour and consequently the same outside heat transfer coefficient as determined in the bench scale experiments.

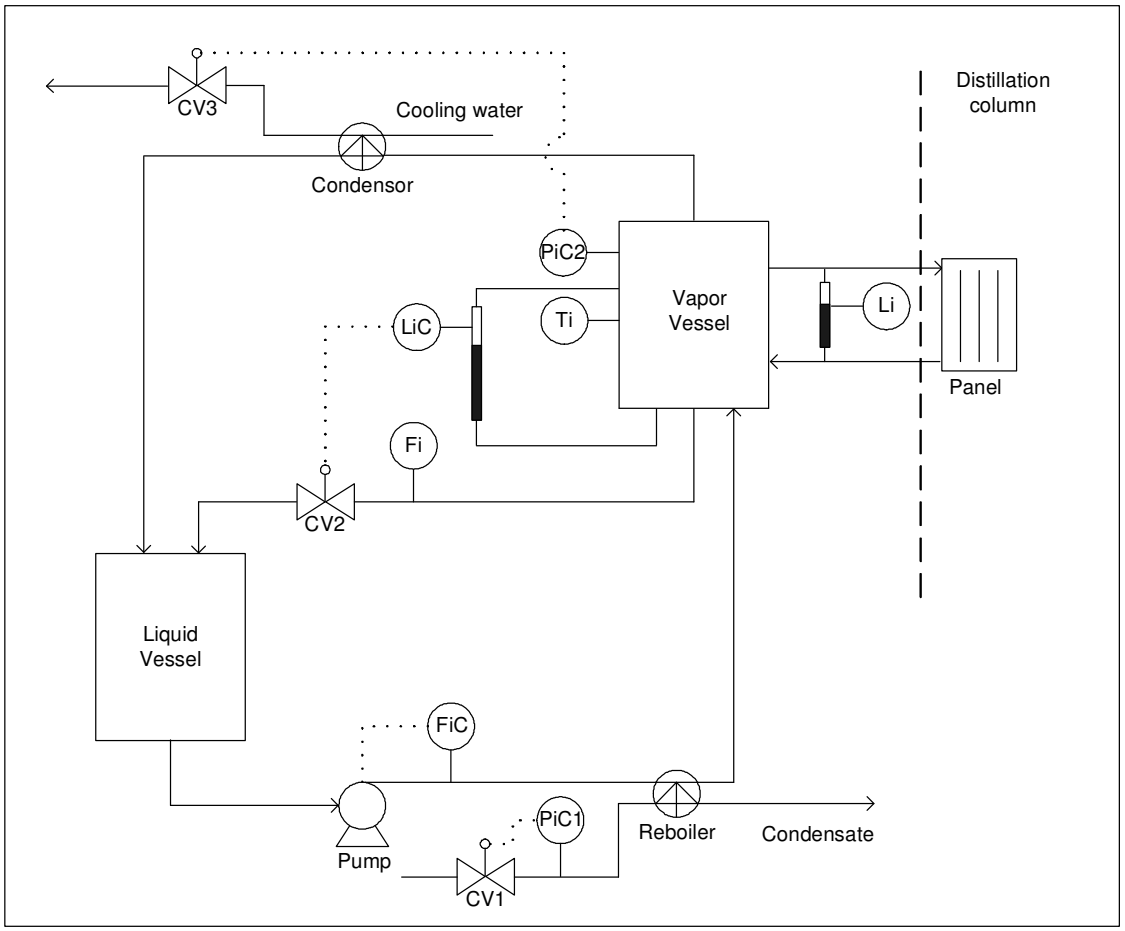

Figure 6: Flowsheet of setup to feed heat transfer panels with hydrocarbon vapour

Consequently the condensation side coefficient of the hydrocarbon mixture could be calculated from the measured overall heat transfer coefficient and the known (from previous experiments) evaporation side coefficient.
A set of four heat transfer panels was placed in the center of the downcomer (*Figure 3 and 7*). The panel dimensions were 200 by 350 mm. The distance between the panels was 20 mm. The bulk of the liquid leaving the tray was

physically separated from the heat panels by a stainless steel plate in order to prevent disturbance of the falling liquid film.
The same set of four heat panels used in the downcomer experiments, were installed above the tray deck for comparison reasons. No liquid distributors were used because the splashing froth present on the tray deck should be able to wet the panels completely. Another set of experiments was carried out with a tray deck that was fully occupied with heat panels. The panel length varied from 180 to 600 mm in the latter layout. (*Figure 7*)

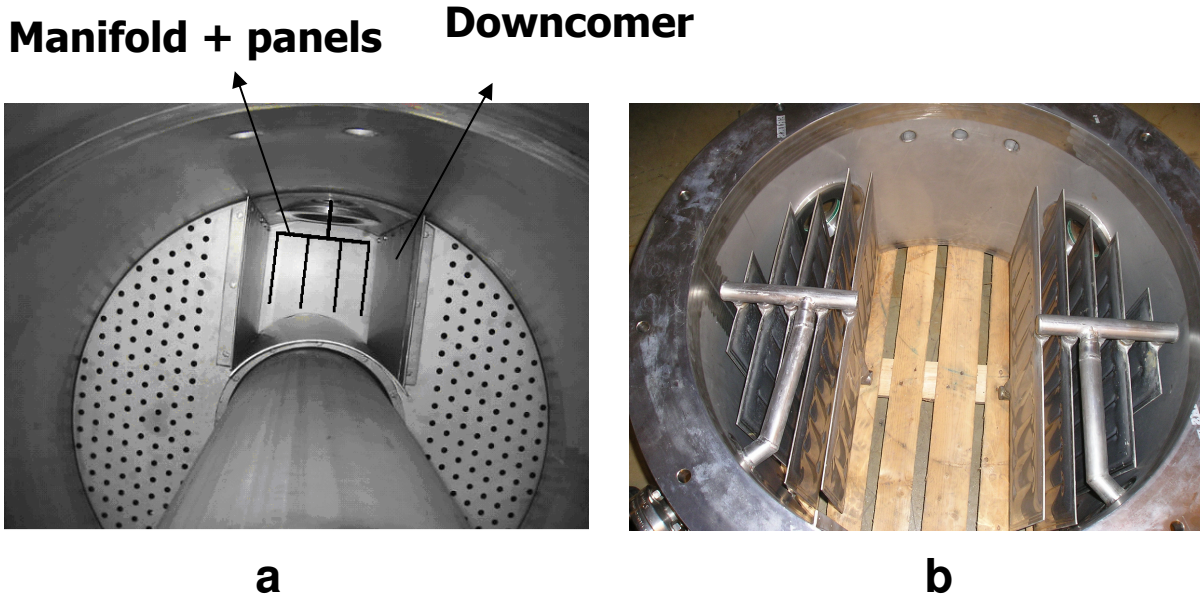

Figure 7: a) placement of heat transfer panels in downcomer b) layout of large set of heat panels on tray active area

3.3 Theory

3.3.1 Condensation of pure component and binary mixtures falling liquid films

As the height of the heat transfer panels used in the present study is relatively small namely 350 mm, the condensate film is expected to remain laminar. For laminar films the condensation side heat transfer process was described with the well known Nusselt equation (12).

$$Nu_{z,l} = \frac{h_{z,l}}{\lambda_l} \cdot \left(\frac{\mu_l^2}{\rho_l^2 \cdot g} \right)^{1/3} = 1.1 \cdot \left(1 - \frac{\rho_v}{\rho_l} \right)^{1/3} \cdot \left(\mathrm{Re}_f \right)^{-1/3} \qquad [1]$$

where, $h_{z,l}$ is the local heat transfer coefficient of condensation, λ_l is the thermal conductivity (W/mK), μ_l is the viscosity of the liquid (Pa s), ρ is the density (kg/m3), g is the acceleration of gravity (m/s2). Re_f is the Reynolds number of the falling liquid film, defined as:

$$\mathrm{Re}_f = \frac{4 \cdot \Gamma_z}{\mu_l} \qquad [2]$$

where Γ_z (kg/s/m) is the liquid mass flow per unit width.

The Nusselt equation is only valid for smooth falling liquid films. At Reynolds numbers higher than 30, waves appear at the vapour-liquid interface and the flow pattern changes to laminar-wavy. In this regime the heat transfer is enhanced by two effects. Kapitza (13) has shown that the average film thickness is less than predicted with the Nusselt theory and the second effect is convection in the film, although the bulk of the film in this region will remain laminar. In both the laminar and the laminar wavy regime the heat transfer coefficient will decrease with increasing film Reynolds number due to an increased film thickness. Slegers and Seban (14) measured that the heat transfer coefficient in the laminar wavy regime is up to 80% higher than that of a smooth laminar film. A correction factor has been proposed by Kutateladze (15):

$$\frac{h_{z,lw}}{h_{z,l}} \approx 0.69 \cdot \mathrm{Re}_f^{0.11} \qquad [3]$$

Where $h_{z,lw}$ is the local heat transfer coefficient of condensation in the laminar wavy regime. The Nusselt equation is extended to include the laminar wavy regime by combining equations [1] and [3]:

$$Nu_{z,lw} = \frac{h_{z,lw}}{\lambda_l} \cdot \left(\frac{\mu_l^2}{\rho_l^2 \cdot g} \right)^{1/3} = 0.76 \cdot \left(1 - \frac{\rho_v}{\rho_l} \right)^{1/3} \cdot \left(\mathrm{Re}_f \right)^{-0.22} \qquad [4]$$

In the laminar and the laminar wavy regime the condensation side heat transfer coefficient of a binary mixture of components with similar physical properties will closely resemble that of the pure component, because the transport of heat through the film is controlled by diffusion. In the turbulent regime however the heat transfer coefficient of a mixture will be lower than that of the pure component, because the preferable condensation of the heavy component at the interface causes a concentration gradient in the film. The local depression of the light component at the interface will lead to diffusive transport of this component in opposite direction to the convective flow of heat, so called mass transfer resistance. This effect results in a lower effective condensation side heat transfer coefficient (22)

3.3.2 Pressure drop

As the vapour velocity in a distillation column is relatively low, wall friction losses are negligible and consequently there will be virtually no pressure drop between the vapour inlet and liquid outlet of a heat transfer panel (Figure 8).

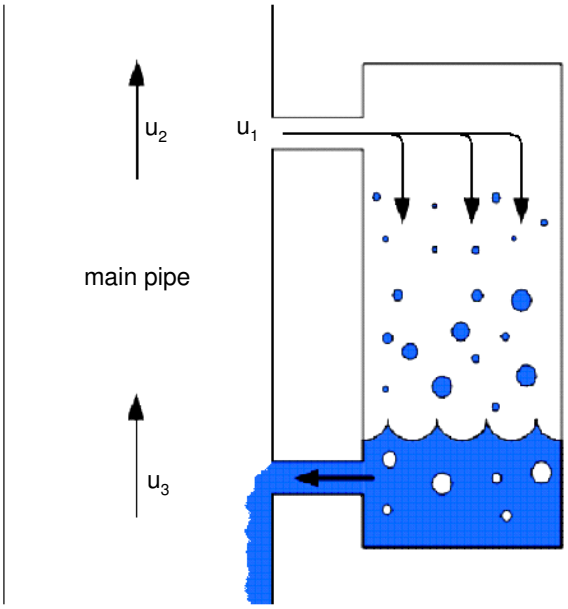

Figure 8: Schematic representation of connection of heat panels to distillation column

Therefore the pressure drop associated with the entrance of the vapour in the heat transfer panel through the vapour manifold, will lead to a static liquid head inside the panels. When friction losses of the entering vapour increase, the condensate level inside the panels will also increase, leading to a decreased surface area available for heat transfer. The pressure drop was calculated using the Darcy-Weisbach equation:

$$\Delta P_f = f \cdot \frac{L}{D} \cdot \rho \cdot \frac{u^2}{2} \qquad [5]$$

where *L* is the length of the pipe (m), *D* is the diameter of the pipe (m), *f* is the Darcy friction factor and u is the velocity of the vapour (m/s).
Since the inlet pipe is relatively short, entrance effects can be expected. In order to get more certainty the pressure drop caused by the entering vapour was also modeled using the commercially available Computation Fluid Dynamics package Fluent.

3.3.3 Evaporation of pure component falling liquid films

In the stripping section the evaporation occurs from the liquid film flowing down the outer surface of the heat transfer panels. For a falling liquid film, different boiling mechanisms can occur, depending on the overall temperature difference which is applied over the heat transfer surface. The boiling mechanisms listed here in the order of increasing temperature difference are:

Surface evaporation. Here it is assumed that heat is conducted through the liquid film which is slightly superheated and evaporation takes place at the liquid-vapour interface.
Nucleate boiling. Here vapour bubbles, which are assumed to form at microscopic cavities in the wall, grow until they are detached from the wall, and migrate to the liquid-vapour interface where they burst and release the vapour.
Film boiling. A film of vapour is assumed to be present between the heated surface and the liquid film. Before evaporation can take place, the heat must be conducted across this vapour film.

As the optimal temperature difference inside a HIDiC appears to be rather small i.e. between 2 and 10 K depending on the model system (2, 9), surface evaporation is considered to be the governing heat transfer mechanism.

A lot of literature information is available on the evaporation of pure component liquid films. Chun and Seban (16) carried out experiments with falling water films and proposed the following relation for the laminar wavy and turbulent regime:

$$h^*_{lw} = 0.606\left(\frac{\mathrm{Re}}{4}\right)^{-0.22} \qquad \text{for Re} < \text{Re}_{tr}$$

[6]

$$h^*_{turb} = 0.0038\,\mathrm{Re}^{0.4}\,\mathrm{Pr}^{0.65} \qquad \text{for Re} > \text{Re}_{tr}$$

[7]

with

$$\mathrm{Re}_{tr} = 5800\,\mathrm{Pr}^{-1.06} \qquad [8]$$

where the subscripts *lw*, *turb* and *tr* refer to wavy laminar film, turbulent and to transition, respectively. The dimensionless Prandtl number is defined as:

$$\mathrm{Pr} = \frac{\nu}{a} \qquad [9]$$

where *v* (m2/s) is the kinematic viscosity and *a* (m2/s) is the thermal diffusivity.

In this model *h** is the dimensionless heat transfer coefficient for falling films, which is defined as:

$$h^* = \frac{h}{\lambda}\cdot\left(\frac{\mu^2}{\rho^2 g}\right)^{\frac{1}{3}} = \mathrm{Nu}\cdot\left(\frac{\mu^2}{\rho^2 g}\right)^{\frac{1}{3}} \qquad [10]$$

where *h* (W/m2K) is the heat transfer coefficient, *λ* (W/mK) is the thermal conductivity, *ρ* (kg/m3) is the liquid density and *g* (m/s2) is the gravitational acceleration (9.81 m/s2).

More recently, Schnabel et al (17) proposed a slightly modified model, based on a larger collection of experimental data. This data collection contains experiments with water (18), and experiments carried out with a refrigerant, R11 (19). Furthermore, Schnabel carried out additional experiments using

another refrigerant, R113. Most importantly he accounted also for a turbulent flow contribution.

$$h_{lw}^{*} = 0.9\left(\frac{\mathrm{Re}}{4}\right)^{-0.33} \qquad [11]$$

$$h_{turb}^{*} = 0.00622\left(\frac{\mathrm{Re}}{4}\right)^{0.4}\mathrm{Pr}^{0.65} \qquad [12]$$

$$h^{*} = \sqrt{\left(h_{lw}^{*}\right)^{2} + \left(h_{turb}^{*}\right)^{2}} \qquad [13]$$

By adopting the quadratic interpolation formula [13], also the transition region between laminar and turbulent, 400 < Re < 3200, is covered.

Alhusseini (20, 21) performed experiments using ethylene glycol and water. His results for water agreed with the Chun Seban model (16). However, the results for ethylene glycol did not. This discrepancy with the Chun Seban model was attributed to the higher Prandtl number of ethylene glycol.

Wavy laminar regime:
The heat transfer in wavy laminar films is enhanced by convection induced by large waves that travel along the free surface. Since wave activity is certainly affected by the surface tension of the fluid, the heat transfer coefficient is also expected to depend in some extent on the surface tension (20).
By dimension analysis, it can be shown that the dimensionless heat transfer coefficient for wavy laminar films should be dependent upon both the film Reynolds number and the Kapitza number, which is defined as

$$\mathrm{Ka} = \frac{g\mu^{4}}{\rho\sigma^{3}} \qquad [14]$$

where σ (N/m) is the surface tension

The following empirical correlation is proposed by Alhusseini et al (20) for the Nusselt number in the wavy laminar region:

$$h_{lw}^{*} = 2.65\,\mathrm{Re}^{-0.158}\,\mathrm{Ka}^{0.0563} \qquad [15]$$

Turbulent regime:
Alhusseini et al obtained an approximate expression for the Nusselt number in the turbulent region based on a turbulence model. For the region near the wall, the following turbulence model was assumed.

$$\frac{\varepsilon_M}{\nu} = \frac{1}{2}\left(-1 + \left\{ 1 + 0.64 \frac{g \cdot \delta}{\nu^2} y^2 \times \left[1 - \exp\left(\frac{\sqrt{\frac{g \cdot \delta}{\nu^2}} \cdot y}{-26} \right) \right]^2 \exp\left(-2.5 \frac{y}{\delta} \right) \right\}^{1/2} \right) \qquad [16]$$

where ε_M (m2/s) is the eddy diffusivity for momentum, δ (m) is the film thickness and y (m) is the distance from the wall and ν (m2/s) is the kinematic viscosity

For the region near the liquid-vapour interface the next equation was used.

$$\frac{\varepsilon_M}{\nu} = \frac{1.199 \cdot 10^{-16} \nu^{2/3}}{\mathrm{Ka}\, g^{1/3}} \cdot \frac{\mathrm{Re}^{6.98\,\mathrm{Ka}^{0.0675}}}{\delta} \left(\frac{\delta - y}{0.0166\,\mathrm{Ka}^{-0.1732}} \right)^2 \qquad [17]$$

The turbulence model was discussed in detail by Alhusseini (20, 21). The model is restricted to cases in which vapour shear at the interface is negligible. Using asymptotic expansion the following expression was proposed for heat transfer under turbulent flow conditions:

$$h^*_{turb} = \frac{\mathrm{Pr}\,\delta^{+1/3}}{(A_1\,\mathrm{Pr}^{3/4} + A_2\,\mathrm{Pr}^{1/2} + A_3\,\mathrm{Pr}^{1/4} + C_1) + (B\,\mathrm{Ka}^{1/2}\,\mathrm{Pr}^{1/2})} \qquad [18]$$

where:

$$A_1 = 9.17$$

$$A_2 = 0.328\pi \frac{130 + \delta^+}{\delta^+}$$

$$A_3 = 0.0289 \frac{152100 + 2340\delta^+ + 7(\delta^+)^2}{(\delta^+)^2}$$

$$B = 2.51 \cdot 10^6 (\delta^+)^{0.333} \frac{\mathrm{Ka}^{0.173}}{\mathrm{Re}^{3.49\,\mathrm{Ka}^{0.0675}}}$$

$$C_1 = 8.82 + 0.0003\,\mathrm{Re}$$

$\delta+$ is the dimensionless turbulent film thickness which can be calculated with Brauer's turbulent film thickness correlation:

$$\delta^+ = 0.0946\,\mathrm{Re}^{0.8} \qquad [19]$$

A combined expression for the heat transfer coefficient for all Reynolds numbers is obtained by a fifth order polynomial interpolation of the wavy laminar and turbulent coefficients:

$$h^* = \left[(h^*_{wl})^5 + (h^*_{turb})^5 \right]^{1/5} \qquad [20]$$

3.3.4 Heat and mass transfer in turbulent falling liquid films of binary mixtures

In binary liquid films, the more volatile component will be preferentially evaporated at the interface, causing a depression in the local concentration of that component. In the steady state condition, axial convection would interact with transverse diffusion to supply a net molar flux of the volatile component towards the interface. For turbulent conditions, Re > 300, this process results in a local concentration profile, as indicated in figure 9, with maximum concentration at the solid surface and minimum concentration at the interface ($x_{A,i}$). A bulk composition ($x_{A,b}$) can be calculated as the integral average of the product of local concentration and velocity. By definition, the bulk saturation temperature at any axial position corresponds to the bubble point (*Ts*) of the bulk mixture. For design purposes, the heat transfer coefficient would be based upon the temperature difference ($T_w - T_s$). Since the interface composition of the volatile component ($x_{A,i}$) would be lower than the bulk composition ($x_{A,b}$), it follows that the true interface temperature (*Ti*) would be

higher than the bulk saturation temperature (T_s). This represents a net reduction in the available driving force (T_w-T_i) for evaporative heat transfer.
Palen (22, 23) found in an experimental investigation that liquid-side mass transfer resistance can be significant for falling films, causing substantial reductions in the effective evaporative heat transfer coefficient and derived a model to describe the heat and mass transfer in a binary liquid film. This model is based on the film theory. The heat transfer coefficient for falling film evaporation is defined as

$$h = \frac{q}{T_w - T_s} \qquad [21]$$

The heat transfer coefficient is based on the temperature difference T_w-T_s in this definition. In the case of single component fluids, the saturation temperature T_s is identical to the interface temperature T_i.

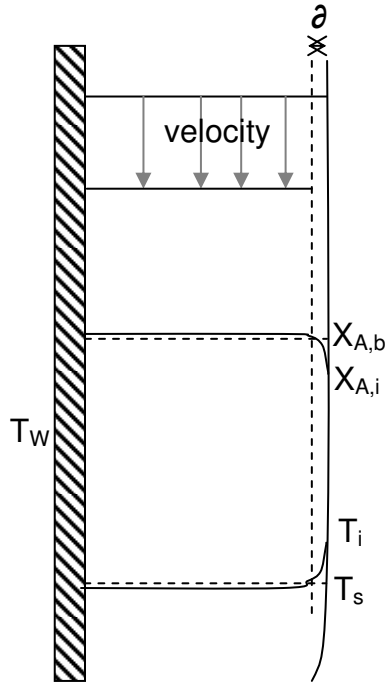

Figure 9: Transport phenomena in a binary turbulent falling liquid film

It is hypothesized that in the case of binary mixtures, the effective heat transfer coefficient would be the same as for single-component films, but with the true interface temperature T_i in place of the bulk saturation temperature T_s. Thus a mixture correction factor can be defined as

$$F_c = \frac{T_w - T_i}{T_w - T_s} = \frac{h}{h_{SC}} \qquad [22]$$

where h_{SC} is the heat transfer coefficient for single component films at same Re and Pr values. The molar flux in the boundary layer for component *A* may be written as

$$N_A = \left(\frac{\rho_A}{M_A}\right) D_{AB} \left(\frac{dx_A}{dy}\right) + Nx_A \qquad [23]$$

where *y* is measured from interface into the liquid film, *N* is the mass flux (kg/m2s) in the –y direction, D_{AB} is the diffusivity of the mixture (m2/s) and *xA* is the mole fraction of the light key component.

Integrating across the composition boundary layer yields

$$\frac{y_{A,b} - x_{A,b}}{y_{A,b} - x_{A,i}} = \exp\left[-\frac{N M_A}{\rho_A k}\right] \qquad [24]$$

where the mass transfer coefficient *k* (m/s) is defined as

$$k \equiv \frac{D_{AB}}{\partial} \qquad [25]$$

In this equation δ is the boundary layer thickness at the interface of the film (m).
With negligible subcooling or superheating, the heat flux *q* (kJ/m2K) is given by

$$q = N(\Delta H_{vap}) M_{vap} \cong N(\Delta H_{vap}) M_A \qquad [26]$$

for binary mixtures with components having significantly different boiling points ($T_B > T_A$).
Now variable *Q* is introduced to make the equations more compact.

$$Q \equiv \frac{q}{\rho_A \cdot \Delta H_{vap}} \qquad [27]$$

Combination of equations [24] and [27] yields the following expression

$$(y_{A,b} - x_{A,i}) = (y_{A,b} - x_{A,b})(e^{Q/k} - 1) \quad [28]$$

A difference approximation for the temperature-composition gradient will be used $T_i - T_s = \left[\frac{dT_s}{dx_A}\right](x_{A,i} - x_{A,b})$ [29]

and combined with equation [28]:

$$T_i - T_s = \frac{dT_s}{dX}(y_{A,b} - x_{A,b})(1 - e^{Q/k}) \quad [30]$$

Combining equations [22], [23] and [30] yields an expression for the mixture correction factor:

$$F_C = \left[1 + \frac{h_{SC}}{q}\frac{dT_S}{dx_A}(y_{A,b} - x_{A,b})(1 - e^{Q/k})\right]^{-1} \quad [31]$$

Schnabel and Schlünder (17) suggested an approximation for the saturation temperature gradient, dT_s/dx. It is recognized that the saturation temperature of the heavy component is its boiling point (T_B) at x_A=0 and the saturation temperature of the light component is its boiling point (T_A) at x_A=1. Then, the overall temperature gradient is approximated as

$$\frac{dT_s}{dx_A} = T_A - T_B \quad [32]$$

The simplified expression for F_c then becomes

$$F_C = \left[1 - \frac{h_{SC}}{q}(T_B - T_A)(y_{A,b} - x_{A,b})(1 - e^{Q/k})\right]^{-1} \quad [33]$$

Schlünder also suggested that a constant value of k in the range of about 0.0002 to 0.0003 m/s could be used as a good approximation for mass transfer for common hydrocarbons. However, since k is an unknown, the logical procedure is to attempt to back calculate this quantity from the

experimental data. Palen e.a. performed this back calculation for their experimental data (ethylene glycol-water and propylene glycol-water) using the following Sherwood number correlation.

$$\mathrm{Sh} = 0.010\,\mathrm{Re}^{0.78}\,\mathrm{Sc}^{0.4} \qquad [34]$$

with

$$Sh = \frac{k\,\delta}{D_{AB}} \qquad [35]$$

and

$$\mathrm{Sc} = \frac{\mu}{\rho D_{AB}} \qquad [36]$$

The thickness of the laminar film is described with the well known Nusselt expression:

$$\delta = \left[\frac{3\mu\,\Gamma}{\rho^2 g}\right]^{1/3} \qquad [37]$$

3.4 Results and Discussion

3.4.1. Heat panel test setup

3.4.1.1 Single Component Evaporation

Figure 10 shows both the experimental values and the model predictions for the evaporation side heat transfer coefficient of a single heat panel as a function of liquid load at various temperature differences. n-Heptane was used as process liquid and experiments were performed in the heat panel test setup. The heat transfer coefficient for evaporation is relatively constant with respect to the driving force for heat transfer. It tends to increase with Reynolds number indicating the presence of turbulent flow conditions in the falling liquid film. It should be noted that at these low Reynolds numbers, the liquid film is not fully turbulent and basically the flow conditions of the falling liquid film are in the transition regime between laminar and fully turbulent flow.

Although the Chun-Seban model is widely used in literature to predict the performance of falling film evaporators, it underpredicts the heat transfer coefficient of n-heptane with roughly 30%, most probably due to the fact that the model development was done using water as model component, which is also the case for the model of Schnabel. The model of Alhusseini appears to be the most suitable one to predict the evaporation heat transfer coefficient of a single component hydrocarbon falling liquid film in the transition regime between laminar and turbulent flow.

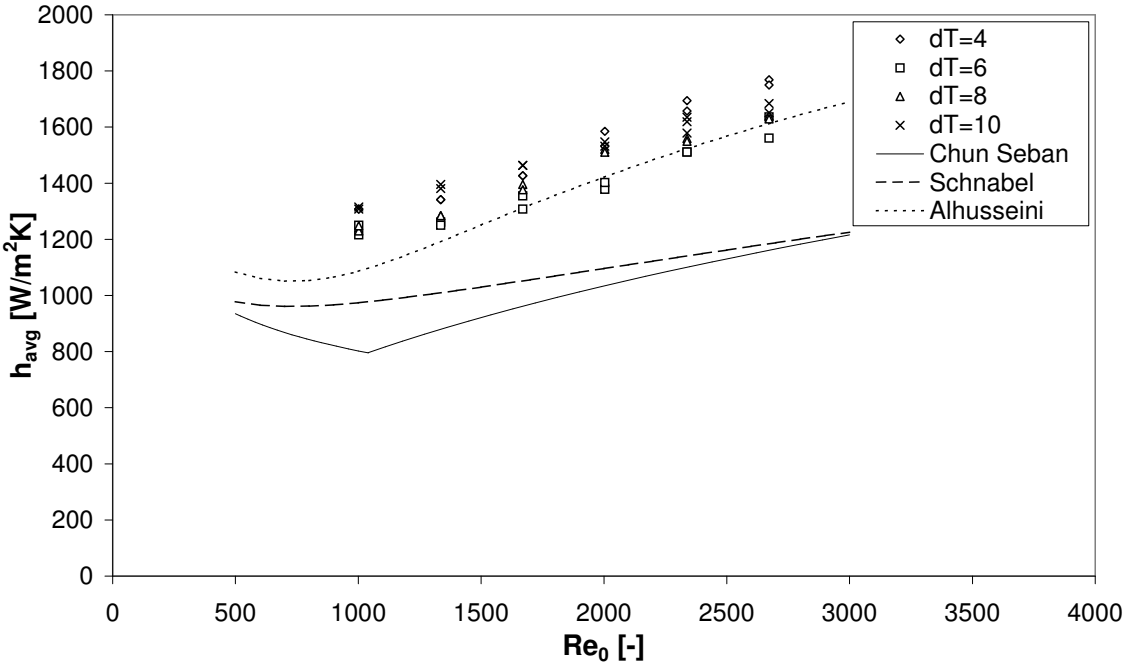

Figure 10: Experimental data and model prediction for evaporative heat transfer coefficient of a falling film of n-heptane

3.4.1.2 Evaporation of Binary Mixtures

The experimental results at a temperature difference of 8 ºC, for different mixtures of cyclohexane/(n)-heptane are given in figure 11 and compared to the Alhusseini model prediction for pure n-heptane. The most important observation is that the average heat transfer coefficient decreases with increasing concentration of cyclohexane in the feed. The preferential evaporation of the light component cyclohexane leads to mass transfer limitations in the falling liquid film, resulting in a lower average heat transfer coefficient. At a 12% concentration of cyclohexane a decrease in heat transfer coefficient of around 20% compared to the pure component is observed. The Palen model was used to describe the effect of mass transfer limitations in the

falling liquid film on the average heat transfer coefficient. Figure 12 shows the Sherwood relation for cyclohexane/(n)-heptane as function of Reynolds number.

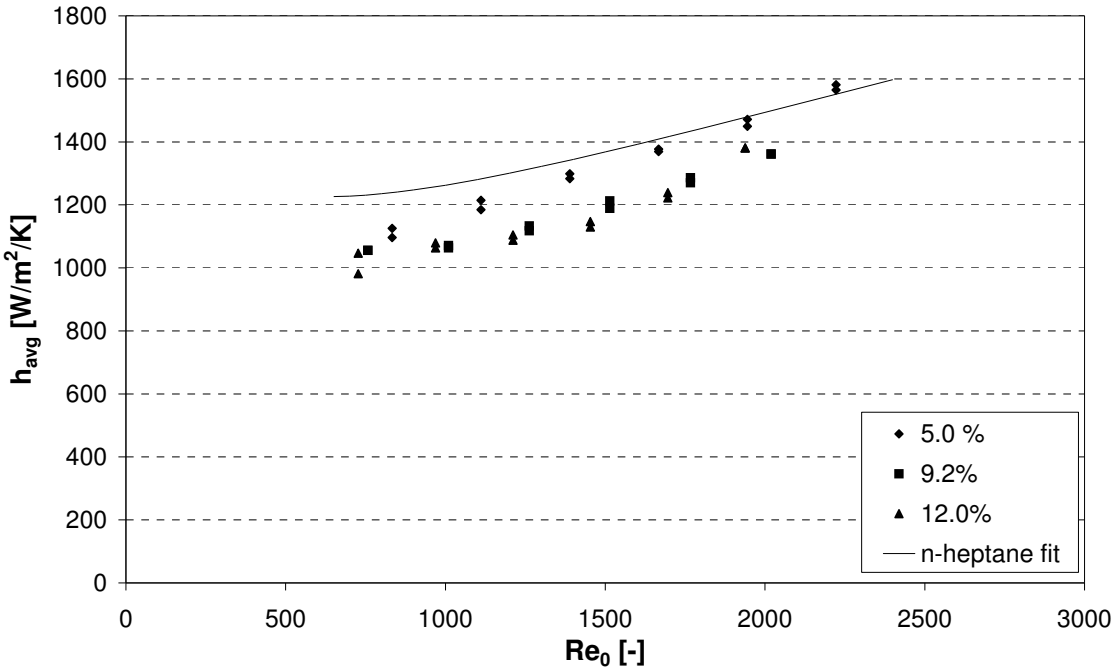

Figure 11: Experimental data for different binary mixtures of cyclohexane/(n)-heptane compared to the Alhusseini model prediction for n-heptane

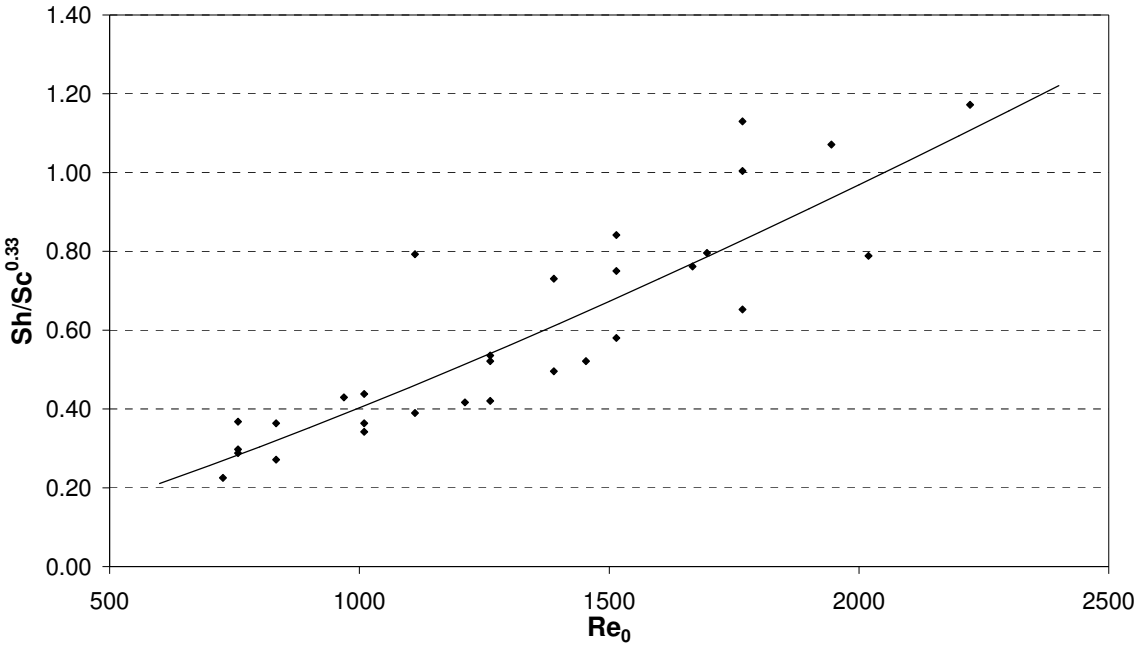

Figure 12: Sherwood regression correlation obtained from the cyclohexane/(n)-heptane experiments

The following correlation was obtained by fitting the calculated Sherwood numbers against the Reynolds and Schmidt number:

$$Sh = 6{,}41 \cdot 10^{-5} \cdot \mathrm{Re}^{1{,}27} \cdot Sc^{0{,}33} \qquad [38]$$

Using Eq [38], the heat transfer coefficients for a mixture were calculated and compared to the experimental data. Figure 13 shows a parity plot of the heat transfer coefficient calculated by the Palen model compared to the experimental values. The average deviation between modeling results and experimental values is less than 5%. It should be noted that the Palen model does not have any predictive value for other model systems as it needs experimental data for a specific model system to calculate the mixture correction factor.

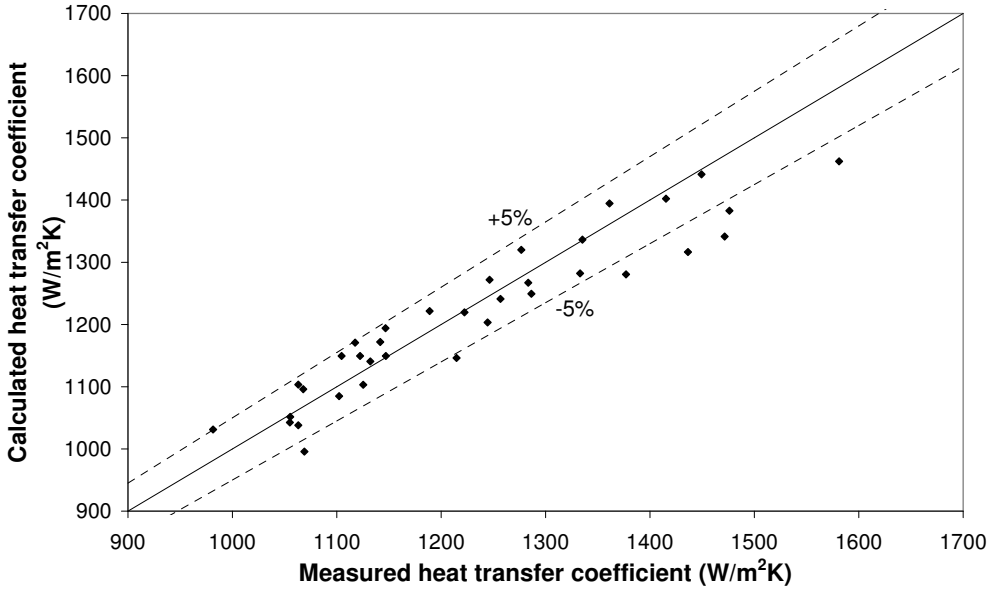

Figure 13: Comparison of calculated and measured heat transfer coefficients for cyclohexane/(n)-heptane mixtures

However a HIDiC appears to be most favourable for the separation of close boiling mixtures in which the effect of mass transfer limitation due to evaporation of the light component is expected to be less pronounced. Figure 14 shows the heat transfer coefficient of a mixture of n(heptane)/methylcyclohexane which has a relative volatility of 1,1. The heat transfer coefficient of a 50% mixture appears to be around 10% less than that of the pure components, where for C6/C7 a 12% mixture already led to a decrease in heat transfer coefficient of around 20% compared to the pure component. Moreover the liquid composition of both the feed and the film leaving the bottom of the panel were measured and there appeared to be virtually no difference between top and bottom composition. Therefore it can be expected that mass transfer limitation will play only a minor role in an industrial HIDiC.

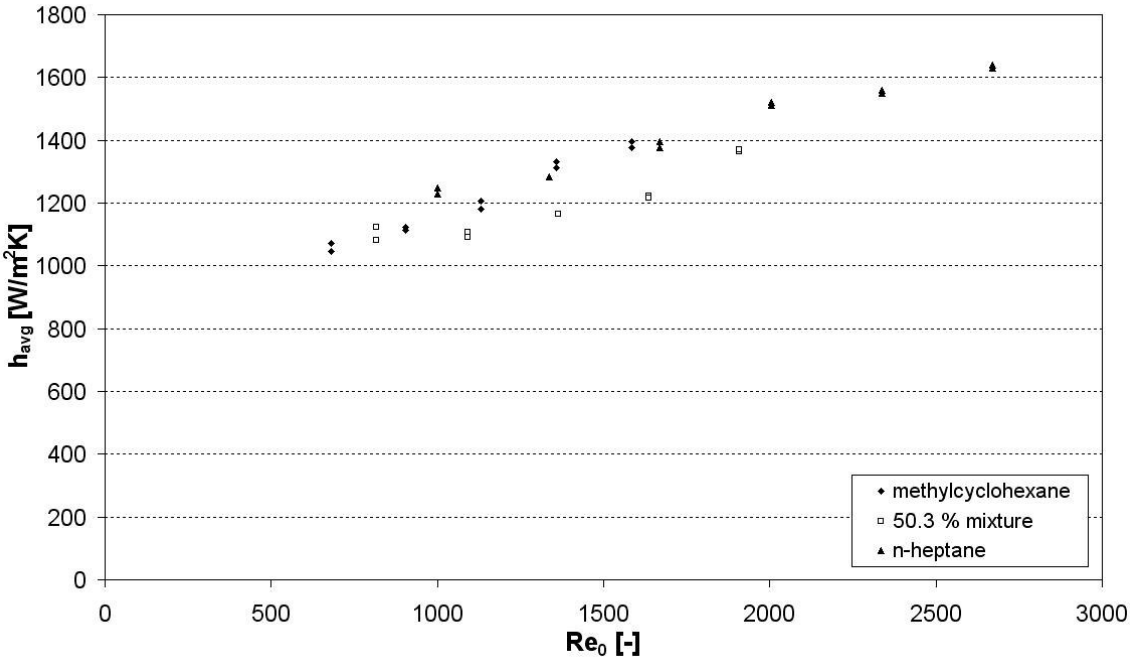

Figure 14: Experimental values for evaporation side heat transfer coefficient for both pure n-heptane, pure methylcyclohexane and a 50% mixture.

3.4.2 HIDiC pilot plant

3.4.2.1 Pressure drop in vapour inlet manifold of heat panels

Figure 15 reveals that the calculated pressure drop in the manifold to the heat panels closely resembles the CFD-simulation. From Figure 16 follows that the velocity of the vapour increases from roughly 1 m/s in the rectification section to around 5 m/s in the inlet tube to the heat panels. However because of the short length of the inlet tube the total pressure drop associated with the entrance of vapour is relatively small. The vapour inlet to the heat panels used in the present study was designed on the basis of this calculation to result in a liquid level inside the panels of 2 to 5 mm. The visually observed liquid height by means of a side mounted viewing glass was approximately 3 mm, which means that Eq [5] can be used with confidence for design purposes.

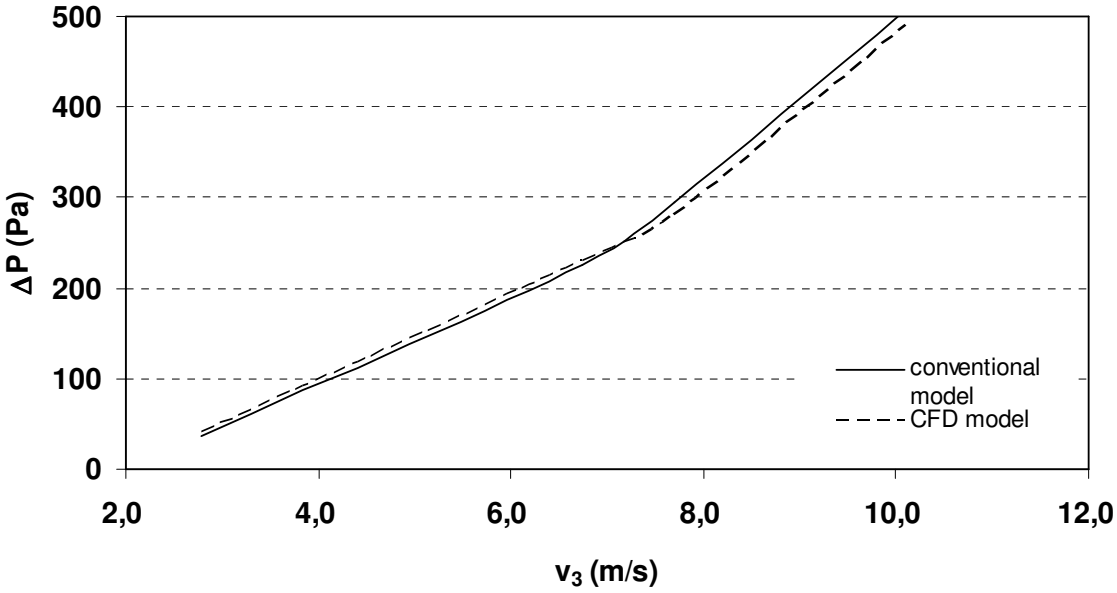

Figure 15: Pressure drop of vapour entering the heat transfer panels at different branch velocities. Dashed lines represent the CFD simulations

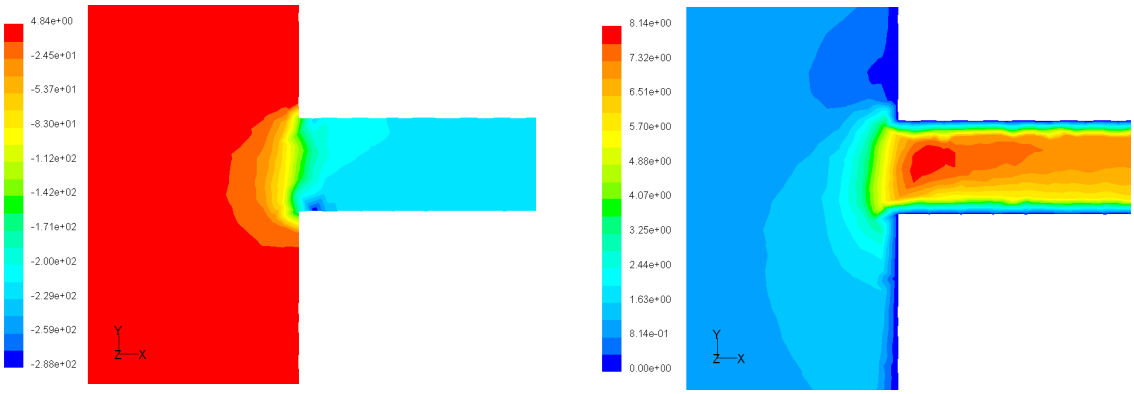

Contours of pressure drop (Pa) Contours of velocity magnitude (m/s)

Figure 16: Fluent plot of the pressure drop and velocity profile at the T-junction to the heat panels

3.4.2.2 Overall heat transfer coefficient for panels in downcomer

Figure 17 shows the overall heat transfer coefficient for a set of heat panels placed in the downcomer of an annular sieve tray in the HIDiC pilot plant. Although the piping was properly insulated the heat loss to the environment

was estimated with engineering correlations to be around 200 W. The effect of this heat loss on the overall heat transfer coefficient is also shown. The heat transfer coefficient decreases with increasing temperature difference. The larger heat duty leads to an increased film thickness of the laminar wavy condensate film inside the heat panel, which means an increased

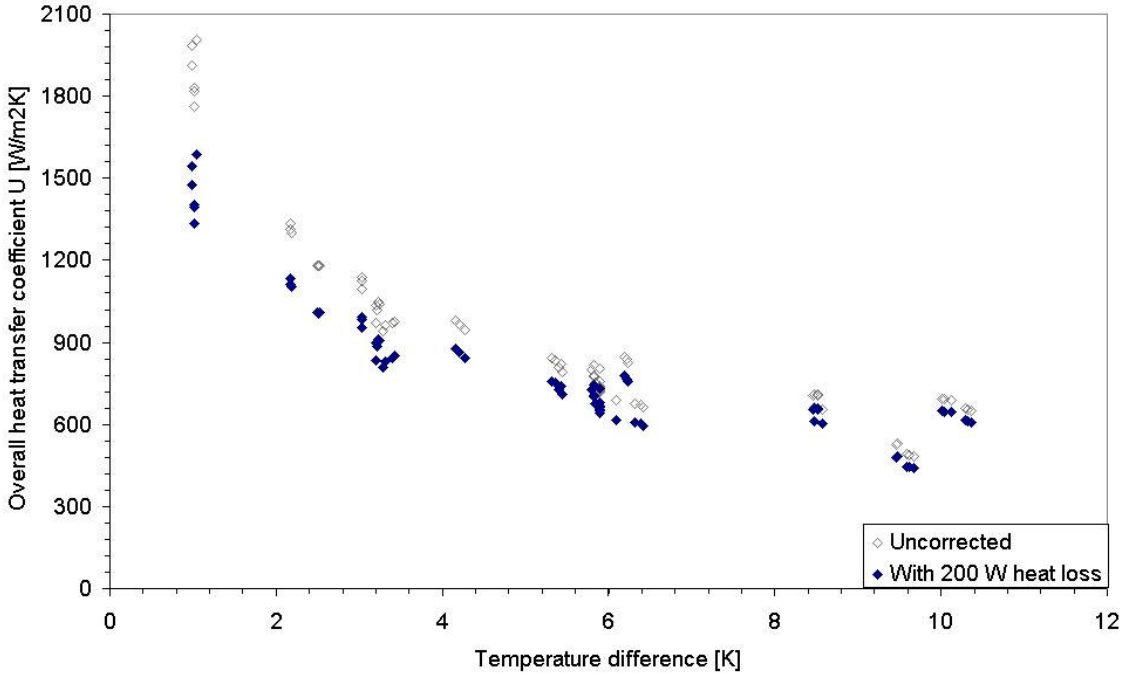

Figure 17: Overall heat transfer coefficient for panels placed in downcomer, without heat loss (uncorrected) and corrected for 200 W heat loss to the environment

resistance for heat transfer. As indicated in Figure 10, the evaporation side heat transfer coefficient seems to be independent of temperature difference. Since the same liquid distributor was used for all experiments, it can be concluded that the influence of temperature difference on overall heat transfer coefficient is caused by the change in flow conditions at the condensation side only.

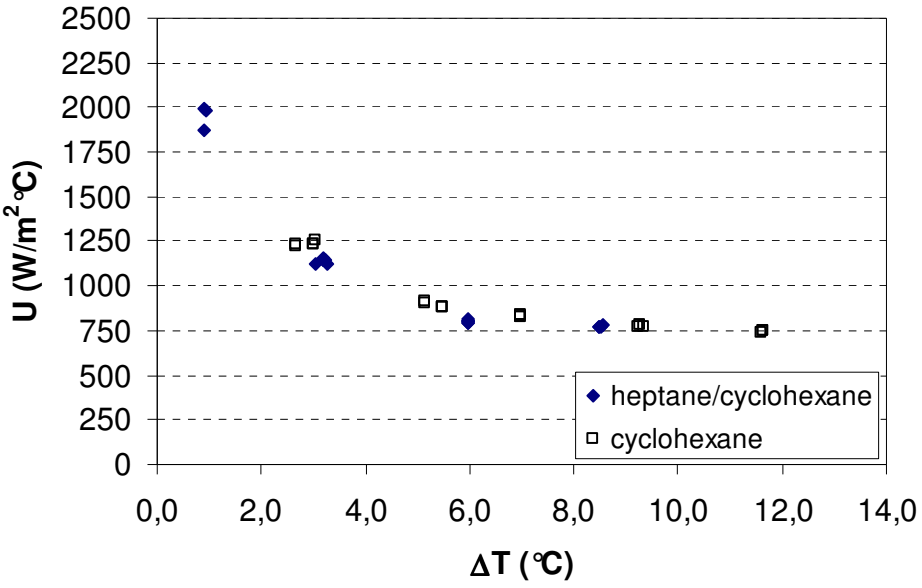

Figure 18: Overall heat transfer coefficient for downcomer experiments. Pure cyclohexane or a C6/C7 mixture on the condensation side

As shown in Figure 18, there was no difference observed between the overall heat transfer coefficient of the pure component cyclohexane and that of a 50 wt% C6/C7 mixture due to the laminar flow conditions in the falling liquid film. In the laminar and the laminar wavy regime the condensation side heat transfer coefficient of a binary mixture of components with similar physical properties will closely resemble that of the pure component, because the transport of heat through the film is controlled by diffusion. It can therefore be concluded that mass transfer limitations don't have a significant effect on the condensation side heat transfer coefficient.

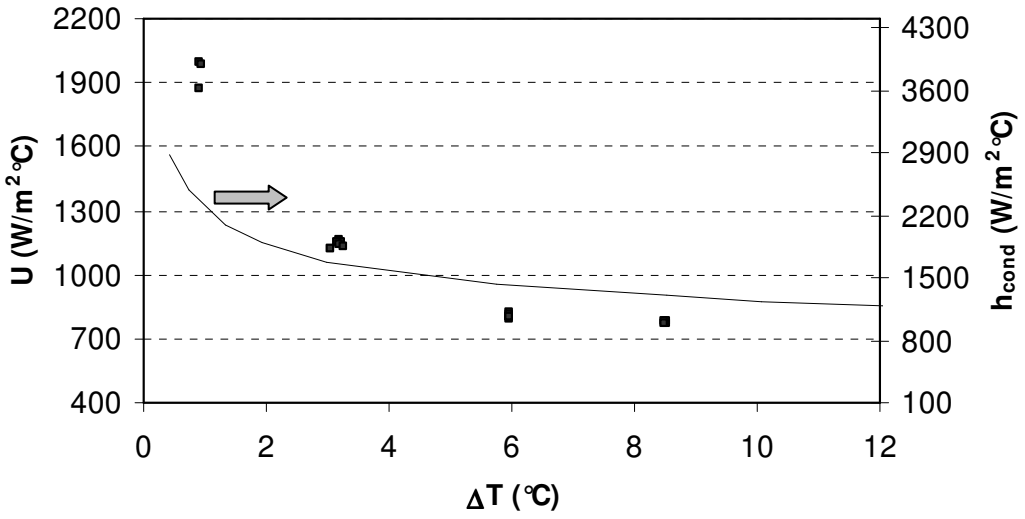

Figure 19: Experimental values of overall heat transfer coefficient (points) and Nusselt model prediction (line) for condensation side heat transfer coefficient

Figure 19 shows the Nusselt model prediction for the condensation side heat transfer coefficient, which appears to be in reasonable agreement with the experimental data. Especially at low temperature differences the model underpredicts the condensation side heat transfer coefficient. This is most probably due the fact that at very low Reynolds numbers, the surface is not fully wetted. El-Genk and Saber (24) report a number of analytical expressions for the minimum liquid film thickness (MLFT) and minimum wetting rate (Γ^{+}_{min}) to ensure that the surface remains covered by a continuous, thin liquid film. The most common one is derived from a force balance and gives the MLFT as a function of contact angle:

$$\delta^{+}_{min} = (1-\cos\theta_L)^{1/5} \qquad [39]$$

Where θ_L is the liquid contact angle (º) and δ^{+} is the film thickness written in dimensionless form:

$$\delta^{+} = \delta\left(\frac{\rho_L^3 g^2}{15\eta_L^2\sigma}\right)^{0.2} \qquad [40]$$

The corresponding minimum wetting rate (Γ^{+}_{min}) based on the Nusselt film theory is proportional to the minimum liquid film thickness to the third power:

$$\Gamma^{+}_{\min} = 1.693 \cdot \left(\delta^{+}_{\min}\right)^{3} \qquad [41]$$

Where Γ^{+} is the liquid load written in dimensionless form according to:

$$\Gamma^{+} = \frac{\Gamma}{\left(\rho_L \eta_L \frac{\sigma^3}{g}\right)^{1/5}} \qquad [42]$$

With these equations the minimum liquid load for a stable film can be calculated when the contact angle between the process liquid and stainless steel surface is known. Unfortunately no measurements could be performed to determine this contact angle. From the experimental data it follows that the transition point is at condensate mass flow of approximately 18 kg/h, which corresponds with an overall heat transfer coefficient of around 1050 W/m^{2}K. For Reynolds numbers below the transition point, the panel surface is considered to be not completely wetted by the film. However, when the contact angle is back calculated using Eqs. [41] to [44] it is found to be 7.8˚, which is an acceptable value for hydrocarbons on a stainless steel surface (24).

3.4.2.3 Overall heat transfer coefficient for panels on active tray area

In case that the panels are placed in the downcomer, a liquid distributor is placed on top, resulting in a smooth liquid film flowing continuously down the panel surface. When panels are placed in the froth, liquid will periodically be splashed against the panel surface due to the oscillatory motion of the froth and flow down until the next batch of liquid splashes up. It was visually observed that a ‘splash’ of liquid from the froth hits the panels once every 1 to 2 seconds. This resulted in the panels being completely wetted and no dry spots could be observed at the outer panel surface. Figure 20 shows the overall heat transfer coefficient for the small panels in the downcomer compared to that of the same set of panels placed on the active tray area.

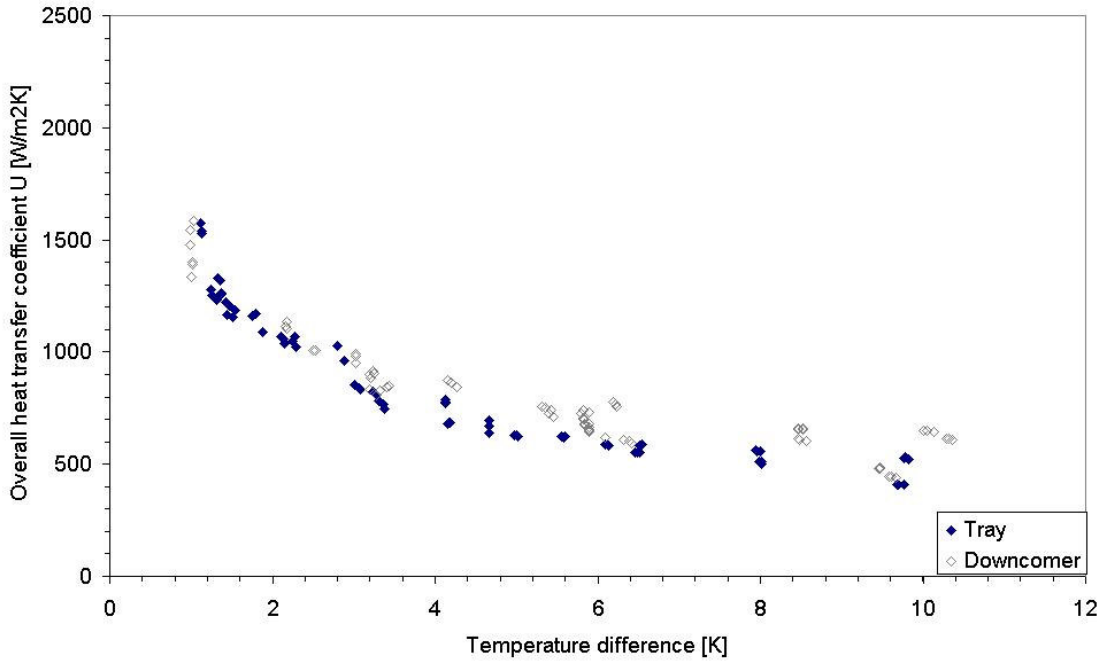

Figure 20: Experimental overall heat transfer coefficients for small set of heat panels placed in the downcomer or on the tray deck

The overall heat transfer coefficient is slightly lower for the tray situation. Apparently the average film thickness and consequently average Reynolds number of the liquid film splashed to the panels by the froth on the distillation tray is lower than that of the controlled liquid film applied in the downcomer experiments. The effect is not very pronounced as the evaporation heat transfer coefficient is not very sensitive to Reynolds number close to the transition regime from laminar to turbulent flow. It also indicates that the condensation side is the rate determining step in this heat transfer process.

The heat transfer coefficient for the large panels is lower than that of the small panels as can be seen in figure 21. The reason for this must be a lower effective condensation side coefficient as the flow conditions on the outside of the panels were the same as for the small panel set. Most probably some stagnant zones were present inside the panels, due to the asymmetric form of the panel set used in the experiments. A symmetric panel form and a well designed vapour feed manifold will prevent this problem. As indicated in Figure 22, if 20 per cent stagnant area is assumed, the heat transfer coefficients of the large panel set resemble that of the small panel set.

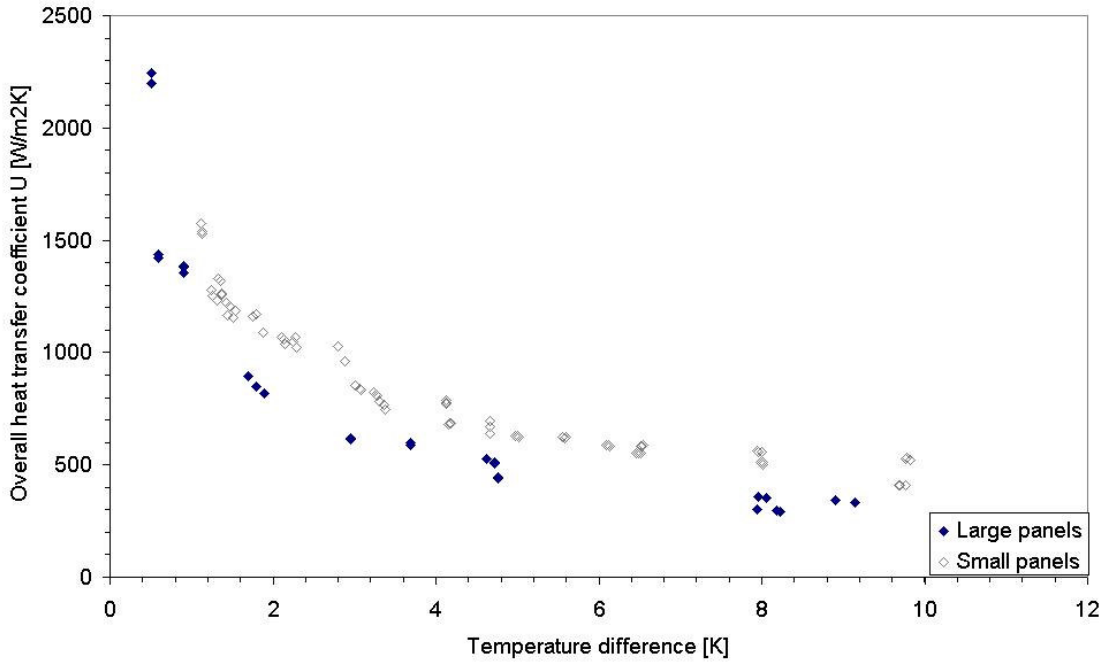

Figure 21: Comparison of experimental heat transfer coefficient of small panels and large panels both placed on active tray area

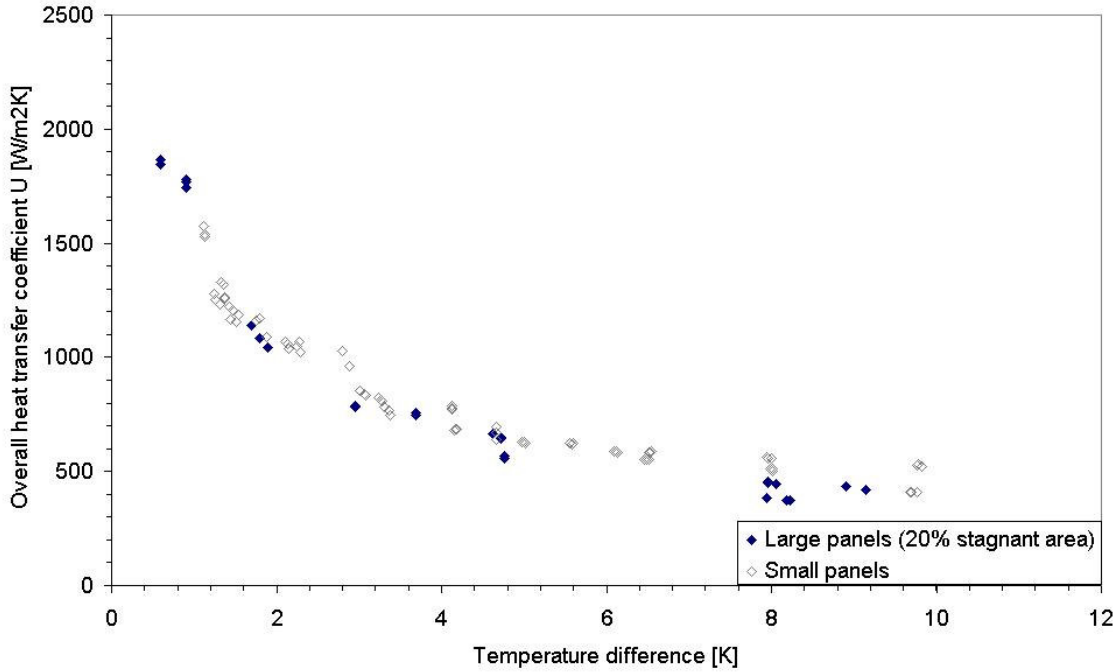

Figure 22: Experimental results for large set of heat transfer panels corrected for stagnant area for vapour flow

Figure 23 shows experimental results for both the tray and downcomer together with the model prediction. The overall heat transfer coefficient drops with temperature difference caused by the increasing film thickness of the

laminar condensate film as explained above. The Alhusseini model was chosen to predict the evaporation side heat transfer coefficient as the mixture on the tray contained more than 85% of cyclohexane and mass transfer limitations have a minor effect on the overall heat transfer coefficient at high concentrations of the light component (21, 22). Moreover it was not possible to obtain experimental data in the heat transfer panel test setup for light mixtures of C6/C7 as atmospheric pressure steam was used as heating medium and consequently driving forces

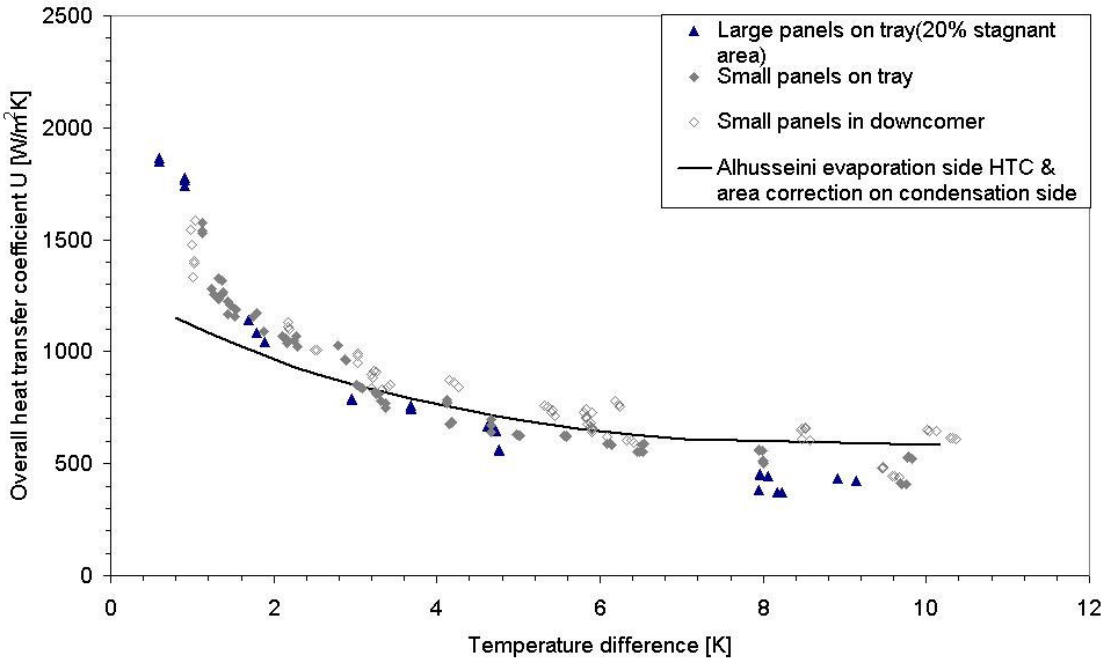

Figure 23: Experimental results and model prediction for overall heat transfer coefficient for small panels in downcomer, small panels on tray and large panels on tray.

for heat transfer were too high for surface evaporation of mixtures containing more than 30% cyclohexane. The Nusselt model was used to predict the condensation side heat transfer coefficient. Partial wetting was taken into account for condensate flows below 18 kg/hr. An inversely linear relation was assumed between the mass flow of condensate and the fraction of the panel wetted by the film. As can be seen Figure 23 the model still under predicts the heat transfer coefficients for temperature differences below 1 ºC. It must be noted that the experimental error at these low temperature differences is relatively large due to the very low condensate flows compared to the large scale of the equipment. Moreover a concentric HIDiC with heat panels won't be operated at such small temperature differences in industrial practice,

because surface area requirement would be too large to be economically justified.

Figure 24 shows the influence of column vapour load (F-factor) on the overall heat transfer coefficient for the panels placed on the tray deck. The effective overall heat transfer coefficient increases linearly with increasing F-factor. This is caused by the fact that the panels are not sufficiently wetted at low F-factor due to the decrease in froth height.

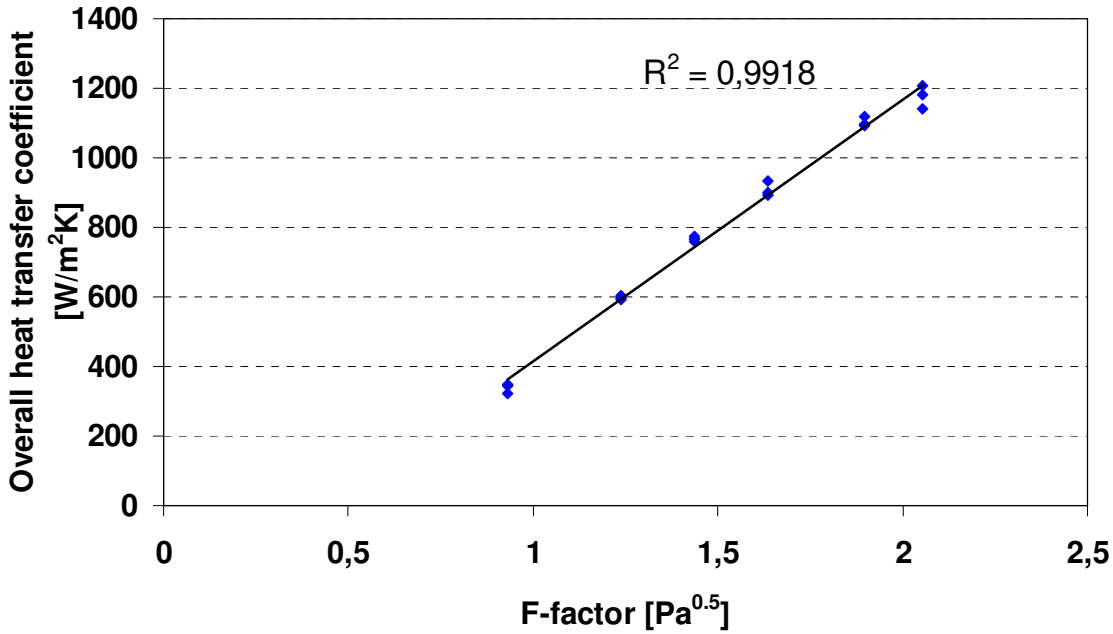

Figure 24: Experimental values and linear regression showing influence of column capacity on measured overall heat transfer coefficient for large panels on tray.

This decrease in froth height was also observed visually. As can be seen in Figure 25 the froth height calculated by the Bennett model (25) also shows a linear relationship with column F-factor for our column operating at total reflux. From these results it is obvious that for a HIDiC equipped with heat panels high vapour load operation is preferred because it ensures good wetting of the panels.

Another option is to place the panels closer to the tray deck. In this study the heat transfer panels were placed at a distance of 90 mm from the tray deck and the height of the panels was 350 mm. As will be discussed elsewhere placing the heat panels closer to the tray deck has a beneficial effect on the separation efficiency as it will hinder the back mixing on the tray, leading to a higher overall tray efficiency (Chapter 4).

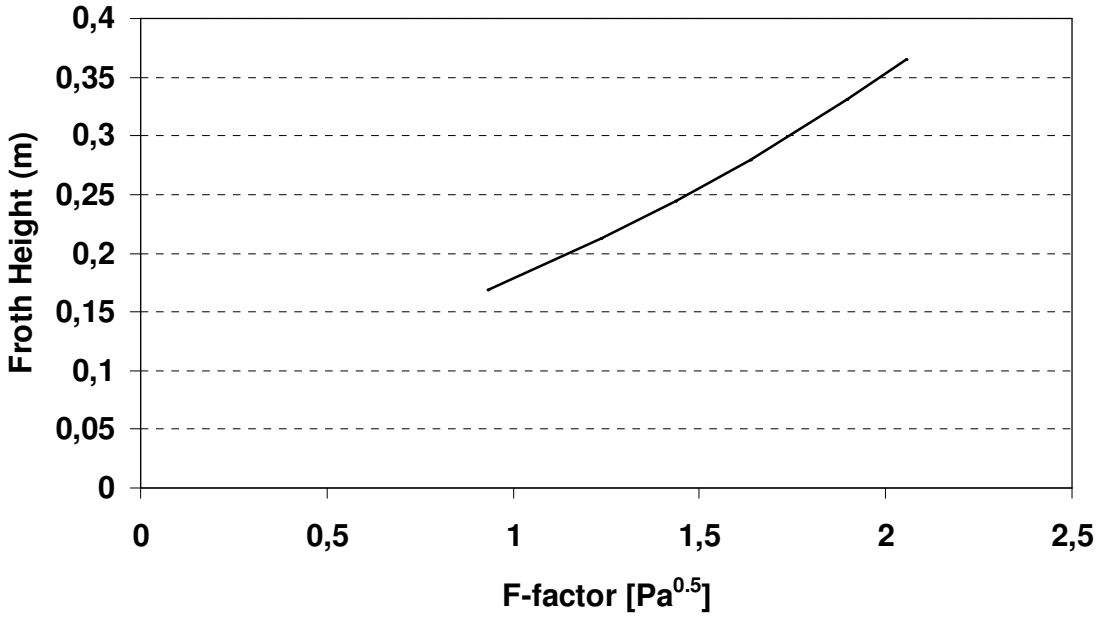

Figure 25: Bennett model for froth height as function of column capacity

3.5 Conclusions

The overall heat transfer coefficient was determined for heat transfer panels placed in the downcomer and on the active area of a sieve tray respectively. Process fluid for both the condensing side and evaporating side of the heat transfer panel was a hydrocarbon mixture of cyclohexane/(n)-heptane.

There appears to be no difference between the overall heat transfer coefficient of panels placed in the downcomer and those placed on the tray deck because of the laminar flow conditions at the condensation side of the heat panels. It follows that the heat transfer is governed by the condensation side.

The overall heat transfer coefficient is strongly dependent on driving force for heat transfer, also because of the laminar flow conditions at the condensation side. Overall heat transfer coefficients varied between 700 and 1500 W/m^2K for operating conditions (mainly temperature difference between stripping and rectifying section) of practical interest to HIDiC.

The Alhusseini model appeared to be the most suitable to predict heat transfer coefficient for an evaporating liquid film in the transition regime between laminar and turbulent flow. The Nusselt model was in good

agreement with the experimental condensation side heat transfer coefficient, except for the low Reynolds numbers, indicating partial wetting of the heat transfer surface.
The vapour inlet manifold to the heat transfer panels must be carefully designed to minimize the pressure drop and to avoid stagnant zones inside the panels.

3.6 Nomenclature

a	thermal diffusivity	m^2/s
D	diameter of pipe	m
D_{AB}	diffusivity of the mixture	m^2/s
f	Darcy friction factor	-
F_c	mixture correction factor	-
g	gravitational acceleration	9.81 m/s^2
h	the heat transfer coefficient	W/m^2K
h^*	dimensionless heat transfer coefficient	-
k	mass transfer coefficient	m/s
Ka	Kapitza number	-
L	length of pipe	m
M	molecular weight	g/mol
N	mass flux	kg/m^2s
Re	Reynolds number	-
Sc	Schmidt number	-
Sh	Sherwood number	-
T_A	boiling point light key component	K
T_i	interface temperature	K
T_s	saturation temperature	K
T_w	wall temperature	K
u	velocity of vapour	m/s
x	mole fraction	-
x_b	mole fraction in bulk	-
x_i	mole fraction at the interface	-
y	distance from the wall	-
Γ	liquid mass flow per unit width	kg/s·m
δ	film thickness	m
δ^+	dimensionless turbulent film thickness	m
ε_M	eddy diffusivity for momentum	m^2/s
η	liquid viscosity	Pa.s
θ	liquid contact angle	º
λ	thermal conductivity	W/mK
μ	viscosity of the liquid	Pa.s
v	kinematic viscosity	m^2/s

ρ	liquid density	kg/m^3
σ	surface tension	N/m

3.7 References

(1) Humphrey, J.L., Seibert, A.F. and Koort, R.A.*,* Separation technologies advances and priorities, Final Report for US Department of Energy, Office of Industrial Technologiest, Washington DC*,* (1991)

(2) Olujic, Z., Fakhri, F., de Rijke, A., de Graauw, J. and Jansens, P.J., Internal heat integration – the key to an energy conserving distillation column, *J Chem Technol Biotechnol*, **78**, 241-248 (2003)

(3) Mah, R.S., Nicholas, J.J. and Wodnik, R.B., Distillation with Secondary Reflux and Vaporization, a comparative evaluation, *AIChE J*, **23** pp 651-658 (1977)

(4) Seader, J.D. and Baer, S.C., Continuous Distillation Apparatus and Method, final report, University of Utah, Salt Lake City (1984)

(5) Glenchur, T. and Govind, R., Study on a continuous Heat Integrated Distillation Column, *Separation Science and Technology*, **22**(12), 2323-2338 (1987)

(6) Nakaiwa, M., Internally Heat Integrated Distillation Columns: a review, *Trans IChemE,* **81** Part A, (2003)

(7) Aso, K., Takamatsu, T. and Nakaiwa, M., Heat Integrated Distillation Column, U.S. Patent 5,873,047 (1998)

(8) De Graauw, J., Steenbakker, M.J., de Rijke, A., Olujic, Z. and Jansens, P.J., Distillation column with heat integration, Patent Application EP1476235 (2004)

(9) Olujic, Z., Sun, L., De Rijke, A., and Jansens, P. J., 2004, Design of an Energy Efficient Propylene Splitter, *Submitted for publication in Energy*

(10) Seader, J.D. and Baer S.C. Continuous Distillation Apparatus and Method, final report, University of Utah, Salt Lake City (1984)

(11) Kaeser, M. and Pritchard, C.L., Heat Transfer at the Surface of Sieve Trays, *Trans ICHemE,* **83**, 1038-1043 (2005)

(12) VDI-Wärmeatlas, 7. Auflage, 1994

(13) Kapitza, P.L. Wave Flow of Thin Films of Viscous Liquids, Collected Papers of Kapitza, Pergamon Press Ltd. 662-689 (1949)

(14) Slegers, L. and Seban, R.A., Nusselt Condensation of n-Butyl Alcohol, *International Journal of Heat and Mass Transfer*, **12**, 237-239 (1969)

(15) Kutateladze, S.S., Fundamentals of Heat Transfer, Academic Press Inc, 303-308 (1963)

(16) Chun, K.R., Seban, R.A. Heat Transfer to Evaporating Liquid Films, *Journal of Heat Transfer*, **89**, 391-396 (1971)

(17) Schnabel, G., Schlünder, E.U. Wärmeübergang van senkrechten Wänden an nichtsiedende und siedende Rieselfilme, Verfahrenstechnik, 14(2), 79-83, (1980)

(18) Haase, B. Beitrag zur Klärung der Wärmeübertragungsverhältnisse an einem siedenden Rieselfilme, Dissertation TH Magdeburg, (1966)

(19) Elle, C. Der Wärmeübergang bei der Rieselfilmverdampfung de Kältemittels R11 und des Kältemittel-Öl-Gemisches R11-51KM33, Dissertation TU Dresden, (1970)

(20) Alhusseini, A.A. et al., Falling Film Evaporation of Single Component Liquids, *International Journal of Heat and Mass Transfer*, **41**, 1623-1632. (1998)

(21) Alhusseini, A.A. Heat and mass transfer in falling film evaporation of viscous liquids, Ph.D. thesis, Lehigh University, Bethlehem, Pennsylvania (1995)

(22) Palen, J.W., Wang, Q., Chen, J.C. Falling Film Evaporation of Binary Mixtures, *AIChE Journal*, **40**(2), 207-214 (1994)

(23) Palen, J.W., Chen, J.C. (1989) Falling Film Evaporation of Wide-Boiling-Range Mixtures: Correlation of Heat Transfer Data, *AIChE Symposium Series*, **85**, 66-71

(24) El-Genk, M.S. and Saber, H.H., *Int. J. Heat Mass Transfer.* **44**, pp. 2809-2825, (2001)

(25) Bennett, D.L., Kao, A.S. and Wong, L.W., *AIChE J.* **41,** pp. 2067-2082 (1995)

Chapter 4:

Mass Transfer Performance of an Annular Heat Integrated Sieve Tray

Abstract

This paper presents the results of a pilot scale experimental study performed with the objective to determine the effects of the heat transfer panels installed above the active area of an annular sieve tray as encountered in a concentric internally heat integrated column (HIDiC). The outer and inner diameters of the stripping section were 0.8 m and 0.3 m, respectively, and the total reflux distillation experiments have been carried out with cyclohexane/n-heptane system at atmospheric pressure. The measured pressure drop and overall tray efficiency of the annular sieve tray resembled that obtained with a cross flow sieve tray at FRI under similar operating conditions, and it appeared that heat transfer panels have a significant enhancing effect on tray efficiency.

Key words: *Heat Integration, HIDiC, Distillation, Murphree efficiency, Tray Efficiency, Pressure drop*

4.1 Introduction

Although the HIDiC concept was already introduced in the seventies and a lot of research was carried out until this moment (1-4), HIDiC is still not implemented in industrial practice. The main barrier for industrial implementation is obviously the complexity of the column design and also the lack of experimental data at sufficiently large scale to prove the practical feasibility of the HIDiC principle. From 1996 a Japanese consortium published experimental results of pilot plant experiments in a HIDiC which is constructed like a shell and tube heat exchanger, in which the tube side is the rectifying section and the shell side is the stripping section. Column internals can be both random or structured packing. (5).

The concentric column concept introduced by Govind (3) has been further developed with respect to heat transfer devices to be placed between the trays of the rectification or stripping section (6). The proposed HIDiC column designs in literature are schematically shown in Figure 1.

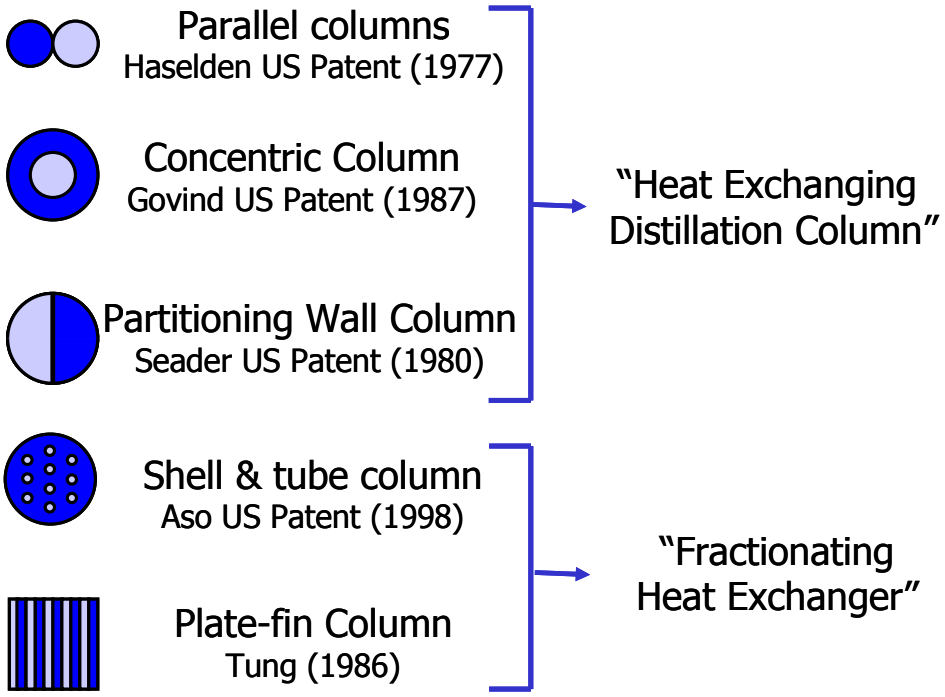

Figure 1: Proposed configurations for a heat-integrated distillation column

A HIDiC is especially favourable for the separation of close boiling mixtures, requiring large heat transfer duties per stage; therefore a lot of internal heat transfer area has to be installed inside the distillation column (7). It is known from industrial practice that close boiling mixtures are separated in tray columns as structured or random packing cannot handle efficiently the large liquid loads in these applications. Therefore a tray appeared to be the preferred column internal for a HIDiC. In the proposed HIDiC design, which is

basically a concentric distillation column, an annular stripping section is configured around the rectifying section. Heat transfer area is provided by heat transfer panels which are placed in the stripping section preferably or the rectifying section. (*figure 2*).

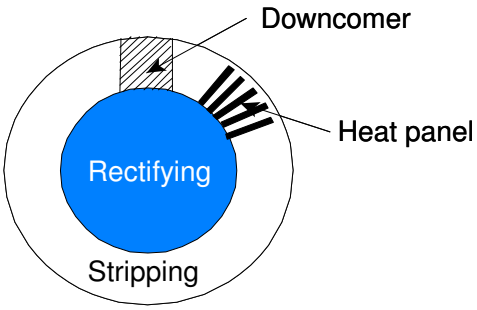

Figure 2: Placement of heat transfer panels in stripping section

In the case that the heat panels are placed in the stripping section, vapour from the rectifying section should enter the panels condense inside and the condensate will flow back into the rectifying section. On the outer surface of the panels simultaneous evaporation of liquid will take place in the stripping section. It should be noted here that the driving force for vapour to enter the panels should be created by the condensation of the vapour inside the panels, as there is virtually no pressure difference between the inlet and outlet of the panels. Although pressure drop calculations showed that the condensation process should start spontaneously, it is clear that this should be validated experimentally. Moreover very little is known of heat transfer characteristics in the froth of an operating distillation tray. Experimental values for both heat transfer coefficient and Murphree tray efficiency for a laboratory scale, 0.1 m diameter sieve tray, in which the heat was provided by means of an external heat transfer medium circulating through a coil mounted inside a thick sieve tray, were reported by Kaiser et al (8) for the model system methanol-water.
The research objectives of the present study are to determine the separation efficiency and pressure drop of an annular sieve tray, compared to a conventional cross-flow sieve tray. The second objective is to study the influence of the presence of heat transfer panels on the separation efficiency. Because the panels are placed on the active area of the distillation tray, they are expected to exhibit some influence on the tray hydraulics and therefore on the separation efficiency. The third objective is to study the influence of the heat transfer process inside the stripping section on the mass transfer efficiency. It was expected that the light component will be evaporated

preferably at the heat exchanger surface and therefore the internal evaporation in the distillation column should have a positive influence on the separation.

4.2 Experimental

A pilot plant has been built, which is basically an annular sieve tray column in which heat transfer panels can be placed in either the downcomer or on the active area of an operating tray. The column data are summarized in *table 1:*

Table 1: Distillation pilot plant data

Diameter outer column	800 mm
Diameter inner column	300 mm
Number of trays	3
Tray spacing	500 mm
Hole size	10 mm
Hole pitch	30 mm
Tray area	0.38 m^2
Downcomer area	0.08 m^2

The model system for this study was cyclohexane/(n)-heptane. The column is operating atmospherically under total reflux and samples can be taken from the top and bottom products in order to determine the separation efficiency of these annular trays. The samples were analyzed with gas chromatography. View glasses were mounted in order to visually observe the behaviour of the froth on the distillation tray. The pressure drop of each tray was measured with high accuracy pressure transmitters.
In order to measure the overall heat transfer coefficient and to study the influence of the internal heat transfer on the mass transfer efficiency a separate setup was built to feed the heat transfer panels with hydrocarbon vapour, (figure 3) which was also a mixture of cyclohexane/(n)-heptane .

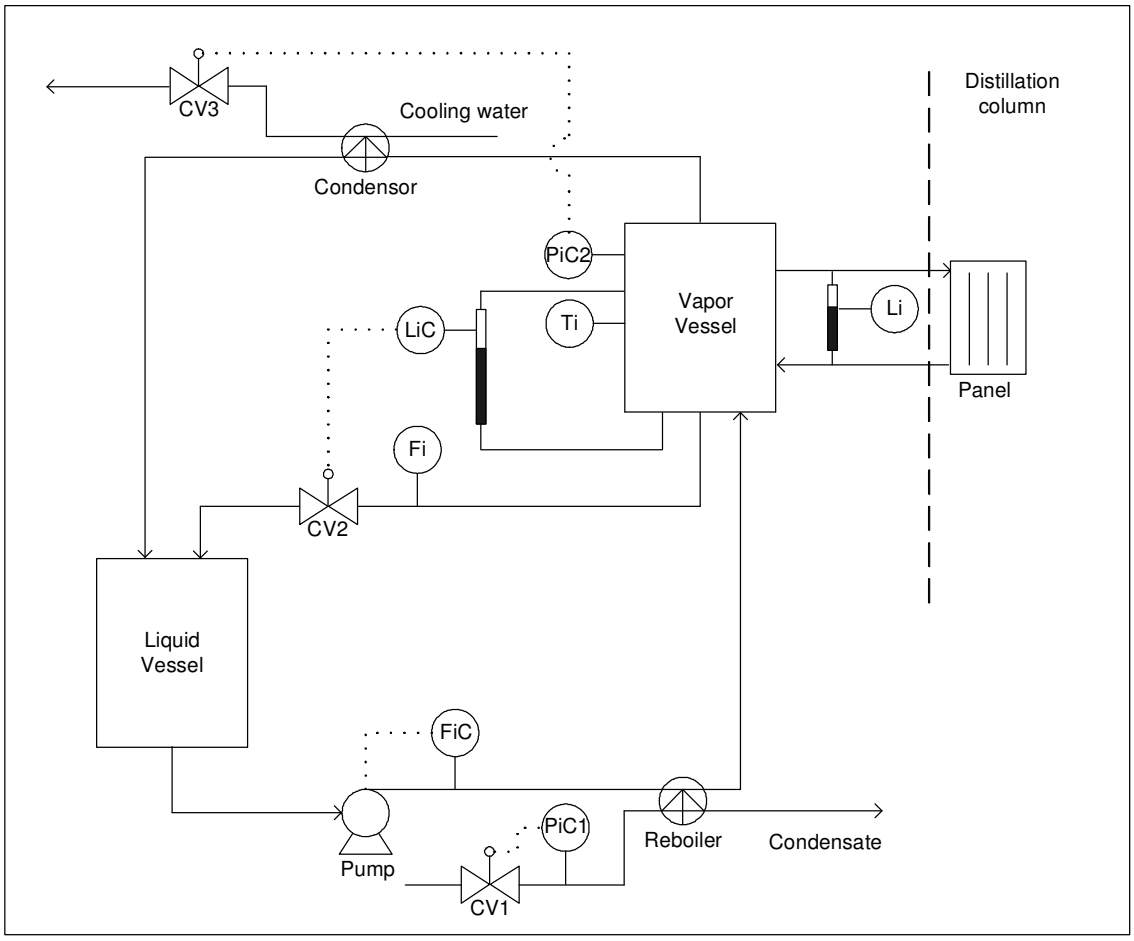

Figure 3: Process Flow Diagram of vapour feed unit

This separate column simulates the behavior of the rectifying section. The operating pressure of the vapour feed column was slightly higher than atmospheric pressure, namely in the range 1.05 to 1.5 bar, to create the desired temperature difference between the two sections. The vapour is slightly superheated to avoid condensation inside the setup, before the vapour enters the heat transfer panels. As a consequence of the condensation process inside the heat transfer panels, there will be a driving force for the vapour to enter the panels and subsequently condense against the colder surface of the heat transfer panels. The condensate quantity is measured with a coreolis mass flow meter.

Figure 4 shows the layout of the heat transfer panels which were placed at the annular tray deck in this study. The height of the panels was 300 mm and the distance between the panels 30 mm. The panels were placed more or less in the direction of the liquid path at a distance of 90 mm above the tray in order to avoid too much interference with the liquid flow over the tray.

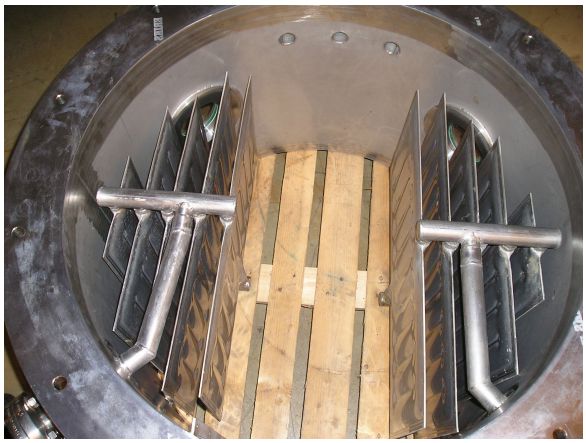

Figure 4: Orientation of heat transfer panels in HIDiC pilot plant.

The third expected effect of the heat transfer panels on separation efficiency is the preferential evaporation of the light component on the panel surface. To determine this additional effect on overall tray efficiency, experiments were carried out both with heated panels and with panels which were not heated. The tests with cold panels are meant to study the effect on tray hydraulics and additional surface area for mass transfer. The tests with hot panels are carried out to determine the additional mass transfer enhancement caused by the evaporation process on the outside of the heat transfer panels.

4.3 Modeling

4.3.1 Mass Transfer Models

Several attempts have been made to develop a method for the reliable prediction of distillation tray efficiency. The need of a more reliable efficiency model was felt strongly by chemical and petrochemical industries which resulted in a large research consortium of three universities sponsored by the chemical industry, which eventually lead to the well known AIChE model (9).
Chan and Fair (10) adjusted the empirical relations for the volumetric mass transfer coefficients based on newly obtained experimental data from the Fractionating Research Institute. Both the AIChE model and the Chan and Fair model use volumetric mass transfer coefficients and no attempts were made to determine the interfacial area between vapour and liquid phase.
Prado and Fair did a pioneering effort to develop a model for the mixing intensity on the tray and of the different regimes which play a role (from froth regime to spray regime) (11). They evaluated bubbling and jetting using electrical conductivity probes and looked at several different contacting regimes in order to determine theoretically the values for interfacial and mass transfer coefficients. The model of Prado however is based on air/water

experiments in a relatively small size tray column and their experimental technique could not be applied systems with non electrical conductive liquids. Therefore their model does not have a predictive value for hydrocarbon systems in large columns. Garcia and Fair (12) continued the work of Prado et al and extended it to model systems of hydrocarbon mixtures, like cyclohexane/(n)-heptane, water/ethylene glycol, ethylbenzene/styrene and isobutane/(n)butane. They developed an extensive database with experimental data both from open source literature and data obtained in a large scale (1,2 m diameter) sieve tray column at the Fractionating Research Institute (FRI). Their model comparison with the experimental data for the system cyclohexane/(n)-heptane obtained in the FRI column (13, 14) is of great interest for the present study as it handles about the same model system in a distillation column of equivalent size. The Garcia model was able to predict the overall tray efficiency of a conventional sieve tray with the C6/C7 system within 5%. (12). At this moment the model of Garcia appears to be the most suitable model to predict the separation efficiency of the annular sieve tray in a HIDiC as it has proven to work for this model system and it is the only fundamental model so far which is checked against an extensive database of experimentally obtained tray efficiencies and proved to be able to predict the efficiency of these different model system with an average deviation of around 10%. Although for example Taylor and Kooijman (15) developed a dynamic, non-equilibrium model to simulate sieve tray distillation columns, their model was not checked against experimental data from literature so far and it is therefore difficult to judge its applicability to HIDiC. Moreover a lot of physical properties are required to apply their model, which are not readily available and have to be estimated, introducing extra uncertainties in the calculated mass transfer coefficients.

4.3.2 Tray efficiency definitions

The mass transfer efficiency of contacting trays may be expressed in several ways, but in this paper only two efficiencies will be used, the point efficiency and the overall tray efficiency.

4.3.2.1 Point Efficiency: The point efficiency is defined as the approach to equilibrium at some point on the tray. The equilibrium relationship takes the concentration in the exit vapour leaving the froth of the tray and the liquid composition at this specific point on the tray. As a consequence the point efficiency can vary across the length of the tray if there is a variation of liquid composition across the tray. By definition the point efficiency cannot be greater than 1.0. The point efficiency (E_{OG}) on tray *n* is defined as:

$$E_{OG} = \left(\frac{y_n - y_{n-1}}{y_n^* - y_{n-1}} \right)_{po\,\mathrm{int}} \qquad [1]$$

Where y is the mole fraction of the light component in the vapour and y^* is the mole fraction of the light component in the vapour, in equilibrium with liquid concentration x.
The efficiency concept is based on two resistance theory. Assuming phase equilibrium at the interface, the overall mass transfer coefficient can be obtained by the sum of the two mass transfer resistances according to the next relationship:

$$\frac{1}{K_{OG}} = \frac{1}{k_G} + \frac{m}{k_L} \qquad [2]$$

Where K_{OG} is the overall mass transfer coefficient, k_G is the gas-side mass transfer coefficient, k_L is the liquid-side mass transfer coefficient and m is the slope of the equilibrium curve dy^*/dx.

Considering a mass balance across a differential element in the froth of the sieve tray, the next expressions can be deduced for the number of mass transfer units (N) in the vapour and liquid phase:

$$N_G = k_G a_i' t_G \qquad [3]$$

and,

$$N_L = k_L a_i' t_L \qquad [4]$$

Where $k_G a_i^{'}$ and $k_L a_i^{'}$ are volumetric coefficients. Volumetric mass transfer coefficients are often used in modeling tray efficiencies as the interfacial area in the froth of a distillation tray is very difficult to determine accurately. t_G and t_L are the residence times in respectively the vapour phase and liquid phase.

The number of overall transfer units (N_{OG}) can be calculated from the individual mass transfer units with:

$$N_{OG} = \left(\frac{1}{N_G} + \frac{\lambda}{N_L} \right)^{-1} \quad [5]$$

Where λ is the ratio of slopes of the equilibrium and operating line:

$$\lambda = \frac{m}{\left(L_M / G_M \right)} \quad [6]$$

L_M is the molar flow rate of liquid and L_G is the molar flow rate of vapour. The point efficiency is next computed from N_{OG}:

$$E_{OG} = 1 - \exp(-N_{OG}) \quad [7]$$

4.3.2.2 Overall Tray Efficiency: The most widely used tray efficiency is the Murphree efficiency (E_{mV}) or overall tray efficiency. The approach to equilibrium is based on the average vapour and liquid composition leaving the tray. Because of its definition the Murphree efficiency can be higher than 100%. The model is based on the assumption that vapor and liquid entering each tray are of uniform compositions. The relation between the point

efficiency and Murphree efficiency depends on the mixing behaviour of the two phases present on the tray.
For the case that the liquid on the tray is completely mixed, the vapour passing through the liquid is in plug flow and the exiting vapour is assumed to mix completely before entering the tray above, the Murphree efficiency is equal to the point efficiency:

$$E_{mV} = E_{OG} \qquad [8]$$

Only if the liquid travel distance across the tray is small, the liquid on a tray will approach complete mixing. Complete liquid mixing will be definitely not the case for large industrial scale distillation columns and even not for the size of the column which was used in this experimental study.

For the case that the liquid on the tray is in plug flow (vapour is in plug flow, exiting vapour will mix completely before entering tray above), the Murphree Efficiency is related to the point efficiency by (Lewis, (34)):

$$E_{mV} = \frac{\left(\exp\left(\lambda E_{OG}\right) - 1\right)}{\lambda} \qquad [9]$$

Equations [8] and [9] represent extremes between complete mixing and no mixing of the liquid phase respectively.
More realistic models account for partial liquid mixing on the tray. The relation of Bennett and Grimm (27) offers improvements over earlier models: it has a fundamental basis not limited to air-water and when compared to axial mixing data it gives significantly lower errors than the previous models. In the Bennett and Grimm model the eddy diffusion coefficient is taken as a function of the height of the froth layer:

$$D_E = 0.02366\left(h_{frothlayer}\right)^{3/2}\sqrt{g} \qquad [10]$$

The height of the froth layer is determined from individual heights of vapour-continuous and liquid-continuous regions as proposed by Bennet et al (28).

The average residence time of the liquid t_L is based on a hold-up correlation given in that paper.
The eddy diffusion coefficient is used to calculate the dimensionless Peclet number (Pe_L):

$$Pe_L = \frac{L_T{}^2}{D_E t_L} \qquad [11]$$

Where L_T is the length of travel across the tray. (m)

The relation of Murphree efficiency and point efficiency was developed by Gerster (35):

$$\frac{E_{mV}}{E_{OG}} = \frac{1 - e^{-(\eta + Pe_L)}}{(\eta + Pe_L)\cdot\left[1 + \frac{\eta + Pe_L}{\eta}\right]} + \frac{e^{\eta} - 1}{\eta \cdot \left[1 + \frac{\eta}{\eta + Pe_L}\right]} \qquad [12]$$

Where

$$\eta = \frac{Pe_L}{2}\left[\sqrt{1 + \frac{4\lambda E_{OG}}{Pe_L}} - 1\right] \qquad [13]$$

4.3.2.3 Column Efficiency

In practice the column efficiency is most widely used and best understood. It is the ratio of theoretical stages, as determined from the observed separation, to the actual number of trays that are installed in the distillation column. In this study the column efficiency is measured and the overall tray efficiency is calculated from the measured column efficiency.

4.3.3 Garcia and Fair Model

To obtain a hydraulic model of the dispersion above the tray deck of a sieve tray, the operating tray is divided in a number of zones, which are characterized by the type of flow which is predominantly present in this zone

and varies from small bubbling through large bubbling to jetting as was discussed thoroughly by Hofhuis and Zuiderweg (16) Jetting occurs at very high gas to liquid loads, when momentum of vapour is relatively large compared to momentum of liquid and the jets therefore are not likely to break up into bubbles.
The froth regime is most commonly found in a distillation column and the principal focus of their work. The froth regime is characterized by a liquid mixture, containing a variety of bubble sizes.

The bubble size distribution must be predicted in order to determine the interfacial area for mass transfer. A bi-modal bubble size distribution for air-water has been observed by many researchers (17-19) and was included in the original Prado model.

Sauter mean bubble diameter at formation The Sauter mean bubble diameter at formation is influenced by the rate of liquid cross-flow. To determine the bubble size at formation a relation was developed which includes the effect of liquid cross flow on the tray deck as suggested by several researchers (21-23). This effect is particularly important in high pressure distillations and also in a total reflux situation.

$$d_{BLS} = \Psi \times 0.605 \frac{d_H^{0.84} u_H^{0.18}}{L_V^{0.07}} \qquad [14$$

$$d_{BSS} = \Psi \times 0.66 \frac{d_H^{0.84} u_H^{0.85}}{L_V^{0.08}} \qquad [15]$$

$$\Psi = \left(h_{W,CBS}\right) \times \left(\eta_{L,CBS}\right) \times \left(\sigma_{CBS}\right) \qquad [16]$$

d_{BLS} Sauter mean diameter at formation of large bubbles [m]
Ψ Correction factor for bubble size [-]
d_H Orifice diameter [m]

u_H Gas phase superficial velocity based on hole area [m/s]
d_{BSS} Sauter mean diameter at formation of small bubbles [m]
L_V Liquid cross flow over tray deck per meter weir length [m^3/s m weir]
$h_{W,CBS}$ Weir height, corrected for bubble size [-]
$\eta_{L,CBS}$ Liquid viscosity, corrected for bubble size [-]
σ_{CBS} Surface tension, corrected for bubble size [-]

Bubble break-up In gas-liquid contactors operating under turbulent conditions, the bubble breakup can be modeled using isotropic turbulence theory. Walter and Blanch (24) applied this theory validated by experimental results and developed a correlation to predict the maximum stable bubble size (d_M):

$$d_M = 1.12 \frac{\sigma^{0.6}}{\left(\frac{P}{V}\right)^{0.4} \rho_L{}^{0.2}} \left(\frac{\eta_L}{\eta_V}\right)^{0.1} \quad [17]$$

Where σ is the surface tension (N/m), ρ_L is the liquid density (kg/m^3) and η is the viscosity (Pa.s)

The power per unit volume (P/V) for a tray was proposed by Calderbank (23)

$$\left(\frac{P}{V}\right)_{SieveTray} = U_{VSA} \rho_L g \quad [18]$$

Where U_{VSA} = the superficial vapour velocity based on the active tray area (m/s) and g is the gravitational constant (m/s^2)

Wilkinson (24) demonstrated that the bubble stability strongly depends on three physical properties, namely surface tension, liquid viscosity and vapour density. Garcia and Fair assumed a linear effect of these properties on the bubble size distribution. A linear regression was conducted using two extreme cases: air-water at atmospheric conditions and i-butane/n-butane at high

pressure. (14), which lead to the next expression for the resulting maximum stable bubble diameter of bubbles present in the froth:

$$D_{BL} = d_M \left[0.83 + 41.5 \left\{ \sigma^{0.6} \left(\frac{\eta_L}{\rho_V} \right)^{0.1} \right\} \right] \qquad [19]$$

The large bubbles formed at a diameter of D_{BLS} are assumed to break up in bubbles with a diameter of the maximum stable bubble size D_{BL}. The small bubbles formed at a diameter of D_{BSS} are assumed not to break up, but will rise through the liquid present at the tray deck. Hence the resulting bimodal bubble size distribution in the bulk froth regime consists of bubbles with a diameter D_{BL} and D_{BSS}.

It is evident that the ratio between the number of small bubbles and number of large bubbles is required to determine the interfacial area. A relation was developed to calculate the number of small bubbles as fraction of the total number of bubbles, which appeared to be a distinct function of the physical properties, of the two-phase system present on the tray.

The fraction of small bubbles in the froth (AJ) was set at 0.532 for air-water at atmospheric pressure in the Prado and Fair model. Garcia and Fair use the following correlation to calculate AJ for other systems:

$$AJ = 1 - 0.463 \left[SP_{RATIO} \right] \qquad [20]$$

$$SP_{RATIO} = \left(\frac{\sigma}{\sigma_{wat}} \right)^{0.6} \left(\frac{\eta_L}{\eta_{wat}} \frac{\eta_{air}}{\eta_G} \right)^{0.1} \left(\frac{\rho_{wat}}{\rho_L} \right)^{0.6} \left(\frac{\rho_{air}}{\rho_G} \right)^{0.1} \qquad [21]$$

AJ Fraction of small bubbles in the bulk froth zone [-]
SP_{RATIO} Stability parameter ratio [-]
σ_{wat} Surface tension of water [N/m]
η_{air} Viscosity of air [Pa·s]
η_{wat} Viscosity of water [Pa·s]
ρ_{wat} Density of water [kg/m^3]
ρ_{air} Density of air [kg/m^3]

4.3.4 Influence of heat transfer panels on tray efficiency

The presence of heat transfer panels will influence the tray hydraulics and therefore it is expected that the panels will influence separation efficiency. At the first place the wetted surface area of the heat transfer panels provides additional surface area for mass transfer in analogy with the mass transfer taking place at the wetted surface of a structured packing. This influence of extra interfacial are can be estimated using the so-called 'Delft-model' which was described in detail by Olujic et al (30), simply by changing the corrugation inclination angle to vertical i.e. 90 degrees.

The second effect of the heat transfer panels on the tray efficiency is the influence of the panels on the liquid and vapour flow patterns on the tray. The panels are oriented in such a way on the tray that they operate as guiding vanes for the liquid and it is therefore expected that the presence of the panels will hinder the back mixing of the liquid i.e: induce a more plug flow character of the moving liquid, leading to an increase in separation efficiency.

Ashley and Haselden (31, 32) performed experiments with baffles above a distillation tray and they found that the panels improved mass transfer because:

- the panels prevent the formation of large bubbles, leading to more interfacial area and therefore to higher point efficiencies and
- the panels will change the fluid dynamics, leading to less back mixing and therefore a higher Murphree tray efficiency

In the study of Ashey and Haselden, however the baffles were placed at a distance of 6.4 mm of the tray deck. This small distance is considered to be the main reason for the prevention of the formation of the large bubbles at the outlet of the sieve tray holes. In the present study the panels are placed at a distance of 90 mm of the tray deck, so that formation of large bubbles, which are in the order of magnitude of 25 mm (13, 19, 20, 21) is not likely to be prevented by the presence of the heat panels. Moreover Ashley and Haselden were not able to measure bubble sizes during their experiments and therefore the assumption of a larger fraction of small bubbles in the froth as a consequence of the presence of the baffles, was not proven.

To model the hindering of back-mixing by the heat transfer panels, the liquid phase on the tray is considered to be a number of ideally mixed tanks in series, which is a classical way to simulate a case where mixing intensity lies between ideally mixed and plug flow. When the number of mixed tanks approximates infinity, the flow will be in complete plug flow. This method was

successfully applied earlier by Gautreaux and O'Connel (33) to calculate the Murphree efficiency for these intermediate cases of mixing.

$$E_{mV} = \frac{1}{\lambda}\left[\left(1+\frac{\exp(\lambda E_{OG})}{n}\right)^{n} - 1\right] \qquad [22]$$

Where n is the number of perfectly mixed tanks on the tray and E_O is the overall tray efficiency.
When the number of pools approaches to infinity, equation [22] reduces to equation [9], which is equivalent to Lewis case I (liquid plug flow, vapour plug flow).

4.3.5 Pressure drop

The pressure drop across the sieve tray is calculated by the method proposed by Bennett (28).
It is assumed that the total tray pressure drop consists of three main contributions: liquid inventory on the tray (h_L) , dry hole pressure drop (h_D) and pressure drop due to surface tension (h_σ) (in mm of liquid):

$$h_T = h_L + h_D + h_\sigma \qquad [23]$$

The clear liquid height is calculated as follows:

$$h_L = \Phi_{Fe}\left[h_W + C\left(\frac{L_{VW}}{\Phi_{Fe}}\right)^{2/3}\right] \qquad [24]$$

$$\Phi_{Fe} = \exp\left(-12.55K_s^{0.91}\right) \qquad [25]$$

$$K_s = u_s\sqrt{\frac{\rho_G}{\rho_L - \rho_G}} \qquad [26]$$

$$C = 0.0317 + 0.0286 \cdot \exp\left[-137.8 h_W\right] \quad [27]$$

Φ_{Fe} Relative froth density [-]
C Constant, defined by equation [27] [-]
L_{VW} Liquid phase volumetric flow rate per unit of weir length [$m^3/s \cdot m$]
K_s Constant, defined by equation [26] [m/s]
u_s Gas phase superficial velocity based on column cross sectional area [m/s]
h_W weir height [m]

The dry hole pressure drop is usually calculated using the following equation:

$$h_D = \frac{a}{c_V^2} \frac{\rho_G u_H^2}{\rho_L g} \quad [28]$$

a Constant [-]
c_V Discharge coefficient [-]
u_H Superficial hole velocity [m/s]

Correlations for a and c_V are given by Leibson (29). A value of 0.499 is suggested for a. c_V is the discharge coefficient.

The pressure drop due to surface tension can be calculated with the following correlation:

$$h_\sigma = \frac{6\sigma}{g \rho_L d_{bub,max}} \quad [29]$$

$$d_{bub,max} = b\left[\frac{d_H \sigma}{g\left(\rho_L - \rho_G\right)}\right]^{1/3} \quad [30]$$

$$b = \left(6 \sin \theta_{bub}\right)^{1/3} \quad [31]$$

$d_{bub,max}$ Departure bubble diameter from sieve tray [m]
b Constant [-]
θ_{bub} Departure contact angle between bubble interface and tray [°]

4.3.6 Influence of heat transfer panels on tray pressure drop

The frictional pressure drop due to vapour flow through narrow channels formed between the heat panels can be described by the following expression:

$$\Delta P_{pp} = \frac{1}{2} f_{pp} \frac{h_p}{d_{hydr,pp}} \rho_L u_{pp}^2 \quad [32]$$

ΔP_{pp} Pressure drop panels [Pa]
f_{pp} Friction factor panels [-]
h_p Panel height [m]
$d_{hydr,pp}$ Hydraulic diameter panels [m]
u_{pp} Gas phase superficial velocity panels [m/s]

The friction factor for parallel plates is defined as:

$$f = \frac{96}{\mathrm{Re}_{pp}} \quad [33]$$

$$\mathrm{Re}_{pp} = \frac{\rho_G u_{pp} d_{hydr,pp}}{\eta_G} \quad [34]$$

Re_{pp} Reynolds number between panels [-]

The hydraulic diameter of the rectangular channel formed between two infinite parallel plates is defined as:

$$d_{hydr,pp} = 2S_{pp} \quad [35]$$

S_{pp} Spacing between panels [m]

4.4 Results and Discussion

The overall tray efficiency of both the annular sieve tray and a conventional, 1.2 m diameter, cross-flow sieve tray which was tested with the mixture cyclohexane/(n)-heptane by the Fractionating Research Institute (14) is plotted in figure 5 as function of the F-factor.

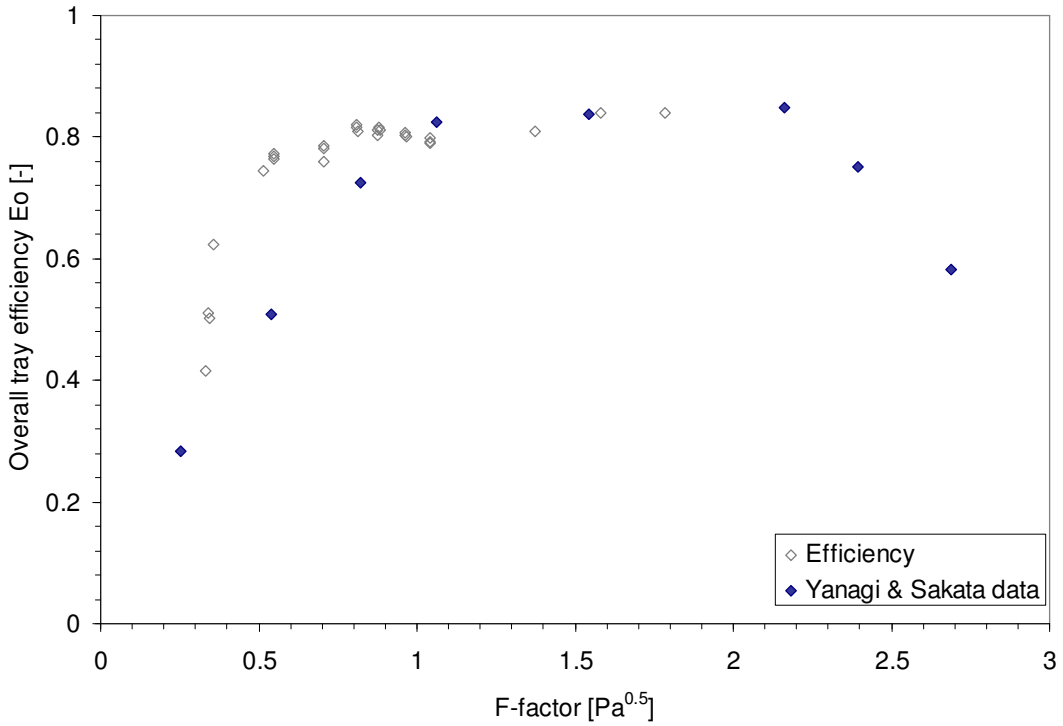

Figure 5: Experimental values for overall tray efficiency of annular tray compared to conventional cross flow sieve tray tested by FRI.

At low column loads the tray efficiency drops steeply due to weeping through the holes of the tray. The sieve tray tested by FRI starts to weep at a slightly higher F-factor due to the fact that the hole area of their tray was 14% compared to 10% for the annular tray. The upper operating limit is determined by flooding i.e.: entrainment of liquid to the next tray. Unfortunately it was not possible to reach the flooding point for the annular tray due to limitation of the reboiler capacity. The main and most important result, however is that the overall column efficiency in the regime in which the sieve trays are operated in practice, is practically equal for both tray layouts. Apparently the annular shape of the tray doesn't influence the Murphree tray efficiency. One could expect a difference in tray efficiency, because the liquid path length at the annular tray is not constant but changes from roughly 200 mm along the inner tube to 950 mm along the outside as a consequence of the annular shape of the tray. At a conventional sieve tray however, the distance between the inlet downcomer and outlet downcomer is constant. Apparently the liquid is so thoroughly mixed at both the tray deck (without heat panels) and in the

downcomers that the difference in liquid path length doesn't influence the overall separation efficiency

Figure 6 shows the experimental results and the model prediction for the overall tray efficiency and pressure drop of the annular sieve tray, respectively The measured overall efficiency in the operating range is in good agreement with the results predicted by the Garcia and Fair model. In the weeping region the model over-predicts the efficiency. Unfortunately it was not possible to check if this was also the case for the model prediction for the cross flow sieve tray as the original publication only shows the model prediction for F-factors above 0.7 for this model system. Moreover this operating region is of limited interest in industrial practice as trays are usually operated at 0.8 of flood limit.

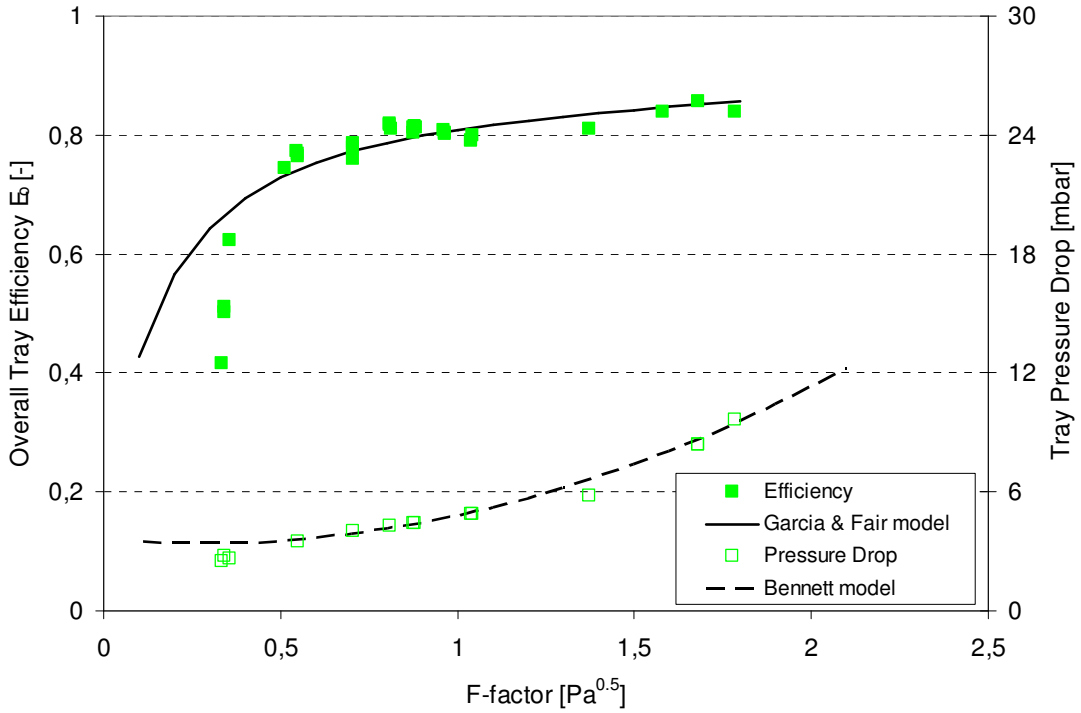

Figure 6: Model Prediction and Experimental Results for Overall Efficiency and Pressure Drop of annular sieve tray without heat panels

The pressure drop model of Bennett appears to be very useful to predict the tray pressure drop (figure 6 & 7). The pressure drop of the annular tray is practically equal to the pressure drop of the cross flow tray operated by FRI (14). The pressure drop increases with F-factor due to the increased vapour velocity through the holes and also the froth height increases at higher column capacity. Both calculations and experimental data (figure 7) indicate that there is no additional effect of the presence of heat transfer panels on the overall tray pressure drop. The vapour velocity between the panels is low, typically in the order of 1 m/s and therefore friction losses and additional

pressure drop can be neglected compared to the pressure drop resulting from dry hole pressure drop, liquid layer pressure drop and the pressure drop resulting from surface tension as incorporated in Bennett's model.

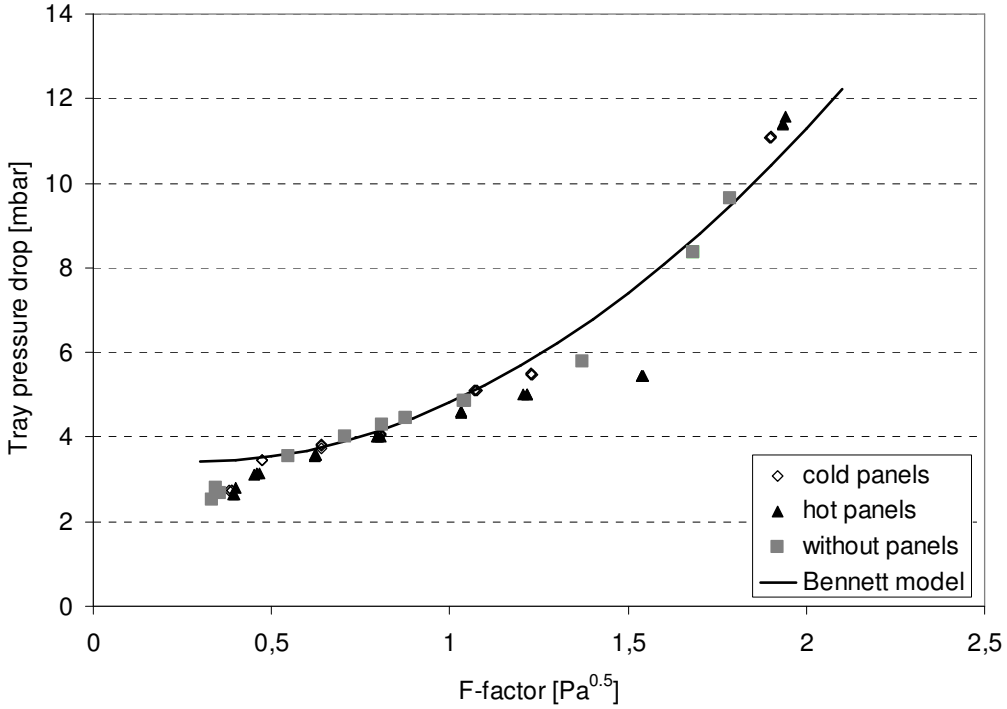

Figure 7: Model prediction and experimental results for pressure drop of annular sieve tray, without panels, equipped with cold panels and equipped with hot panels

Figure 8 shows that the efficiency of the tray with heat panels is substantially higher than that of the empty tray. It should be noted that liquid samples were taken from the top and the bottom of the column and only one the middle tray out of three, namely the central tray, was equipped with heat transfer panels. So both top and bottom trays were operating without panels and only the effect of the panels on the mean tray efficiency could be determined experimentally. The enhancing effect on the tray equipped with heat panels was determined by assuming that the efficiency of the top and bottom tray was not influenced by the presence of heat panels at the central tray. The increase in efficiency for the single tray equipped with heat panels is around 10% in the usual operating range for sieve trays. Also it was found that there is no difference between the cold panels series and the panels which were in operation, due to the fact that the amount of vapour formed at the panel surface was too small compared to the total vapour flow in the column, namely about 2,5 per cent compared to the total vapour flow rate of the column. Although according to theory preferential evaporation of the light

component should take place at the panel surface, having an enhancing effect on the separation, this could not be validated experimentally.

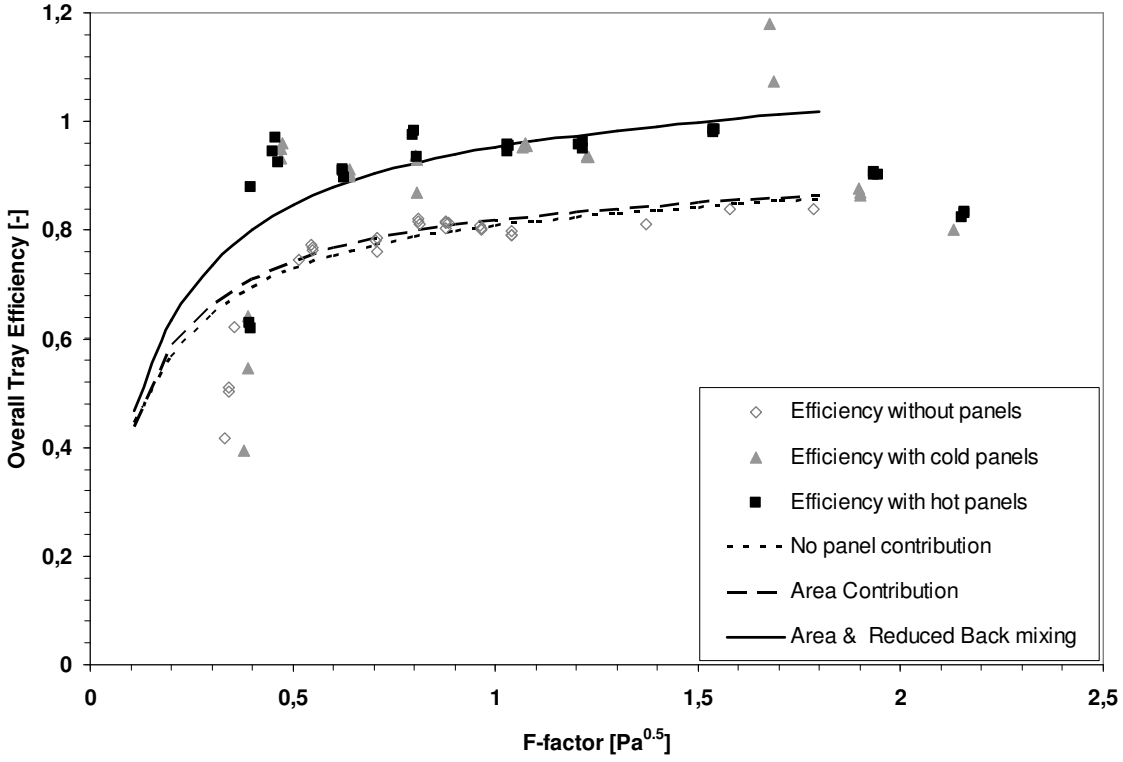

Figure 8: Experimental results and model prediction of overall Tray Efficiency of annular sieve tray without panels, equipped with cold panels and equipped with hot panels

The efficiency increase due to the additional surface area of the heat transfer panels was calculated, using the "Delft-model". As can be seen in figure 8, the additional surface area enhances the separation indeed, but has a relatively low impact, compared to the total increase in efficiency. The main and most important factor is the effect on tray hydraulics, namely the panels hinder the mixing of the liquid at the tray deck, due to the orientation of the panels parallel to the direction of the flow. To calculate this additional effect of the panels on the mixing intensity of the liquid, the tray was divided into a number of perfectly mixed tanks in series as suggested by Gautreaux and O'Connell (33). The resulting model prediction of both the effects of additional surface area and the influence of mixing intensity is depicted by the solid line in figure 8. The number of ideally mixed tanks to predict the measured increase in efficiency is equal to 2. The mixing intensity is influenced by the presence of panels and shows intermediate behaviour between ideally mixed and complete plug flow, but obviously the panels do not create near plug flow as only 2 ideal tanks in series are sufficient to predict the measured separation

efficiency. It is expected that other smart panel configurations, e.g. panels placed at a smaller distance above the tray deck, a smaller spacing between the panels or an orientation more parallel to the direction of the flow, will lead to an extra reduction of back-mixing and therefore a further increase in overall tray efficiency. This could lead to a densely packed tray with a high potential for internal heat transfer. On the other hand a too small spacing between the panels could possibly prevent the full wetting of the panel surface by the splashing froth, leading to a decrease in overall heat transfer coefficient.

4.5 Conclusions

Large scale experiments have been performed with a 0.8 m diameter concentric HIDiC column, operated with the model system cyclohexane/n-heptane to establish the effect of the annular tray layout on the separation efficiency and to determine the influence of heat transfer panels on the overall tray efficiency.

Comparison of the data obtained in this study with measurements by the Fractionating Research Institute shows that separation efficiency of an annular sieve tray resembles that of a conventional cross-flow sieve tray.

The model of Garcia and Fair is able to predict the separation efficiency of the annular sieve tray for F-factors higher than 0.5.

The tray pressure drop was modeled successfully with the Bennett model. The model predicted that the heat transfer panels did not influence the tray pressure drop which was in agreement with experimental results.

Heat transfer panels do have a positive influence on tray hydraulics and enhance the separation efficiency of the tray by roughly 10%, which proves to be a strong advantage of the proposed column design with heat transfer panels placed on the active tray area. The main reason for the increase in tray efficiency is the reduction of back mixing by the panels, which increases the driving force for mass transfer. This additional effect could be simulated by regarding the liquid as two ideally mixed tanks in series.

The heat panel surface provides extra interfacial area which has a minor enhancing effect on the separation efficiency.

4.6 Nomenclature

AJ	fraction of small bubbles in the bulk froth zone (-)
c_V	discharge coefficient (-)
d_{BLS}	Sauter mean diameter at formation of large bubbles (m)
d_{BSS}	Sauter mean diameter at formation of small bubbles (m)
$d_{bub,max}$	departure bubble diameter from sieve tray (m)
D_E	eddy diffusion coefficient (m^2/s)
d_H	orifice diameter (m)

$d_{hydr,pp}$ hydraulic diameter between panels (m)
E_{mV} Murphree tray efficiency (-)
E_{OG} tray point efficiency (-)
f friction factor (-)
f_{pp} friction factor between panels (-)
g gravitational acceleration (m/s^2)
$h_{frothlayer}$ height of froth layer (m)
h_p panel height (m)
h_W weir height (m)
$h_{W,CBS}$ weir height, corrected for bubble size (-)
k_G gas-side mass transfer coefficient (m/s)
$k_G a_i'$ volumetric mass transfer coefficients vapour phase (s^{-1})
k_L liquid-side mass transfer coefficient (m/s)
$k_L a_i'$ volumetric mass transfer coefficients liquid phase (s^{-1})
K_{OG} overall mass transfer coefficient (m/s)
K_s Constant, defined by equation [26] (m/s)
L_G molar flow rate of vapour (mole/s)
L_M molar flow rate of liquid (mole/s)
L_T length of travel across the tray (m)
L_V liquid cross flow over tray deck per meter weir length (m^3/s m weir)
L_{VW} liquid phase volumetric flow rate per unit of weir length ($m^3/s \cdot m$)
m slope of the equilibrium curve dy^*/dx (-)
n number of perfectly mixed tanks on the tray (-)
N_G number of mass transfer units in the vapour phase (-)
N_L number of mass transfer units in liquid phase (-)
N_{OG} number of overall mass transfer units (-)
Pe_L Peclet number (-)
Re_{pp} Reynolds number between panels (-)
S_{pp} spacing between panels (m)
SP_{RATIO} stability parameter ratio (-)
t_G residence time in vapour phase (s)
t_L residence time in liquid phase (s)
u_H gas phase superficial velocity based on hole area (m/s)
u_H superficial hole velocity (m/s)
u_{pp} gas phase superficial velocity between panels (m/s)
u_s gas phase superficial velocity based on column cross sectional area (m/s)
U_{VSA} superficial vapour velocity based on the active tray area (m/s)
y mole fraction of the light component in the vapour (-)
y^* mole fraction of the light component in the vapour, in equilibrium with liquid concentration x (-)

ΔP_{pp}	pressure drop between panels (Pa)
η	viscosity (Pa.s)
η_{air}	viscosity of air (Pa·s)
$\eta_{L,CBS}$	liquid viscosity, corrected for bubble size (-)
η_{wat}	viscosity of water (Pa·s)
θ_{bub}	departure contact angle between bubble interface and tray (°)
λ	ratio of slopes of the equilibrium and operating line (-)
ρ_{air}	density of air (kg/m^3)
ρ_L	liquid density (kg/m^3)
ρ_{wat}	density of water (kg/m^3)
σ	surface tension (N/m)
σ_{CBS}	surface tension, corrected for bubble size (-)
σ_{wat}	surface tension of water (N/m)
Φ_{Fe}	relative froth density (-)
Ψ	correction factor for bubble size (-)

4.7 References

(1) Mah, R.S., Nicholas, J.J. and Wodnik, R.B., Distillation with Secondary Reflux and Vaporization, a comparative evaluation, *AIChE J*, **23** pp 651-658 (1977)

(2) Seader, J.D. and Baer, S.C., Continuous Distillation Apparatus and Method, final report, University of Utah, Salt Lake City (1984)

(3) Glenchur, T. and Govind, R., Study on a continuous Heat Integrated Distillation Column, *Separation Science and Technology*, **22**(12), 2323-2338 (1987)

(4) Nakaiwa, M., Internally Heat Integrated Distillation Columns: a review, *Trans IChemE,* **81** Part A, (2003)

(5) Aso, K., Takamatsu, T. and Nakaiwa, M., Heat Integrated Distillation Column, U.S. Patent 5,873,047 (1998)

(6) De Graauw, J., Steenbakker, M.J., de Rijke, A., Olujic, Z. and Jansens, P.J., Distillation column with heat integration, Patent Application EP1476235 (2004)

(7) Olujic, Z., Sun, L., De Rijke, A., and Jansens, P. J., 2006, Design of an Energy Efficient Propylene Splitter, *Energy* (2006)

(8) Kaeser, M. and Pritchard, C.L., Heat Transfer at the Surface of Sieve Trays, *Trans IChemE*, **83**, 1038-1043 (2005)

(9) American Institute of Chemical Engineers, Research Committee. Tray Efficiencies in Distillation Columns, AIChE: New York (1958)

(10) Chan, H. and Fair, J.R., Prediction of Point Efficiencies on Sieve Trays. 1. Binary Systems. *Ind. Eng. Chem. Process Des. Dev.* **23**, 814-820 (1984)

(11) Prado, M. and Fair, J.R., Fundamental Model for the Prediction of Sieve Tray Efficiency, *Ind. Eng. Chem. Res.* **29**, 1031 (1990)
(12) Garcia, J.A. and Fair, J.R., *Ind. Eng. Chem. Res.* **39**, 1809-1825 (2000)
(13) Sakata, M:, Yanagi T, Performance of a Commercial Scale Sieve Tray, *Inst. Chem. Eng. Symp. Ser.* **56**, 21 (1979)
(14) Yanagi, T., Sakata, M., Performance of a Commercial Scale 14% Hole Area Sieve Tray. *Ind. Eng. Process Des. Dev.* **21**, 712-717 (1982)
(15) Kooijman, H.A. and Taylor, R, A Non-equilibrium Model for dynamic Simulation of Tray Distillation Columns, *AIChE Journal*, **41**, 1852-1863 (1995)
(16) Hofhuis, P.A.M., Zuiderweg, F.J., Sieve Plates, Dispersion Density and Flow Regimes, *Inst. Chem. Eng. Symp. Ser.* **56**, 2.2/1 (1979)
(17) Hofer, H., Influence of Gas Phase Dispersion on Plate Column Efficiency, *Ger. Chem. Eng.,* **6**, 113 (1983)
(18) Kaltenbacher, E., On the Effect of Bubble Size Distribution and the Gas-Phase Diffusion on the Selectivity of Sieve Trays, *Chem. Eng. Fundam.* **1**, 47 (1984)
(19) Locket, M.J. *Distillation Tray Fundamentals*, Cambridge University Press, Cambridge, U.K. (1986)
(20) Jiang, P., Lin, T.J., Luo, X., Fan, L.S., Flow Visualisation of High Pressure (21 MPa) Bubble Column: Bubble Characteristics, *Trans. Inst. Chem. Eng.* **73**, Part A, 269, (1995)
(21) Tsuge, H., Nakaijima, Y., Terasaka, K., Behaviour of Bubbles Formed from a Submerged Orifice under High System Pressure, *Chem. Eng. Sci.,* **47**, 3273 (1992)
(22) Ponter, A.B., Tsay, T., Sieve Plate Simulation Study: Contact Angle and Frequency of Emission of Bubbles from a Submerged Orifice with Liquid Cross-flow, *Chem. Eng. Res. Des.* **61**, 259 (1983)
(23) Calderbank, P.H.; Pereira, J., The Prediction of Distillation Plate Efficiencies from Froth Properties. *Chem. Eng. Sci.* **32**, 1427 (1977)
(24) Wilkinson, P.M., Schayk, A.V., Spronken, J.P., Dierendonck, L.L.V., The influence of Gas Density and Liquid Properties on Bubble Break-up. *Chem. Eng. Sci.,* **48**, 1213 (1993)
(25) Marshall, S.H., Chudacek, M.W., Bagster, D.F., A Model for Bubble Formation from an Orifice with Liquid Cross-flow, *Chem. Eng. Sci.,* **48**, 2049 (1993)
(26) Walter, J.F., Blanch, H.W., Bubble Break-up in Gas-Liquid Bioreactors: Break-up in Turbulent Flows, *Chem. Eng. J.* **32**, B7 (1986)
(27) Bennett, D.L., Grimm, H.J., Eddy Diffusivity for Distillation Sieve Trays, *AIChE J.* **37**, 589-595 (1991)
(28) Bennet, D.L., Agrawal, R., Cook, P.J., New Pressure Drop Correlation for Sieve Tray Distillation Columns, *AIChE J.*, **29**, 434 (1983)

(29) Leibson, I., Kelley, R.E., Bullington L.A., *Petrol. Ref.* **36**, 127-133 (1957)
(30) Olujić, Ž., Behrens, M., Colli, L., Paglianti, A., *Chem. Biochem. Eng.*, **18**, 89-96 (1994)
(31) Ashley, M.J., Haselden, G.G., The Improvement of Sieve Tray Performance by Controlled Vapour-Liquid Contacting, *Trans. I. Chem. E.* **51**, 188-191 (1973)
(32) Haselden, G.G., British Patent 1460709 (1972)
(33) Gautreaux, M.F., O'Connell, H.E., *Chem. Eng. Prog.* 51, 232-237 (1955)
(34) Lewis, W.K., *Ind. Eng. Chem,* **28**, 399 (1936)
(35) Gerster, J.A., Hill, A.B., Hochgraf N.A., and Robinson, D.G., Tray Efficiencies in Distillation Columns, AIChE, New York (1958).

Chapter 5:

Design of an internally Heat Integrated Distillation Column for Propylene-Propane

Partially published as:
Conceptual design of an internally Heat Integrated Distillation Column, Energy, 31, 3083-3096 (2006)

Abstract

Immense quantities of energy are required in distillation columns used for polymer grade separations of close boiling mixtures. The purpose of this paper is to introduce an industrially viable, internally heat integrated (HIDiC) version of a state of the art propylene-propane splitter. A novel asymmetric HIDiC column configuration is introduced. The energy efficiency of HIDiC appears to be strongly dependent on the column configuration. The most viable HIDiC configuration can save up to 50% of exergy compared with its vapour recompression counterpart. The base case is one of the world's largest, heat-pump assisted, stand-alone columns of this type. The actual plant data formed the basis for the techno-economic evaluation, which indicated that the HIDiC could become an economically attractive option for new designs, provided the barriers with respect to related design complexity could be overcome.

5.1 Introduction

An internally heat-integrated distillation column (HIDiC), which combines advantages of a low-pressure ratio vapor recompression system with a diabatic operation, offers ultimate potential for energy saving in distillation (1,2). As such, it is particularly suitable for most demanding, close boiling mixtures separations (1). A column with vapor recompression system (VRC) is shown schematically in Fig. 1 together with its HIDiC counterpart. A HIDiC, with two sections in parallel to each other reduces the total height, in ideal case by factor two, however it requires heat coupling between the trays of stripping and rectification sections. Its obvious complexity seems to be the main barrier for a successful implementation in industrial practice. So far, a small diameter pilot plant demonstration column equipped with packings has been build and operation of this column proved the principle (3). However, few design considerations have been reported so far; the mainstream of research effort went into overall performance evaluation as well as to control and dynamics aspects (2).

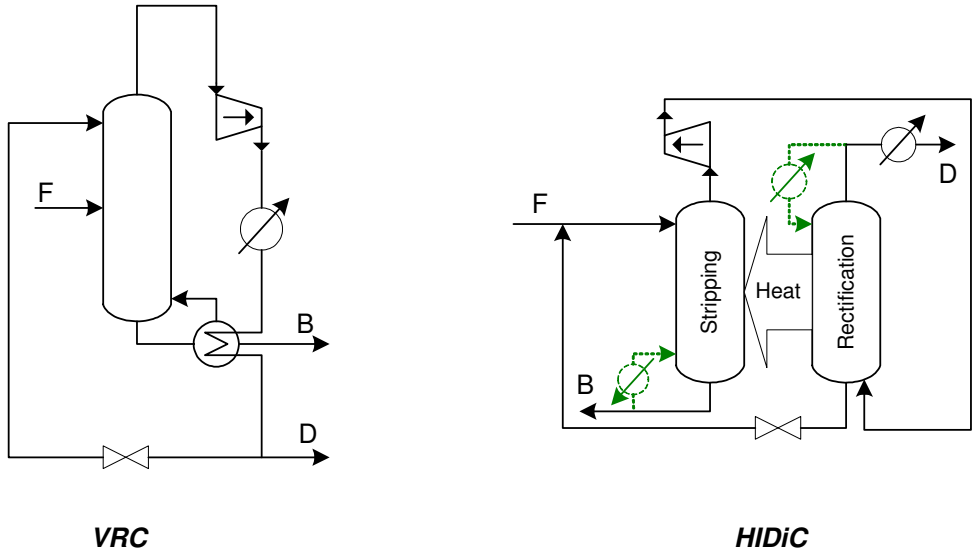

Figure 1 Schematic illustration of the operating principle of a column with the direct vapour recompression (VRC) and a HIDiC.

Because of its nature, a HIDiC is considered as an alternative for self-standing large vapor recompression columns, such as that widely utilized in industrial practice for separation of propylene and propane and similar close boiling mixtures. Because of the large production capacity in conjunction with high product purity, low relative volatilities and consequently very high reflux ratios involved, these rather big columns require usually up to 100 MW of energy,

which is immense in any respect. As demonstrated earlier (4), by adopting the HIDiC concept, the energy requirement of a heat pump assisted propylene-propane splitter (PP-splitter), which uses only one sixth of the energy required in a conventional steam heated column, could be reduced by nearly 50%, i.e. to the values close to theoretical limit. However, such a gain is at the expense of increased design complexity. Unfortunately, in the open literature there is no evidence that could be of some use in estimating the mechanical design effort and related cost of a HIDiC PP-splitter.

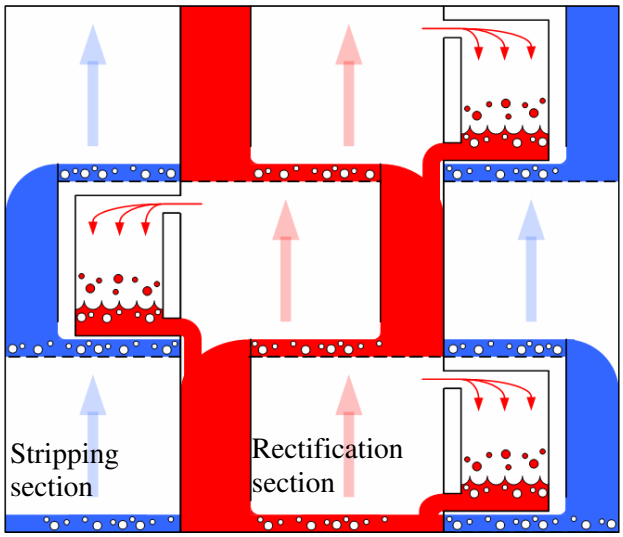

Figure 2 Drawing illustrating the heat transfer panels placed in between trays in annular stripping section.

Conceptually, a HIDiC is a column with vapor leaving the stripping section, compressed to a higher pressure, which upon entering the rectification section starts to condense and in this way provides the heat duty for evaporation in the stripping section. This implies that the vapor load in rectification section decreases steadily downward the column/section, while the vapor load increases correspondingly upwards the stripping column/section. In this way some sort of a continuous operating line is obtained, which follows in parallel the equilibrium line at a minimum distance, ensuring nearly a reversible operation, as expected in diabatically-operated distillation columns (5,6). In a concentric column with rectification section placed inside the stripping column, the wall surface area is not sufficient to transfer the required heat at a rather small temperature difference, which implies that on each stage a substantial amount of additional heat transfer area must be installed to enable desired operation, to ensure continuous increase in the vapor flow rate, from a minimum at the bottom to a maximum value at the top of the stripping section.

In case of a PP-splitter, which is usually designed as a tray column, a feasible way of doing this would be to provide annular stripping column trays with a multiplicity of heat transfer panels with inner body in open contact with the equivalent trays in the rectification section (7). In this way, it is possible for vapor from the rectification section tray to enter the panels placed on the stripping section tray and condense inside releasing the heat which is transferred through the panel walls to the liquid film on the outside walls, which evaporates generating the vapor phase in the stripping section. Figure 2 shows schematically such a configuration.

In general, for a certain constant heat transfer duty per stage, a known value of the overall heat transfer coefficient and a given temperature difference, there will be a heat transfer area requirement per actual stage (i.e. a tray). The heat transfer area translated into a number of panels fitting into the space available in between trays can be used to estimate related material and installation costs as well as additional weight of a tray, which in turn affects the column shell thickness. This additional weight will to some extent compromise the saving in wall thickness, which might be expected from a significant reduction in the column height.

5.2 Effect of Column Configuration

Another potential problem with practical implementation of HIDiC is the fact that an ideal HIDiC in principle requires symmetrical distribution of stages, i.e. equal number of stages in both sections. This condition is conflicting with optimum feed position, which in turn is governed by the feed composition, feed thermal condition and products specification. In case of PP-splitters, usually only the distillate (propylene) is required at high purity, which implies that practically all columns of this type contain more stages in rectification than in the stripping section. In the cases evaluated in this and previous studies, approximately one third of the stages are contained in the stripping section and other two third in the rectification section. It must be noted that with respect to optimum feed position a HIDIC does not differ from a conventional column. So the main conceptual design question is how to arrange a HIDiC with different number of stages in rectification and stripping sections. Possible configurations, compared in this study are shown in Fig. 3.
The basic configuration called *HIDiC_basic*, shown in Fig. 1, is the fully symmetrical configuration structure as known from the literature (2,3), which, regarding the base case implies operation with a feed introduced well above the optimal location. In this way, each stage in the rectification section is connected through a heat exchanger with a corresponding stage in the stripping section.

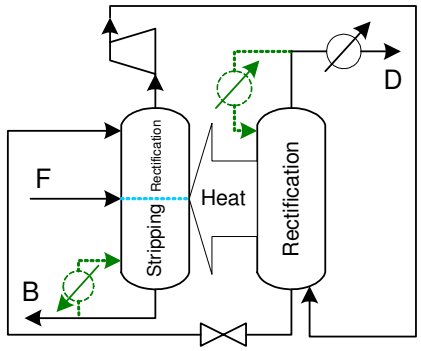

(HIDiC_optimum feed)

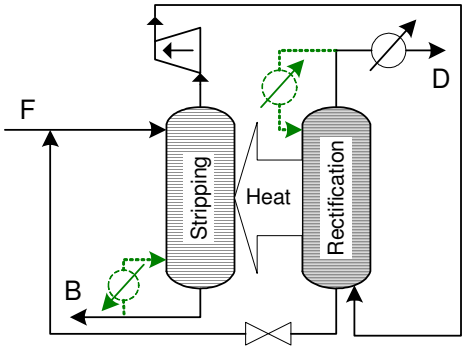

(HIDiC_all)

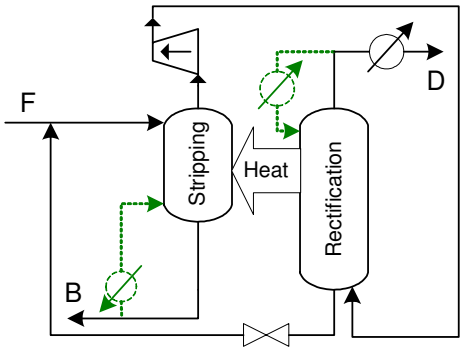

(HIDiC_top)

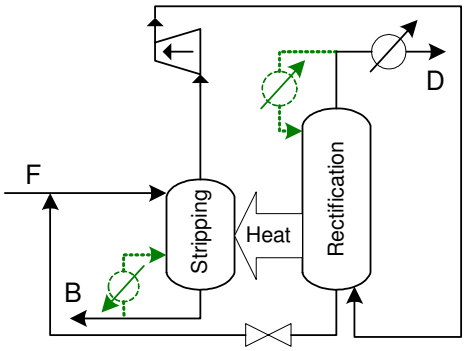

(HIDiC_bottom)

Figure 3. Other possible configurations of the HIDiC, in addition to that of (HIDiC_basic) shown in Figure. 1

HIDiC_optimum feed is the modification of *HIDiC_basic* where the feed is introduced on the stage, which represents the optimal one for a conventional column. In order to get the same number of stages in the low- and high pressure/temperature sections of the column, a number of rectification section stages is placed directly above the stripping section. *HIDiC_top* and *HIDiC_bottom* represent two extreme asymmetric configurations, with the stripping section stages connected with the same number of stages in the rectification section in the respectively upper and lower part of the rectification section. In these cases a part of the rectification section resembles the conventional column design. Finally, a HIDiC with a smaller number of stages

in stripping than in rectification section can be arranged to have equal length of the sections, simply by adapting the stripping section tray spacing accordingly. This configuration, called *HIDiC_all* implies the heat exchange between each of stripping section stages with one or more stages in the corresponding segment of the rectification section.

The objective of the current work is to present the results of a thermal analysis study indicating a strikingly strong effect of HIDiC configuration on the energy/exergy requirement of a hypothetical PP-splitter. As it will be demonstrated later on, it appears possible to arrive at a HIDiC design that could compete with the conventional vapor recompression design.

5.2.1. Energy & Exergy Savings

Figure 4 shows the energy and exergy requirements of the VRC (column with vapour recompression system) and the HIDiC relative to that of the conventional column. As expected a VCR enables a huge energy saving with respect to conventional column and the asymmetric HIDiC with upper part of rectification section coupled thermally to the striping section seems to be the best configuration in this respect. Interestingly the performances of five compared configurations of HIDiC differ significantly and some of them, (*HIDiC_basic and HIDiC_bottom*), appeared to be less favourable than the VRC itself. This may not be so surprising if we consider the fact that the HIDiC's in question are that with feed stage far from optimum and the one with a number of rectification stages placed in the low-pressure part of the column. In fact, striking is the extent of bad performance of the HIDiC with the bottom part of the rectification section coupled to the stripping section (*HIDiC_bottom*). The relative exergy requirement plot shown in Fig. 4 indicates that the exergy efficiency of this configuration is more than factor two worse than that of the conventional column.

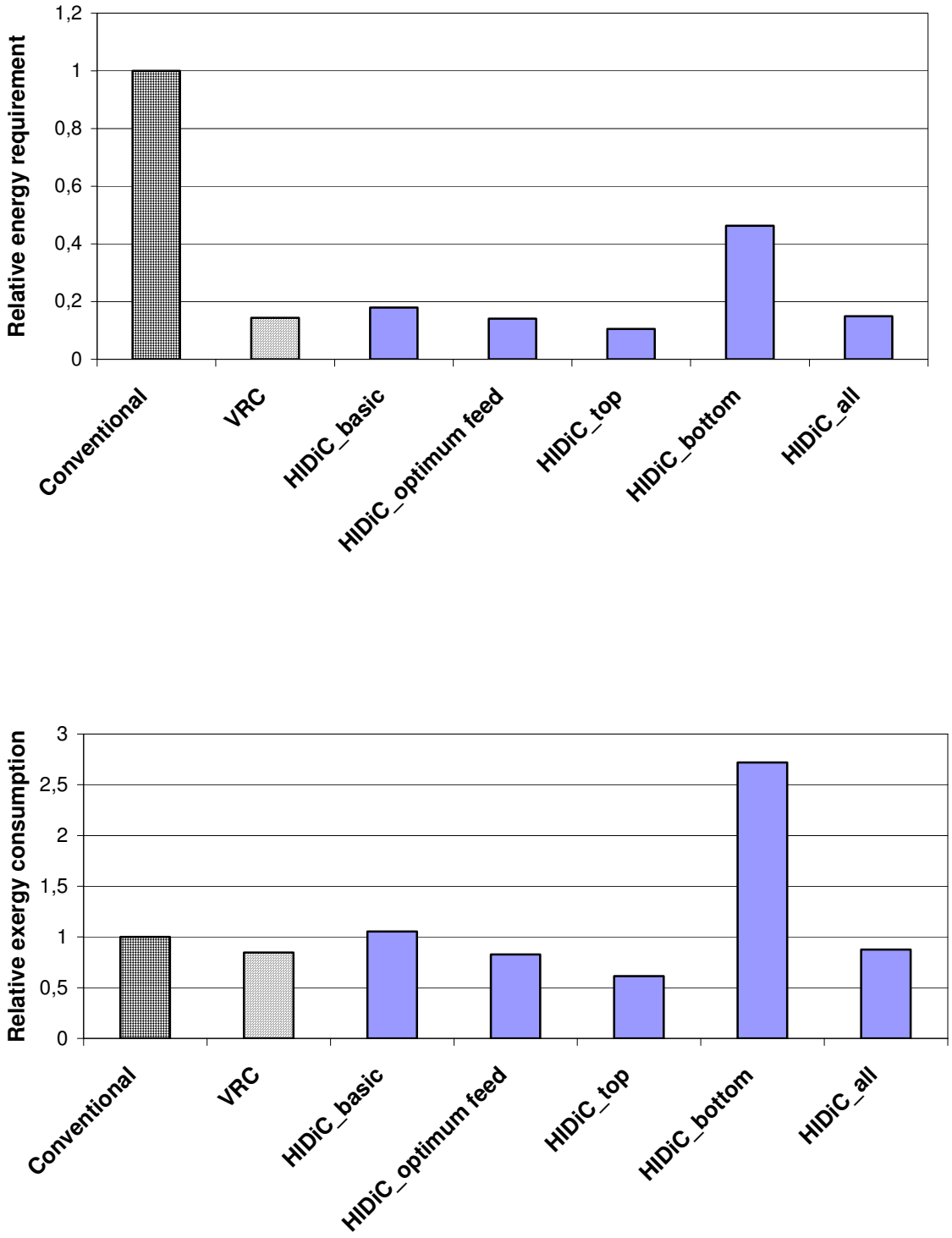

Figure 4. Relative energy (above) and exergy (below) requirement of HIDiC (compression ratio = 1.4) compared to the conventional column

5.2.2 Vapour Flow Profiles

Figure 5 shows the vapor flow profiles of VRC and its HIDiC equivalent. As expected, the vapor flow profile of the VRC is nearly constant (around 850 t/h), while the changing profile of HIDiC indicates the nature of this type of internally heat-integrated column. The vapor flow increases steadily from zero at the bottom of the stripping section to a maximum value (around 1100 t/h) at the top of the stripping section. This vapor, plus that contained in partially vaporized feed and that generated during the pressure reduction of the liquid passing through the throttling valve on its way from the high pressure rectification section (14.6 bar) to low pressure stripping section (11.2 bar) enters the compressor and is delivered to the rectification section. In this normal part of the rectification section, containing 109 stages, the vapor flow is nearly constant. Upon entering the HIDiC part of the rectification section, containing 61 stages the vapor flow continuously decreases to a value, which corresponds to the sum of the flow rates of the top product and the necessary reflux, which are equal.

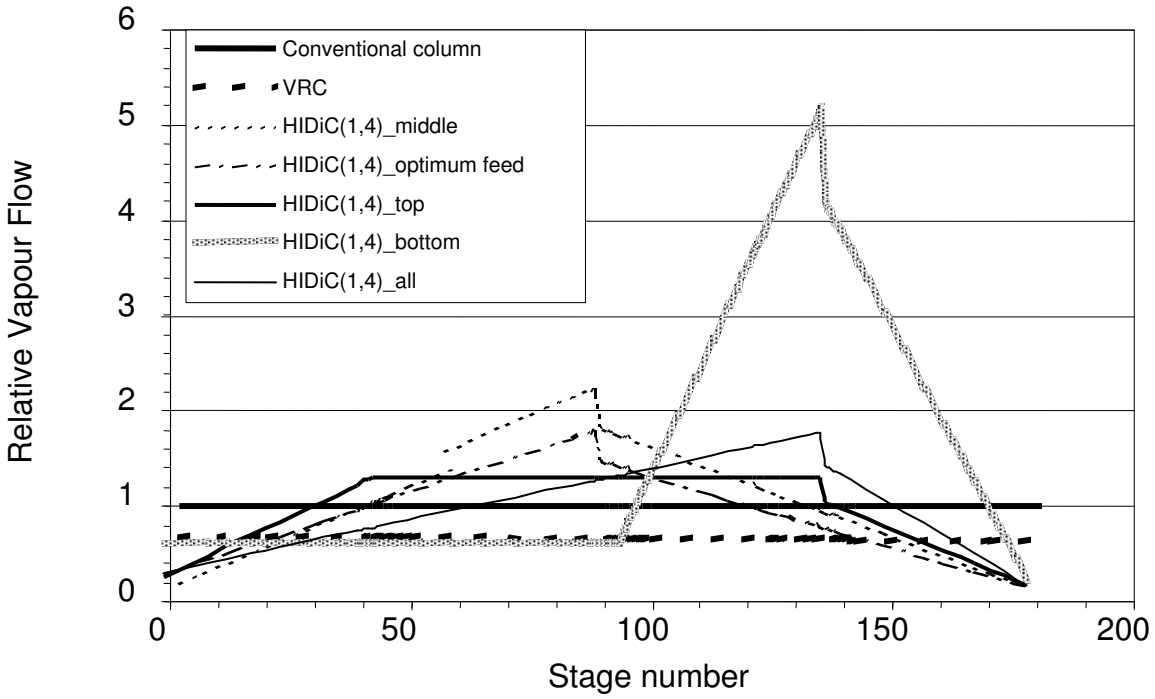

Figure 5: Vapour flow profiles of different HIDiC configurations (compression ratio = 1,4) compared to those of a VRC and a conventional column

In addition to the compression ratio, which is equal for all HIDiC configurations, the compressor duty depends also on the mass flow rate of the vapour. As indicated in Fig. 5 the latter one varies considerably, in one case extremely, depending on the configuration. The peaks of vapour rate curves shown in Fig. 5 indicate the compressor load associated with HIDiC configurations considered here. It can be seen that the vapour flows through compressors of *HIDiC_top*, *HIDiC_optimum feed*, *HIDiC_all*, *HIDiC_basic* and *HIDiC_bottom* are 1.7, 2.4, 2.4, 3.1 and 7.5 times of that of the VRC, respectively. This observation reveals a latent weak point of HIDiC, i.e. a relatively much larger vapour load of the compressor compared to that of the VRC. Therefore it is not surprising that in some cases a HIDiC consumes more energy/exergy than the VRC. According to Fig. 5, *HIDiC_a*ll and *HIDiC_optimum feed* exhibit the same vapour load peak, which is that high that it leads to approximately equal energy/exergy requirement as in the case of VRC. Such a strongly pronounced deteriorating effect of the vapour load could be reduced to some extent by increasing appropriately the number of stages. Anyhow, to perform better than the VRC these configurations should be operated at a lower compression ratio, which, as it will be shown later, is associated with a heat transfer area requirement that may become impractical.

5.2.3 Internal Reflux and Separation Efficiency

The horizontal part of the vapour flow profiles of two asymmetric HIDiCs indicates a constant flow rate operation, similar to that of the conventional column and the VRC. Indeed, this is so, and the bad performance of the *HIDiC_bottom* can be attributed to the fact that the upper, normal column part of the rectification section operates at a constant internal reflux ratio equivalent to the distillate flow rate, which is roughly factor two and three times lower than that encountered in respectively the VRC and the conventional column. An inspection of the propylene composition profile along the column for two asymmetric HIDiC's and the conventional column shown in Figure 6 indicates that in case of *HIDiC_bottom* the separation effort is concentrated in the thermally coupled part of the column. In fact, this part of the column operates with a rather low number of theoretical stages, which must be compensated by correspondingly increased internal reflux ratio (roughly 75!). This is needed to compensate effectively for highly inefficient performance of the upper, strongly under-refluxed part of the rectification section, which uses more than 100 stages to bring the distillate to the specification. On the other hand, the separation performance of *HIDiC_top* resembles that of the conventional column. As shown in Fig. 5, the vapour flow in the normally operating lower part of the rectification section is somewhat larger indicating correspondingly larger internal reflux (around 24.5). As indicated in Fig. 6, this leads to somewhat enhanced separation

performance in this part of the column, which compensates certain loss in the thermally coupled part of the column.

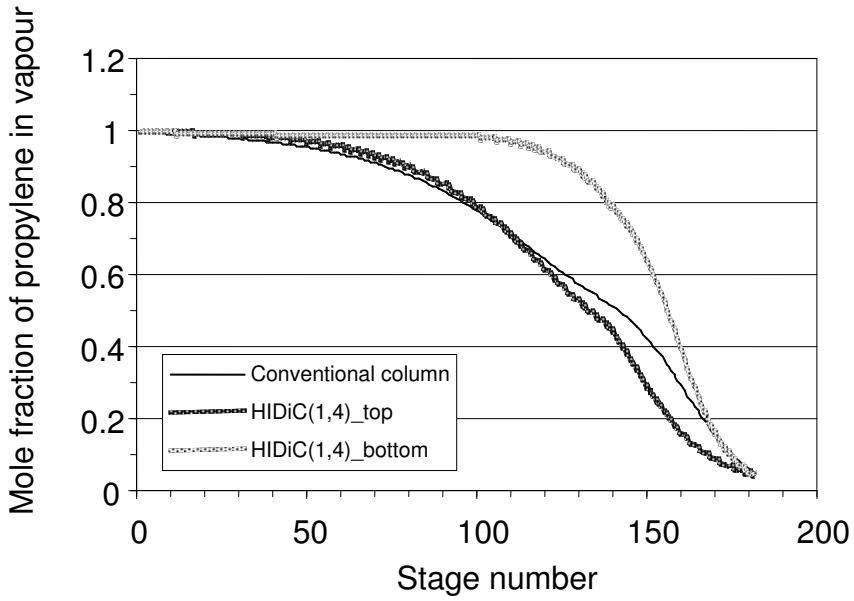

Figure 6: Mole fraction of propylene in vapour as function of stage number for different HIDiC configurations compared to the conventional column

Obviously, the performance of a HIDiC strongly depends on the configuration chosen. From thermal integration point of view the asymmetric HIDiC with upper part of rectification section interconnected thermally with stripping section appears to be the best option. Therefore this HIDiC configuration was chosen to be compared to and industrial scale VRC.

5.3 Design case

5.3.1. The base case

As the base case, a stand alone, heat pump assisted PP-splitter is used, considered in a previous study (4). It is one of the largest columns of this sort, 110 m tall, with an internal diameter of around 6.5 m, containing 230 four pass sieve trays. This column operates at an overall efficiency of around 91%, which means that at given reflux ratio (around 15) 211 theoretical trays (equilibrium stages) are contained in the column, 47 in the stripping section and 164 in the rectification section. The flow rate of a partly vaporized feed (vapor fraction = 0.37) is around 112 t/h. The overall composition of the vapor

and liquid feed mixture is: 52 mole % propylene, 47 mole % propane and a small fraction, say around 1 mole % of isobutane and heavier components. The top product (57.9 t/h) is polymer grade propylene (99.6 mole %), and only 1.1 mole % propylene is allowed in bottoms, which contains mainly propane (96.5 mole %). The top pressure is around 11.2 bar, and the column pressure drop is around 6 mbar per stage, which results in a column pressure drop of approximately 1.2 bar. The compressor ratio employed in this case is around 1.7, which means that the top vapor is compressed to around 18 bar. This results in a temperature increase of roughly 21 ^{0}C, i.e. a vapor temperature of 45 ^{0}C at the reboiler inlet.

5.3.2. Simulation tool

The simulation of separation performances of the base case and the HIDiC PP-splitters was carried out using ASPEN Plus facilities. The HIDiC part of the alternative design (called generally HIDiC) was simulated as a pair of thermally interconnected columns/sections. In this case, the stripping section stages were thermally integrated with the equivalent number of the stages in the upper part of the rectification column. Lower part of the rectification column, containing some 105 stages, operates as a normal column at given operating pressure. The heat transfer area requirement and the equipment cost of the HIDiC were estimated by an interactive sequential calculation effort, by combining ASPEN and Excel.

5.3.3. Column layout and dimensions

Overall dimensions of the actual VRC PP-splitter and its HIDiC equivalent are given in Fig. 7. The dimensions of HIDiC were obtained by assuming the same tray type (sieve) and tray spacing (0.46 m). The column height is based on the number of actual trays and the adopted tray spacing. The VRC height corresponds to that of the actual column, and the alternative column (HIDiC) is realized in one piece, with the heat integrated part placed above the normal, lower part of the rectification section. This hybrid column, containing in total 20 more trays is 20 m shorter than the VRC. As illustrated schematically in Fig. 7b, the ideal form of the HIDiC is the conical shape of the internal column, i.e. upper part of the rectification column. Certainly, this is not feasible, and therefore the HIDiC part has to be arranged into a number of sections with decreasing/increasing column diameter. This has been arranged by adopting a tray turndown ratio of two. So, the stripping section diameter was based on the common 80 % of flood limit, and the same diameter kept for all trays

above, until the lower limit was reached. As illustrated in Fig. 7c, this procedure delivered seven different diameters in the HIDiC part of this hybrid column. This may look to be complicated but a more detailed consideration including trays with a larger turndown ratio would reduce this to say three different diameters. Anyhow, it should be noted that applying the default sizing procedure from ASPEN delivered quite unrealistic (too large) diameters of the VRC and the HIDiC. Since a more appropriate correlation, proposed by Kister and Haas (8), requires unknown tray design details a correction factor for capacity coefficient was adopted to arrive at the diameter of the actual VRC and consequently a realistic diameter of the HIDiC.

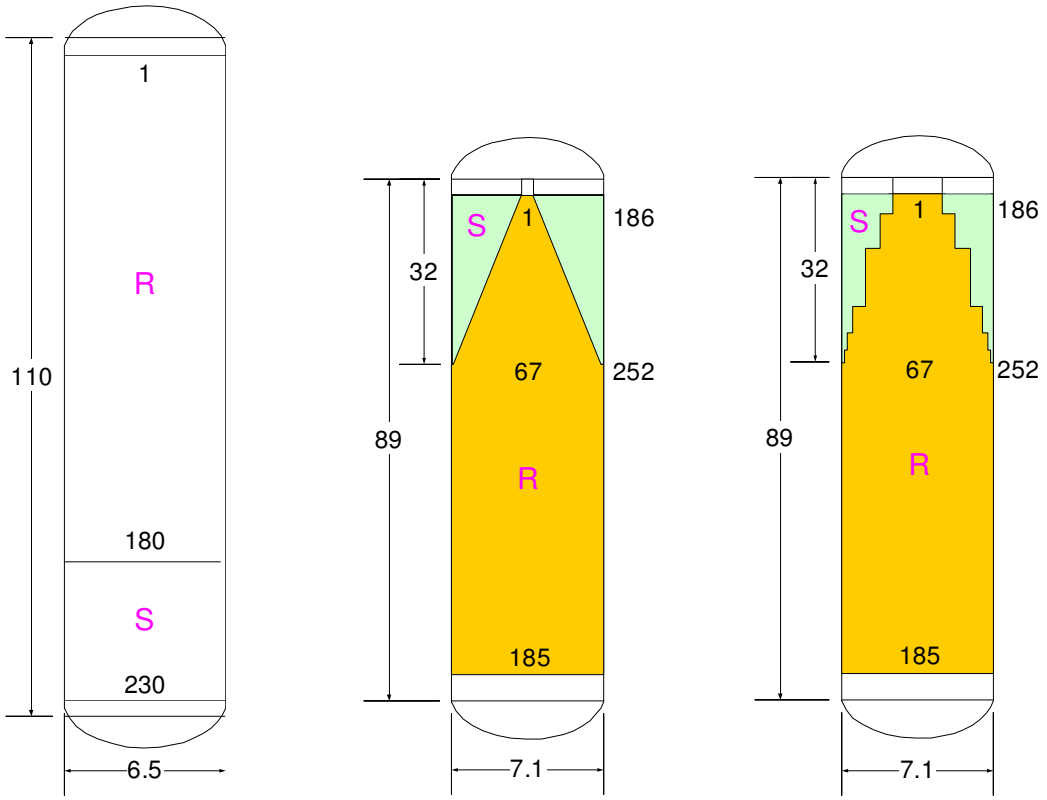

Figure 7: Column dimensions of: (a) VRC, (b) ideal HIDiC, and (c) a multi-diameter HIDiC.

Regarding the fact that the available cross sectional area increases in the stripping and decreases in the rectifying section, from the bottom to the top of the section, a feasible design could be to distribute the heat transfer area accordingly, by installing heat transfer panels at stripping section trays as long

as this is feasible and then switch to the trays in the rectification area. To get an idea about the space needed for installation of heat transfer panels in the active area in between two trays a constant height (0.35 m) and width (15 mm) was chosen for panels. The length depends on the size of the active area on the tray, and the spacing between panels may vary between one and two panel thicknesses. This allows a layout similar to that shown schematically in Fig. 8 for a stripping section (annular) tray. It should be noted that in this study it is assumed that such a configuration will not affect the tray performance adversely.

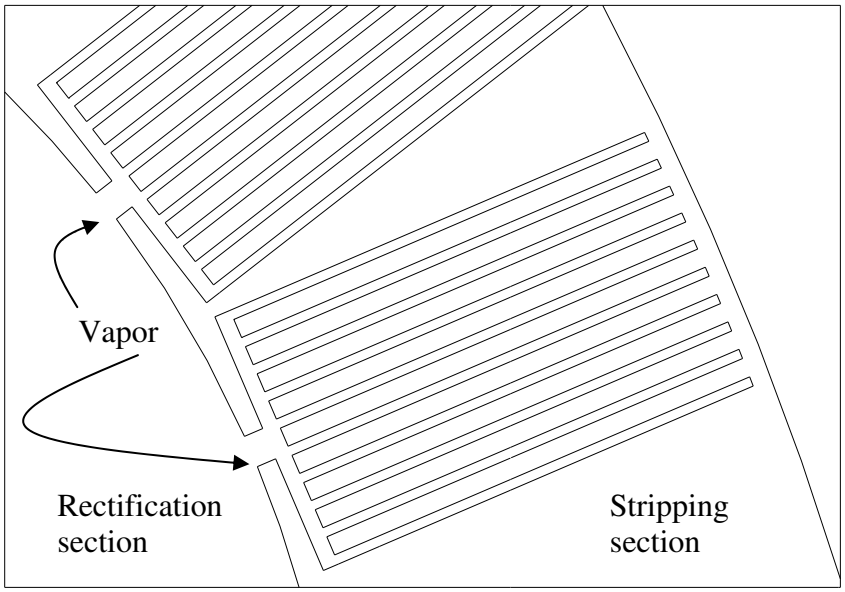

Figure 8: Top view of the layout of a stripping section tray containing heat transfer panels.

The configuration shown in Fig. 8 is an approximation of a practical solution for installation of the heat transfer panels in a HIDiC equipped with trays. Obviously, the available area is not fully occupied and to do so a more complex configuration of heat panels is required. However, a tray with the active area fully occupied by a multiplicity of parallel heat transfer panels implies a significant reduction in the free area available for the vapor flow and consequently a faster approach to the entrainment flooding limit, which can be

counteracted only by a corresponding increase in the tray cross sectional area, i.e. increasing capital cost.

Another reason for this could come from the fact that in this study a 100% heat transfer efficiency of installed panels is assumed, which will be difficult to achieve in a real world situation. This implies that a larger heat transfer area and consequently a larger diameter will be required in practice. Nevertheless, we expect that pilot plant studies will be revealing in this respect as well as to the mass transfer performance of so densely packed tray. With the heat transfer and mass transfer efficiency as well as accompanying pressure drop numbers from a pilot plant scale experiment we expect to be able to provide a realistic basis for the evaluation of practical feasibility of a HIDiC.

Since the heat transfer panels considered here belong to an established technology, it is possible to make reliable estimates of the unit weight and consequently the capital cost involved. Preliminary estimates indicated that the weight of panels may exceed the weight of trays significantly. This could impose two shells configuration as more appropriate HIDiC configuration regarding the material and financial effort needed to ensure mechanical integrity of a one-shell HIDiC.

5.3.4. Cost estimation procedure

By adopting the column efficiency and tray design and spacing of the base case VRC, and assuming the same for HIDiC, the basic dimensions, column diameter(s) and height(s) are easily calculated. Table 1 summarizes main simulation results. As indicated in Table 1, optimized HIDiC operates with a compression ratio of 1.3 and contains few more stages, with feed location moved upwards accordingly.

Table 1:Characteristic parameters of the compared PP-splitter designs

	VRC	HIDiC
Rectification section top pressure (bar)	11.2	14.6
Stripping section top pressure (bar)		11.2
Pressure drop per stage (mbar/stage)	6.2	6.2
Number of stages/trays, rectification section (-)	164/179	170/185
Number of stages/trays, stripping section (-)	47/51	61/66
Total number of stages/trays (-)	211/230	231/251
Feed stage/tray (-)	165/180	171/1860

To enable calculation of the installed cost of the HIDiC configuration shown in Fig. 7c, a simplified approach was chosen, i.e. HIDiC was divided into two main parts: the concentric column with the upper part of the rectification section placed inside the stripping section, and the lower part of rectification section, which is essentially a common one-shell column. For costing purposes the concentric part is considered to consist of two constant (average) diameter shells. Since it appeared that the outer diameter of the concentric part is nearly equal to that of the normal part of the column (lower part of the rectification section), these two are taken equal and one outer shell obtained. To be on the safe side with the cost estimate, for this shell the rectification section pressure is taken as reference. The cost of this big shell is added to the cost of the small diameter shell of the upper part of the rectification section to produce overall shell cost. The same approximation was made for the cost of trays. The stripping section trays were taken as full cross sectional area trays, i.e. not as annular trays. In other words these trays were taken to be equal in the area to that of the normally operating lower part of the rectification section. This effectively means an increase in total tray area equivalent to the area of the trays installed in the upper part of the rectification section. In order to account for (unknown) costs associated with the complexity of the construction of HIDiC, beside these internal provisions the estimated overall shell cost value is multiplied by a factor 1.5.

The installed cost estimates, based on correlations proposed by Douglas (9), were updated using the Marshall and Swift index (M&S = 1115.8, reference year 2003) (10, 11). The installed cost of the column shell, made of carbon steel, is estimated as a function of column diameter, d_{col} (m), and the total column (tangent to tangent) height, h_{col} (m):

$$CSC_{inst} = \left(\frac{M\ \&\ S}{280} \right) \cdot C \cdot d_{col}^{1.066} \cdot h_{col}^{0.802} \qquad (1)$$

where the coefficient C varies, depending on the pressure range. In fact, the values of these coefficients, given in Table 2, include both the correction factors for the pressure effect and the construction material. The latter one is 1, because the column shell is built of carbon steel. Additional complexity of HIDiC is accounted for by multiplying the value obtained from Eq. (1) by a factor of 1.5.

Table 2: Coefficients of Eq. (1)

Pressure range (bar)	*C*
0 – 3.4	3919.32
3.4 – 6.8	3966.20
6.8 – 13.6	4059.96
13.6 – 20.5	4106.85

The tray cost is estimated as a function of column/section diameter and the height of the column occupied by trays, h_{tray} (m):

$$TC_{inst} = \left(\frac{M\ \&\ S}{280} \right) \cdot 97.243 \cdot d_{col}^{1.55} \cdot h_{tray}\ F_C \tag{2}$$

The overall correction factor comprises contributions of the construction material (0), the type of tray (0) and for tray spacing (1.4): F_C= 0 + 0 + 1.4 = 1.4.

The calculation of the heat transfer area is straightforward from the duty, *Q* (kW or MW*)*, temperature difference, ΔT (K), and the most appropriate value for the overall heat transfer coefficient, *U* (kW/m^2):

$$A = \frac{Q}{U\ \Delta T} \tag{3}$$

Depending on the type of the device, constant values of heat transfer coefficients are used, as generally employed for kettle reboilers (1000 W/m^{2}K), thermosyphon reboilers (1200 W/m^{2}K), and condensers (800 W/m^{2}K), respectively. For heat transfer panels installed in the HIDiC, a similar value was assumed (1000 W/m^{2}K). The installed cost was estimated as a function of the heat transfer area, *A* (m^2), using:

$$HEC_{inst} = \left(\frac{M\ \&\ S}{280} \right) \cdot c \cdot A^{0.65} \tag{4}$$

The values of the coefficient *c* are shown in Table 3. These values include corrections for effects of the construction material, pressure range and the

type of the exchanger. For instance, for the condenser a floating head device is chosen and the heat transfer panels are considered as fixed tube devices. The coefficient for the heat transfer panels is based on manufacturing cost per m^2 of such devices employed in common heat exchanger applications.

Table 3: Coefficients of Eq. (4)

Heat exchanger	c
Thermosyphon reboiler	1799.00
Kettle reboiler	1775.26
Condenser	1609.13
HIDiC panel	1466.72

It should be noted that the column/heat exchanger dimensions involved in this study are larger, i.e. outside the range of the validity of used cost estimation correlations. However, this is not of essence for this study, which is concerned mainly with the relative costs of the compared designs.

The installed cost of the centrifugal compressor, driven by an electro-motor, is based on the brake power, *bp*, only:

$$CC_{inst} = \left(\frac{M\ \&\ S}{280} \right) \cdot 2047.24 \cdot bp^{0.82} \tag{5}$$

This expression is valid in the range of: 22 < bp (kW) < 7457. The value of the coefficient includes corrections for the type (centrifugal, with electro-motor), construction material and the pressure range.

5.3.5. Economic evaluation

In order to evaluate properly the economic feasibility of HIDiC, it is chosen here to compare total annual costs (TAC) of the VRC and the HIDiC, which includes both the yearly operating costs and 10% of capital cost, according to assumed plant life time of 10 years. The capital cost is obtained by summing up individual equipment costs, determined using the method described in the preceding sub-chapter. Also, for the sake of simplicity, operating costs are taken to be identical to utility costs, i.e. the number resulting from the

summation of electricity (0.1 $/kWh), low pressure steam (13 $/ton) and cooling water (0.03 $/ton) costs for a year containing 8000 operating hours. Practically no steam is required during the operation of VRC or HIDiC and some water is needed to produce minimum reflux required to initiate liquid flow at the top tray. So main utility cost is that related to compressor duty, 8.09 MW in case of VRC and 6.04 MW in case of a HIDiC operated at the stripping section pressure equal to that of the VRC. This means that exergy, i.e. utility requirement of HIDiC is some 25 % lower than that of the VRC.

The estimated capital and operating costs for VRC and the HIDiC operating at lower operating pressures are summarized in Table 4. Column and auxiliaries are more expensive in the case of HIDiC however this is compensated by a cheaper compressor, resulting in a lower capital cost. The cost of the compressor is the largest among the capital cost components and the cost of electricity is by far the largest contributor in the total annual cost. For VRC and HIDiC the electricity costs make roughly 73 % and 69 % of the total annual cost, respectively. The relative contribution of other components of total annual costs is shown in Table 5.

Table 4: Comparison of estimated capital (main equipment) and operating (utilities per year) costs in millions of US $ for the VRC and the HIDiC (p_r = 14.6 bar; p_s = 11.2 bar)

Cost component	VRC	HIDiC
Hardware		
Column shell	5.15	6.05
Trays	1.03	1.10
Panels	0	2.00
Condenser	0.42	0.66
Reboiler	2.01	0
Compressor	13.06	10.27
Total:	**21.67**	**20.08**
Utilities		
Electricity	6.47	4.83
Cooling water	0.23	0.20
Steam	0	0
Total:	**6.70**	**5.03**
TAC	**8.87**	**7.04**

Table 5: Relative contributions (in percents) of main components of capital and operating costs to total annual cost (TAC)

Cost component	VRC	HIDiC
Column shell	5.81	8.60
Trays	1.16	1.57
Panels	0	2.85
Condenser	0.48	0.94
Reboiler	2.27	0.00
Compressor	14.73	14.59
Electricity	72.95	68.61
Cooling water	2.60	2.84
Steam	0.00	0.00
Total	100.00	100.0

Regarding the fact that the estimated cost of the compressor is based on the brake power only, it may be that the cost of HIDiC compressor is significantly underestimated. Namely, as indicated in Fig. 5, the vapor flow rate entering the compressor of a HIDiC is much larger than that leaving the top of the rectification section of the VRC. This means that for the same application the vapor load of the compressor is significantly higher in case of HIDiC. If, for instance, the cost of HIDiC compressor would be increased by factor 1.3, which corresponds with the ratio of molar flow rates of vapor streams leaving the top of HIDiC and the VRC, the capital cost of HIDiC would exceed that of VRC. However, this would have a limited effect on TAC, i.e. only a 4 % increase. With this increase, the TAC of HIDiC would still be 20% lower than that of VRC. In other words, due to dominating role of operating costs, the sensitivity of TAC to significant variations or errors in estimated equipment costs is limited.

It is interesting to note that the cost of heat transfer panels is appreciably larger than the tray cost, however, in absolute sense, it is not so high to be of significant influence on total costs. This means that costs related to increased complexity of construction of a HIDiC are not a crucial factor, which implies that the cost of heat transfer devices and associated installation costs should not be considered as a real barrier for implementation of HIDiC concept in practice.

5.4. Results & Discussion

5.4.1. Compression ratio effects

In order to arrive at optimum operating conditions, and to be able to make a comparison to VRC, the operating compression ratio was varied. However the absolute values were kept between the stripping section pressure (11.2 bar) and the compressor outlet/reboiler inlet pressure of the VRC (18.1 bar), which corresponds with the rectification section pressure of a conventional column. Column/section pressure drop was considered in all simulations.

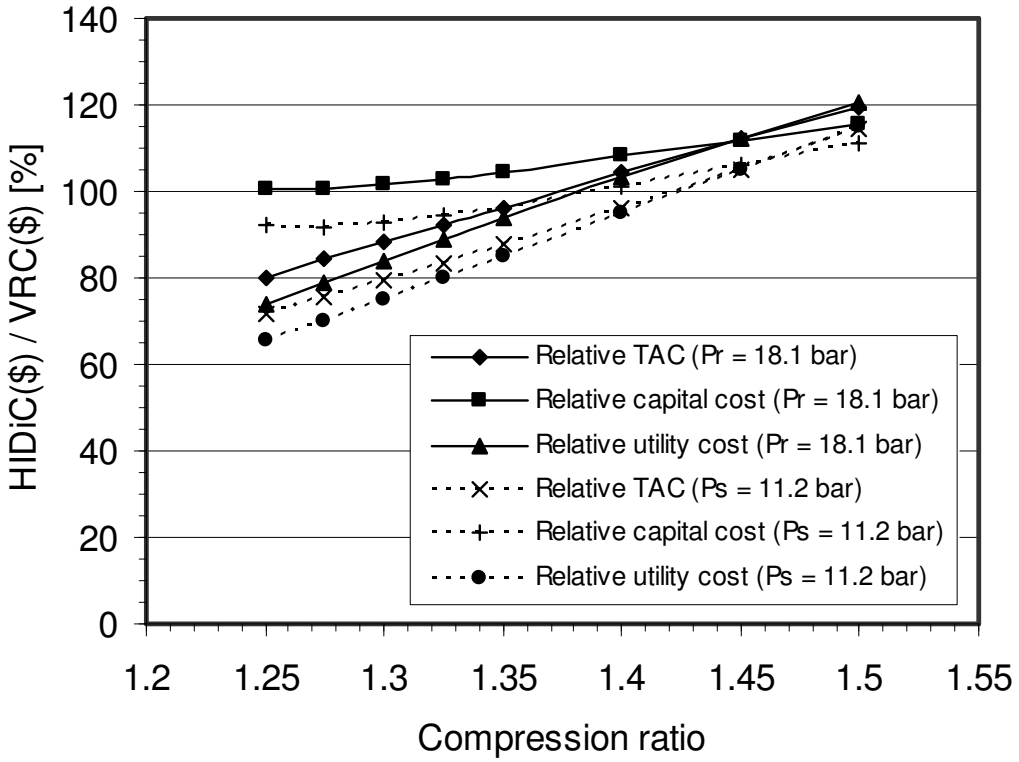

Figure 9: Annual costs as a function of the compression ratio, for high and low (dotted lines) operating pressure, respectively.

Figure 9 shows relative operating, capital and total annual costs as a function of the compression ratio for two HIDiCs based on the upper limit operating pressure (rectification section). Obviously, all costs increase with increasing compression ratio, the capital cost less pronounced than the operating costs, i.e. the cost of utilities. In general, the lower the compression ration the larger the advantage of a HIDiC, which becomes more pronounced at lower range of operating pressures. However, as indicated in Fig. 10, the heat transfer area requirement and related costs increase with decreasing compression ratio due

to the decreasing temperature difference. Anyhow, this is less pronounced than the increase in the cost of the compressor, which increases nearly proportionally to the break power. Obviously, there is a strong relation between the compression ratio and the required area per stage, indicating that operating at otherwise advantageous minimum compression ratio requires a very large heat transfer area, so that a ratio of 1.3 seems to be a compromise in this situation. By increasing the compression ratio above 1.35 would result in a break-even situation, with respect to reference, VRC costs. Most interestingly, this figure indicates that, based on present assumptions, a HIDiC is feasible and, most importantly, could compete with VRC.

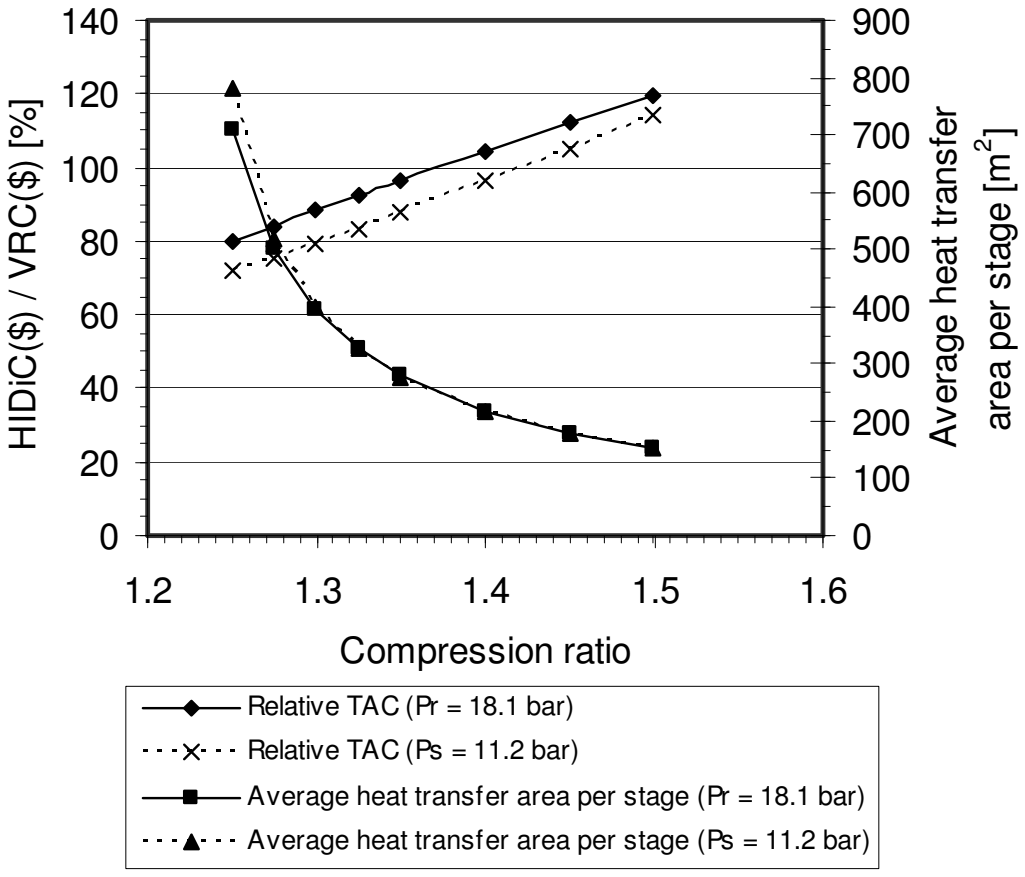

Figure 10: Relative total annual cost and the average heat transfer area per stage as a function of the compression ratio for high and low operating pressure cases, respectively.

Certainly, a concern is a rather large heat transfer area requirement, around 400 m^2/stage, related to the most beneficial compression ratio. This is considered in more detail later on.

Unfortunately, the situation is not as simple as suggested by the trends of overall performance curves shown in Fig. 10. Figure 11 shows the temperature difference profile over the HIDiC length for the compression ratios considered in this study. They all exhibit the same trend, indicating that the temperature difference decreases toward the column bottom. At lowest value, 1.2, it appears that in the bottom part a temperature inversion occurs, resulting in a negative driving force, indicating that in this case stripping stages are hotter than related rectification section stages. This is possible and can be considered as lower theoretical limit for the compression ratio in conjunction with a HIDiC. As indicated in Fig. 12, the operation at such low temperature differences would require a correspondingly increasing heat transfer area, which at lower compression ratios, particularly in the bottom part of the column could lead to prohibitive values. Obviously, a trade off between the compression ratio and the heat transfer area is an important consideration in designing a HIDiC.

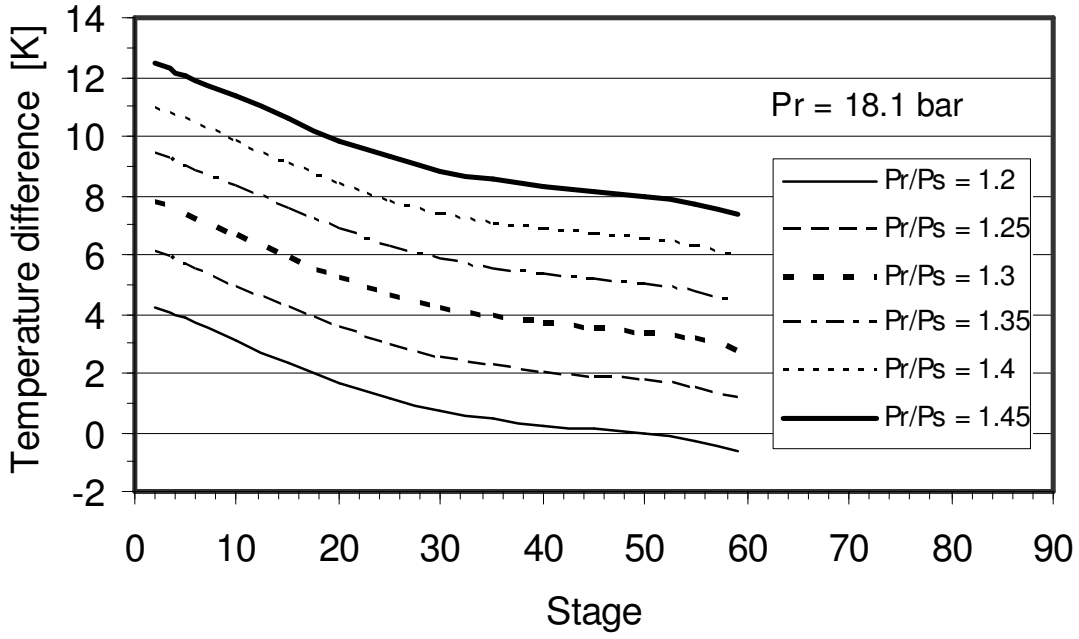

Figure 11: Temperature difference profiles at different compression ratios along the HIDiC, from the top to the bottom of stripping/rectification section.

In fact, the problem is that relatively much more heat transfer area is required in the bottom of the stripping section, where the cross sectional area of trays

is minimal. In other words, the heat transfer area requirement and the space available for installation of the heat transfer panels exhibit opposite trends, which poses a real threat to feasibility of HIDiC. On the other hand, the cross sectional area of the trays in the rectification section is at its maximum in the bottom part of the HIDiC. Therefore, an option is to switch with the installation of heat transfer panels from the stripping section to the rectification section trays at the point that the active tray area available in the stripping section becomes insufficient. This option, elaborated in more details elsewhere (6) requires a more complex type of heat transfer device than the simple panels. Because of related performance uncertainties (countercurrent vapor/liquid flow involved), there is a reason for concern, i.e. placing the heat transfer devices into rectification section could potentially prove impractical. This will be considered in more detail in the next stage of this project.

A potential remedy for this problem could be excluding ten to twenty most critical trays from the heat integration, by operating the bottom part of the stripping section as a normal column with an external reboiler. However, this configuration requires a parallel column configuration, with a hybrid column, comprising a HIDiC placed above a normal stripping section in one shell, as one, and the normally operating part of the rectification section with more stages as the other column.

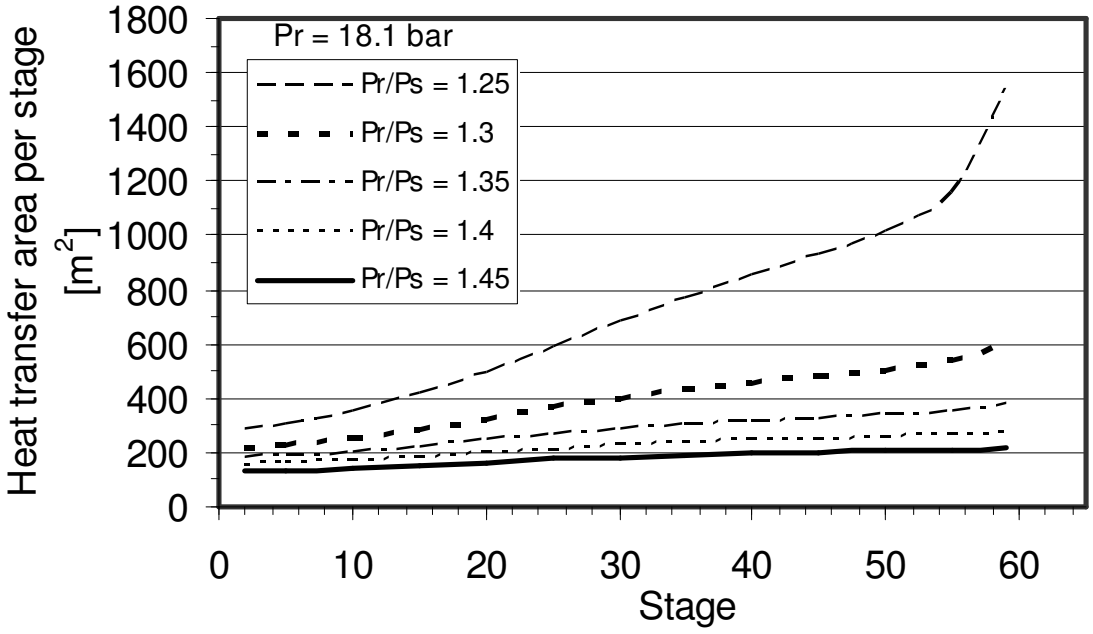

Figure 12: Heat transfer area profiles at different compression ratios along the HIDiC, from the top to the bottom of stripping/rectification section.

Fortunately, as indicated by dot lines in Fig. 10, the costs of a full scale HIDiC can be pushed down significantly if operating pressure is minimized, in this case that based on the stripping section pressure of 11.2 bar. At the same compression ratio, this results in a lower rectification section pressure (14.6 bar). Comparison of total annual costs for these two options indicates that TAC for low operating pressure option is some 10 % lower and that the break-even point is pushed to higher compression ratio (above 1.4). This is mainly because of the fact that at fixed number of stages the reflux ratio will decrease with decreasing operating temperature/pressure, and this is directly reflected in decreasing operating costs. It should be noted that a 14 bar vapor leaving at the top of the column (35 ^{0}C at compression ratio of 1.3) still can be condensed using water, at the expense of using a larger condenser to compensate for a reduced temperature difference. However, this is of negligible impact on overall costs. Therefore, the low operating pressure version of HIDiC is preferred.

5.4.2 Sensitivity to the number of stages

It is inherent to a distillation process that by increasing the number of equilibrium stages to infinity the operating costs proportional to the reflux ratio will decrease to a minimum. So, by operating a conventional column, a VRC or a HIDiC at maximum number of stages will force the operating costs, which dominate the overall annual costs of both VRC and HIDiC, to decrease accordingly. This is illustrated for VRC and HIDiC version of the PP-splitter in Fig. 13, which shows the relative TAC and the average heat transfer area per stage as a function of the number of stages. The asymptotic trend in TAC at high end indicates that a HIDiC with 230 stages should be considered as reasonable choice, regarding the fact that this means installation of more than 250 actual trays in a column, which is demanding, but could be realized in one shell, as suggested in Fig. 7c.

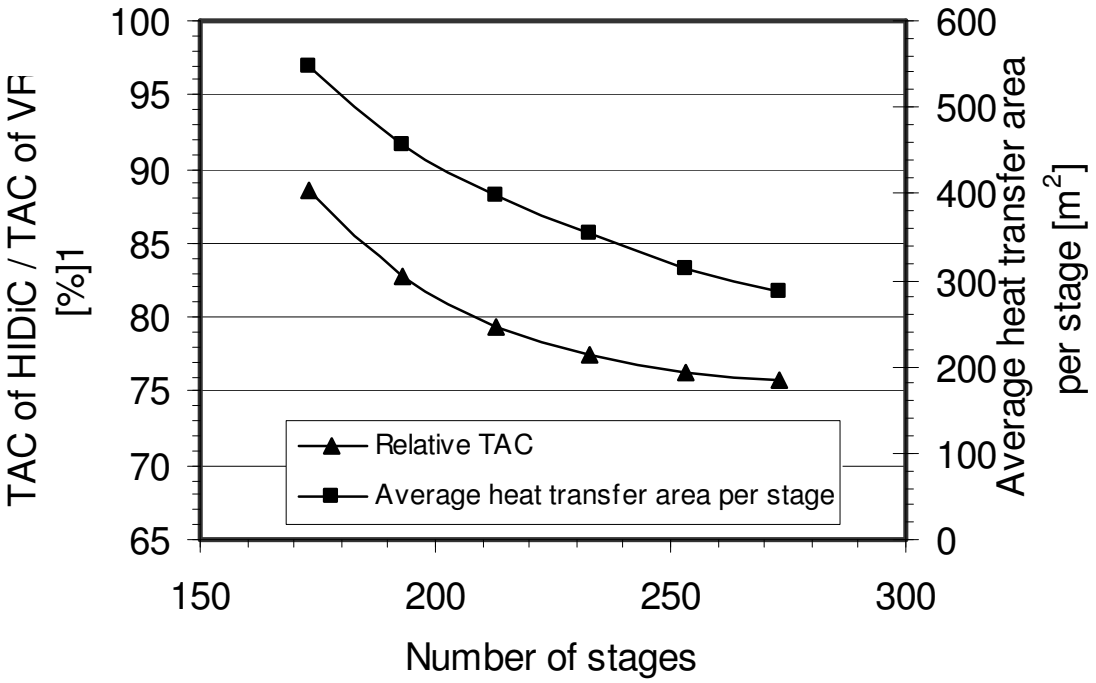

Figure 13: The effect of the number of stages on relative TAC and the average heat transfer area per stage (p_r = 14.6 bar).

5.4.3. Sensitivity to utilities cost

Figure 14 shows the relative TAC's as a function of the electricity and cooling water costs. Obviously, the effect of the variation in cooling water cost is practically negligible, while the effect of the electricity cost is very strong; indicating that with increasing electricity cost HIDiC becomes more attractive option for a PP-splitter.

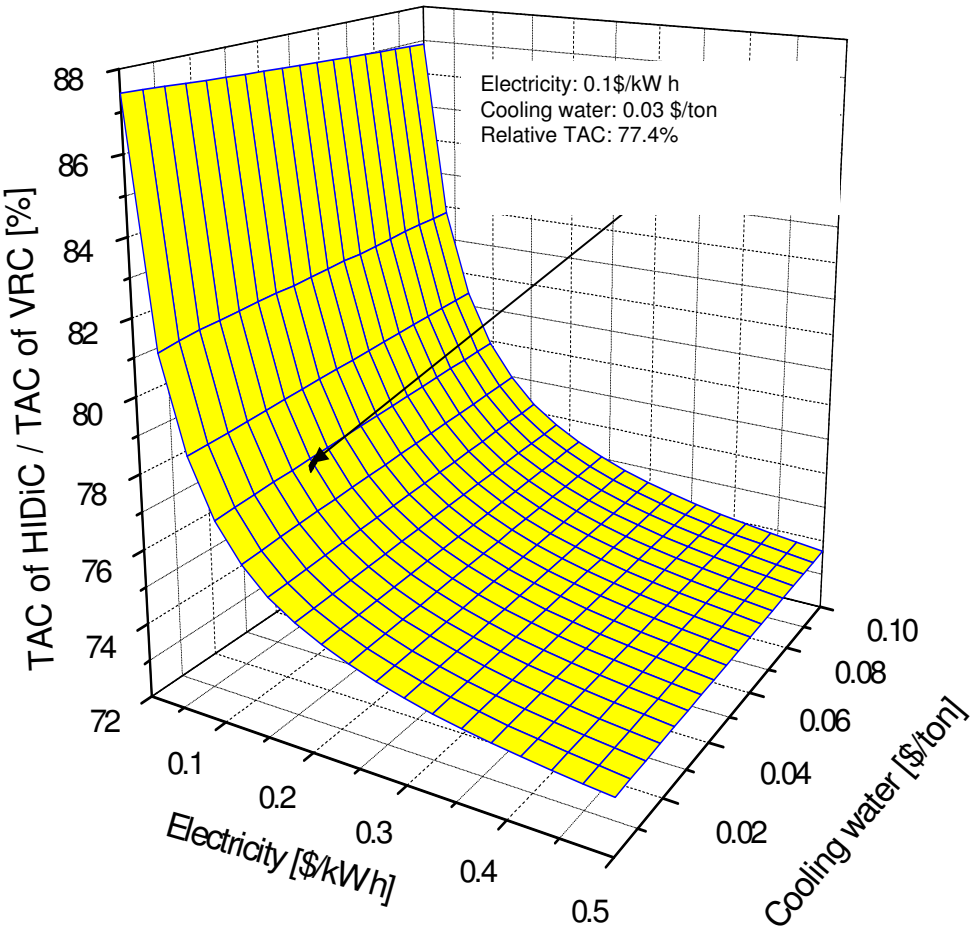

Figure 14: Effect of the variation in electricity and cooling water costs on the relative TAC's (for P_r=14.6 bar, P_r/P_s=1.3, relative TAC is equal to 77.4%).

5.5 Conclusions

A new type of asymmetric HIDiC is introduced which allows for optimization of the feed location by partial thermal coupling of stripping and rectification section. The energy requirements of HIDiC appear to be strongly dependent on the way how the stripping and rectifying section are thermally integrated. The top design HIDiC in which the stripping section is thermally coupled with the top trays of the rectification section is the best configuration for a HIDiC PP-splitter, which can save approximately 50% of energy compared to the VRC.

Based on the simulation results presented in this study, it may be concluded that HIDiC is feasible and could be competitive to a VRC. A PP-splitter could be designed as a one-shell column, with the HIDiC part placed above the part of rectification section operating as a normal column.

This study indicates that relative gain in total annual cost could be up to 20 %. Compressor capital cost and strikingly large operating cost are the main factor affecting the economy of a HIDiC. Both, the increasing number of stages and decreasing pressure ratio and operating pressure of the top of the column are beneficial in this respect.

A trade off between the heat transfer area and the compression ratio is required to arrive at an optimum, and particular attention must be given to the distribution of heat transfer area in the bottom part of the HIDiC. The heat transfer area requirement per stage is rather high and should be considered as a serious threat to the feasibility of HIDiC. A reduction in the column pressure drop could help shift the optimum toward the larger values of the compression ratio, i.e. lower heat transfer requirement per stage.

5.6 Nomenclature

A	heat transfer area (m^2)
bp	break power (kW)
CC_{inst}	purchase and installation costs of centrifugal compressor ($)
d_{col}	column diameter (m)
F_C	correction factor (-)
HEC_{inst}	purchase and installation costs of heat exchangers ($)
h_{tray}	height of the column occupied by trays (m)
M&S	Marshall & Swift index (-)
Q	Heat transfer duty (W)
TAC	total annual cost ($)
TC_{inst}	purchase and installation costs of trays ($)
U	overall heat transfer coefficient (W/m^2K)
ΔT	temperature difference (K)

5.7 References

(1) Olujic, Z., Fakhri, F., de Rijke, A., de Graauw, J., Jansens, P.J. Internal heat integration- the key to an energy conserving distillation column, J. Chem. Technol. Biotechnol. 2003;78:241– 48.

(2) Nakaiwa, M., Huang, K., Endo, A., Ohmori, T., Akiya, T., Takamatsu, T. Internally heat integrated distillation columns: a review, Trans IChemE, Part A, Chem. Eng. Res. Des. 2003;81: 162-77.

(3) Naito K, Nakaiwa, M, Huang, K, Endo, A, Aso, T, Nakanishi, T, Nakamura, T, Noda, H. and Takamatsu T, Operation of a bench-scale HIDiC: an experimental study, Computers and Chemical Engineering 2000; 24: 495-99.

(4) Sun, L., Olujic, Z., de Rijke, A., Jansens, P.J. Industrially viable configurations for a heat-integrated distillation column, Better Processes for Bigger Profits, Proceedings of the 5th International Conference on Process Intensification for Chemical Industry, Maastricht, The Netherlands, 13-15 October 2003, BHR Group 2003, Edited by M. Gough, 151-66.

(5) LeGoff, P., Ramadane, A., Rivero, R., Cachot, T., Diabatic distillation: simulation-optimization of a column with integrated heat exchangers, IChemE Symp. Series 1992; No. 128: A77-A90.

(6) Rivero, R., Exergy simulation and optimization of adiabatic and diabatic binary distillation, Energy; 2001; 26: 561-93.

(7) de Graauw, J., de Rijke, A., Olujic, Z., Jansens PJ, Distillation column with heat integration, European Patent no. EP1332781 (06-08-2003).

(8) Kister, H., Haas, J.R., Predict entrainment flooding on sieve and valve trays, Chem. Eng. Prog. 1990;86(9):63-9.

(9) Douglas, J.M., Conceptual Design of Chemical Processes, New York, McGraw-Hill, 1988.

(10) Emtri, M., Miszey, P., Rev, E., Fonyo, Z., Economic and controllability investigation and comparison, Chem. Bio. Eng. 2003;17(1):31-42.

(11) Chemical Engineering 2003;110(6):82.

Chapter 6:

Optimized HIDiC Designs for Different Industrial Applications

Abstract

A HIDiC is essentially a fractionating heat-exchanger. Therefore the temperature profile dictates the trays which are feasible for internal heat transfer. A better exploitation of driving forces for heat transfer, leads to less overall heat transfer area requirement and moreover to a more feasible design. Optimized HIDiC designs for different industrial applications are presented, namely for the separation of propylene-propane, methanol-water and ethyl benzene-styrene. The choice for an ideal HIDiC without external reboiler or a partial HIDiC is strongly dependent on the model system. The column configuration has a large effect on the feasibility of HIDiC. When the stripping section is shorter than the rectifying section the top design HIDiC, in which the stripping section is thermally coupled with the top part of the rectification section, is favourable. When the stripping section is longer than the rectifying section, the optimal column configuration is the bottom design HIDiC, in which the rectifying section is thermally coupled with the bottom part of the stripping section. HIDiC appears to be favourable for the separation of close boiling mixtures in moderate to high pressure applications, where an optimal HIDiC design allows halving the energy consumption compared to conventional heat pump technology.

6.1. Introduction

A very efficient but capital intensive way to improve the thermal efficiency of a single distillation column is to implement so called vapour recompression. In a vapour recompression column (*figure 1*) (VRC) the top vapour is compressed to such a pressure and temperature level that it can be used as heat source for the reboiler. An internally heat integrated distillation column, HIDiC, offers the maximum energy saving potential for difficult and energy intensive separations, such as propylene-propane (PP-splitter), ethanol-water, etc. (1)

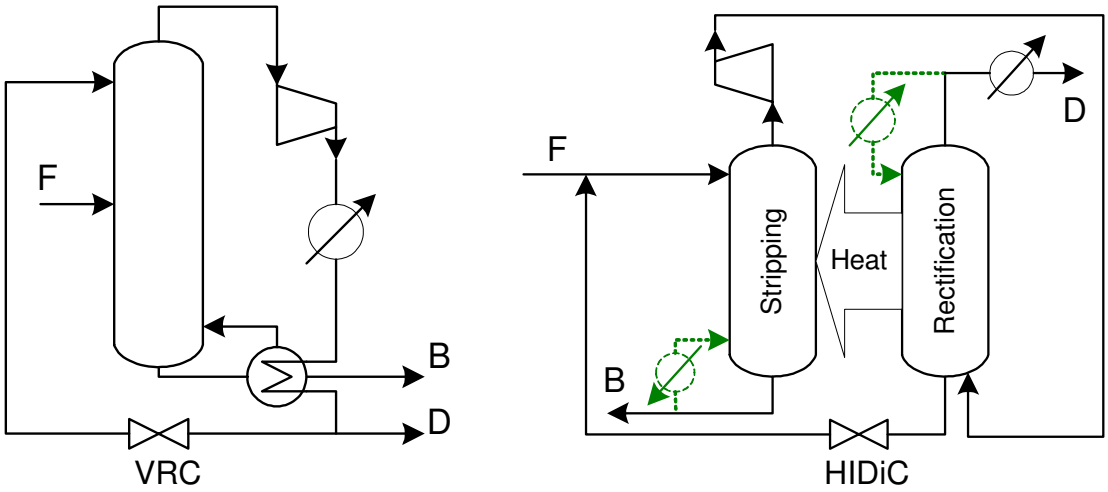

Figure 1: Schematic representation of the vapour recompression column and the HIDiC

In this concept the well established heat pump principle is applied in combination with a diabatic operation (1) and HIDiC should as such compete with conventional vapour recompression technology. (*figure* 1)
In an ideal HIDiC the distillation column is fully heat integrated internally so that no external reboiler is required. A partial HIDiC uses an external reboiler to provide part of the vapour in the stripping section and consequently less internal heat transfer is required. As will be shown in this paper the choice for an ideal or partial HIDiC depends strongly on the mixture which has to be separated.

Background

Although the HIDiC concept was already introduced in 1977 by Mah et al (2) and a lot of promising research studies have been carried since that time (2-7), HIDiC is still not implemented in industrial practice. The complexity of equipment design appeared to be a barrier for industrial implementation. The HIDiC design which was proposed by de Graauw et al (8,9) is based on a

concentric stripping section which is configured around the rectifying section. Heat is transferred by heat transfer panels which can be placed in either the stripping section or the rectifying section.(*figure 2 and 3)*.

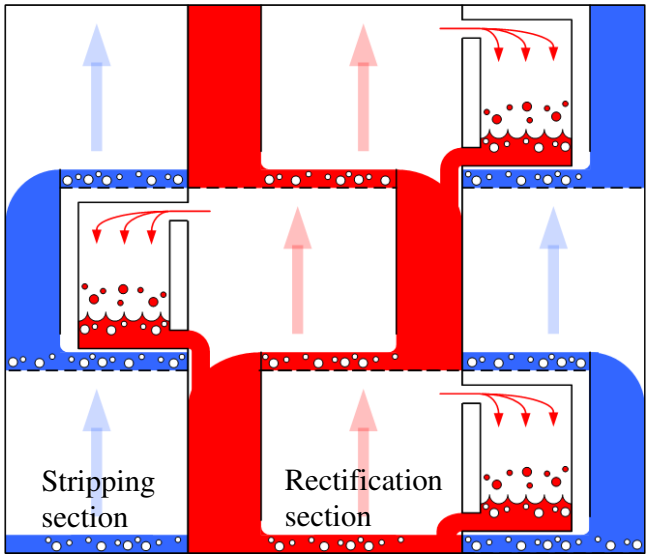

Figure 2: Cross section of concentric HIDiC with heat panels in stripping section

Gadalla et al (10) performed a study on the thermo-hydraulic design of a concentric HIDiC and developed a software tool to determine the optimum heat panel configuration. In this paper this tool is used to calculate how much heat transfer area can be realized physically in a concentric HIDiC.
Previous work showed that the energy efficiency of an asymmetric HIDiC strongly depends on the column configuration (11, see Chapter 5). From this study the so-called top design, in which the stripping section is in heat exchanging contact with the top of the rectifying section appeared to be the most favourable column configuration for a HIDiC PP-splitter, which can save 50% of energy compared to a VRC. An economical evaluation (Chapter 5, 11) revealed that a HIDiC PP-splitter can save 20% of total annual cost compared to a state of the art vapour recompression column (VRC).
The simulation studies on the PP-splitter carried out so far were based on the assumption of a constant heat transfer duty per stage (Chapter 5). Gadalla et al (10) suggest that both from heat transfer and equipment design point of view it could be better to use a constant heat transfer area per stage, resulting in a duty profile which follows the temperature driving force profile. The aim of the present work is to compare the results for a PP-splitter based on constant heat transfer area per stage with those of the aforementioned design based on constant heat duty per stage.

The second case study is the separation of water-methanol. The separation of aqueous mixtures by distillation is energy intensive due to the large heat of evaporation of water. The large energy requirement makes it a possible interesting candidate for HIDiC technology.
The third model system chosen for this design study is the separation of ethyl benzene-styrene, Due to the tendency of the styrene to polymerize at alleviated temperatures, distillation is performed under vacuum. As a low pressure drop along the column is essential in a vacuum application, the preferred column internals for this separation are structured packings. Because of the high purity requirements and a rather low relative volatility of this mixture, which is around 1.4, this separation appeared to be a good candidate for vapour recompression and a simulation study indicated that up to 60% of energy could be saved, when a conventional sieve tray column was revamped to a heat pump column equipped with structured packings (13). For the same reasons, this application could also be a very interesting candidate for a HIDiC. Another interesting aspect of this separation is that the desired high purity product is the bottom product of the distillation column, which is exceptional as in most columns the distillate is the desired product. The high purity requirement of the bottom stream leads to a distillation column in which the stripping section contains more stages than the rectifying section. It is therefore a very attractive model system to study the influence of column configuration in the case that the length of the stripping section exceeds that of the rectifying section.

6.2. Design Guidelines

The key parameter in HIDiC design is the compression ratio (1). A lower compression ratio is beneficial from an energy requirement point of view. A lower compression ratio also results in a lower temperature driving force between rectifying and stripping section and consequently in increased heat transfer area. Therefore, the optimum compression ratio is a trade-off between electricity consumption of the compressor and the amount of heat transfer area which can be physically placed in the distillation column.

Because a HIDiC is essentially a fractionating heat exchanger, a very important design guideline is the temperature profile. The first step in the design procedure is therefore to simulate a high pressure rectifying section and a low pressure stripping section, without internal heat transfer. The resulting temperature profile is used to provide a guide for the choice of the compression ratio. Moreover the temperature profile will give insight where heat transfer panels should be preferably placed i.e. at stages with maximum temperature driving force. Stages with low or even negative temperature

driving force must be excluded from the heat integration process, which is easy to realize with the HIDiC with panels.

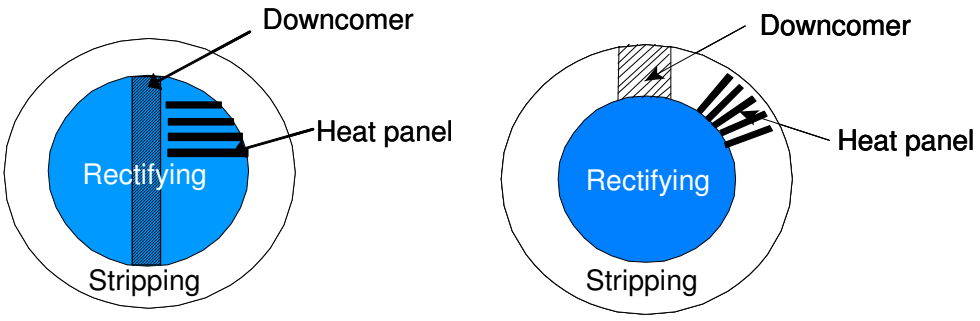

Figure 3: Placement of heat transfer panels in rectifying or stripping section

The second design guideline is the heat transfer area. The column diameter, i.e the overall cross sectional area per tray of a distillation column is determined by the vapour load. From this column diameter follows the maximum amount of heat transfer area that can be physically placed on the active tray area. The configuration of the heat transfer panels in both the annular stripping section and the rectifying section is schematically drawn in *figure 3*. In this study the distance between two adjacent panels is 30 mm. The height of a heat transfer panel is 300 mm, the length depends on the column diameter and the width of a panel is 15 mm. A heat transfer coefficient of 1000 W/m^{2}K was assumed, based on the experimentally obtained results for the overall heat transfer coefficient of a cyclohexane/(n)-heptane mixture in the HIDiC pilot plant.

After determining the initial compression ratio and the heat transfer stages from the temperature profiles, the internal heat transfer rate is stepwise increased by either increasing the duty per stage or alternatively increasing the heat transfer area per stage. The objective is to realise the most economical HIDiC configuration either partial or ideal. Total Annual Costs are calculated simultaneously by linking Excel with ASPEN as to determine which degree of internal heat integration is optimal. The cost estimation procedure was based on correlations by Douglas (12) and is described elsewhere (11, see Chapter 5).

6.3. Results and Discussion

6.3.1 Propylene Propane splitter

The base case for the simulation studies is an actual state of the art, stand alone VRC PP-splitter. The feed conditions and column data are summarized in *table 1*.

Table 1: PP-splitter column specification

Column specification		
Feed		propylene-propane
Composition	propylene mole %	50
Flow rate	t/h	111.6
Pressure	bar	12.2
Temperature	°C	31.7
Rectifying pressure	bar	19.2
Stripping pressure	bar	12.2
Rectifying stages	-	154
Stripping stages	-	57
Top product purity	propylene mole %	99.6
Stripping stages	propylene mole %	1.1

From previous work (1, see Chapter 5) the optimal compression ratio of a top design HIDiC PP-splitter appeared to be between 1,3 and 1,4.

Figure 4 shows the temperature profile of the top design HIDiC PP-splitter at zero internal heat transfer rate. The temperature driving force is relatively large in the upper part of the stripping section and gradually decreases to around 4 ºC in the bottom part of the stripping section. There is a positive, sufficiently large, temperature driving force at all stages and therefore heat transfer panels should be placed at every tray in the heat integrated part of this PP-splitter.

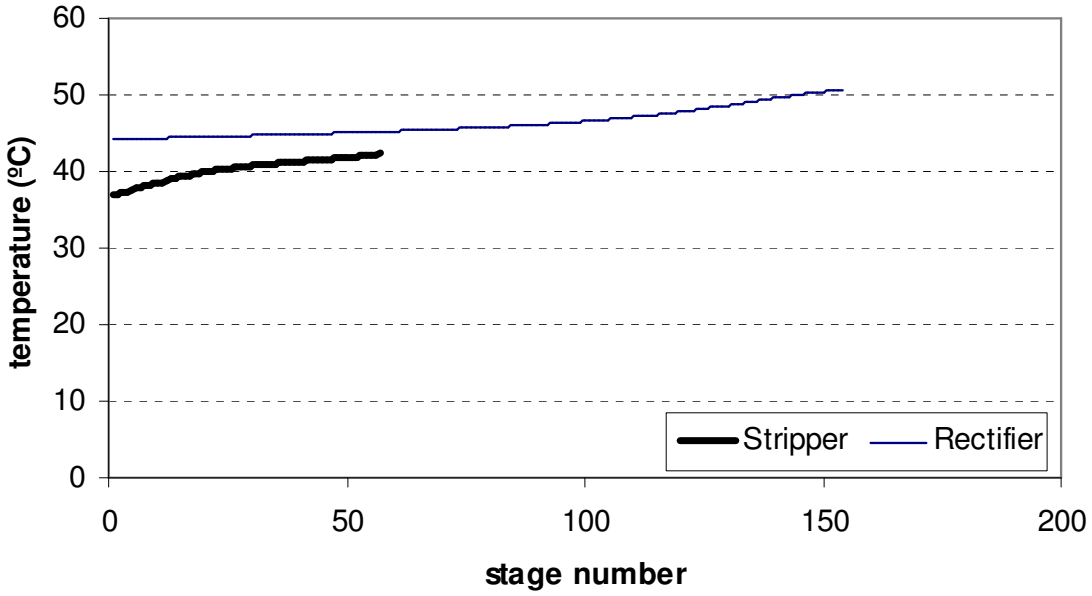

Figure 4: Temperature profile of stripping and rectifying section PP-splitter

Figure 5 shows the reboiler, condenser and compressor duty as function of heat transfer area per stage. Both reboiler and condenser duties decrease almost linearly with increasing internal heat transfer area. The compressor duty remains more or less constant. A heat transfer area of 402 m^2/stage is required to obtain an ideal HIDiC. The corresponding compressor duty is 7500 kW. It should be mentioned that at zero reboiler duty, still a small top condenser is required. The heat duty of this condenser is decreased with 93% compared to the conventional distillation column.

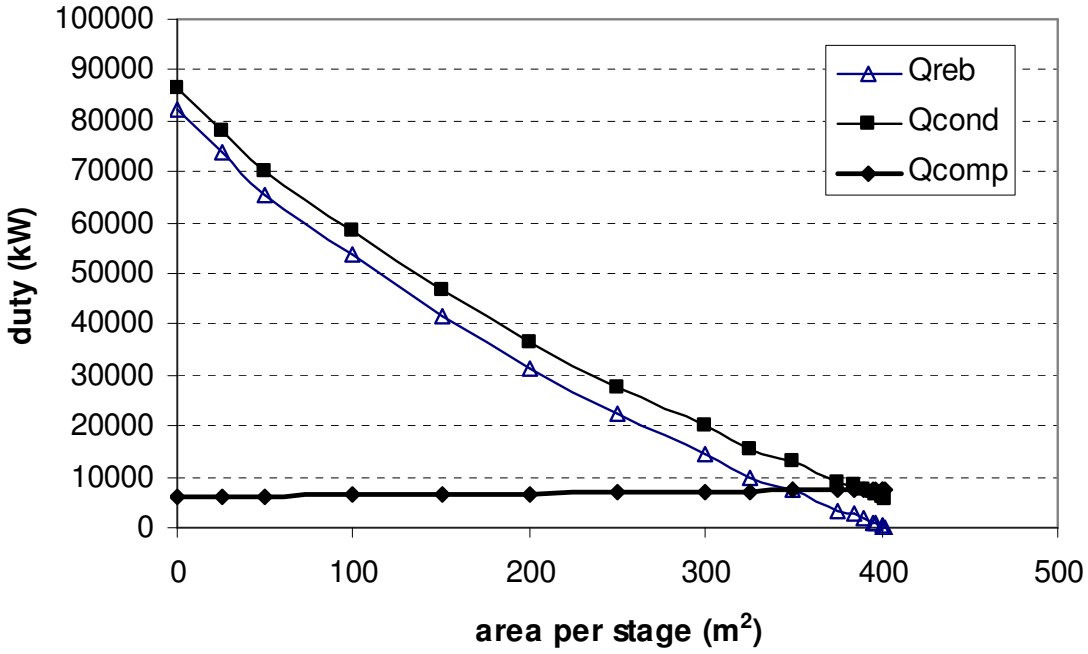

Figure 5: Reboiler, condenser and compressor duty PP-splitter as function of heat transfer area per stage

The Total Annual Cost shows a negative slope as function of heat transfer area per stage. (*Figure 6*). Hence for the PP-splitter an ideal HIDiC with zero reboiler duty is the most economical option, which can save 20% of Total Annual Cost compared to its VRC counterpart (table 2). Certainly a small reboiler and a condenser are inevitable for start-up purposes.

Table 2: Economic evaluation HIDiC for PP-splitter

	HIDiC	VRC
Column	8.38	6.98
Reboiler	-	1.90
Compressor	9.73	12.37
Condenser	0.62	0.39
Trays	1.82	1.65
Heat Panels	1.89	-
Capital Cost (M$)	22.45	23.29
Steam	-	-
Electricity	4.83	6.47
Cooling water	0.44	0.51
Variable Cost (M$/yr)	5.27	6.98
Total Annual Cost (M$/yr)	7.52	9.31

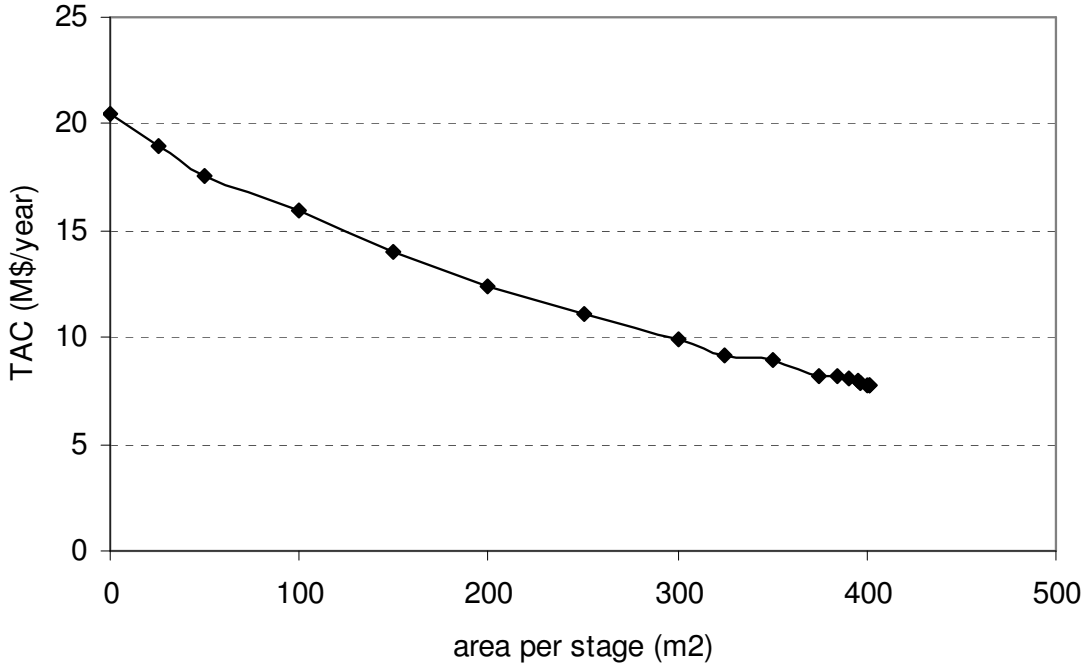

Figure 6: Total Annual Cost PP-splitter as function of heat transfer area per stage

In table 3 the most important results for the HIDiC PP-splitter with constant area per stage are compared with those obtained for constant heat duty per stage.The performance of both HIDiC designs is roughly the same. Less surface area is required in the HIDiC with constant area per stage because the temperature driving forces are better exploited. When considering the second design guideline, namely the amount of heat transfer area that can be physically mounted inside the column an important difference between the two design options appears.

Table 3: Design results for constant duty and area scenarios

Design specification		Constant duty	Constant area
Stage duty	kW	1817	variable
Heat transfer area	m^2	variable	402
Reboiler duty	kW	0	0
Condenser duty	kW	5782	5812
Compressor duty	kW	7489	7415
Total heat transfer area	m^2	25364	22914

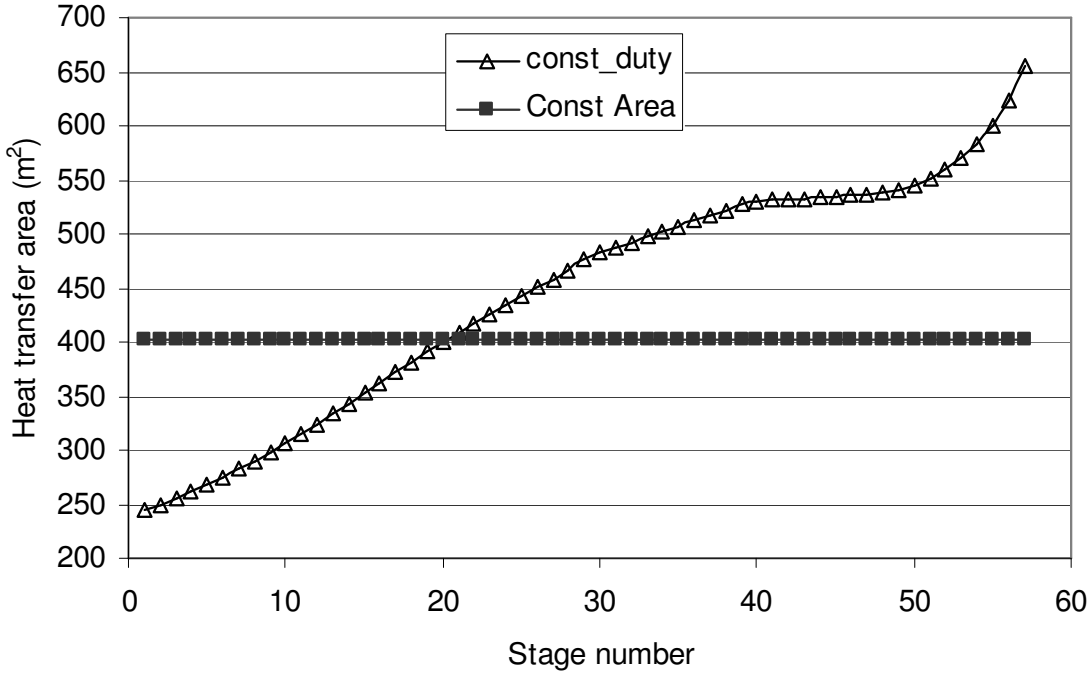

Figure 7: Heat transfer area requirements PP-splitter for constant area design and constant duty design

In figure 7 the heat transfer area for both cases is plotted against the stage number of the stripping column. Calculation of the hydraulic constraints show that in this PP-splitter the maximum amount of heat transfer area that can be placed is 450 m^2 per stage. When this constraint is applied to the HIDiC design with constant duty per stage it follows that it is not possible to physically place the required heat transfer area at all stages without increasing the column diameter, which in turn would adversely affect the hydraulics. The stages with a relatively low temperature driving force in the bottom section require a heat transfer area which is larger than 450 m^2. Roughly half of the stages, namely stage 27 to 57 require a larger heat transfer area than 450 m^2 and it must be concluded that it is practically impossible to build such a HIDiC without increasing the column diameter, changing the panel geometry or by intensifying the heat transfer somehow.

In the constant area design, the required heat transfer area is 402 m^2 per stage which is well below the maximum allowable heat transfer area from the hydraulic calculation (450 m^2 per stage). The advantage of applying a constant heat transfer area per stage is two-fold: First the temperature driving

forces are better exploited and less total surface area is required. Secondly the hydraulic calculation shows that the maximum amount of heat transfer area that can be placed along the length of the heat integrated section of the distillation column is more or less constant for every stage. Also, the hydraulic analysis tends towards constant area per stage as the most appropriate design. In the bottom, panels will be placed preferably in the rectifying section, because vapour load and consequently diameter is much larger than in the corresponding stages of the stripping section. In the top, panels will be placed preferably in the stripping section, because vapour load and hence diameter of the stripping section is largest in the top of the heat integrated section.

6.3.2 Methanol water separation

Base case for the methanol-water separation is an atmospheric conventional distillation column with a capacity of 76 ton/hr and a reboiler duty of 45 MW, which is huge in every respect. The operating conditions are summarised in table 4. In this distillation column the stripping section (30 trays) is also shorter than the rectifying section (65 trays) because of the non-ideality of this system. The relative volatility increases from roughly 2 in the top to 7 in the bottom of the column. In the McCabe-Thiele plot the equilibrium line nearly touches the operating line at high water purities, which is the reason that the rectification section contains much more trays than the stripping section.

Table 4: Methanol-water column specification

Column specification		
Feed		Methanol-water
Composition	water wt %	21.4
Flow rate	t/h	76.8
Rectifying pressure	bar	2.6
Stripping pressure	bar	1.3
Rectifying stages	-	65
Stripping stages	-	30
Top product purity	methanol mole %	99.9
Stripping stages	water mole %	99.9

The temperature profile of a HIDiC with zero internal heat transfer and a compression ratio of 2 is plotted in figure 8. The temperature in the bottom of

the stripping section increases sharply because the composition changes quickly to pure (>99.99 %) water in the bottom stages. A temperature cross occurs at stage 25 i.e.: from stage 26 and upwards the temperature of the stripping section exceeds that of the rectifying section. Obviously these trays must be excluded from the heat transfer process as they would work reversely i.e.: heat would be transferred in opposite direction. Tray 24 has a positive, but very low temperature driving force and is for this reason also not heat integrated.

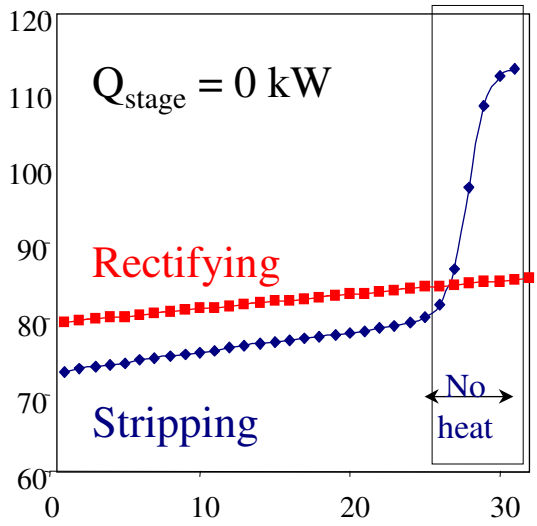

Figure 8: Temperature profiles of stripping and rectifying section Methanol-water separation

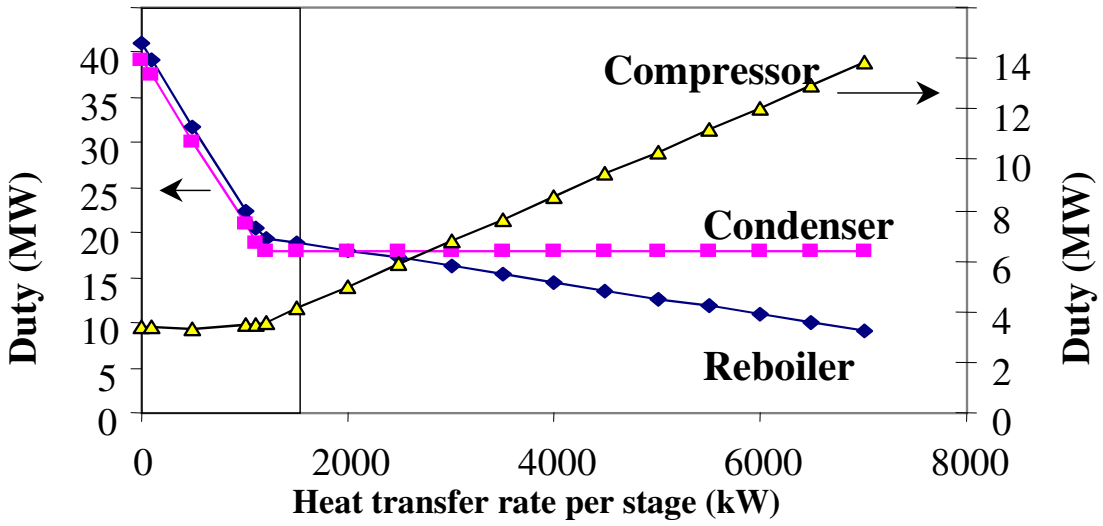

Figure 9: Reboiler, Condenser and compressor duty HIDiC Methanol-water as function of internal heat transfer rate

Figure 9 shows the reboiler, condenser and compressor duty as function of heat transfer duty per stage. In the range between zero to 1150 kW/stage, both reboiler and condenser duty decrease sharply and compressor duty remains constant. When internal heat transfer rate is further increased, only the reboiler duty decreases at the cost of a sharp increased compressor duty. It is not possible to reduce the condenser duty further than around 19,5 MW. The secondary reflux in the rectifying section, caused by internal condensation against the heat transfer surface, is not sufficient to reach the top product specification. Primary reflux from the condenser must be supplied in order to get the desired methanol purity. It is clear from this graph that an ideal HIDiC without external reboiler will not be the most economical column configuration. When internal heat transfer rates higher than 1150 kW/stage are applied, a reduction of 1 kW reboiler duty is at the cost of 0,65 kW compressor duty. Taking into consideration the fact that the compressor is driven by electricity and that for the production of 1 kW of electricity approximately 3 kW of fuel has to be consumed due to inefficiencies in the electricity generation process, a higher internal heat transfer rate than 1150 kW/stage will lead to an increased overall energy requirement. Hence for the separation of given methanol-water mixture a partial HIDiC is the preferred option.

Table 5: Simulation results for different HIDiC designs

	Conventional Column	Top design HIDiC with constant duty per stage	Top design HIDiC with constant area per stage	Bottom design HIDiC with constant area per stage
Reboiler duty (MW)	45	19.5	19.9	19.9
Condenser duty (MW)	40	17.9	17.9	17.9
Compressor duty (MW)		3.5	3.5	5.6
Total heat panel area (m^2)		9410	4140	4095

A bottom design, where the stripping section is in heat exchanging contact with the bottom of the rectifying section is also taken into consideration. The temperature profile shows the same trend and tray 24 to 30 are again excluded from the heat transfer process. Moreover the top design was also carried out with constant heat transfer area per stage. The results for these three design options are summarised in table 5. The compressor duty which is required in the bottom design is significantly larger than in the top design.

This is due to the fact that roughly half of the rectification column has to operate at a low reflux ratio compared to the conventional column. The primary reflux supplied by the top condenser is roughly a factor two lower than desired in a conventional distillation column and this causes a lower separation performance of the conventional part of the rectification section, i.e. the top trays without heat transfer bodies. This decrease in separation performance has to be balanced in the heat integrated part of the distillation column, thus leading to higher secondary reflux rates and consequently a higher compressor duty. Similar behaviour was observed for the bottom design PP-splitter (16).

Table 6: Economic evaluation HIDiC for methanol-water separation

	HIDiC	Conventional
Column	2.64	1.83
Reboiler	0.34	0.76
Compressor	6.22	-
Condenser	0.33	0.61
Heat Panels	0.62	-
Capital Cost (M$)	10.16	3.19
Steam	3.40	7.65
Electricity	2.80	-
Variable Cost (M$/yr)	6.20	7.65
Total Annual Cost (M$/yr)	7.22	7.98

The comparison of constant area versus constant duty shows the same effects as were observed in the PP-splitter, however for the separation of methanol-water these effects are more pronounced. The heat transfer area requirement is decreased with more than 50% when switching from constant duty to constant area per stage, because temperature driving forces are better exploited. From a hydraulic calculation follows that maximum 230 m^2/stage can be placed within the calculated column diameters. Considering the constant duty design, only trays 1 to 5 in the stripping section require a heat transfer area which is lower than the upper limit. The required surface area increases up to 900 m^2/stage in the bottom of the stripping section, which is obviously not a realistic value. With constant area assumption, the required heat transfer area is 172 m^2/stage, which is well below the maximum area from hydraulic calculations.

In summary for this case a partial HIDiC with a constant heat transfer area is the optimal design, which can save 50% of energy compared to the conventional distillation column.

However, as indicated in table 6, the capital costs of HIDiC exceed that of the conventional column, mainly due to the purchase cost of the compressor. On the other hand operating costs of HIDiC are substantially less than that of the conventional column, leading to a lower total annual cost of 9% compared to the conventional column.

6.3.3 Ethylbenzene-Styrene separation

The base case used for this study is an industrial 70 t/h heat pump EB/ST splitter. The column specifications are given in table 7.

Table 7: Ethylbenzene-Styrene Vapour recompression column specification

Column specification		
Feed Composition	Styrene mole % Ethylbenzene Toluene Benzene Heavy ends	64,4 33,6 1,27 0,60 0,07
Flow rate	t/h	70
Column top pressure	bar	0.24
Column bottom pressure	bar	0.30
Rectifying stages	-	24
Stripping stages	-	60
Bottom product purity	Styrene mole %	99.8
Top product purity	Styrene mole %	1.1

It should be noted that this heat pump assisted column, equipped with corrugated sheet packing, is operated under higher pressure (in vacuum) than the conventional column in order to minimize the actual volume flow through the compressor. Although the large volumetric flows associated with vacuum applications are definitely disadvantageous, compared to high pressure applications, the lower circumferential velocities of the compressor and lower compression performances in vacuum applications are advantageous. Namely for vacuum to moderate pressure applications, single- or two stage turbo blowers can be applied, instead of the high compression performance centrifugal compressors required for high pressure applications. For economic reasons turbo blowers are applied whenever possible in distillation plants. Large volumetric flow rates are accommodated by using a number of blowers in parallel. This allows the application of standard types, and the performance can be regulated over a wide range with high efficiency

(13). The largest standard type turbo blower, which can be manufactured at this moment, has a suction capacity of 200.000 m^3/h. (14). The actual volume flow through the compressor in the present heat pump EB/ST splitter is 350.000 m^3/h. The compression ratio is 3, requiring a double-stage blower. Therefore two double-stage turbo blowers are applied in parallel. The cost of a turbo blower depends on both compression ratio and capacity.
A relation for the purchase cost of different types of turbo blowers is given by Peters & Timmerhaus (15) For a turbo blower with a maximum delivery pressure of 0,7 bar:

$$PurchaseCost = \left(\frac{M\ \&\ S}{260} \right) \cdot 0.0597 \cdot Q^{0,598} \qquad [1]$$

where, Q is the capacity (m^3/s) and the Marshal & Swift index was taken to be 1116 (11). An installation factor of 4 is recommended by Douglas (15). For the cost estimation of the structured packing a HETP of 0,5 m, and an installed price of $ 1000/ m^3 packing was assumed. The cost estimation procedure for column shell, reboiler, condenser and heat panels was equivalent to that for the PP-splitter and methanol water separation (11).

6.3.3.1. Bottom design

The simulations were carried out at different pressure ratio's for both top and bottom design HIDiC with constant area per stage. The temperature profile of the bottom design HIDiC with a compression ratio of 1,9 is given in figure 10. It is clear that there are no obvious limiting stages with very low temperature driving force and therefore no stages were excluded from the heat transfer process.

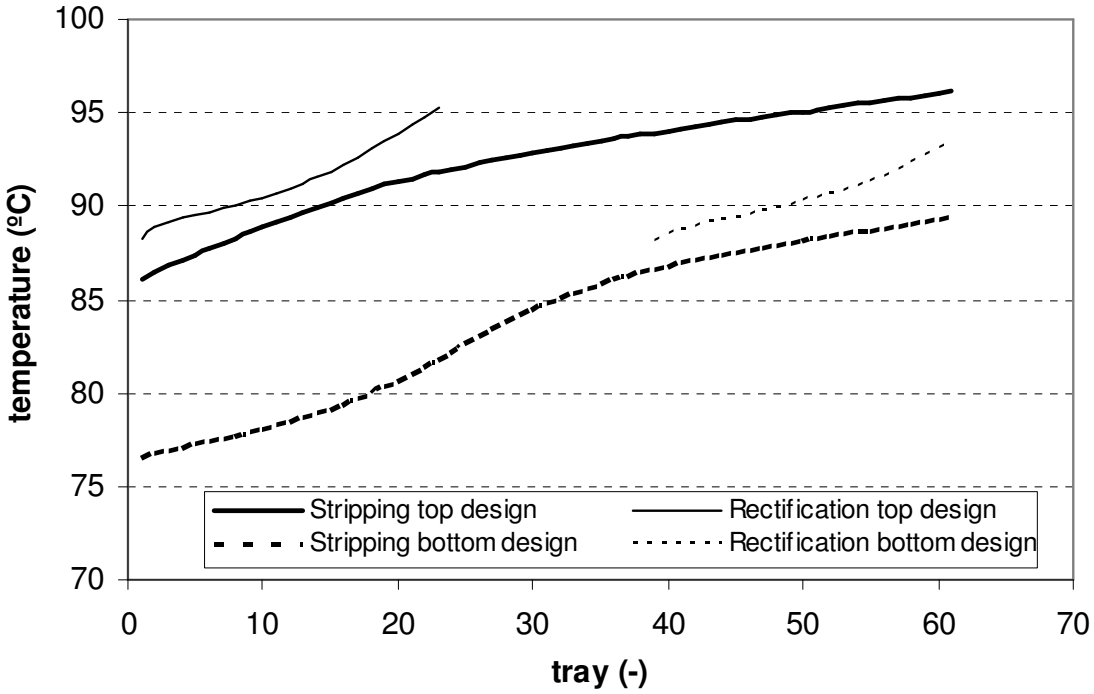

Figure 10: Temperature Profile for top design (pressure ratio = 1,4) and Bottom design (pressure ratio = 1,9) HIDiC Ethyl benzene-Styrene separation.

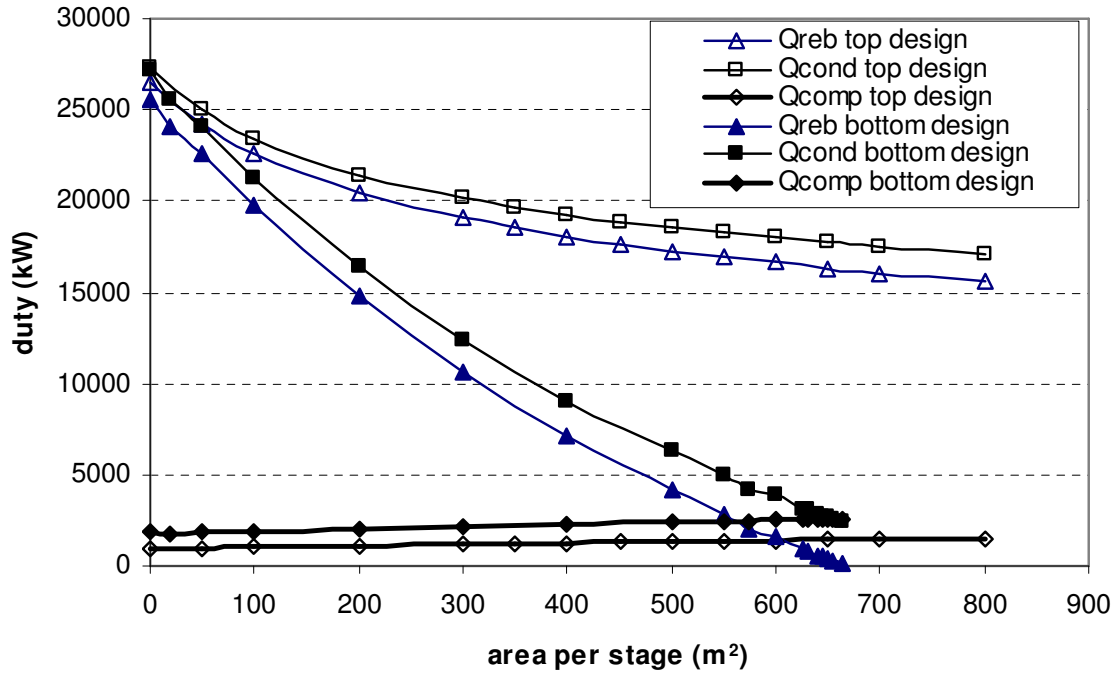

Figure 11: Reboiler, condenser and compressor duties as function of heat transfer area per stage for both top design (Pressure ratio = 1,4) and bottom design (Pressure ratio = 1,9) HIDiC Ethyl benzene-Styrene separation.

Figure 11 shows the reboiler, condenser and compressor duties as a function of the installed heat transfer area per stage. For the bottom design, both reboiler and condenser duties decrease sharply as the internal heat transfer rate increases and it appears possible to obtain an ideal HIDiC with zero reboiler duty. The compressor duty increases slowly to 2,6 MW and a condenser duty of approximately 10% of the original duty is still required in order to generate sufficient primary reflux in the top of the rectifying section. Also the total annual costs (Figure 12) decrease continuously as function of installed heat transfer area per stage, showing the same behaviour as the PP-splitter (Figure 6) and an ideal HIDiC appears to be the most economical option with a Total Annual Cost of 3,6 M$ per year. However a huge amount of heat transfer area, namely 650 m^2/stage, is required, due to the fact that all heat has to be transferred on only 24 stages of the distillation column, which is the number of stages in the stripping section. The average column diameter for the stripping section appeared to be 7,3 m and that of the rectifying section 5,2 m. A hydraulic calculation shows that for these column diameters the maximum amount of heat transfer area, which can be placed per stage is 270 m^2/stage. It can therefore be concluded that a required heat transfer area of 650 m^2/stage is not feasible in practice.

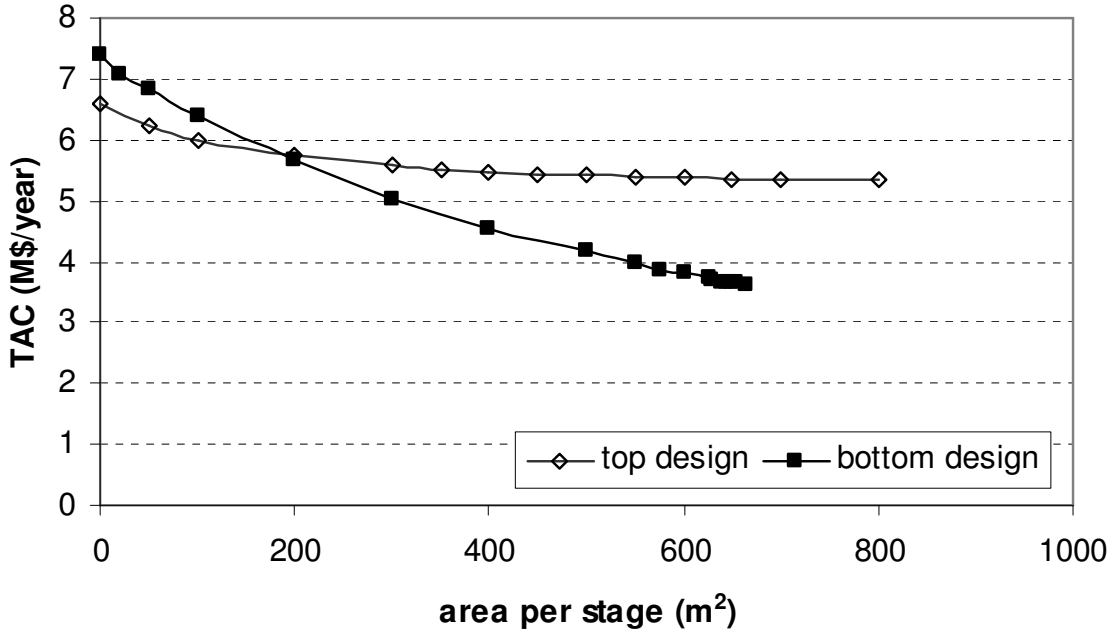

Figure 12: Total Annual Cost as function of heat transfer area per stage for Top design (pressure ratio = 1,4) and Bottom design (pressure ratio = 1,9) HIDiC Ethyl benzene-Styrene separation

Figure 13 shows the influence of pressure ratio on the total annual cost and on the required heat transfer area. The required heat transfer area increases sharply at low compression ratios as a consequence of the low temperature driving force between rectifying and stripping section. Although from this graph a compression ratio of 1,9 seems to be the most economical option, the Aspen simulation did not take into account the practical implications of a heat transfer area which is too large to be installed, according to hydraulic calculations. At a compression ratio of 2,2 the surface area requirement is 260 m^2/stage for an ideal HIDiC, which can be physically installed inside the column without increasing the column diameter. The total annual costs for this design are M$ 3,9.

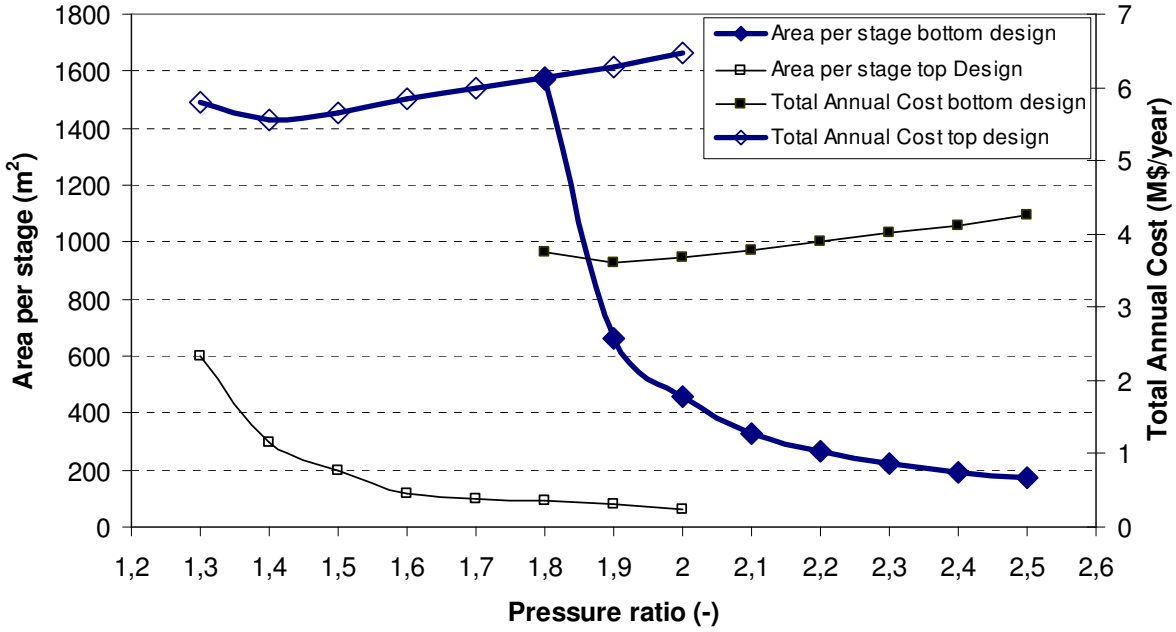

Figure 13: Total Annual Cost and Required heat transfer Area per stage as function of pressure ratio for HIDiC Ethyl benzene-Styrene splitter

The vapour flow profile of the ideal HIDiC operating at a compression ratio of 2,2 is given in figure 14. Starting with zero vapour flow in the bottom of the stripping section (stage 84) , the vapour flow increases due to internal evaporation in the heat integrated part of the stripping section. As the total length of the stripping section is 60 stages and the top part of the stripping section is not in heat exchanging contact with the rectifying section, this upper part of the stripping section is operating like a conventional column with a constant vapour flow along the column. After the compressor the vapour is gradually condensing in the rectifying section. The vapour flow profile of this bottom design EB/ST splitter closely resembles that of the top design PP-splitter (16). The composition profile is very similar to the composition profile

of the conventional distillation column, which shows that the generated secondary boil-up and reflux by the internal evaporation and condensation well allows a good separation performance of the distillation column. The conventional, not heat-integrated part of the stripping section shows slightly worse separation efficiency than the corresponding trays in the conventional column. This is due to the fact that the ratio of molar flow rates of liquid to vapour in this part of the column is 0,88 compared to 0.94 for the conventional column. This lower ratio of liquid to vapour leads to a decrease in slope of the straight operating line in the McCabe-Thiele diagram. The feed is entering the column at the top of the stripping section, which has a given composition, i.e: a fixed point in the McCabe Thiele diagram. Therefore a decrease in the slope of the operating line implies that the operating line is closer to the equilibrium curve and therefore more stages are required for a given separation, or vice versa less separation will be obtained in a fixed number of stages, as was observed in the HIDiC simulation.

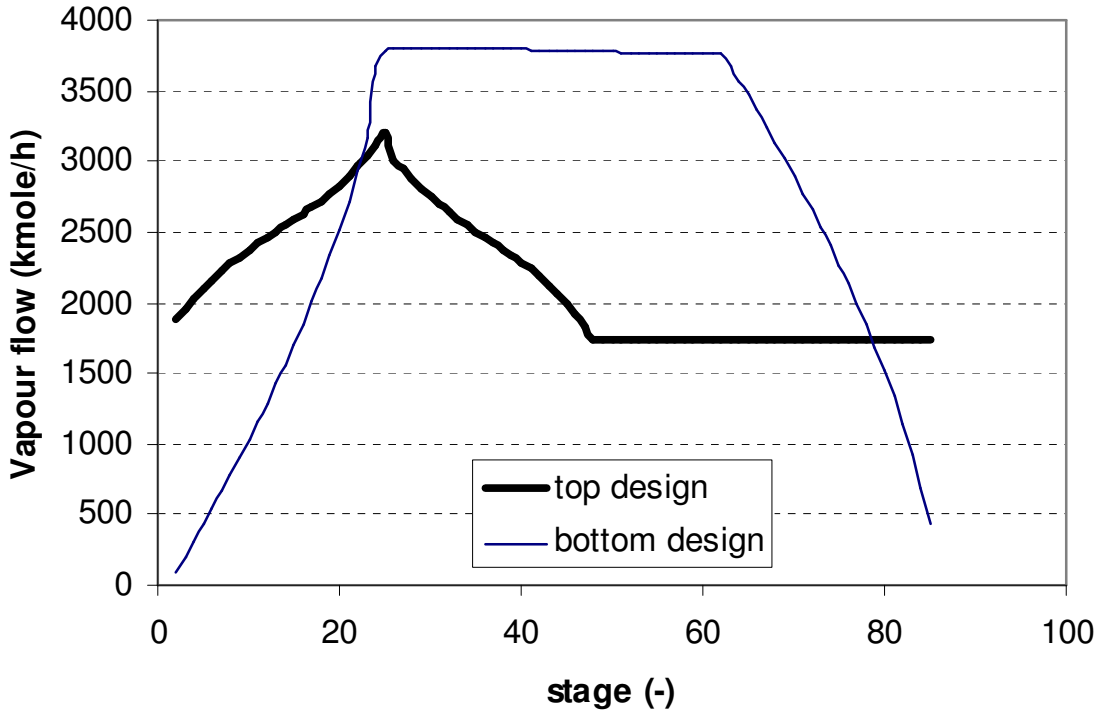

Figure 14: Vapour flow profile for HIDiC Ethyl benzene-Styrene splitter

6.3.3.2 Top design

Figure 10, shows the temperature profile for the top design HIDiC, operating at a pressure ratio of 1,4. In analogy to the bottom design, no stages are limiting with respect to temperature driving force and consequently all 24 stages will be equipped with heat transfer panels.

The condenser and reboiler duties, however show completely different behaviour as function a internal heat transfer area. (Figure 11) It appears not possible to reduce the reboiler duty to zero when the internal heat transfer rate is increased. This could be expected because reducing the reboiler duty to zero would mean that the 35 bottom stages of the stripping column, would be operating without vapour flow, which is obviously not possible. A top design HIDiC of a distillation column with a longer stripping section than the rectifying section implies that a bottom reboiler is required to operate the bottom part of the stripping section. Therefore no ideal HIDiC can be obtained in this configuration. As the major goal of a HIDiC is to reduce reboiler duty, a top design HIDiC of this type of asymmetric distillation columns is inherently disadvantageous compared to
the bottom design.
When we take a closer look to the Total Annual Costs as function of the installed heat transfer area (Figure 12), it becomes clear that also from an economical point of view, installing of extra internal heat transfer area does not lead to substantial cost reduction. Table 8 shows that a reboiler duty of 19 MW remains necessary in order to generate enough boil-up in the stripping section. Therefore the most economical option was chosen at an internal heat transfer area of 300 m^2/stage. The second reason to choose this number is that this is the maximum amount which can be placed inside the distillation column, without the need to increase the column diameter. Namely the average stripping section diameter appeared to be 7,6 m and the average rectifying section diameter 4,7 m, allowing for slightly more surface area per stage than the bottom design.
Figure 13 shows the required heat transfer area and total annual costs of a partial top design HIDiC as function of compression ratio. A compression ratio of 1,4 appears to be the most economical option, which is also feasible taking into account the space which is physically available inside the column to install the required heat transfer area. The compression ratio appears to be significantly lower than that of the bottom design HIDiC. This is due to the shape of the temperature profile in the stripping section, where the top design allows for a lower compression ratio in order to obtain the same temperature driving force for internal heat transfer. Another advantage of the top design is that the actual volume flow through the compressor is significantly lower than in the bottom design, mainly due to the fact that the inlet pressure of the compressor in the top design is higher (0,19 bar) than that of the bottom design (0,12 bar). (table 8).
The vapour flow profile is plotted in figure 14. The bottom of the stripping section, namely the stages 48 to 84, is not heat integrated and therefore the vapour flow is constant along the column. It should be noted that both vapour (2170 kmol/h) and liquid flow (1740 kmol/h) are substantially lower than in the

conventional column, where vapour and liquid flow are 2720 and 2475 kmol/h respectively. The lower capacity of the column leads to a lower separation performance in this part of the stripping section compared to the conventional column, because of the lower internal reflux ratio. Analogous behaviour was observed for the bottom design PP-splitter (16) and bottom design methanol-water separation, where the not heat integrated top part of the rectifying section was operating at a significantly lower capacity than the conventional column and therefore had a worse separation performance than the corresponding trays in the conventional column. This reduced separation performance of must be compensated for in the heat integrated part of the column (stage 48 to 25 of the stripping section and stage 24 to 1 in the rectifying section), in order to reach the desired styrene purity, leading to higher vapour and liquid flows in this part of the column, and also to a high vapour flow through the compressor. The vapour flow through the compressor is 3200 kmol/h for the top design; where the reboiler duty is reduced from 28 MW to 20 MW as a consequence of internal heat transfer. In the bottom design a reduction of reboiler duty from 28 MW to zero requires a vapour flow through the compressor of 3400 kmol/h, which is relatively small taking into consideration the limited degree of internal heat transfer in the top design.

Table 8, shows the key parameters of both HIDiC designs compared to that of the heat pump and the conventional column. The pressure ratio of both HIDiC designs appear to be lower than that of the heat pump because the HIDiC has to overcome only the temperature range of 24 stages in the rectifying section increased with the desired temperature driving force for heat exchange. The VRC has to overcome the temperature range of the complete distillation column, increased with the desired temperature driving force for heat transfer. When an efficiency of 33% is assumed for the conversion from one unit of energy out of fuel to one unit of energy in electrical power, the energy savings for the top and bottom design HIDiC are 26% and 80% compared to the conventional distillation column. The energy savings of the VRC are 79% compared to the conventional column, which means that HIDiC does not lead to extra energy savings than the VRC. Although the HIDiC is able to operate at a lower compression ratio this advantage is balanced by the disadvantage of the higher molar vapour flow through the compressor.

Table 8: Energy Requirements, Pressure ratio and Vapour flow through compressor for Ethyl benzene-Styrene separation

	Conven-tional Column	VRC	Top design HIDiC with constant area per stage	Bottom design HIDiC with constant area per stage
Pressure ratio		2,8	1,4	2,2
Reboiler duty (MW)	28,7		19,0	0
Condenser duty (MW)	28,8		20,1	2,5
Trim cooler duty (MW)		2,9		
Compressor duty (MW)		3,0	1,2	2.9
Vapour flow compressor (kmol/h)		2700	3200	3400
Inlet pressure compressor (bar)		0.24	0.19	0.12
Vapour flow inlet compressor (m3/h)		330.000	540.000	810.000

From table 8 follows also that the actual vapour flow through the compressor is much larger for the HIDiC than for the VRC. The actual vapour flow determines the size of the compressor and therefore the cost of this machine. An inherent disadvantage of HIDiC compared to VRC in the present case is the fact that the inlet pressure of the compressor in HIDiC will always be lower than that of a VRC, leading to a significant increase in actual vapour flow through the compressor. The only way to increase the inlet pressure of the HIDiC compressor is to increase the column pressure, which is not possible in this case due to the increased tendency of the styrene to polymerize at temperatures above 90 ºC. As indicated in table 9, the much higher actual vapour flows through the compressor have a strong influence on the economy of HIDiC. As the largest commercially available turbo blowers have a suction capacity of 200.000 m^3/h, for the vapour recompression column 2 double-stage turbo blowers can be applied. For the top design partial HIDiC 3 single-stage turbo blowers are required and for the bottom design ideal HIDiC even 4 single-stage turbo blowers are necessary. The main difference between HIDiC and the VRC are the investment costs for the turbo blowers. The column diameter for the HIDiC shell is 7,3 m for the top design and 7,6 m for the bottom design, compared to 5,7 m for that of the conventional column and that

of the VRC. Therefore the cost of both column and column internals are higher for both HIDiC configurations.

Table 9: Economic evaluation HIDiC Ethyl benzene-Styrene separation

	Ideal HIDiC Bottom design	Partial HIDiC Top Design	Heat Pump	Conventional
Column	5.0	4.9	3.9	3.9
Reboiler	-	1.0	2.0	1.1
Compressor	8.9	6.7	4.4	-
Condenser	0.1	0.3	-	0.4
Heat Panels	0.8	0.9	-	-
Capital Cost (M$)	14.8	13.7	10.4	5.4
Steam	-	3.2	-	4.9
Electricity	2.3	1.0	2.5	-
Variable Cost (M$/yr)	2.3	4.2	2.5	4.9
Total Annual Cost (M$/yr)	3.9	5.6	3.5	5.4

It is clear from this table that a HIDiC EB/ST splitter cannot compete to a VRC. The energy savings of HIDiC are not higher that those of a VRC. The extra investments and also increased column complexity of a HIDiC are not justified for this separation.
Although the initial investment for a VRC is a factor two higher than for a conventional distillation column, the total annual cost are considerably lower leading to a payback time of 2,6 years.

6.4. Conclusions

The optimal HIDiC design appears to be strongly dependent on the type of application. For the close boiling mixture Propylene-Propane an ideal HIDiC appears to be the most viable option. For the separation of water-methanol, which has a much large relative volatility, a partial HIDiC with both an external reboiler and condenser is favourable. For the separation of Ethylbenzene-Styrene, which has an intermediate relative volatility, an ideal HIDiC is the best option, but is is too capital intensive to compete with VRC.

In the case that the stripping section of the distillation column contains fewer stages than the rectifying section, which is the case in most industrial

separations, a top design HIDiC, where the stripping section is in heat exchanging contact with the equivalent number of stages in the top of the rectifying section, will always be the preferred option.

In case that the stripping section of the distillation column contains more stages than the rectifying section, a bottom design HIDiC, where the rectifying section is in heat exchanging contact with the equivalent number of stages in the bottom of the stripping section is favourable, because the top design requires an external reboiler to operate the bottom stages of the stripping section.

From both a heat transfer point of view and tray hydraulics requirements, a HIDiC with constant area per stage is preferred over a HIDiC with constant duty per stage.

A disadvantage of HIDiC compared to VRC in a vacuum application is the lower inlet pressure of the HIDiC compressor, leading to larger actual volume flows and therefore to costlier equipment.

HIDiC can save a substantial amount of energy, compared to the conventional distillation column at the cost of an increased initial investment due to the compressor and the increased complexity of the distillation column. Total annual costs are decreased with respectively 9 %, 20% and 28% for the separation of Methanol-Water, Propylene-Propane and Ethyl benzene-Styrene, respectively

6.5 References

(1) Olujic, Z., Fakhri, F., de Rijke, A., de Graauw, J. and Jansens, P.J., Internal heat integration – the key to an energy conserving distillation column, *J Chem Technol Biotechnol*, **78**, 241-248 (2003)

(2) Mah, R.S., Nicholas, J.J. and Wodnik, R.B., Distillation with Secondary Reflux and Vaporization, a comparative evaluation, *AIChE J*, **23** pp 651-658 (1977)

(3) Glenchur, T. and Govind, R., Study on a continuous Heat Integrated Distillation Column, *Separation Science and Technology*, **22**(12), 2323-2338 (1987)

(4) Naito, K., Nakaiwa, M., Huang, K., Endo, A., Aso, K., Nakanishi, T., Nakamura, T., Noda, H. and Takamatsu, T., Operation of a bench-scale ideal heat-integrated distillation column (HIDiC): an experimental study, *Computers and Chemical Engineering*, **24**, 495-499 (2000)

(5) Nakaiwa, M., Huang, K., Naito, K., Endo, A., Akiya, T., Nakane, T. and Takamatsu, T., Parameter analysis and optimization of ideal heat-integrated distillation columns, *Computers and Chemical Engineering*, **25**, 737-744 (2001)

(6) Nakaiwa, M., Huang, K., Owa, M., Akiya, T., Nakane, T., Sato, M. and Takamatsu, T., Energy savings in Heat-Integrated distillation columns, *Energy* **22**(6), 621-625 (1997)

(7) Nakaiwa, M., Internally Heat Integrated Distillation Columns: a review, *Trans IChemE,* **81** Part A, (2003)

(8) De Graauw, J., Steenbakker, M.J., de Rijke, A., Olujic, Z. and Jansens, P.J., Distillation column with heat integration, Dutch Patent P56921NL00 (2003)

(9) De Graauw, J., Steenbakker, M.J., de Rijke, A., Olujic, Z. and Jansens, P.J., Distillation column with heat integration, Patent Application EP1476235 (2004)

(10) Gadalla, M., De Rijke, A., Olujic, Z. and Jansens, P.J., A Thermo-Hydraulic Approach to Conceptual Design of an Internally Heat Integrated Distillation Column (HIDiC), ESCAPE proceedings, Lisbon (2004).

(11) Olujic, Z., Sun, L., De Rijke, A., and Jansens, P. J., 2004, Design of an Energy Efficient Propylene Splitter, *Energy* **30**(3), 1764-1778 (2006)

(12) Douglas, J.M., Conceptual Design of Chemical Processes, New York, McGraw-Hill (1994)

(13) Sulzer Chemtech, Distillation with Vapour Recompression (1992)

(14) MAN, Turbo AG, Personal Communication (2006)

(15) Peters, M.S. and Timmerhaus K.D., Plant Design and Economics for Chemical Engineers, Mc Graw-Hill, 4th ed. (1991)

(16) L. Sun, Z. Olujic, A. de Rijke, P. J. Jansens, Industrially Viable Configurations for a Heat Integrated Distillation Column, Conference Proceedings Process Intensification Conference, Maastricht, Netherlands (2003)

Chapter 7:

Further Opportunities for Application & Optimization of the HIDiC concept

7.1 Introduction

This thesis proves that the concentric column with heat panels is a technically sound design, which can be applied for an industrial scale HIDiC. However, when the total annual costs of HIDiC are compared to state of the art vapour recompression technology, it appears that HIDiC is around 20% cheaper than a VRC, which may be not enough for the process industry to seriously consider the application of HIDiC.
This paragraph elaborates on the possibilities to further decrease the costs of HIDiC and discusses some opportunities for further improvement and development of this technology.

7.2 Retrofitting Existing VRC

In an industrial heat pump assisted column with an asymmetric feed stage, one option could be to revamp the existing VRC to a HIDiC. When considering the HIDiC PP-splitter, it appears that roughly half of the trays in the column are not equipped with heat panels. In the case that a VRC PP-splitter would be revamped to a HIDiC, the existing VRC column could be used to serve as the conventional column part of HIDiC i.e. the column part in which the trays are not equipped with heat panels. In this option the heat integrated column part of the HIDiC, containing the complete stripping section and approximately one third of the rectifying trays could be placed adjacent to the existing column.
It should be noted that this also presents opportunities for increasing the column capacity. Namely the existing VRC column shell contains two times more trays than are required in the conventional part of the rectifying section of the HIDiC. The opportunities for capacity increase become clear when considering the option of splitting the existing VRC column physically in a bottom and top section each containing the same number of trays. In this case the bottom section and top section of the existing VRC column would be transformed into two different columns, which should be operated in parallel. As the required number of trays in the conventional, not heat integrated, part of the HIDiC is half of the number of trays in the VRC this option would allow a capacity increase of 100%, assuming no change in process parameters such as vapour flow, vapour density and relative volatility. From the simulation studies (Chapters 5 and 6) followed that the diameter of the bottom part of the rectification section of the HIDiC PP-splitter is larger than the column diameter of the VRC PP-splitter, mainly due to the fact that the vapour flow in this part of the HIDiC column is around 30% larger compared to the vapour flow in the VRC. Also the increased vapour density and decreased relative volatility as a consequence of the higher operating pressure (15 bar compared to 11 bar) are limiting the possibilities for capacity increase of the existing VRC column. Therefore splitting the VRC column into two, parallel operated, partial

rectification sections, offers opportunities for a significant increase in column capacity but it will obviously not lead to a capacity increase of 100%. Moreover a capacity increase of 100% will not be feasible due to limitations in other process equipment.

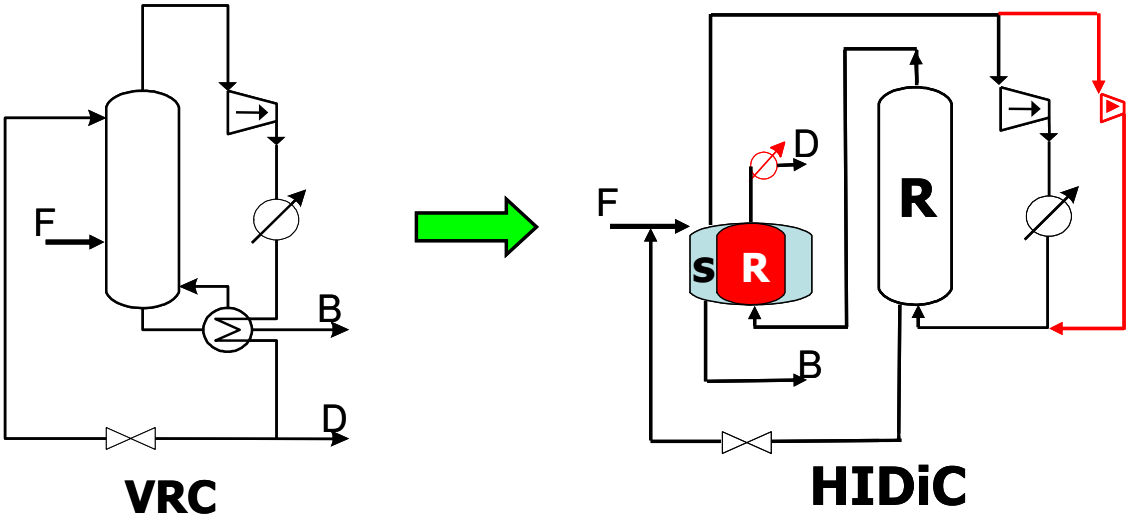

Figure 1: Revamp of VRC PP-splitter into HIDiC

A second option could be to change column internals or to increase the tray spacing in the existing VRC column. It should be noticed that the new internals must be capable to handle an increased vapour flow of 30%, compared to the VRC and even more when an increase in feed flow rate is also desired.
From mechanical point of view the VRC shell should be able to handle the increased operating pressure as stress and wall thickness calculations showed that the wall thickness is governed by wind and weight imposed stresses that are much larger than the stresses caused by the internal pressure itself. (1)

The second piece of process equipment of the existing VRC column that should be reused in a HIDiC is the compressor. This is technically possible because the compression ratio of HIDiC is lower than that of a VRC. A drawback however is the fact that the vapour flow through the HIDiC compressor is larger than through the VRC compressor, thus requiring a second compressor when a VRC is revamped to a HIDiC. Depending on the compressor curve of the VRC compressor, the second compressor has to handle approximately 20% of the vapour flow, assuming no increase in column capacity. Obviously this second compressor is much cheaper than a full size HIDiC compressor.

For economical reasons the revamp option should be considered in combination with an increase of column capacity.

7.3 Concentric HIDiC for Inter-Column heat transfer

Another opportunity would be to apply the concentric column with heat panels to inter-column heat transfer, thus minimizing or eliminating the reboiler duty of the low temperature column. This opportunity was mentioned before by Nakaiwa et al for the separation of azeotropic mixtures e.g. for the pressures swing distillation of acetonitrile-water (2).
A compressor, which is the most capital intensive equipment in a HIDiC, is not required in this case because the model systems should have a suitable temperature profile for inter-column heat transfer.

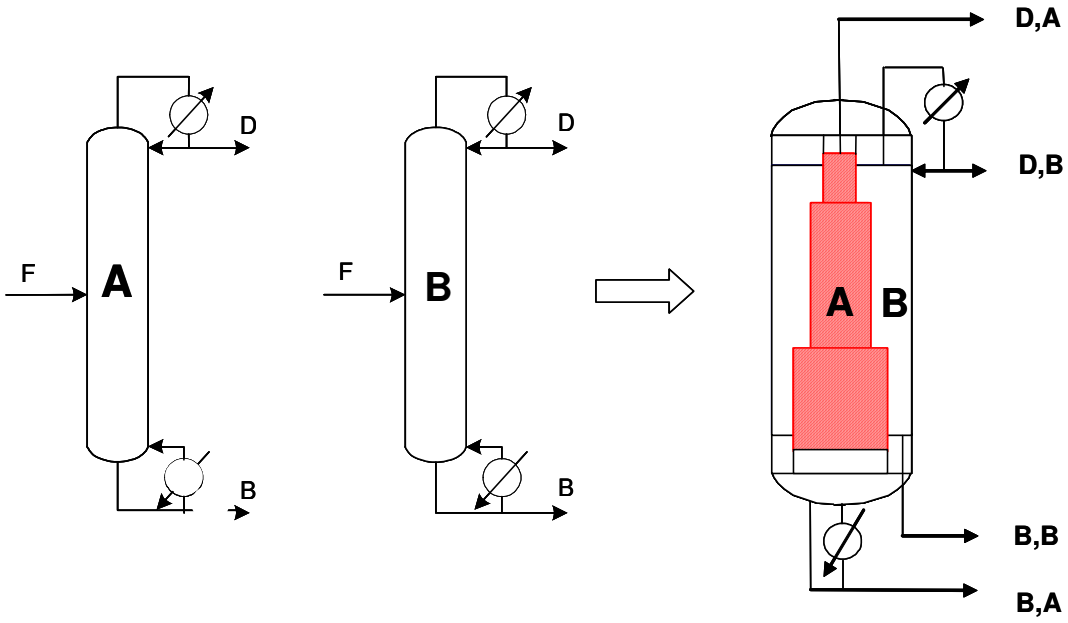

Figure 2: HIDiC concentric column concept for two adjacent distillation columns A and B

7.4 Layout of Heat Transfer Panels

Since the heat panels positively influence the separation efficiency by hindering the back mixing on the tray, it would be interesting to further optimize this effect by placing the panels closer to the tray deck or by changing the panel orientation with respect to the flow along the tray deck.

7.5 Increasing or Enhancing the Heat Transfer Area

The compression ratio is the key parameter in HIDiC design. A low compression ratio is favourable from energy saving point of view, but it leads to a large surface area for internal heat transfer. It is recommended to further intensify the heat transfer area by applying surface roughness techniques or fins. It would be especially favourable to break the laminar film at the condensation side of the heat panels, thus increasing the overall heat transfer coefficient.

Increasing the surface area per tray could also be accomplished by choosing another type of equipment for HIDiC e.g. a plate-fin device as proposed by the Energy research Centre of the Netherlands (ECN) (3) which could lead to a further reduction in pressure ratio. At lower compression ratios a relative cheap turbo blower could be used instead of a centrifugal compressor.

7.6 Application of External Heat Exchangers

An even more flexible design, from an operational point of view, would be reached when the stripping section and rectifying section would be realized as adjacent distillation columns without internal heat transfer surface. Heat transfer surface could be realized in external plate heat exchangers. In this design the amount of heat transfer area and the cross sectional area of the distillation column are not coupled. Moreover it would not be necessary to make vapour and liquid connections on every tray. It is recommended to make the vapour and liquid connections only at the positions along the column where the column diameter changes. In this way the number of vapour and liquid connections between the stripping and rectifying section are reduced. Another advantage of this concept is consequently that both vapour and liquid flows along the different column sections are constant and it would not be necessary to optimize the tray layout for every individual tray.

It should be noted that a drawback of this design is that larger distances are involved for the working fluids, compared to the concentric column with heat panels. Liquid from the cold column needs to enter the heat exchanger to be (partially) evaporated. The liquid flow could be facilitated by gravity. It will be more difficult to get vapour in these external heat exchangers. The vapour manifolds should be designed in such a way that the ‘pull’ created by condensation in the external heat exchanger is strong enough to overcome the inevitable pressure drop in the vapour manifold. However, this may lead to manifold diameters which are impractical.

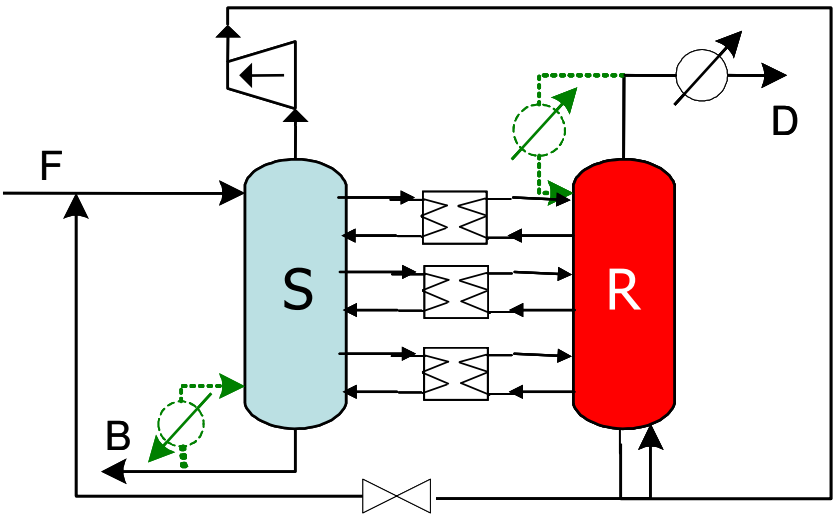

Figure 3: HIDiC constructed as intercoupled columns with separate plate heat exchangers

7.7 References

(1). Edzard Leeuw, Preliminar Mechanical Design of a HIDiC Propylene-Propane Splitter, Graduation Thesis, Delft University of Technology, (2004).

(2). Nakaiwa, M., Huang, K., Endo, T., Ohmori, T., Akiya, T., and Takamatsu, T., Internally Heat Integration Columns: A Review, *Trans IChemE,* **81**, part A. (2003)

(3). Hugill, J.A., and van Dorst, E.M., The Use of Compact Heat Exchangers in Heat-Integrated Distillation Columns, *Proceedings of the Fifth International Conference on Enhanced, Compact and Ultra-Compact Heat Exchangers: Science and Technology,* **40,** 310-317 (2005)

Appendix 1

Reducing CO_2 emissions of internally heat-integrated distillation columns for separation of close boiling mixtures

Partially published as:
Reducing CO_2 emissions of internally heat-integrated distillation columns for separation of close boiling mixtures,
Energy, 31, (2006), 2073-2081

Abstract
A model developed originally for crude oil distillation units has been applied to a standalone internally heat integrated distillation column (HIDiC) to evaluate emissions levels and to generate design options for direct carbon dioxide emissions reduction. Simulations indicate that for propylene-propane separation, an ideal (no reboiler) HIDiC enables a reduction in emissions of 83 % and of 36 %, compared to conventional and heat pump alternatives, respectively. Integrating a turbine to drive the compressor, in conjunction with a suitable fuel is the key to the minimization of the emissions associated with the operation of a HIDiC. Importantly, while substantial emission reductions are achieved, the process economics are improved.

1. Introduction

Since distillation columns separating close-boiling mixtures are highly energy intensive, vapour recompression (heat pumping) has been adopted as a technique to increase the energy efficiency of distillation (1-4). In a direct vapour recompression column (VRC), the vapour leaving the top of the distillation column is compressed and is then condensed in the reboiler of the same column, providing the heat needed for vapour generation at the bottom of the column. Further intensifications of this concept led to the development of internally heat-integrated distillation column (HIDiC). These configurations can have significantly lower energy demand than conventional distillation columns and heat pump assisted alternatives (5-7).

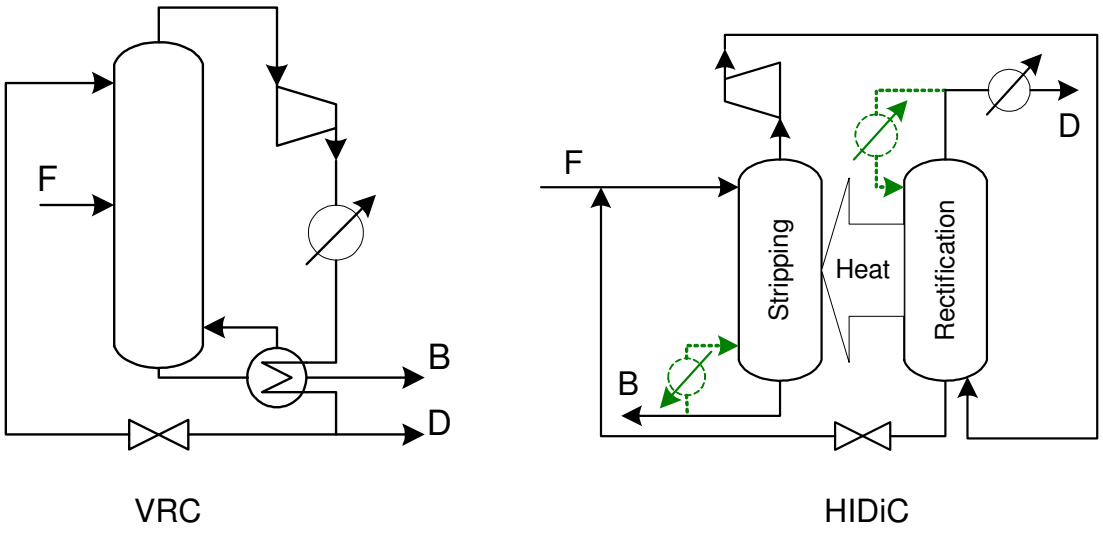

Figure 1: Schematic representation of the vapour recompression column and the HIDiC

As illustrated in Fig. 1, the HIDiC configuration contains two separate distillation columns, the stripping and rectifying columns. There is a pressure difference between the two columns; the overhead vapour of the stripping column is compressed and then enters the bottom of the rectifying column. The rectifying column operates at a higher pressure, *i.e.* a higher temperature. The liquid from the bottom of the rectifying column is fed into the top of the stripping column, as is the column feed. The pressure of the recycled liquid stream from the rectifying column is equalised with that of the stripping column through a throttling valve. The vapour leaving the top of the rectifying column is the light product, while the heavy product is the bottom stream of the stripping column. The two columns are configured in a particular way so that the energy of the hot rectifying column is used to heat the stripping column. As a result, continuous condensation of the vapour phase occurs

along the rectifying column and continuous evaporation, *i.e.* vapour generation takes place in the stripping column. The heat is transferred on each integrated column stage through the indirect contact of the rectifying hot vapour and the stripping cold liquid streams. The amount of heat transfer between the two columns can vary, and correspondingly the reboiler duty will change. When no heat is transferred, the reboiler duty will be the greatest, *i.e.* equal to that of the conventional column. In other words, a HIDiC may be *partial*, when the reboiler energy requirement is reduced, compared to that of a conventional column, or *ideal*, when the reboiler duty is zero.

The HIDiC concept was first introduced and evaluated by Mah and co-workers (8, 9) under the name 'Secondary Reflux and Vaporization' (SRV). Seader (10), and Glenchur and Govind (11) suggested different column configurations for HIDiCs implementation. A shell and tube-type packed column was introduced for HIDiC by Aso *et al.* (12). Recently, a group of Japanese researchers (13, 14 and 15) studied HIDiCs, concentrating on theoretical evaluation and pilot plant testing. Most recently, Gadalla *et al.* (16) developed a design approach using pinch analysis principles for improving performances of exiting designs of internal heat-integrated distillation columns. All these studies indicate significant, practically ultimate energy savings potential with respect to energy requirements of conventional columns.

Certainly a reduction in energy requirements implies a corresponding indirect reduction of the associated CO_2 emissions. However there is an increasing need for quantification of the accompanying emissions. Most recently, a model has been developed by Gadalla *et al.* (17) for the purpose of quantifying the emissions associated with large heat integrated distillation systems, such as those employed in refineries in crude oil distillation units. Internally heat-integrated distillation columns are expected to show a good opportunity for emissions reduction due to their large potential for energy savings. The objective of the present study is to use this method to quantify CO_2 emissions from existing designs of HIDiC separating a mixture of propylene-propane. Also the potential of these column designs for further emissions reduction compared to conventional alternatives is evaluated, by considering the effect of changing fuels and using gas turbines. The latter one appeared to be the key to minimization of emissions associated with operation of a HIDiC.

2. Calculation of CO_2 emissions from HIDiCs

In the combustion of fuels, air is assumed to be in excess to ensure complete combustion, so that no carbon monoxide is formed. CO_2 emissions, $(CO_2)_{Emiss}$ (kg/s), are related to the amount of fuel burnt, Q_{Fuel} (kW), in a heating device as follows:

$$[\,CO_2\,]_{Emiss} = \left(\frac{Q_{Fuel}}{NHV}\right)\left(\frac{C\%}{100}\right)\alpha \qquad (1)$$

where α (=3.67) is the ratio of molar masses of CO_2 and C, while *NHV* (kJ/kg) represents the net heating value of a fuel with a carbon content of *C%* (-). Typical fuels used in heating devices, such as steam boilers or furnaces are light and heavy fuel oils, natural gas and coal.

Equation 1 shows that the types of both the fuel used and the heating device affect the amount of CO_2 emissions. The heating device affects emissions through the amount of fuel burnt, which is directly related to its efficiency or performance. However, the effect of the fuel can be seen in the terms *C%, NHV* and *α.* These effects can be lumped in a so-called *fuel factor,* $Fuel_{Fact}$ (kg/kJ), defined as:

$$Fuel_{Fact} = \left(\frac{\alpha}{NHV}\right)\left(\frac{C\%}{100}\right) \qquad (2)$$

2.1. CO_2 Emissions from steam boilers

Boilers produce steam from the combustion of fuel; this steam is delivered to the process at the temperature required by the process or obtained at a higher pressure and then throttled. In distillation systems, steam is used either for heating purposes, indirectly in reboilers. For the flame temperature in a boiler the theoretical flame temperature of 1800 °C may be used (18). The stack temperature should not be lower than the corrosion limit; a typical stack temperature of 160 °C is used in the calculations. (20) The amount of fuel burnt can be calculated from (18):

$$Q_{Fuel} = \frac{Q_{Proc}}{\lambda_{Proc}}\left(h_{Proc} - 419\right)\frac{T_{FTB} - T_o}{T_{FTB} - T_{Stack}} \qquad (3)$$

where λ_{Proc} (kJ/kg) and h_{Proc} (kJ/kg) are the latent heat and enthalpy of steam delivered to the process, respectively, while T_{FTB} (°C) is the flame temperature of the boiler flue gases.

The above equation is obtained from a simple steam balance around the boiler to relate the amount of fuel necessary in the boiler to provide a heat duty of $Q_{proc;}$ the boiler feed water is assumed to be at 100 °C with an enthalpy of 419 kJ/kg (18). Equations (1) and (3) can calculate the CO_2

emissions from steam boilers. Note that the duty, $Q_{Proc,}$ in Eq. (3) includes the heat duty required by the process and that provided by the stripping steam.

2.2. CO_2 emissions from gas turbines

A gas turbine is used in process industry either as a stand-alone unit or in an integrated context with a process. In both cases, the gas turbine provides heat to the process and delivers power. Fuels such as natural gas and light fuel oil can feed gas turbines. Integration of a gas turbine with a process enables refineries to produce electricity for the same heat requirement. The generated power can be either consumed in the refinery site or exported to other consumers. The integration of gas turbines then leads to a reduction in the operating costs due to fuel savings, and it also provides flexibility in importing and exporting power. Two different models will be used in modelling CO_2 emissions from gas turbines. The model of Delaby (18) is used when a gas turbine is used separately to provide the process heat duty. On the other hand, when a gas turbine is integrated with a process, a more detailed model is used (19).

In an ideal HIDiC, operating without a reboiler a gas turbine could deliver the electricity to drive the compressor. A partial HIDiC still requires a reboiler and in this case also the excess heat associated with the combustion of fuels in the gas turbine can be used as process heat for the column reboiler.

When a gas turbine is used to supply the process heat duty, Q_{Proc}, the amount of fuel burnt can be calculated from the relationship between the efficiency of a gas turbine, η_{GT} (-), and the Carnot factor, η_C (-) (18):

$$Q_{Fuel} = \frac{Q_{Proc}}{\eta_{GT}} \frac{1}{1-\eta_C} \tag{4}$$

The Carnot factor for a gas turbine is defined as (18):

$$\eta_C = \frac{T_{inlet} - T_{outlet}}{T_{inlet} + 273} \tag{5}$$

The temperature at the inlet ($T_{inlet;}$ ^oC) of the gas turbine (combustion temperature) and the temperature at the outlet ($T_{outlet;}$ ^oC) of the gas turbine (flue gas temperature) vary according to the turbine design. However, a value of 1027 ^oC for the inlet and 720 ^oC for the outlet temperatures may be used (20). Any correlation that calculates the outlet temperature can be used, as will be seen for the case of integrated gas turbines. The efficiency of the gas

turbine (η_{GT}) is defined as the ratio of the useful heat delivered by the gas turbine to the total heat available in the exhaust (18):

$$\eta_{GT} = \frac{T_{outlet} - T_{Stack}}{T_{outlet} - T_o} \tag{6}$$

The power (electricity) delivered by a gas turbine, W_{GT} (kW), is obtained from the Carnot factor and the amount of fuel burnt in the gas turbine, as follows (18):

$$W_{GT} = 0.90\eta_C Q_{Fuel} \tag{7}$$

The carbon dioxide emissions from a gas turbine can then be calculated from Eqs. (1), (4) and (5).

When a gas turbine is integrated with a process furnace, power is generated for the same heat requirement. Furnaces have a high combustion temperature and low heat losses, but do not produce power. On the other hand, gas turbines have a large power output, but the exhaust temperatures are too low to satisfy most process heat requirements. Thus, integrating a gas turbine with a process furnace combines the advantages of both units. The exhaust gas from the gas turbine is partially fired in the furnace, together with extra fuel. It should be noted that this may lead to a substantial increase in NOx contribution to emissions due very high temperature of the combustion air (up to 720^{o}C) and the presence of oxygen in the turbine outlets. However, the harmful effect of the NOx is not considered in this work, which is concerned exclusively with CO_2 emissions. In this case, the process heat duty is partially provided by the gas turbine by burning a certain amount of fuel. The rest of the heat duty to the process is provided in the furnace. To model the integration of a gas turbine with a process furnace, the exhaust gas is assumed to provide the heat duty from the theoretical flame temperature after firing in the furnace to the stack temperature (21). Also, the amount of exhaust flue gases does not change much after combustion in the furnace (22).

The power generated in the gas turbine, W_{GT}, is correlated with the flow rate of flue gases ($M_{FG;}$ kg/s), as follows (22):

$$W_{GT} = \frac{1000M_{FG}}{2.9} \tag{8}$$

The flow rate of the flue gases required can be calculated from:

$$M_{FG} = \frac{Q_{Proc}}{C_P\left(T_{FTF} - T_{Stack}\right)} \tag{9}$$

where C_P (kJ/kg °C) is the heat capacity of the flue gases, which can be taken to be equal to that of air (≈1.1). This assumption is not critical since typical hot flue gases can be considered as hot air (18).
The part of heat duty provided by the gas turbine, Q_{GT} (kW), is calculated from:

$$Q_{GT} = C_P\left(T_{Exhaust} - T_{Stack}\right)M_{FG} \tag{10}$$

where $T_{Exhaust}$ (°C) is the outlet temperature of the exhaust gases from the gas turbine, which can be calculated from Eq. (11). Note that Eqs. (8), (9) and (10) use the same value of $M_{FG,}$ since the flow rate of the flue gases from the turbine is assumed almost constant.

$$T_{Exhaust} = 0.4(10)^{-3}W_{GT} + 493.42 \tag{11}$$

Then, the heat duty required from the furnace, Q_{Furn} (kW), can be calculated from an enthalpy balance:

$$Q_{Furn} = Q_{Proc} - Q_{GT} \tag{12}$$

The fuel equivalents consumed in the gas turbine (Q_{Fuel}^{GT}; MW) and furnace (Q_{Fuel}^{Furn}; kW), respectively, are calculated as follows:

$$Q_{Fuel}^{GT} = 2.84(10)^{-3}W_{GT} + 7.33 \tag{13}$$

$$Q_{Fuel}^{Furn} = \frac{Q_{Furn}}{\eta_{Furn}} \tag{14}$$

Then, the total fuel consumption (Q_{Fuel}; kW) in the gas turbine and furnace, assuming that there is no heat loss, is:

$$Q_{Fuel} = Q_{Fuel}^{GT} + Q_{Fuel}^{Furn} \tag{15}$$

The CO_2 emissions from the gas turbine integrated with the process furnace can be calculated from Eqs. (1) and (8) to (15).

2.3. Global CO_2 emissions estimation

In the above calculation of CO_2 emissions, we considered only the process plant including the furnace, boiler and the gas turbine. The emissions calculated in this case are called *local emissions* (18), since we account only for the process plant. The power generated from the gas turbine is either consumed at the site itself or exported to other consumers. In both cases, the central power station, which is situated outside the plant boundaries, has the possibility of reducing electricity production by the amount that can be generated by the gas turbine. Thus, certain amounts of fuels can be saved at the central power station. This leads to a reduction in the CO_2 emissions, or in other words, a saving in the emissions at the central power plant. Therefore, integration of a gas turbine with a process enables the central power station to reduce its emissions. So, we should consider the central power station together with the process plant as one unit in emission calculations. The CO_2 emissions calculated in this case are called *global emissions* (18).

The reduction in fuel consumption at the central power station (ΔQ_{Fuel}^{PS}; kW) is related to the amount of electricity generated by the gas turbine (W_{GT}) and the power station efficiency, η_{PS} (-), as follows (22):

$$\Delta Q_{Fuel}^{PS} = \frac{W_{GT}}{\eta_{PS}} \tag{16}$$

The efficiency of the central power station is assumed to be 28% (18). The reduction in CO_2 emissions at the power station can then be calculated from Eqs. (1) and (16), for a given type of fuel. Coal is used in majority of power stations as a fuel. The global CO_2 emission from the process plant and the central power station is defined as:

Global emissions = Emissions from process plant – Emissions saved at power station (17)

Although the integration of a gas turbine with a process furnace reduces the operating costs by reducing fuel consumption, it incurs a substantial capital investment. There is a trade-off between the capital cost of the gas turbine and the benefits obtained. The capital cost of the gas turbine, $Cost_{GT}$(k$), can be calculated from (22):

$$Cost_{GT} = 195.1(10)^{-3} W_{GT} + 2529.2 \tag{18}$$

The gas turbine enables the process plant to increase its profit by producing electricity; the value of electricity generated ($Cost_{Power}^{GT}$; \$/h) is a function of the unit cost of electricity ($PUnit_{Cost}$; \$/kW h):

$$Cost_{Power}^{GT} = PUnit_{Cost} W_{GT} \tag{19}$$

So, when a gas turbine is to be integrated with a process, the CO_2 emissions can be calculated locally or globally and, at the same time, the capital investment and the value of the power generated are evaluated.
In summary, the overall model for CO_2 emissions calculation in heat-integrated distillation systems comprises of all the equations presented above to estimate the emissions from all the individual devices, *i.e.* furnace, boiler and gas turbine. For an existing crude oil distillation plant, the CO_2 emissions will be calculated individually for each device. Then, the total (or global) emissions are determined for the process plant and for the process together with the central power station. The capital expenses and process income can also be evaluated.

Regarding the modelling approach the same working equations as those introduced in the above mentioned reference are used to estimate CO_2 emissions, *i.e.* fuel equivalents consumed by different configurations of HIDiC. In this case the total process heat requirement is equal to the reboiler duty involved, which varies from zero for an ideal HIDiC to a certain value for a partial HIDiC. Certainly, in an ideal HIDiC case no emissions are produced due to heating; however, there are still emissions at the central power station for providing compressor power (electricity) requirement.
The only exception in the calculations procedure is the ideal HIDiC with a turbine used to drive the compressor. In this case, the required compressor power, which is equal to the power produced by gas turbine, W_{GT} (kW), is given and is used to estimate the mass flow rate of the flue gas, M_{FG} (kg/s), needed by the turbine via the following empirical equation: $M_{FG} = 0.0029\, W_{GT}$. Therefore, in this case no excessive power is available, *i.e.* the CO_2 emissions are equivalent to the amount of the fuel consumed by the turbine. However, the equivalent heat of the hot effluent gases of the turbine can be used to provide heat for other processes (energy export or steam saving), including the reboiler duty in case of partial HIDiC, as it will be elaborated in more detail later on.

3. Case study – A propylene-propane splitter

Propylene-propane splitters are notorious for their immense energy requirements, and as such main candidates for implementation of energy

conserving concepts to single columns. An internally heat-integrated distillation column was designed for separating an equimolar propylene-propane mixture based on actual plant data for a state of the art heat pump assisted column (VRC) (23). The design specifications are shown in Table 1. In this design, the stripping stages are integrated with the top stages of the rectifying column, *i.e.* the total 57 stripping stages are heated by the first top 57 stages of the rectifying section. The ideal HIDiC requires 1.54 MW of energy to be transferred per stage from the rectifying column to the stripping column. The corresponding compressor power is 5.84 MW.

Table 1: HIDiC column data and specifications for propylene-propane separation

Column specifications		
Feed		propylene- propane
Composition	propylene, mole %	50
Flow rate	t/h	111.6
Pressure	bar	12.2
Temperature	^{o}C	31.7
Rectifying pressure	bar	19.2
Stripping pressure	bar	12.2
Rectifying stages	-	154
Stripping stages	-	57
Top product purity	propylene, mole %	99.6
Bottom product purity	propylene, mole %	1.1

A conventional column with the same number of stages (basic data are given in Table 1) requires 89.2 MW; a traditional VRC requires 75.8 MW of heat and its compressor electricity demand is 8.1 MW. Note that in VRCs, the reboiler does not require steam, since the compressed top vapour is used for heating purposes. These results were obtained by using a rigorous model for distillation column calculations available in Aspen Plus (24). The physical and thermodynamic properties of feed, intermediate and product streams were calculated by the Peng Robinson model (24). Although ideal HIDiC requires no reboiler for heating purposes, a reboiler unit is necessary for startup procedure. In this study, the cost of a start-up reboiler is not included, however this issue will be considered in greater detail in a later stage of design where controllability and operability aspects of HIDiC and related costs will be stressed on. Namely, for CO_2 emissions studies, which compare different HIDiC configurations, the consideration of start-up reboilers is not

essential. In the situations with a partial HIDiC, the same reboiler is used for start-up purposes.

In this study different levels of heat integration are considered, leading to different reboiler duties. Emissions are calculated for a range of reboiler duties, from zero (ideal HIDiC) to the maximum value. When increasing the heat integration level between the two columns, the reboiler duty will reduce. At zero reboiler duty (ideal HIDiC), complete heat integration is exploited; this requires an energy transfer of 1.54 MW per stage. This case represents a full energy saving (100%). Note that by increasing heat integration, compressor loads are also increasing. This means that extra money will be spent on both the capital cost and electricity requirement of the compressor unit. Therefore, an optimisation is required to arrive at the best conditions of heat integration levels and the corresponding reboiler duty (16). In what follows, the emissions from HIDiC, with and without turbine, are compared with that associated with conventional and VRCs, for respectively heavy oil and natural gas as fuels.

4. Results and discussion

4.1 CO_2 emissions quantification

Fig. 2 shows the CO_2 emissions calculated for the HIDiCs with different reboiler duties, compared with those from conventional and heat pump columns. The emissions are produced in the boiler that provides the required steam and in the power station. A conventional column (fed by fuel oil) produces CO_2 emissions of about 32 t/h. On the other hand, heat pump design (VRC using fuel oil) produces 8.7 t/h of CO_2 globally. Note that for the vapour recompression column, emissions are produced only at the power station. The local emissions (see Fig. 2) account for emissions from the boilers, while the global emissions include the emissions of the power station. Thus, the difference between the two emissions represents emissions produced at the power station. As shown, emissions reduce significantly with reducing the reboiler duty. This indicates that less steam is needed for heating and consequently the load of the boilers that produce CO_2 emissions is reduced. Obviously, the level of emissions is strongly dependent on the nature of the fuel used. Compared to heavy oil, the natural gas can be considered as an environmentally friendly fuel.

The local emissions start (equivalent to maximum reboiler duty) from the same emissions value produced by a conventional alternative and then reduce to zero when an ideal HIDiC is operated, *i.e.* no reboiler is used. Along the local emissions line, the emissions from the power station are not considered. The global emissions start (no heat integration) at a value higher than that of the conventional column and then end at a value higher than zero, which is equivalent to the emissions of electricity production. It is clear that at

the ideal HIDiC conditions, the emissions from HIDiCs are smaller than those from VRCs. This is because the HIDiCs consume less electricity than heat pumps. In order to operate a HIDiC in an environmental friendly manner, the reboiler duty needs to be lower than 7.5 MW (see Fig. 2); this value is equivalent to the emissions which are produced by heat pump designs. At this reboiler duty, HIDiCs will have the same environmental impact as VRCs. The emissions from an ideal HIDiC are reduced by 83% compared to a conventional column, and by 36% compared to a heat pump. These emissions savings are roughly equivalent to the energy savings experienced in these two cases.

When a gas turbine is integrated with a HIDiC, the global emissions are expected to rise compared to the original case (without turbine). This is due to an extra amount of fuel which is burnt by the gas turbine to provide the required compressor power and heat duty. It is assumed that the excess power produced by the turbine will be exported to the neighbouring site. In addition, the hot flue gases of the gas turbine have a surplus heat that can be exported to other processes and thus extra savings in steams will be gained. This is valid when HIDiC is ideal*, i.e.* no reboiler is used

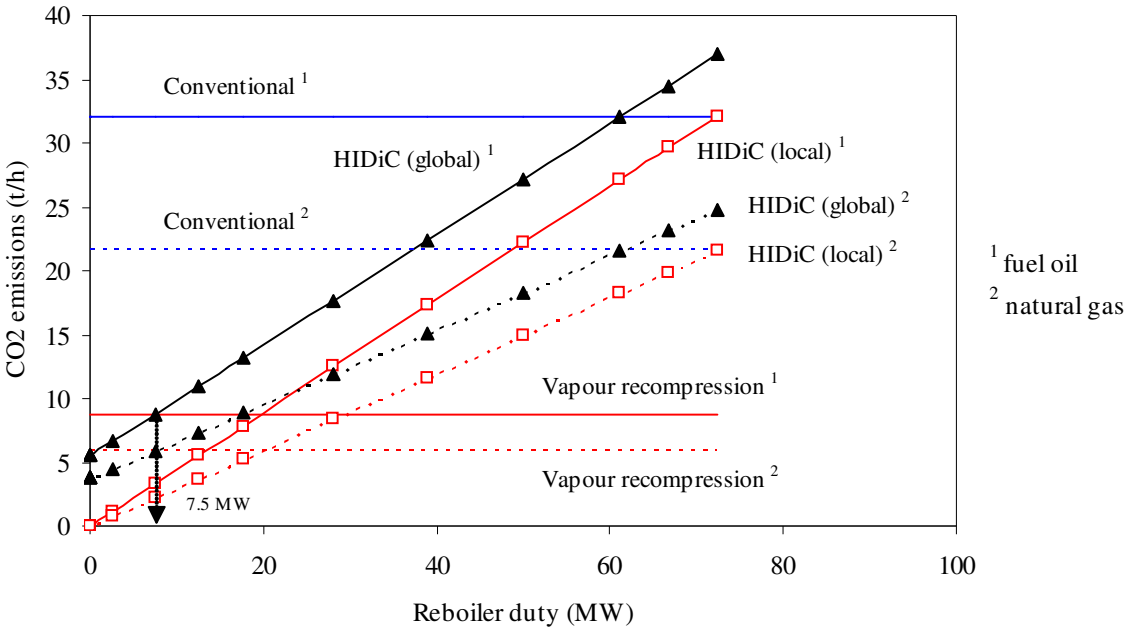

Figure 2: CO_2 emissions from a HIDiC without gas turbine integration; fed by fuel oil or natural gas (column details are given in Table 1)

Fig. 3 illustrates the global CO_2 emissions for a HIDiC equipped with a gas turbine, fed either by heavy fuel oil or natural gas. As shown, the emissions from the unit with a gas turbine reduce significantly compared to the base case (without gas turbine). It must be noted that the emissions in this case are

divided into three parts, emissions from the steam boiler, the gas turbine and the power station.

As shown in Fig. 3, the emissions for a HIDiC with very small reboiler duties and integrated with a gas turbine are lower than those for a VRC. There is also a sharp decrease in the global emissions below a reboiler duty of approximately 40 MW. This is because, below this reboiler range, the power generated in the gas turbine is exactly that required by the compressor. Hence, there is no excess power to be produced and consequently no additional fuel is burnt by the gas turbine, which reduces emissions.

Furthermore, as indicated in Fig. 3, when the HIDiC is operated with no reboiler and the power required by the compressor is supplied by the gas turbine the global emissions are negative (-570 kg/h; for fuel oil). This is due to the fact that no emissions are produced locally by the HIDiC, from the steam boilers or globally due to power consumption. Moreover, the gas turbine has a surplus heat that can be exported. This exported heat provides an opportunity for other processes to save emissions. Therefore, the reductions in emissions for HIDiCs with turbine are estimated to be above 100%, compared to heat VRCs.

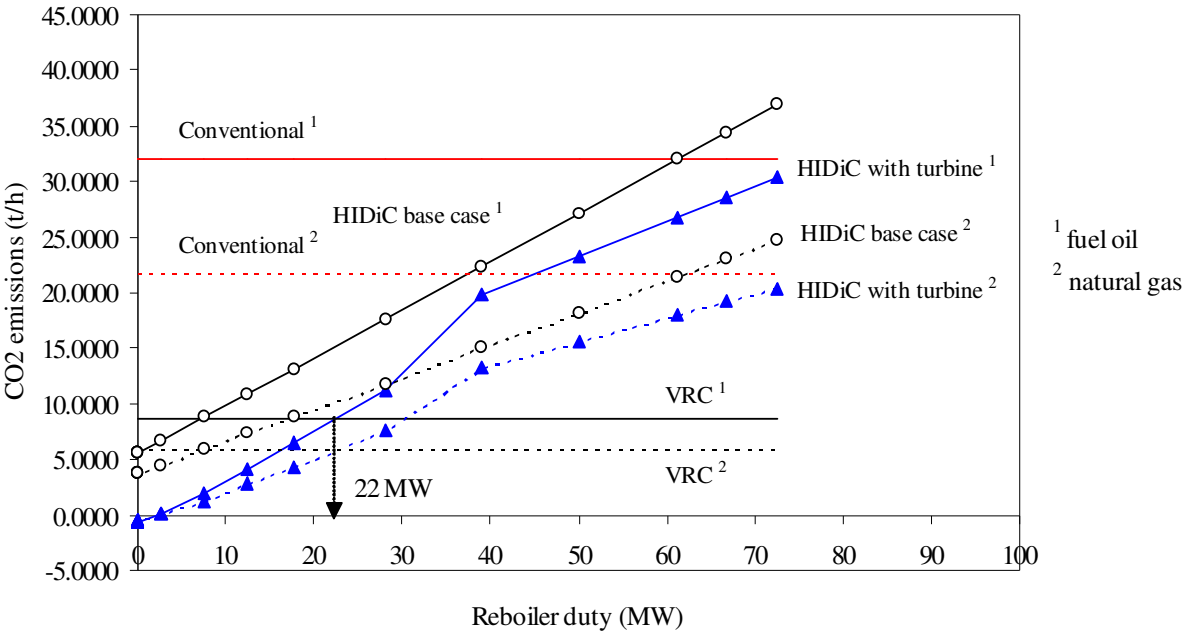

Figure 3: Global CO_2 emissions from a HIDiC with a gas turbine (fed by fuel oil or natural gas)

When a HIDiC is to be operated with a reboiler, there should be an optimum value for the reboiler duty; this value could be economically driven, related to control issues or related to environmental consequences. For the environmental perspective, the results of Fig. 3 may suggest that the reboiler duty should be below 22 MW. At these conditions, the emissions from HIDiCs will be less than or equal to those of the heat pumped alternative. Therefore, the environmental impact will be no greater than that for an efficient VRC design.

The power generated by the gas turbine integrated with a HIDiC is shown in Fig. 4, and compared with the power demand of the compressor. At large reboiler duties, there is a surplus in the power production, which can be exported. Fig. 5 compares the steam flow rates of the base case HIDiC (without gas turbine) and a HIDiC integrated with a gas turbine with those of a conventional column. A conventional column consumes approximately 118 t/h of steam in its reboiler.

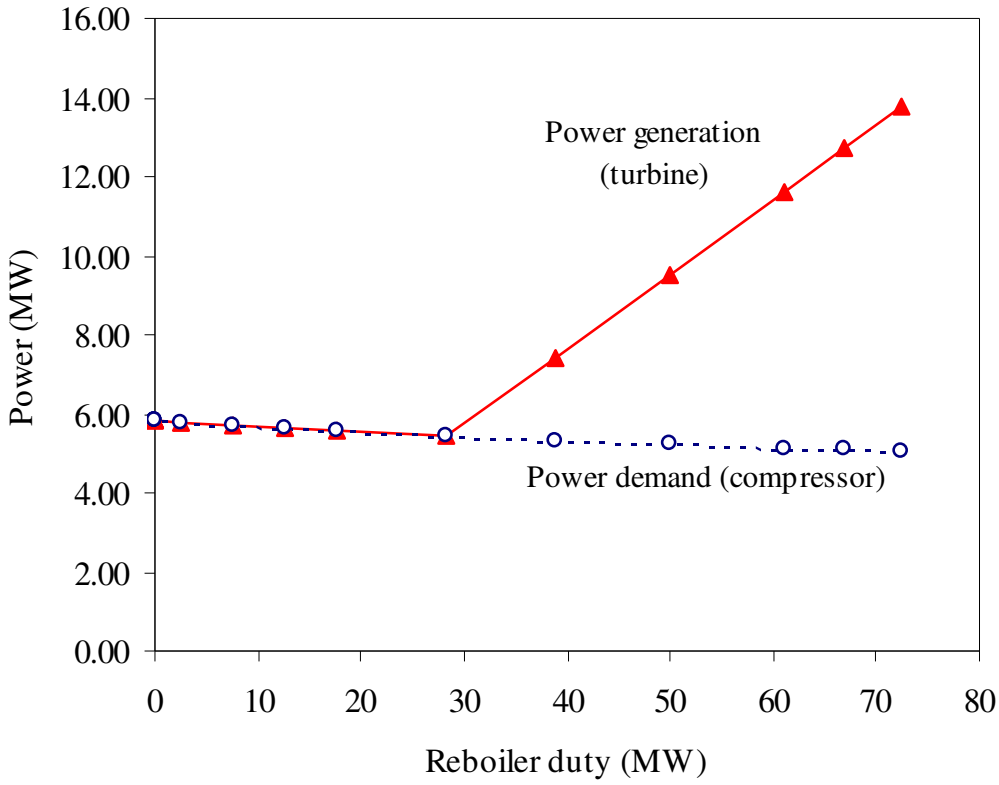

Figure 4: Power demand/generation from a HIDiC with an integrated gas turbine (fed by fuel oil)

When a HIDiC configuration is adopted, steam consumption is reduced as the reboiler duty decreases; no steam is consumed in an ideal HIDiC. Moreover,

when a gas turbine is integrated with the HIDiC, more steam can be saved. This saving results from the part of the reboiler duty that can be provided by heat from the gas turbine. While the steam consumption of the base case ideal HIDiC is zero, the net steam consumption of the ideal HIDiC with a gas turbine can theoretically be below zero. This implies that there is no steam consumption and may even allow steam savings in a neighbouring process if heat or steam is exported.

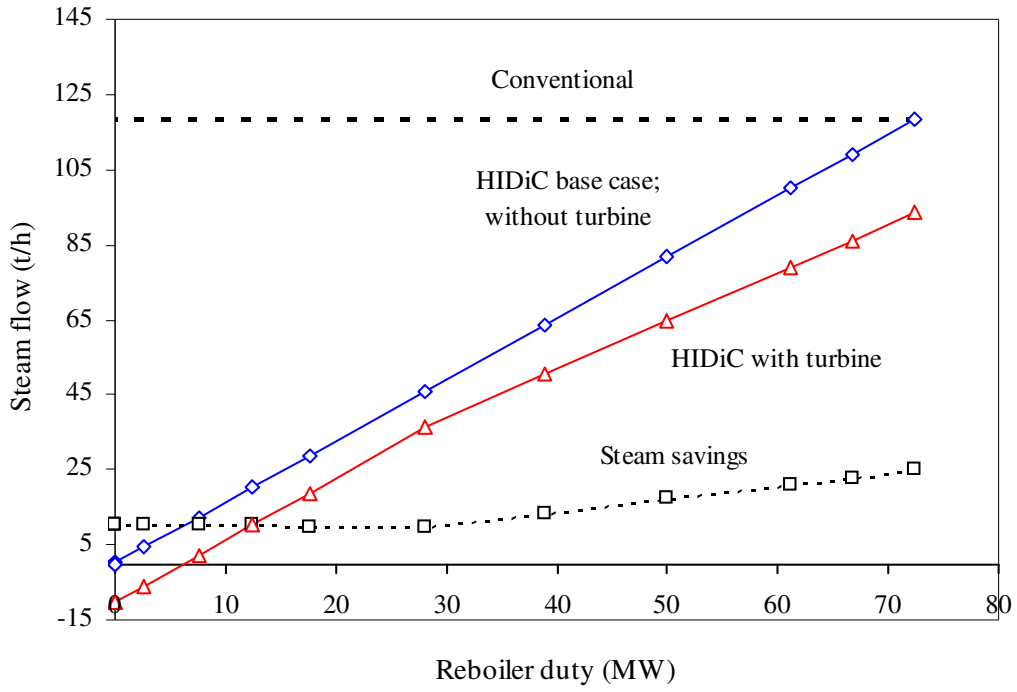

Figure 5: Steam consumption of HIDiC configurations

Fig. 6 summarises the reductions in the emissions from both the base case HIDiC and the HIDiC integrated with a gas turbine, relative to both conventional and VRC. HIDiC integrated with the turbine reduces CO_2 emissions by 6 to 102%, relative to a conventional column. At reboiler duties larger than 60 MW, the base case generates more CO_2 globally than does a conventional column. Integrating a gas turbine with a HIDiC generates less CO_2 than a VRC for HIDiC reboiler duties of less than 23 MW. If the reboiler duty of the base case HIDiC is less than 8 MW, its emissions will be less than those of a VRC.

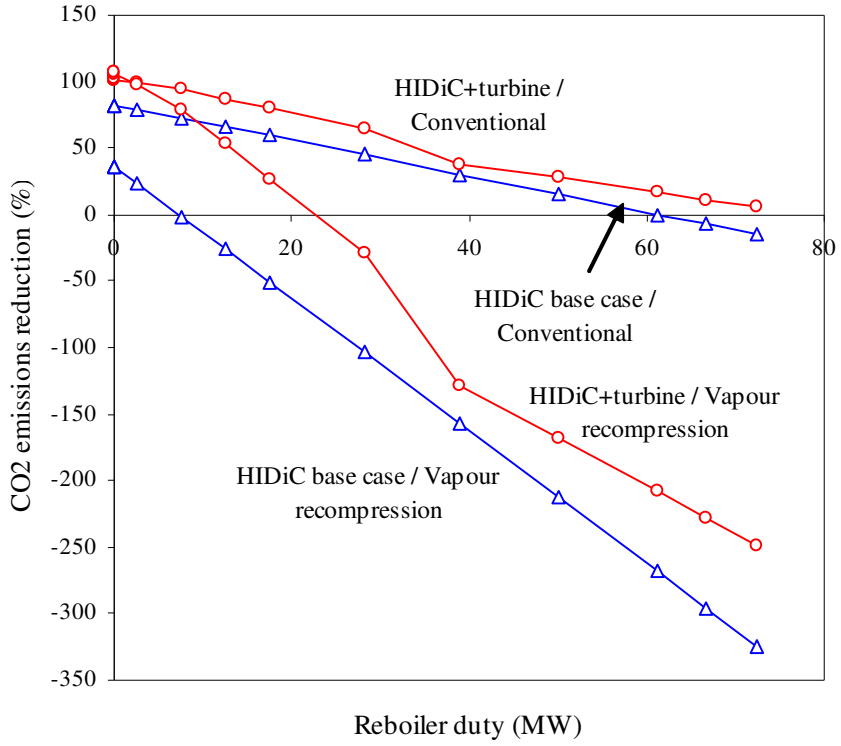

Figure 6: Reductions in CO_2 emissions from a HIDiC, relative to conventional column and VRC

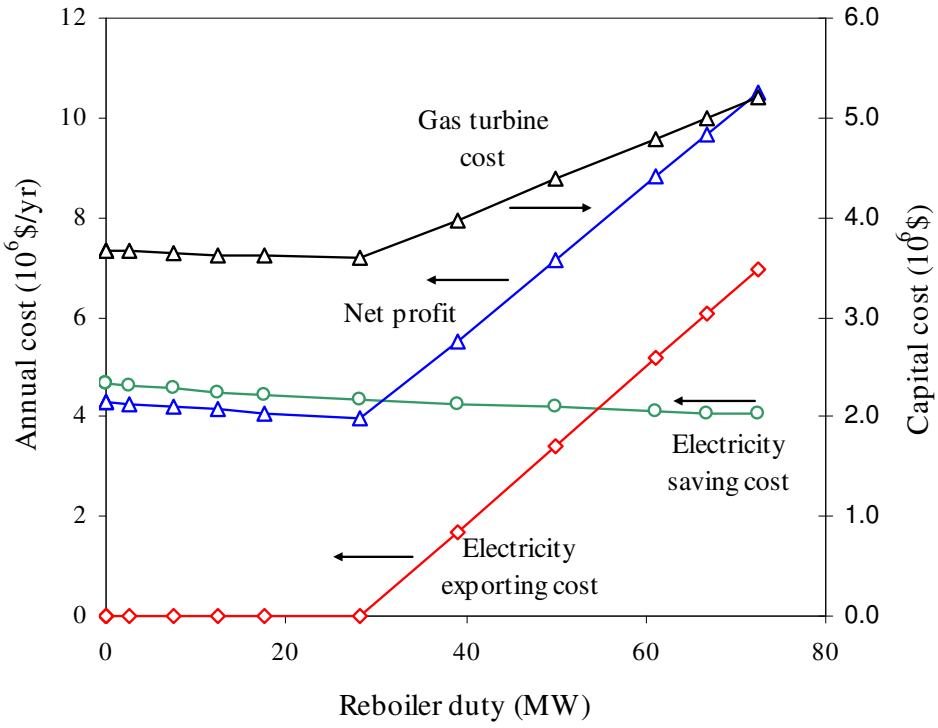

Figure 7: Economic analysis of a HIDiC with a gas turbine

4.2 Economic evaluation

Fig. 7 summarises the economic evaluation of HIDiCs with integrated gas turbines. Electricity saving is equal to the power demand of the compressor, which will be provided by the gas turbine. Similarly, exported electricity is that provided by the gas turbine, and is in excess of that required by the compressor. The net profit is the value of exported power and saved imported power less the annualised cost of the gas turbine (17). As shown, the net profit is relatively high when the reboiler duty is large (partial HIDiCs). This is because the power output of the gas turbine is large and consequently greater amounts of electricity can be exported, increasing income. For near ideal HIDiCs, the net profit is decreased from 10.5 to 4.0 million dollars per year because no power is exported (see also Fig. 4). However, as illustrated in Fig. 8, since the turbine capital cost is at the minimum and significant amount of heat is exported the payback time is also minimized, to 0.8 years. This case study illustrates that HIDiCs can offer a good opportunity for emissions reduction, in addition to economic benefits. Certainly, the benefits increase when a gas turbine is integrated with the HIDiC.

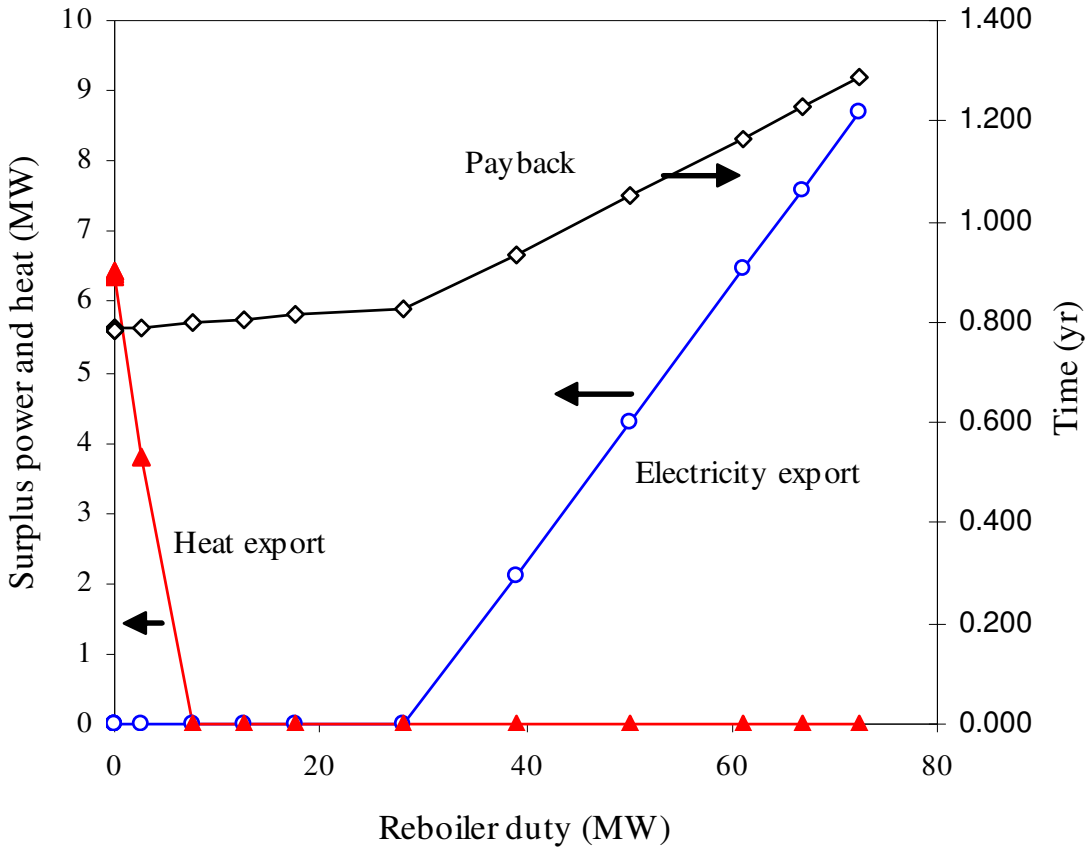

Figure 8: Surplus power and heat from a HIDiC with a gas turbine

5. Conclusions

Potential for CO_2 emission reduction of an internally heat integrated column has been evaluated and demonstrated using a state of the art propylene-propane splitter as the base case. It has been shown that the CO_2 emissions of such column configurations can be decreased by 83% compared to conventional alternatives, and 36% compared to the state of the art heat pump designs. This is roughly equivalent to the reduction of the energy requirement. The emissions of these columns are reduced further significantly when a gas turbine is added to the existing design and/or natural gas is used as the fuel. Most importantly, by exporting excessive electricity, the process economics are improved in parallel with emissions reductions.

6. References

(1) Linnhoff B, Dunford H, Smith R. Heat integration of distillation columns into overall processes. Chem. Eng. Sci. 1983; 38(8): 1175-1188. Stupin W J., Lockhart F J. Thermally coupled distillation – a case history. Chemical Engineering Progress 1972; 68(10): 71-72.

(2)

(3) Freshwater D C. Thermal economy in distillation. Trans IChemE 1951; 29: 149-160

(4) Sulzer Chemtech. Distillation and heat pump technology. Brochure 22.47.06.40-V.91-100, 1991.

(5) Nakaiwa M, Huang K, Owa M, Akiya T, Nakane T, Sato M, Takamatsu T. Energy savings in heat-integrated distillation columns. Energy 1997; 22: 621-625.

(6) Nakaiwa M, Huang K, Naito K, Endo A, Owa M, Akiya T, Nakane T, Takamatsu T. A new configuration of ideal heat integrated distillation columns (HIDiC). Computers and Chemical Engineering 2000; 24: 239-245.

(7) Olujic Z., Fakhri F, de Rijke A, de Graauw J, Jansens P J. Internal heat integration – the key to an energy-conserving distillation column. Journal of Chemical Technology and Biotechnology 2003; 78: 241-248.

(8) Mah R S H, Nicholas J J, Wodnik R B. Distillation with secondary reflux and vaporization: a comparative evaluation. AIChE J 1977; 23: 651-658.

(9) Fitzmorris R E, Mah R S H. Improving distillation column design using thermodynamic availability analysis. AIChE J 1980; 26(2): 265-273.

(10) Seader J D. Continuous distillation apparatus and method. US Patent, 4,234,391, 1978/1980.

(11) Glenchur T, Govind R. Study on a continuous heat integrated distillation column. Sep. Science Tech. 1987; 22: 2323-2328.

(12) Aso K, Matsuo H, Noda H, Takada T, Kobayashi N. Heat integrated distillation column, US Patent 5,783,047, 1996/1998.

(13) Nakaiwa M, Huang K, Naito K, Endo A, Akya T, Nakane T, Takamatsu T. Parameter analysis and optimization of ideal heat integrated distillation columns. Computers and Chemical Engineering 2001; 25: 737-744.

(14) Naito K, Nakaiwa M, Huang K, Endo A, Aso T, Nakanishi T, Nakamura T, Noda H, Takamatsu T. Operation of bench-scale HIDiC: an experimental study. Computers and Chemical Engineering 2000; 24: 495-499.

(15) Nakaiwa M, Huang K, Endo A, Ohmori T, Akiya T, Takamatsu T. Internally heat-integrated columns: a review. Trans IChemE 2003; Part A(81): 162-177.

(16) Gadalla M, Olujic Z, Sun L, de Rijke A, Jansens P J. Pinch analysis-based approach to conceptual design of internally heat-integrated distillation columns. Chemical Engineering Research and Design 2005; 83 (A8): 1-7.

(17) Gadalla M, Jobson M, Smith R, Estimation and reduction of CO_2 emissions, Energy 2005, in press.

(18) Delaby O. Process integration for the reduction of flue gas emissions. PhD Thesis, UMIST, Manchester, UK, 1993.

(19) Manninen J. Flowsheet synthesis and optimisation of power plants. PhD Thesis, UMIST, Manchester, UK, 1999.

(20) Smith R, Delaby O. Targeting flue gas emissions. Trans IChemE November 1991; Part A(69): 493-505.

(21) Linnhoff March Report. GRI Multiple Utility Design Procedure, 1987

(22) Manninen J, Zhu X X. Optimal gas turbine integration to the process industries. Ind. Eng. Chem. Res. 1999; 38(11): 4317-4329.

(23) Sun L, Olujic Z, de Rijke A, Jansens P J. Industrially viable configuration for a heat integrated distillation column. The 5th international Conference on Process Intensification for the Chemical Industry, Maastricht, the Netherlands, 13-15 October 2003, BHR Group, M. Gough (Ed.), 151-166.

(24) Aspen Plus. Version 10.2. Aspen Technology Inc., February, 2000.

Samenvatting

De toenemende vraag naar energie, de resulterende hoge olieprijzen en de groeiende zorg over CO_2 emissies zijn belangrijke aanjagers voor de ontwikkeling van energetisch efficiëntere en meer milieuvriendelijke processen en unit operations in de chemische procesindustrie.
Destillatie is veruit de meest toegepaste scheidingstechniek. Een groot nadeel is de degradatie van energie in het destillatieproces, die wordt veroorzaakt door het temperatuurverschil tussen de condenser en verdamper van een destillatiekolom. Deze degradatie van energie is er de oorzaak van dat het thermodynamische rendement van destillatie laag is, typisch in de orde van 10%. Gedurende de laatste decennia zijn er verschillende technologiëen ontwikkeld en geïmplementeerd om de thermische economie van destillatiekolommen te verbeteren. De aandacht was voornamelijk gericht op de warmte-integratie van een trein van destillatiekolommen. Damprecompressie is een manier om het energetisch rendement van een enkele destillatiekolom te verbeteren en wordt industrieel toegepast voor de scheiding van mengsels met een lage relatieve vluchtigheid.
Een intern warmte-geïntegreerde destillatiekolom (HIDiC) combineert de voordelen van damprecompressie en diabatische operatie met als doel de energiebehoefte van een enkele destillatiekolom te verminderen. Het theoretische voordeel van HIDiC ten opzichte van een damprecompressiekolom is gelegen in het feit dat de compressor in een HIDiC alleen hoeft te opereren over de stripsectie van de kolom. Daarom zou een HIDiC met een lagere compressieverhouding moeten kunnen opereren, resulterend in een lager benodigd compressorvermogen. In een HIDiC is de stripsectie van de kolom fysiek gescheiden van de rectificatiesectie. Warmte wordt in de destillatiekolom van de rectificatiesectie naar de stripsectie overgedragen, omdat de operatiedruk van de rectificatiesectie wordt verhoogd door de compressor. Hoewel het HIDiC concept al werd geïntroduceerd rond 1970, is het nog steeds niet industrieel toegepast vanwege het complexe apparaatontwerp en het ontbreken van experimentele data op voldoende grote schaal om het principe van HIDiC aan te tonen.
Op de TU Delft is een nieuw type concentrische HIDiC ontwikkeld, waarin de lage druk annulaire stripsectie rondom de hoge druk rectificatiesectie is geconfigureerd. Warmtepanelen kunnen boven het actieve schoteloppervlak worden geplaatst om een voldoende groot warmtewisselend oppervlak te verkrijgen. Er is een experimentele studie uitgevoerd om dit concept voor intra-kolom warmteoverdracht te bewijzen. De experimentele resultaten zijn gebruikt om de toegepaste modellen te valideren.

Warmteoverdracht in een Concentrische HIDiC met warmtepanelen

Er zijn op grote schaal experimenten uitgevoerd in een concentrische HIDiC met een diameter van 0.8 m, die werd geopereerd met het modelsysteem cyclohexaan/(n)-heptaan. De overall warmteoverdrachtscoëfficiënt werd bepaald voor respectievelijk, warmtepanelen geplaatst in de downcomer of boven het actieve oppervlak van de zeefschotel. De warmtepanelen blijken voldoende te worden bevochtigd door de boven de schoteldek aanwezige spattende en schuimende massa. De overall warmteoverdrachtscoëfficiënt hangt sterk af van het temperatuurverschil tussen de rectificatie- en de stripsectie, veroorzaakt door de laminaire stromingscondities aan de condensatiekant van de warmtepanelen. Voor procescondities die voor HIDiC praktisch interessant zijn, lag de overall warmteoverdrachtscoëfficiënt tussen de 700 en 1500 W/m^2K.

Het Alhusseini model voorspelde het beste de warmteoverdrachtscoëfficiënt van een verdampende, vallende vloeistoffilm met stromingscondities in het transitiegebied tussen laminaire en turbulente stroming. Het Nusselt model kwam goed overeen met de experimentele warmteoverdrachtscoëfficiënt aan de condensatiezijde, uitgezonderd bij lage Reynolds getallen, wat een indicatie is voor gedeeltelijke bevochtiging van het warmtewisselend oppervlak.

De dampinlaat naar de warmtepanelen moet zorgvuldig worden ontworpen om stagnante zones in de warmtepanelen te voorkomen.

Scheidingsefficiency van een annulaire zeefschotel

Er zijn experimenten uitgevoerd om het effect van de annulare schotelgeometrie op de scheidingsefficiency te bepalen en om de invloed vast te stellen van de aanwezigheid van warmtepanelen op het stromingsgedrag van de schotel en daardoor op het overall schotelrendement.

Wanneer de gemeten data vanuit deze studie worden vergeleken met die van het Fractionating Research Institute, blijkt dat de scheidingsefficiency van een annulaire schotel overeenkomt met die van een conventionele cross-flow schotel.

Het Garcia en Fair model is gebruikt om de overall schotelefficiency te voorspellen. De drukval van de schotel is gemodelleerd met het model van Bennett. Zowel metingen als berekeningen tonen aan dat de panelen geen invloed hebben op de drukval van de schotel.

Warmteoverdrachtspanelen hebben een positive invloed op het stromingsgedrag van de schotel en verbeteren de scheidingsefficiency van de schotel met ruwweg 10%, wat een belangrijk voordeel is van het voorgestelde kolomontwerp waarin warmtepanelen boven het aktieve schoteloppervlak zijn geplaatst. De belangrijkste reden voor de toename in schotelefficiency blijkt

de door de panels veroorzaakte vermindering van terugmenging op de schotel te zijn. Dit additionele effect kon worden gesimuleerd door het vloeistof mengsel boven de schotel te beschouwen als een aantal ideaal gemengde tanks in serie.
De film langs het oppervlak van de warmtepanelen is tevens een extra uitwisselingsoppervlak voor stofoverdracht resulterend in een kleine verbetering van de scheidingsefficiency.

Ontwerp van HIDiC voor diverse industriële destillatie toepassingen
Een HIDiC versie van een state of the art Propaan-Propyleen scheider wordt geïntroduceerd. De referentie is één van 's werelds grootste, alleen staande, kolommen die met een warmtepomp is uitgerust. De actuele kolomdata vormde de basis voor een technisch-ecomische evaluatie, die aangeeft dat HIDiC economisch interessant kan worden voor nieuwe ontwerpen.
De thermische efficiency van HIDiC is erg afhankelijk van de kolomconfiguratie, dat is de wijze waarop de stripsectie en rectificatiesectie thermisch worden geïntegreerd. Ten tweede blijkt de verdeling van de interne warmtelast langs de kolom erg belangrijk te zijn. Omdat een HIDiC in essentie een fractionerende warmtewisselaar is, dicteert het temperatuurprofiel de schotels waarop interne warmteoverdracht haalbaar is. Een betere exploitatie van de drijvende krachten voor warmteoverdracht leidt tot een reductie van het benodigd warmtewisselend oppervlak en resulteert bovendien in een ontwerp met een hogere haalbaarheid. De keuze voor een ideale HIDiC, zonder externe verdamper, of een partiële HIDiC hangt sterk af van het modelsysteem. HIDiC blijkt de voorkeursvariant te zijn voor de scheiding van mengsels met een lage relatieve vluchtigheid in toepassingen met een gemiddelde tot hoge operatiedruk, waar een optimaal HIDiC ontwerp de energiebehoefte met 50% reduceert ten opzichte van conventionele damprecompressietechnologie.

Aris de Rijke

Dankwoord

Allereerst dank ik God, die me in staat stelde om dit werk uit te voeren en met goed resultaat af te ronden.

Verder, Daniëlle, en onze jongens, Martin en Timon. Ik ben ontzettend dankbaar dat ik dit werk niet zonder jullie heb hoeven uitvoeren.

Peter Jansens die me adviseerde om dit promotieonderzoek uit te voeren naast mijn taak als beheerder van API. Hoewel de bedrijfsvoering van API vaak top priority was en daardoor het promotieonderzoek op de tweede plaats kwam, heb ik nooit spijt gehad van de keuze om deze twee jobs te combineren.

Zarko Olujic beschouw ik als een leermeester die met een niet aflatende ijver zijn jongeren het destillatievak bijbrengt. Zijn boodschap tijdens het 3^{e} jaars college Scheidingstechnologie “and don’t forget the pressure drop” zal ik niet snel vergeten.

Jan de Graauw de uitvinder van “onze” HIDiC. Dank voor uw praktische en tevens uitstekend doordachte adviezen in de ontwerpfase van de HIDiC kolom.

‘Mijn’ afstudeerders, Maarten Steenbakker, Maarten Wichhart, Edzard Leeuw en Warbout Tesselaar voor de vele discussies en het werk dat jullie binnen dit projekt hebben verricht.

The HIDiC post-docs, Lanyi Sun, Mamdouh Gadalla and Pieter Schmal. Without your simulation results, this dissertation would not have been written at all.

De projektpartners, ABB Lummus Heat Transfer, Akzo Nobel Chemicals, BP, DSM, ECN, Sulzer Chemtech en Shell Global Solutions voor hun deelname en steun aan dit projekt.

SenterNovem voor het beschikbaar stellen van subsidie voor de ontwikkeling van HIDiC in het kader van de EET (Economie Ecologie Technologie) regeling.

De heer Cousaert van Borealis Antwerpen die de plant data van de damprecompressie PP-splitter beschikbaar heeft gesteld om te gebruiken binnen dit projekt.

Carel van Dissel voor jouw expertise en hulp bij het beheer van API en het “in de klauwen” houden van onze collega-wetenschappers, die geen enkel belang leken te hechten aan de financiën van hun projekten en de daaruit voortvloeiende verplichtingen. Als ik terug denk aan de vele uren die we hebben doorgewerkt onder het genot van een sigaret in de historische rookkamer, ben ik geneigd weer met roken te beginnen.

Brenda, m’n maatje binnen API, met wie ik eigenlijk alles in vertrouwen kon bespreken.

De mannen van API, Jan, Stefan, Theo, André, Gerard en Martijn voor jullie bijdrage aan het ontwerpen en bouwen van de HIDiC destillatie pilot plant. Zonder de werkplaats is het onmogelijk experimenteel onderzoek op grote schaal uit te voeren. Jullie waren altijd bereid een stapje harder voor me te lopen.

Paul Durville voor jouw immer opgeruimde humeur en voor het VGWM-bewust maken van de API-gemeenschap.

Marcel Behrens en Martijn van der Kraan voor jullie niet aflatende bereidwilligheid even een frisse neus te halen in het rookhol.

‘Het secretariaat’, Annemarie, Petra, Helma en Leslie voor alle dingen die jullie hebben georganiseerd.

Maarten de Groot en Ad den Hollander voor jullie betrokkenheid en coaching op het gebied van financiëel beheer.

Martin Pander voor jouw lessen betreffende de ontwikkeling en het management van vastgoedprojekten. En voor de gelegenheid die je me gaf om naast het werk binnen FMVG ook dit promotieonderzoek af te ronden, hoewel we langzamerhand tot de conclusie kwamen dat een promotieonderzoek nooit af is.

Allemaal **BEDANKT**, Aris

About the Author

Aris de Rijke was born at January 20, 1975 in Delft, the Netherlands. After finishing his secondary education, he studied Chemical Engineering at Delft University of Technology from 1993 to 1998. On completing his study, he worked as a process engineer for Norsk Hydro. In 1999, he accepted a job as manager of the Laboratory for Process Equipment of Delft University of Technology. His PhD study was started in this laboratory in 2002, covering the development of an internally Heat Integrated Distillation Column (HIDiC). In 2005 and 2006, he was departmental secretary of the Process & Energy department of TU Delft. From 2004 till 2007 he was project leader of some real estate projects at the university campus, all projects involving design and implementation of large scale experimental equipment and laboratory facilities. Recently, he joined the department Distillation and Thermal Conversion of Shell Global Solutions.

List of Publications

Patents

J. de Graauw, M.J. Steenbakker, A. de Rijke, Z. Olujic, P.J. Jansens. *Heat Integrated Distillation Column*, NL102244 (29-07-2003), WO 03061802 (31-07-2003), EP1476235 (17-11-2004), CA2474061 (22-07-2004), US2005121303 (09-06-05)

Papers

Z. Olujic, F. Fahkri, A. de Rijke and P.J. Jansens, *Internal heat integration-the key to an energy conserving distillation column,* J. Chem. Technol. Biotechnol. 78 (2003) 241-248

L. Sun, Z. Olujic, A. de Rijke and P.J. Jansens, *Industrially Viable Configurations for a Heat Integrated Distillation Column*, Proceedings of the 5th Process Intensification Conference, Maastricht, Netherlands, 13-15 October 2003, 151-166

M. Gadalla, Z. Olujic, A. de Rijke and P.J. Jansens, *A Thermo-hydraulic approach to conceptual design of a internally heat integrated distillation column*
ESCAPE 14, European Symposium on Computer Aided Process Engineering, Lisbon, Portugal, May 16-19, 2004, Volume A, p 181-186

M. Gadalla, Z. Olujic, A. de Rijke, P.J. Jansens, *A Pinch Analysis based approach to the design of internally heat integrated tray distillation columns*, TransIChemE, Part A, Chem. Eng. Res. Des. 2005, 83 (A8), 987-993

Z. Olujic, L. Sun, A. de Rijke, P.J. Jansens, *Conceptual Design of an Energy Efficient Propylene-Propane Splitter*, Proceedings of the 17th International Conference on Cost, Optimization, Simulation and Environmental Impact of Energy Systems (ECOS 2004), July 20-22, 2004, Guanajuato, Mexico, Volume 1, 61-78

A. de Rijke, L. Sun, M. Gadalla, Z. Olujic, P.J. Jansens, *Finding an Optimal HIDiC Configuration for Various Industrial Distillation Applications*, Proceedings of the 7th World Conference of Chemical Engineering, Glasgow Scotland, 10-14 July 2005.

M. Gadalla, Z. Olujic, A. de Rijke, P.J. Jansens, *Reducing Carbon Dioxide Emissions of internally Heat Integrated Distillation Columns for the Separation of Close Boiling Mixtures*, Energy 31, 2006, 2073-2081

Z. Olujic, L. Sun, A. de Rijke, P.J. Jansens, *Conceptual Design of an internally Heat Integrated Propylene Propane Splitter*, Energy 31, 2006, 3083-3096

A. de Rijke, Z. Olujic, P.J. Jansens, *Heat and Mass Transfer Characteristics of an Annular Sieve Tray*, Proceedings of the Distillation and Absorption '06 Conference, 2-4 September 2006, London.

Presentations

Industrially Viable Configurations for a heat integrated distillation column,
Oral Presentation 5th Process Intensification Conference, Maastricht, Netherlands, 13-15 October 2003, 151-166

Industrially Viable Configurations for a heat integrated distillation column
Oral Presentation 3rd Netherlands Process technology Symposium, 28 October 2003, Veldhoven, Netherlands

A Thermo-hydraulic approach to conceptual design of a internally heat integrated distillation column
Poster Presentation ESCAPE 14, European Symposium on Computer Aided Process Engineering, Lisbon, Portugal, May 16-19, 2004 , Volume A, p 181-186

A Pinch Analysis based approach to HIDiC Design
Oral Presentation CHISA 2004 Conference, 22-26 August 2004, Prague

Reducing Carbon Dioxide Emissions and Energy Consumption of Heat Integrated Distillation Systems
Keynote Lecture CHISA 2004 Conference, 22-26 August 2004, Prague

Force-Flux Analysis of a Heat Integrated Distillation Column
Oral Presentation 4th Netherlands Process technology Symposium, 26 October 2004, Veldhoven, Netherlands

Conceptual Design of a Heat Integrated Propylene Propane Splitter
Poster Presentation 4th Netherlands Process technology Symposium, 26 October 2004, Veldhoven, Netherlands

Finding an Optimal HIDiC Configuration for Various Industrial Distillation Applications
Oral Presentation 7th World Conference of Chemical Engineering, Glasgow, Scotland, 10-14 July 2005.

Heat and Mass Transfer Characteristics of an Annular Sieve Tray
Oral Presentation Distillation and Absorption Conference, London UK, 2-4 September 2006.